BERGISCHE
UNIVERSITÄT
WUPPERTAL

Analysis of framed structures under fire loading

Dissertation

zur Erlangung eines Doktorgrades (Dr. Ing)

in der

Fakultät für Architektur und Bauingenieurwesen

der

Bergischen Universität Wuppertal

vorgelegt von

Davoud Pirzadeh

Aus Esfahan, Iran

Wuppertal 2017

Die Dissertation kann wie folgt zitiert werden:

urn:nbn:de:hbz:468-20190626-113708-8
[http://nbn-resolving.de/urn/resolver.pl?urn=urn%3Anbn%3Ade%3Ahbz%3A468-20190626-113708-8]

DOI: 10.25926/r961-y369
[https://doi.org/10.25926/r961-y369]

Foreword

This dissertation is submitted for the degree of Dr.Ing at Wuppertal University, Civil engineering department. The research described herein was conducted under the supervision of Professor Dr. Ing. Reinhard Harte.

Firstly, I would like to express my sincere gratitude to my supervisor Professor Dr. Ing. Reinhard Harte for the continuous support of my Ph.D study and related research, for his patience, motivation, friendship and immense knowledge. His guidance helped me in all the time of research and writing of this thesis.

Besides my supervisor, I would like to thank my thesis committee: Prof. Dr. Ing. Casimir Katz and Prof. Dr. Ing. Markus Schäfer for their insightful comments and encouragement, but also for the hard question which incented me to widen my research from various perspectives.

My sincere thanks also go to Univ.-Prof. Dr.-Ing. Georg Pegels who provided me an opportunity to join the team in Wuppertal.

Thanks to my friends and to the people who helped me at Wuppertal University during my time in Wuppertal.

Finally, I take this opportunity to express my gratitude to my wife and my parents for their love, encouragement, and support.

Wuppertal, Germany 2017

Davoud Pirzadeh

Abstract

Fire is categorized under accidental loads in Eurocodes. Accidental fire loads are almost unpredictable loads that depend on time, the fire compartment, live loads, and the type of such loads. In case of complicated structural systems, some aspects—such as the buckling of columns, the effects of elevated temperatures on global structure, the redistribution of loads and internal forces, and the unloading process—can be investigated only by applying advanced calculation methods based on the Eurocode classification, which apply the coupled finite element fields to analyse the structure. The solution process of complicated systems can be time-consuming, costly, and—sometimes—impossible. The abovementioned methods are complicated and time-consuming for modelling the accidental fire loading process as different scenarios in combination with other loads. The motivation of this research study is to simplify the modelling of the fire loading processes.

By combining the simulation procedure of Levels 2 and 3, based on Eurocode, a FEM model of analysis for mathematizing the fire loading process is developed. Based on the results of the two-dimensional thermal FEM equation, the developed method obtains the reduced time-dependent stiffness (integrated over the cross-section area) of warm members as a function of time. The variable stiffness of warm members will be applied to mathematize the global structural behaviour for calculating the distribution of internal forces, considering geometrical nonlinearity. The developed method is able to apply different fire scenarios and combine them with other service loads to obtain global structural behaviour and distribution of internal forces. To achieve this, a FEM code has been developed in Microsoft Visual C# (C sharp), and the results are verified with those of the ANSYS Workbench software. To investigate the fire resistance of steel structures, the method that has been developed will give convincing results at lower temperatures. The developed method considers a cold analysis under an assumption of variable stiffness for the warm members and, so, is suitable to just determine an estimation.

The developed method attempts to decrease the cost of analysis and give a rough estimation of the structural response. The results of the developed method can be trusted to obtain an estimation of the global behaviour of structure. The results depend directly on stiffness curves. The simplified method that has been developed is not suitable to determine exact and accurate structural behaviour. Material nonlinearity, crashes in concrete members, 3D thermal stresses and strains in cross-sections, buckling, and shear deformations are some of the parameters not considered by the method that has been developed.

Table of contents

List of illustrations

List of symbols

ε_p	Maximum strain related to linear behaviour
ε_y	Yield strain
E_T	Modulus of elasticity at temperature θ
$\theta \ and \ T$	Temperature
σ	Stress or Stefan-Boltzmann constant (see Chapter 4)
$f_{y,T}$	Yield stress at temperature T
$k_{T,E}$	Reduction factor for modulus of elasticity
$k_{T,y}$	Reduction factor for yield stress
E_{in}	Input energy to control volume
ΔU	Change in stored energy in control volume
E_{out}	Output energy to control volume
q_x	Heat flux
$E_{generated}$	Generated energy inside control volume
A	Cross-sectional area
Q	Internal heat generated by heat source
K_{xx}	Thermal conductivity in x direction
h	Heat transfer coefficient
T_∞	Surrounding temperature or temperature of fluid
ε	Emissivity in heat transfer problems
c	Specific heat
ρ	Density
m	Mass
q_0	Boundary heat flux
l_x, l_y, l_z	Direction cosines in x, y, z directions
V	Volume of the finite volume
S	Area of the boundary

T_i	Nodal temperature for node i
x_i, y_i, z_i	Nodal coordinates
N_i	Shape function for element i
a_i, b_i, c_i	Constants of shape functions
$[T]$	Temperature vector of an element
$[N]$	Shape function vector of an element
$I^{(e)}$	Functional of an element
$[K]$	Stiffness matrix of an element
$[D]$	Material properties matrix of an element
t	Thickness of an element
$[f]_e$	Force vector of an element
$[f]$	Force vector of a system
$[K]_1$	Stiffness matrix related to conduction effects
$[K]_2$	Stiffness matrix related to convection effects
$[K]_3$	Consistent matrix
Δt	Time step increment
$[T_i]$	Temperature field at step i
$[\dot{T}]$	Variation of a temperature with respect to time
W_x, W_y, W_z	Distributed loads in x, y, z directions
P_x, P_y, P_z	Point loads in x, y, z directions
u, v, w	Deformation in x, y, z directions
u_1, u_2, u_3	Deformations in tensor form
$\theta_1, \theta_2, \theta_3$	Rotations in tensor form
$\theta_x, \theta_y, \theta_z$	Rotations in x, y, z directions
$\sigma_{xx}, \sigma_{yy}, \sigma_{zz}$	Normal stress in x, y, z directions
$\sigma_{xy}, \sigma_{yz}, \sigma_{zx}$	Shear stress in x, y, z directions
$\sigma_{11}, \sigma_{22}, \sigma_{33}$	Normal stress in tensor form

$\sigma_{12}, \sigma_{23}, \sigma_{31}$	Shear stress in tensor form
$\varepsilon_{xx}, \varepsilon_{yy}, \varepsilon_{zz}$	Normal strain in x, y, z directions
$\varepsilon_{xy}, \varepsilon_{yz}, \varepsilon_{zx}$	Shear strain in x, y, z directions
$\varepsilon_{11}, \varepsilon_{22}, \varepsilon_{33}$	Normal strain in tensor form
$\varepsilon_{12}, \varepsilon_{23}, \varepsilon_{31}$	Shear strain in tensor form
b_x, b_y, b_z	Body force x, y, z directions
$[\sigma]$	Stress tensor matrix
$[\varepsilon]$	Strain tensor matrix
a	Acceleration
$\ddot{u}_x, \ddot{u}_y, \ddot{u}_z$	Accelerations in x, y, z directions
ϑ	Poisson's ratio
α	Thermal elongation coefficient
$[\varepsilon_0]$	Initial strain matrix
π	Potential energy of a system
W_{ext}	Work done by external forces
$\pi_{int.}$	Work done by stresses
$[P]$	External force vector
$[B]$	Body force vector
$[N]$	Shape function vector of an element
$[U]$	Displacement vector
$[K_e]$	Element stiffness matrix
$[P_e]$	Element force matrix
$[A]$	Transformation matrix
I_{xx}, I_{yy}	Second moment of inertia
l	Length of a line element
G	Shear modulus of material
l_i, m_i, n_i	Direction cosines

M_x, M_y, M_z	Bending moment about x, y, z axes
$[K_e]_{ij}$	Stiffness matrix of an element between nodes i and j
$\eta_{xx,NL}$	Nonlinear strain in x direction
$\eta_{yy,NL}$	Nonlinear strain in y direction
$\eta_{zz,NL}$	Nonlinear strain in z direction
$\left[\sigma_{ij}^{t}\right]$	Stress at time t
$\left[\Delta\sigma_{ij}^{t}\right]$	Stress increment at time t
$\left[\varepsilon_{ij}^{t}\right]$	Strain at time t
$[K]_L$	Linear stiffness matrix
$[K]_{NL}$	Non-linear stiffness matrix
$[K]_G$	Non-linear geometric stiffness matrix
l_0	Initial length of the beam
dl	Axial deformation of a beam
ε_{th}	Thermal strain

1 Introduction

1.1 Preamble

Designing structures and making them withstand loads is a topic that has engaged the attention of specialists. Structures can be under different load types, which can be categorized by their roots and sources viz. gravity, earthquake, fire, and wind. One of the goals of structural designing is to protect human life and capital. Fire loads can rapidly affect the serviceability of the structures and endanger human life and capital. Fire loads are accidental and difficult to be mathematized by engineers. The vital importance of the safety of the structures against fire loads becomes visible when the safety of infrastructures, high-rise buildings, political buildings, etc. are of interest. Recent large-scale experiments, such as the ones in Cardington, and real-life events like the Windsor Tower fire in Madrid and the World Trade Center (WTC) collapse in New York, have shown the real impact of structural continuity in the global response of buildings subjected to fire hazards. There are many examples in which fire loads have led to catastrophes. Since then, a lot of work has been undertaken to understand the global fire response, especially of steel and composite structures. In Figures 2-1 and 2-2, the effect of thermal loads on steel structures can be seen.

Buildings have to be designed to withstand all the loads, including fire loads. Specialists has developed safety rules and strategies to protect human life against accidental thermal loads. Fire Safety Engineering has been developed

to achieve these goals. Fire Safety Engineering integrates the rules of Fire Protection Engineering and Structural Fire Engineering. Fire safety is normally considered to cover both the safety of people and of property (in the building concerned and in the surrounding area). The structural engineer and architect should set two goals: safety of life and property protection. Other objectives may sometimes be relevant, but these will normally only be variations on, or combinations of, these two principles. For example, in the fire safety design of hospitals, the maintenance of the service should be provided. The structural engineer and architect seek to minimize deaths and ensure the protection of properties. The structure must be able to continue its functionality during the fire and after the fire, and be repairable. The building should also remain safe for firefighting operations during the fire.

Figure 1-1: Deformation of steel beams under a test fire [1]

Figure 1-2: Deformation of beams near a column after a fire test [1]

Structural Fire Engineering (SFE) can be considered a constituent of a general multi-disciplinary approach to determine safety for buildings subjected to fire, in which structural stability is achieved by providing passive fire protection. After taking the above statements into consideration, it can be stated that SFE is the branch of engineering that is concerned with the design and analysis of structures when exposed to fire hazard. Its main goal is to ensure that the building is so designed and constructed that in the event of a fire, its stability will be maintained for a reasonable period. In other words, it deals with the analysis of thermal and structural effects of fire on buildings and defines the regulations to maximize the stability of the structure in order to ensure that the structure presents the required load-bearing resistance when subjected to fire.

The structural fire engineer has to provide acceptable levels of Fire Protection Engineering, which minimize the risks from the following products: combustion, heat, and smoke. The regulations and steps that have to be respected and performed can be considered the components of fire safety. These components

are concerned with what is built or installed, including the fire doors, sprinklers, escape stairs, alarm, etc.

Five tactics are available to the architect seeking to fulfil the objectives of fire protection engineering:

1. Prevention: Precisely controlling the fuel and heat sources;
2. Communication: Installing devices that are sensitive to heat and smoke to inform the occupants if an ignition has occurred;
3. Escape: Providing enough—and safe—ways of escape;
4. Containment: Trying to limit the fire to a closed compartment;
5. Extinguishment: Ensuring that the fire can be rapidly extinguished and with minimum consequential damage to the building.

Considering the rules of structural fire engineering and simplifications, this research deals with the development of a method of analysis to mathematize the structural behaviour under fire loads.

1.2 Problem statement and objective

Structural analysis and design of the buildings under fire loads is a complicated process, one that is categorized under passive protection methods. To investigate the behaviour of a structure under fire loads, different parameters, such as material properties, chemistry, fire, etc. will be considered. Reinforced concrete and steel structures—or a combination of both—have been used as the main construction materials worldwide. The goal of this research is to simplify the analysis of the steel and concrete structures under fire loads. To attain this goal, the structural behaviour of the structural members subjected to fire is mathematized by the variable stiffness of the members.

Structural standards and codes, such as EN 1992-1-2 [2] and EN 1994-1-2 [3], have taken the first steps in the pursuit of a comprehensive model that enables structural engineers to assess the real level of the fire safety of concrete and steel buildings. EN 1992-1-2 and EN 1994-1-2 (EN 199x-1-2) present three levels of analysis to simulate the behaviour of a structure:

- Level 1: This procedure of analysis is a conservative method based on tabulated data and diagrams that are related to the type and cross-section of the members subjected to fire;
- Level 2: This consists of simplified calculation methods based on reduced stiffness and strength of members subjected to thermal loads;
- Level 3: This level is based on material properties at elevated temperatures and non-linear behaviour of the global structure under fire. This level consists of thermal analysis and mechanical analysis.

In the current research, the simulation procedure of Level 2, based on Eurocodes, will be applied to obtain the reduced cumulative (integrated over the cross-section area) time-dependent stiffness of warm members as a function of time. The variable stiffness of warm members will be exercised to mathematize the global structural behaviour, calculating the distribution of internal forces after considering geometrical nonlinearity. Therefore, the developed method is a combination of Levels 2 and 3.

Structural members under fire behave in a nonlinear and time-dependent manner. Thermal loads can change the geometry and material properties of the warm members and can change the distribution of gravitational loads. Apart from the abovementioned effects, thermal loads lead to rapid decreases in the modulus of elasticity, thermal strains, and stresses in three directions. The thermal stresses and strains cause the internal and axial forces. Although consideration of the reduced cumulative time-dependent stiffness for warm members cannot give accurate results (because of material nonlinearity), this assumption may give a rough estimation of global structural behaviour.

This research considers the following points:

- the three-dimensional thermal strains are neglected;
- the thermal axial stress along the frame members length is considered as a cumulative stress (integrated over the cross-section area);
- conductivity, convection, and radiation are considered to obtain the temperature field;
- the analysis allows the effects of geometric nonlinearity;
- the developed method uses the variable stiffness of cross-sections, which is dependent *just* on the temperature field.

The regulations of Eurocodes are implemented in many advanced structural analysis software, which can perform thermal and non-linear structural analysis. The goal is to develop a faster and simple method which considers the variable stiffness of structure instead of a complicated thermal/structural analysis.

As mentioned above, if the variation of a member’s stiffness for a fire scenario is available, the behaviour of the structure can be calculated. This assumption is used to develop a software that uses the stiffness curve of members to obtain the structural behaviour of members during the fire loading process. A FEM code has been developed in Microsoft Visual C# (C sharp), and the results are compared with those of the ANSYS Workbench software, which have some coupled three-dimensional elements. The three-dimensional transient thermal and transient structural analysis of ANSYS Workbench software can calculate the temperature field and equations of motion for a structure.

The code that has been developed is named Fire-Loading. The temperature curve, loads, and geometry of the structure will be imported as Microsoft Excel files to the program. The material properties for steel and concrete, based on Eurocodes, are predefined in the program. Fire-Loading can calculate the temperature field and reduced cumulative time-dependent stiffness for the warm members. It can consider the geometric nonlinearity. Finally, the structural response can be calculated under an assumption of time-dependent stiffness.

To obtain the temperature distribution, the cross-section geometry and FEM mesh will be imported to Fire-Loading. Fire-Loading can consider only the pre-defined thermal boundary conditions. The sample importable Excel files can also be generated by the software. Fire-Loading can calculate structural response for 3-D or 2-D framed structures under point or distributed loads. It needs to be noted that Fire-Loading is developed to reduce the costs of analysis and to obtain an estimation of structural behaviour. Modelling the thermal loads with the help of variable stiffness cannot give accurate results. At higher temperatures, material non-linearity and thermal stresses are more important factors that can affect the accuracy of the results. Fire-Loading is suitable to obtain an estimation of the structural response.

1.3 Previous research works

The investigation of structures at elevated temperatures has been—and will be—the aim of many researchers' works, which form the basis of the building codes such as Eurocodes. Some of the subject researches will be presented here.

- Bizri H. [4] used two independent computer programs to calculate the framed structures under thermal actions. His program solves the differential equations for the heat transfer and defines a two-dimensional, non-linear, and non-stationary temperature field in the cross-section of the warm members. Thermal properties of the material are assumed to be temperature-dependent. A second iterative procedure—which is based on FEM, the deformation method, and the secant stiffness—performs a non-linear static analysis. The second program performs the analysis by using the results of the thermal analysis. To obtain the stiffness characteristics of the cross-section and internal forces, the cross-section is divided into sub-elements, considered one-axis prisms. It makes the program able to consider only the axial deformation and bending. The shear deformations and possible slip between concrete and bars are neglected. The developed program can consider the following aspects: the change of the element dimensions as a result of thermal dilation, the temperature-dependent material properties of the concrete and steel, the degradation of the cross-

section as a result of concrete cracking and crushing, reinforcement yielding, and the shrinkage and creep caused by temperature.

- Becker, J.M. and Bresler, B. [5] continued the research work of Bizri, H. They improved the two computer programs developed by Bizri, H. They also considered the redistribution of the stresses and strains in fire conditions.
- In 1977, a computer program named FIRES-RCII was developed by the University of California. It was developed to model the structural response of the reinforced concrete frames in fire environments. The material models of concrete and steel account for changes in mechanical properties of the material, degradation of the section by cracking and crashing, and increased rates of shrinkage and creep. Nonlinear stress-strain laws are used in FIRES-RC II to model concrete and steel behaviour.
- Chandrasekaran, V. and Mulcahy, N.L. [6] presented a method for the analysis of unprotected steel columns in fire conditions. Beam finite elements are used to model the columns that are concentrically loaded with initial out-of-straightness and temperature-dependent elasto-plastic material properties. They determined the accuracy of the model by comparing it with available experimental results for column strength at elevated temperature and for time of collapse with time-varying temperatures. They studied the unprotected steel column under a range of load levels, column sections, and slenderness of the column.
- Ellingwood, B. and Shaver, J.R. [7] considered a simply supported concrete beam under thermal actions. They applied the temperature curve based on ASTM E119. They tested six concrete beams under fire load of ASTM E119 and the design fire SDHI. The fire resistance, which is obtained by experiments, and the measured deformations formed the base for the verification of a modified version of the computer program FIRES-RC [5].
- Kodur V.K.R. et al. [8] developed the computer program SAFIR, which is the improved version of the computer program CEFICOSS. CEFICOSS was developed in the 1980s at the University of Liege in Belgium. The program is able to obtain the thermal field and perform the three-dimensional static analysis under fire loads by applying FEM. The structural analysis considers the material and geometric non-linearity. The fire load can be defined as a standard line or it may be a parametrically defined fire. The program can consider conduction, convection, and radiation, as well as temperature-dependent thermal characteristics of structural materials.
- Jukka Myllymaki and Djebar Barboudi [9] modelled the concrete-filled tubular composite columns under fire loads. They applied the one-dimensional Galerkin approach to model the heat transfer and the simple design method of Eurocode 4 to obtain the load-bearing capacity of the tubular composite columns. Calculated temperatures and load-bearing capacities are compared with the test

results of concentrically loaded circular and square tubular columns, filled with reinforced and non-reinforced concrete. They developed a spreadsheet program in Microsoft Excel to model the structural and thermal effects, and compared the calculated temperatures and capacities of the columns with the test results.

- Saab [10] was concerned with the development of a finite element approach and its subsequent use for behavioural studies on steel frames in fire conditions. The nonlinear structural analysis he assumed is based on a tangent stiffness formulation with large deformations. He performed the analysis by using an incremental Newton-Raphson iterative procedure and obtained the collapse load or critical temperature for two-dimensional multi-storied steel frames. A beam element with two nodes and three degrees of freedom at each node was used in the analysis. He tested the validity of the method with experimental and analytical data, covering as wide an arrangement of problem parameters as possible.
- Lien and colleagues [11] modelled the nonlinear behaviour of steel structures in the cooling phases of a fire by the Vector Form Intrinsic Finite Element (VFIFE) method. They verified the numerical model by comparing the results with the published analytical and experimental results for steel structures in the cooling phase. The numerical results show that the boundary conditions, temperature distributions, and properties of the high-temperature steel significantly affect the fire response of steel structures. They stated that structures with constraints in fires will induce thermal stresses, and the members of those structures will reach the plastic stage at lower temperatures when they are cooled to room temperature. This phenomenon indicates that these structures will probably reach the plastic phase in the early stage of a fire, and induce a considerable permanent deformation that causes great damage even after the fire is put out.
- Gelien, M. [12] investigated the fire resistance of reinforced concrete columns. The simplifications made in comparison with the exact thermal and mechanical analysis are demonstrated and analysed with reference to the effects on the result of calculation. She developed a new calculation model that is applicable to all types of usual cross-sections, systems of columns, and various flame impingements i.e. as of three or four sides. The model she developed can be calculated as a simple composite column with a rectangular cross-section.
- In 2004, an analysis of nonlinear frame elements under fire loads was investigated by two researchers [13] (Enrico Spacone and Sherif El-Tawil). They presented the current state-of-the-art of nonlinear analysis of steel-concrete composite structures. The focus was on frame elements that are computationally faster than continuum finite element models. Section models, fibre models, and a discussion of possible practical applications were presented. Models with lumped and distributed inelasticity, as well as models with perfect

and partial connections, are covered in their research. They focused on the developments that have stemmed from the recently completed National Science Foundation-sponsored U.S.-Japan program on composite and hybrid structures.

- Mihajlov, V. [14] developed a computer program called Fire Statik 3D (FS3D) to determine the construction behaviour during and after a fire exposure. FS3D calculates the temperature distribution in the cross-section of fire-exposed elements using the techniques based on FEM coupled with the time step integration. The numerical model implemented in FS3D is capable of achieving steady state linear and nonlinear heat transfer problems as well as unsteady state nonlinear heat transfer problems on an arbitrary domain (cross-section) with an arbitrary thermal boundary condition associated with fire. A non-linear beam-column element that can consider both material and geometric nonlinearity is included in the formulation of FS3D. The developed program applied the fibre method. Each segment (fibre) can have different material properties and a different temperature. FS3D is able to consider the material non-linearity, the thermal expansion, initial steel stresses, crashing and cracking of concrete, the residual concrete strength, and the constitutive material properties.
- Pauli [15] focused on the stability of carbon steel columns subjected to fire, especially on the interaction of material, cross-sectional, and member behaviour. The model she developed for the structural response considers factors that include the type of steel, the column slenderness, the support, and heating conditions. She defined an ideal model that should be easily calculable, be based on commonly used and available material parameters, show no discontinuities at the intersections of the different segments, and be adaptable to all the different non-linear shapes of the stress-strain relationship of any given material. All these requirements are met by exponential models of Eurocodes.
- Yi Zhuang [16] investigated the stability of unbraced steel frames due to abnormal loadings or fire loads, and developed practical methods to evaluate the stability capacity of unbraced steel frames in fire. He stated: ‘The problem of determining the elastic buckling strengths of unbraced steel frames subjected to variable loadings can be expressed as an optimization problem with stability constraints based on the concept of storey-based buckling. The optimization problem can be solved by the linear programming method, which is considerably simpler and more suitable for engineering practice than the nonlinear programming method.’ He suggested an alternative method to assess the lateral stiffness of an axially loaded column, derived by using two cubic Hermite elements to signify the column that is proposed.
- Bergmann [17] developed a simplified method for partially encased I-sections, which can be carried out by hand calculation. The developed design method

closely follows the design method for composite columns in accordance with DIN EN 1994-1-1. He determined the load bearing curve with respect to the residual stresses in accordance with DIN EN 1993-1-1.

Eurocodes define the regulations of the calculation models for the determination of temperature and load effects. For the fire design, different time-temperature curves for the determination of the hot gas-temperature are provided. Eurocodes also deal with the design of concrete (EN 1992-1-2), steel (EN 1993-1-2), and composite (EN 1994-1-2) structures for the case of fire. They state the design values for material properties and combination factors for actions, treating methods of the passive and structural fire precautions; active fire protection methods are not included. The current research is based on the regulations and material properties of the Eurocodes.

1.4 Organization of the Thesis

An investigation into the properties of fire as a chemical process and the concepts of Fire Safety Engineering is not of interest here. The application of the finite element method in structural analysis is of interest. The current thesis is divided into the following chapters:

- Chapter 1: Introduction

  State of the art, the goal of the current research, and the results of the research are explained in brief.

- Chapter 2: Fire Loads

  The fire is described as an accidental fire load. Developing a fire in a fire compartment and modelling the temperature rise in the fire compartment as a fire curve is explained.

- Chapter 3: Structural material at elevated temperatures

  In this chapter, mechanical and thermal properties of structural materials, including concrete and steel, are described. Mechanical properties as a function of temperature are especially presented in this chapter. The main parameter that affects the analysis process is the modulus of elasticity as a function of temperature. Annexures A and B are a part of this chapter. Annexure A represents the stress–strain curves of concrete as a function of time and concrete type. In Annexure B, thermal properties, such as thermal conductivity and the specific heat of material for transient state analysis, are discussed.

- Chapter 4: Thermal analysis

In this chapter, we consider the heat transfer problems. First of all, the heat transfer equation is presented in two-dimensional form. The two-dimensional heat transfer equation will be used to analyse the temperature distribution of a given cross-section, which is also stated in this chapter. The finite element formulation of a heat transfer equation will be presented and the stiffness matrix and force vector in the two-dimensional form will be obtained. The effects of temperature distribution on bending and axial stiffness of cross-sections and the mathematical method to obtain bending and axial stiffness will be explained in this chapter.

- Chapter 5: Linear and Nonlinear Mechanical Analysis

  In Chapter 5, a mechanical analysis of a structure, in which the stiffness of warm members varies in accordance with the stiffness curves, is proposed. A large deformation analysis will be applied to make the mathematical model of the structure more realistic. The basic equations and finite element formulation of linear and nonlinear three-dimensional space frames are presented. Geometric nonlinearity of space frames and variable stiffness of members facing fire are presented and included in the formulation.

- Chapter 6: The developed method

  In this chapter, the developed method, and the required assumptions are explained and discussed.

- Chapter 7: Validation of the simplified method

  In Chapter 7, the results of the computer code are going to be validated by applying the multi-phase analysis of ANSYS Workbench software. To do this, seven examples are solved by using the developed code and ANSYS Workbench. The results of Example 10 of DIN EN 1991-1-2 [18] are also compared with the results of the developed method.

2 Fire Loads

2.1 Introduction

Fire is a series of rapid and uncontrollable chemical processes between a fuel and oxygen, usually oxygen from the air. These chemical processes release energy in the form of heat and light. Three sources must be present to have a fire: 1- Oxygen, 2- Fuel, and 3- Energy—in the form of heat—to start the chemical process. These three ingredients of a fire are so essential that they are referred to as the 'triangle of fire'. The removal of any of these three (heat, fuel, or oxygen) will terminate the reaction and put out the fire. The major products of fire are light, smoke, and heat. Heat and smoke can be very dangerous for humans. In the process of a fire, we have:

$$Combustible\ material\ (Fuel) + O_2 \xrightarrow{Heat} H_2O + Smoke + Ash + Energy$$

Flames are the visible part of the chemical reaction between a gaseous fuel and oxygen. If the fuel and oxygen are mixed together in gaseous form, the mixed materials are named pre-mixed flame; if the fuel is a solid or liquid and the mixing occurs only during combustion, as the fuel gives off flammable vapours, then the flames are described as diffusion flames. Therefore, the solid or fluid material is changed to gaseous form and then mixed with oxygen. The gasification of a solid or liquid fuel occurs as it is heated. To obtain fire, the vaporized fuel and oxygen will have to be ignited. Therefore, it is not the fuel itself that burns, but the vapours. After the ignition has occurred, the vapours

burn, and the generated heat increases the fuel temperature and rate of vaporization. The combustion process must be self-sustaining for stable flames.

Underwriters Laboratories, Inc., has developed a classification that categorizes combustible materials into four types [19]:

1. Class A fires involve ordinary combustibles and are readily extinguishable by water or cooling, or by coating with a suitable chemical powder;
2. Class B fires involve flammable liquids where smothering is effective and where a cooling agent must be applied with care;
3. Class C fires are those in live electrical equipment where the extinguishing agent must be nonconductive. Since a continuing electrical malfunction will keep the fire source active, circuit protection must operate to cut off current flow, after which an electrically conductive agent can be used with safety;
4. Class D fires involve metals that burn, such as magnesium, sodium, and powdered aluminium. Special powders are necessary for such fires, as well as special training for operators.

2.2 Developing and growing the fire loads

There are three mechanisms of heat transfer that occur in structural fire scenarios: conduction, convection, and radiation [20].

- Conduction is the mode of heat transfer within solids. A negligible part of heat is transferred by conduction in fluids and gases.
- When the warm material moves in gaseous and liquid form, heat transformation also occurs, which is named convection heat transfer.
- Radiation is a form of heat transfer that does not require an intervening medium between the source and the receiver. It is heat transformation by light or waves.

The fires that grow inside structures behave in a completely different manner from those that grow outside in open areas. If the fire occurs in enclosed areas, which are named the fire compartment, the radiation effects increase, and the heat loss is reduced; as a result, the temperature of fuel rises more rapidly. A fire compartment is a structurally delimited area that burns out as intended in the event of fire. With sufficient fuel and ventilation, an enclosed fire will pass through a series of stages after ignition: a period of growth, one of stability, and then one of cooling. The temperature can be plotted as a function of time, which shows how the gas temperature has risen. It should be noted that the temperatures of fuel, gas, and structural elements around a fire are all different. The temperature curves are extremely useful to fire scientists when they

consider the consequences of changes in the conditions. The duration of the growth period depends on many factors, but a critical moment is reached when the flames reach the ceiling. As they spread out under the ceiling, the surface area increases greatly. Consequently, because of the warmed ceiling, the radiant heat transfer back to the surface of the fuel increases intensively. The remaining unburned material now reaches its fire point and begins to burn. This sudden process, which releases a lot of energy, is known as flashover, and is the beginning of a stable phase of the fire. If one of the members—for example, oxygen—vanishes, it is possible that a flashover may not occur. The fire may die out completely, or it may continue to smoulder; such a smouldering fire can be extremely hazardous because of toxic vapours. These toxic gases are hot enough, requiring only an oxygen source to explode. This effect is known as back draught. This can be highly dangerous for firefighters when they attempt to enter rooms to search for survivors. When the fire reaches the stable phase, it will begin to be distributed in the fire compartment. In the stable phase, depending on the combustible material(s) and ventilation, the maximum temperature will be reached. Once all combustible materials are burnt, the cooling phase will begin, which is the final phase.

To fight against fire, one of the three members of the fire triangle would have to be removed from the chemical reaction. Many extinguishing agents operate by limiting the amount of oxygen available to the fire (e.g. carbon dioxide, foam, sand). The most common extinguishing agent (water) works by cooling the materials involved in the reaction. Without heat, the reaction cannot start; and if the materials are suddenly cooled, the reaction will cease. The third method of extinguishing a fire is by interrupting the reaction itself, and dry powder and the halogenated hydrocarbons (commonly known as halons) do this by slowing down the reaction until it ceases to be self-sustaining.

The combustible material(s) or the fuel(s) within a building are described as that building’s fire load. Estimating the fire load can provide basic knowledge about the building category and fire risk. The fire load is difficult to estimate because the live load of the structure varies over time and depends on variable reasons. The greater the surface areas of the fuel(s) exposed, the greater is the potential for a rapid development of the fire. The denser the arrangement of the fuel, the longer will the fire take to build up to full heat output, and the longer it will last. Ventilation is another important factor. The amount of ventilation will be determined by the shape and size of the window openings. When the windows are small, the size of the fire may be limited by the amount of oxygen that can be provided (a ventilation-controlled fire).

Smoke is the general term for the solid and gaseous products of the combustion in the rising plume of heated air. Smoke contains both burnt and unburned gases, which are produced during the process of fire. These gases are extremely toxic; almost all the deaths in fire situations are caused by smoke. The designer of the building must control the smoke ventilation and prepare facilities that can help people survive. The smoke produced forms a layer of hot gas below the ceiling and heats the walls and ceiling. In this process, the temperature can rise to 1200°C.

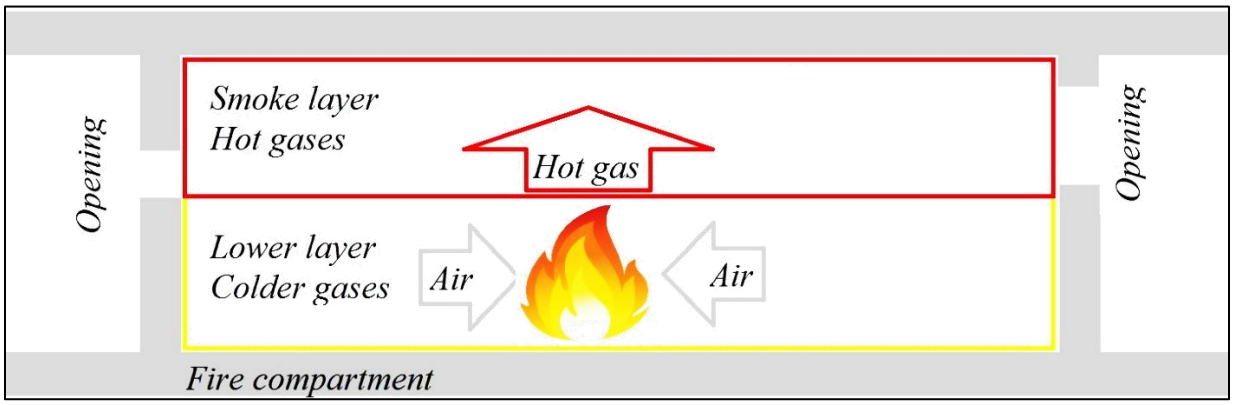

Figure 2-1: Fire development for localized fires in a fire compartment

Fire resistance requirements should, however, be based on all parameters influencing the growth of the fire and its development, such as fire risk and the probability of fire occurrence, the ventilation conditions, the fire compartment and its properties, the importance of the structure or members, evacuation conditions, safety of the rescue teams, fire spread to other buildings, and the active firefighting measures. The fire curve is the variation of temperature in a fire compartment as a function of time. Figure 2-2 shows a comparison between natural fire curves based on tests and the standard fire curve. The fire growth curve (experimental curve), shown in Figure 2-2, can be divided into five regions as follows:

1. Ignition, which is the start of the fire;
2. The growing phase, called pre-flashover. In this step, the fire is localized, and depending on the fire compartment, can develop or can demolish;
3. The flashover, which represents the sudden and short-time development of the fire in the whole compartment;
4. The post-flashover fire, which corresponds to a fully developed fire in the whole compartment. The duration and gas temperature depend on compartment and ventilation;
5. The cooling phase: In this phase, all combustible material in the fire compartment will burn.

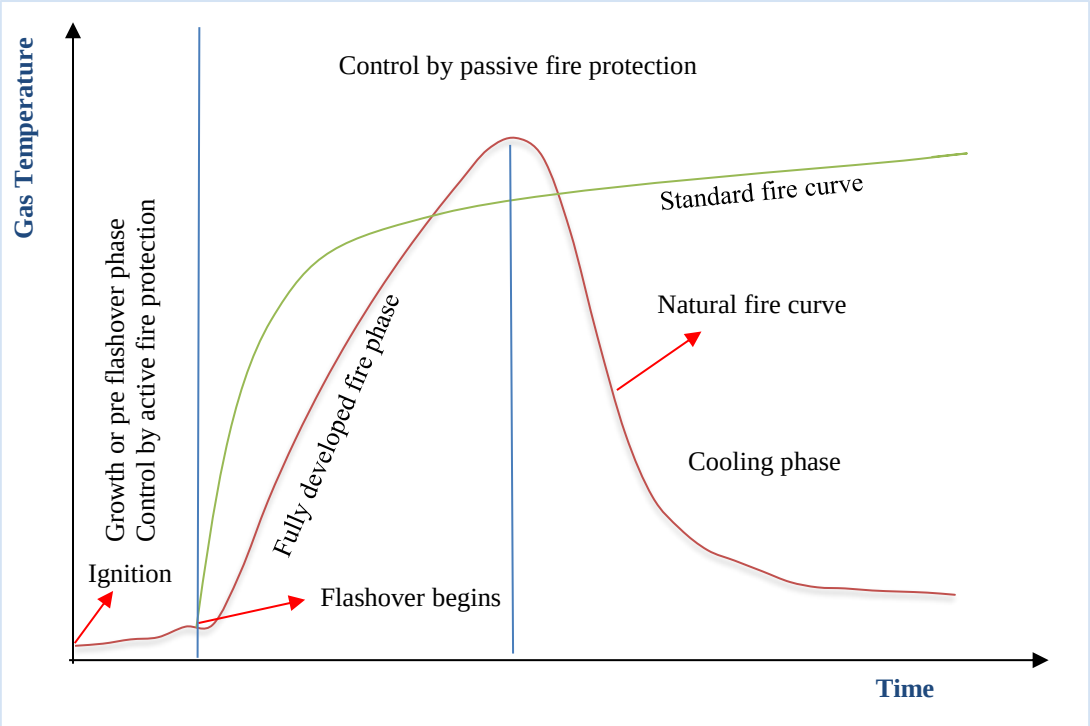

Figure 2-2 Phases of fire for natural fires [20]

2.3 Safety of structures

A performance-based approach to analyse the structures in case of fire, which takes account of the real fire characteristics and of active firefighting measures, has been developed by scientists and engineers. This approach, named Global Fire Safety concepts, consists of the following steps:

- Based on the building characteristics relevant to fire growth, the fire scenario, fire load, pyrolysis rate, compartment type, and ventilation conditions will be determined
- The risk of a fire scenario will be calculated by considering the size of the fire compartment, the occupancy, and the influence of active firefighting measures. The risk analysis is based on the existing statistical data of real fires and on probabilistic procedures. To analyse the risk of a fire scenario, a building life, and a target failure probability will be determined (55 years) [20]. Three levels of probabilistic analysis are defined: a full probabilistic approach (Level 0) and two semi-probabilistic approaches (Levels 1 and 2). Level 0 requires establishing the limit state function and, hence, the mathematical expression of the probability of the physically relevant failure in the fire situation. In Level 0, the characteristic fire load is considered when establishing the limit state function and the danger of fire. Level 1 and Level 2 are based on the procedure for structural design at the ambient temperature, which defines a design fire load. The design

fire load will be used to determine the temperature distribution in the fire compartment [20].
- Establishing the design value for the main parameters—for example, the design fire load.
- Determining the design fire (temperature) curve as a function of the design fire load and calculating the temperature distribution in the fire compartment and structural members.
- Calculating the global structural response under combination of static and thermal loads (accidental fire combinations).
- Deducing the design fire resistance time.
- Verifying the safety of the structure by comparing the design fire resistance time with the required time based on the resistance class of a structure.

The fire resistance class of a structure stands for the duration for which a structure retains its function in accordance with standards. The European standard EN 13501 Part 2 [21] introduces the fire resistance classes. The classification in accordance with the resistance duration of the structure (30, 60, 90, 120, and 180 minutes). The resistance criteria of the members are abbreviated in detail with the following letters:

- R- Structural resistance of the structure
- E- Integrity separating function
- I- Thermal insulating separation function

The abovementioned criteria can be implemented individually or in combination. For example, R30 means a structural resistance for a maximum of 30 minutes.

Fire loads can be modelled using several possibilities as follow [14]:

- nominal fire curves;
- parametric fire curves;
- one-zone models assuming a uniform, time-dependent temperature distribution in the compartment;
- two-zone models assuming an upper layer with time-dependent thickness and with time-dependent uniform temperature, as well as a lower layer with a time-dependent uniform and lower temperature;
- Computational Fluid Dynamic models giving the temperature evolution in the compartment in a completely time-dependent and space-dependent manner.

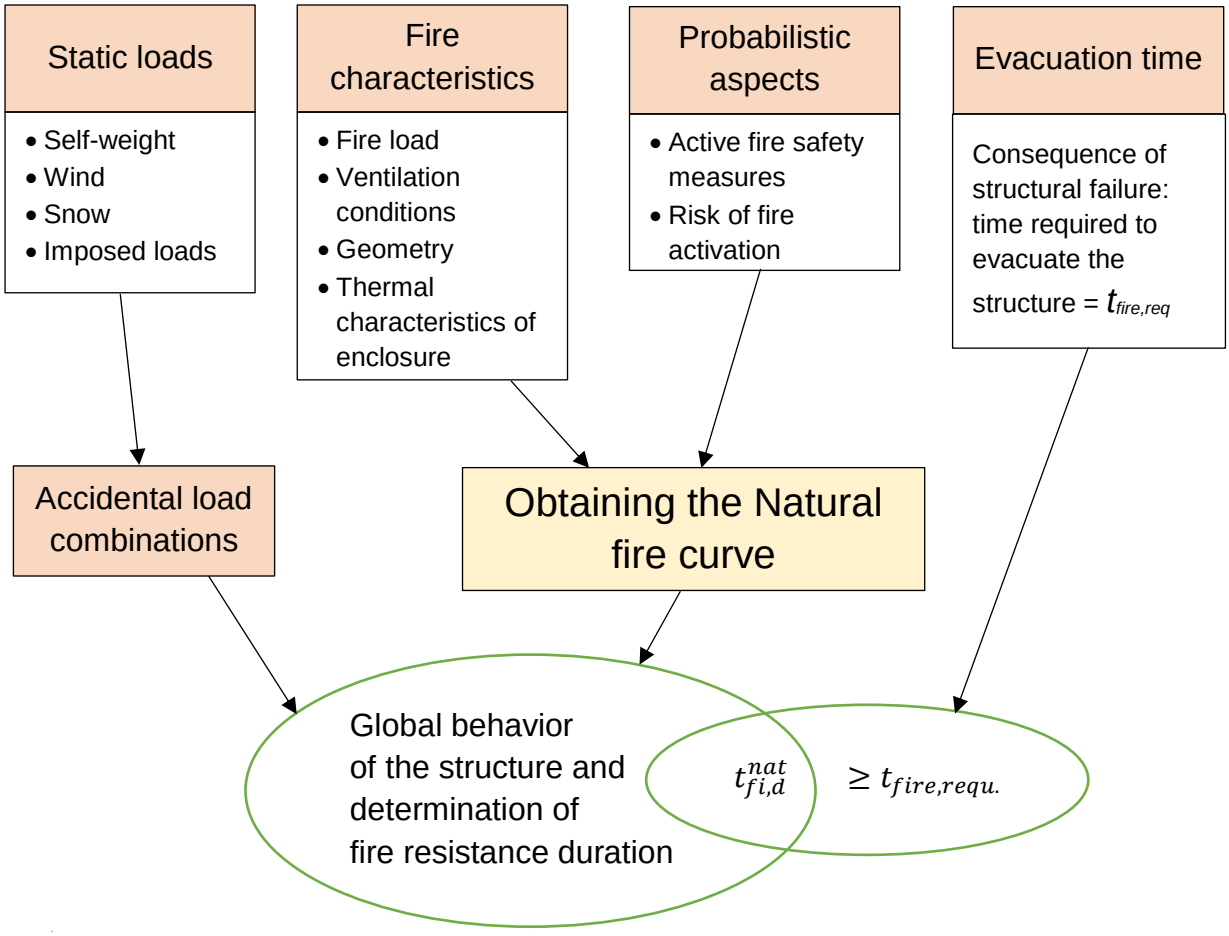

Figure 2-3: Global fire safety concept [20]

2.4 Natural fire curves

Natural fire models are the growth curve of real fires or fires expected to occur in a compartment. The size of the buildings, openings, the amount of fire load, and the ventilation conditions can change the heat flux and, so, the properties of natural fire curves. The natural curves, in comparison with the nominal curves, are more realistic, and will be calculated for each fire compartment and fire scenario. In Germany, the natural fire curve may be calculated in accordance with the National Annexure of EN 1991-1-2 [18].

When natural curves are of interest, the structural designer will perform the following steps to determine the curves:

- Determine the load density;
- Determine the fire activation risk for the compartment;
- Calculate the design fire load density;
- Obtain the surface factors for hot surfaces of the compartment, including walls, floors, and openings;
- Calculate the opening factor;
- Obtain the limiting time and maximum temperature for the compartment;

- Determine the fire curve, including the cooling phase.

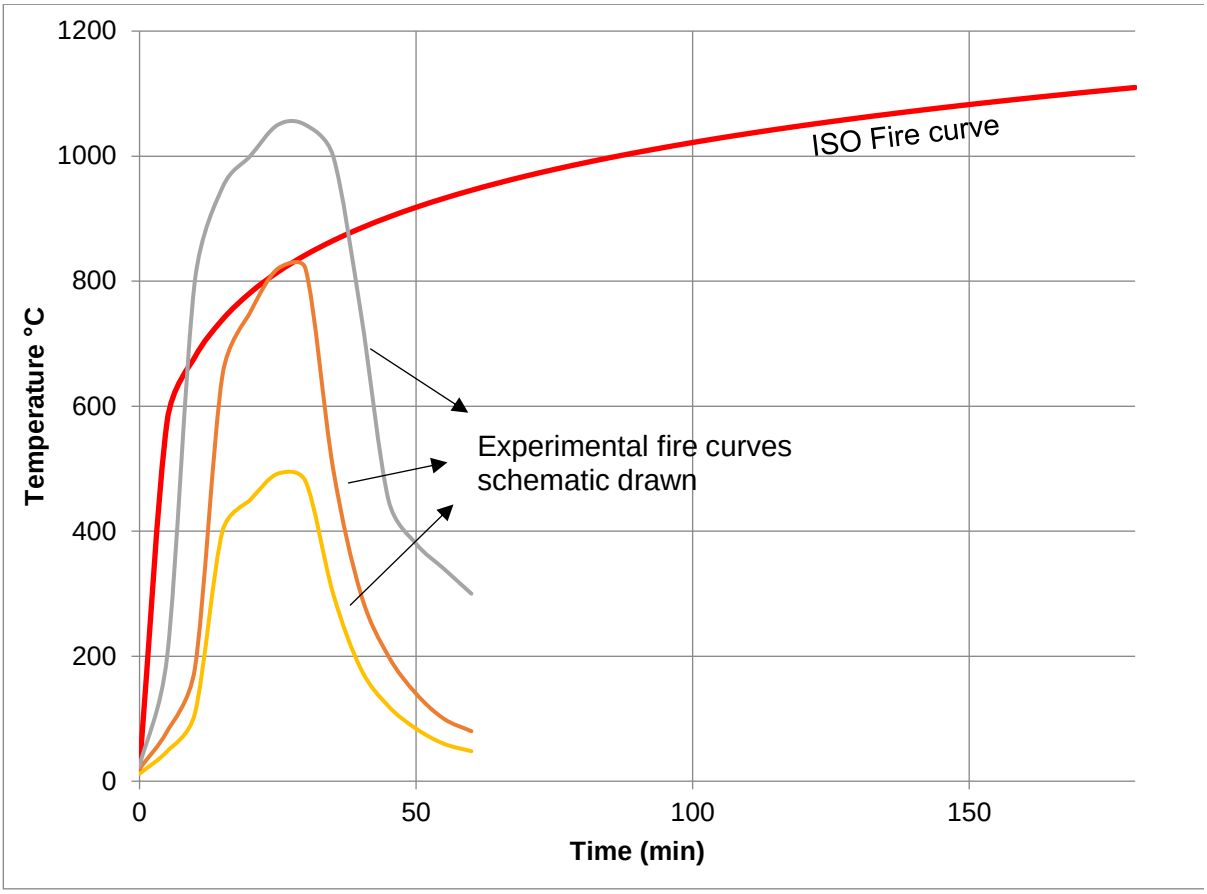

Figure 2-4 Natural fire curves and ISO fire curve

2.5 Nominal fire curves

The temperature–time curves are gas temperatures in the environment of member surfaces as a function of time. Obtaining the nominal fire curves is the simplest way to model the fire. These do not depend on ventilation and boundary conditions of the fire compartment. The nominal fire curves are illustrated in Figure 2-5. In EN 1991-1-2, three temperature–time nominal curves are defined:

1. *Standard temperature–time curve (ISO834):* Nominal curve defined in prEN 13501-2 for representing a model of a fully developed fire in a compartment.

$$T_{gas} = 20 + 345log_{10}(8t + 1), \alpha_c = 25\frac{W}{m^2K} \quad (2.1)$$

2. *External fire curve:* Nominal temperature–time curve intended for the outside of separating external walls which can be exposed to fire from different parts of the façade, i.e. directly from the inside of the respective fire compartment or from a compartment situated below or adjacent to the respective external wall.

$$T_{gas} = 660(1 - 0.687e^{-0.32t} - 0.313e^{-3.8t}) + 20, \alpha_c = 25\frac{W}{m^2K} \quad (2.2)$$

3. *Hydrocarbon curve:* Nominal temperature–time curve for representing the effects of a hydrocarbon-type fire.

$$T_{gas} = 1080(1 - 0.325e^{-0.167t} - 0.675e^{-2.5t}) + 20, \quad (2.3)$$

$$\alpha_c = 50\frac{W}{m^2K}$$

With a fire model, the temperature analysis of the structural members will be made for the full duration of the fire, which may include the cooling phase. The mechanical analysis will be performed for the same duration as the temperature analysis. It has to be understood that these nominal fires correspond to a fully developed fire, which means that the corresponding compartment is fully engulfed in fire. Figure 2-5 compares the nominal fire curves obtained from Equations 2.1, 2.2, and 2.3. It can be noticed that the nominal fire curves do not cover the cooling phase.

For the assumption of liquid fuel burning, the proposal is to use the hydrocarbon curve in the fire safety design. The rest of the nominal curves can be used for any other building fires [22], [14]. The natural fire curves are obtained in laboratories. The maximum temperature, heating rate, intensity of fire, and fire duration are differences between nominal and natural fire curves. The results of the structural and thermal analyses when using nominal and natural curves obviously show the difference in the curves. Structures designed using nominal curves might fail under natural fires.

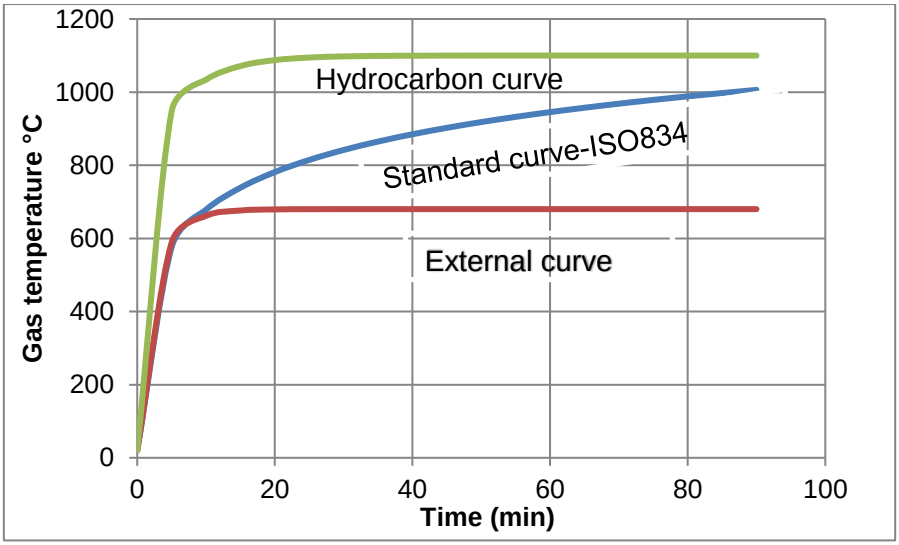

Figure 2-5 Nominal temperature–time curves in accordance with EN 1991-1-2 [18]

2.6 Parametric fire curves

The parametric fire curves enable us to describe the fire by taking into account the most important physical aspects of the fire [20]. The parametric curves

describe the fire as a function of time under the influence of the following aspects:

- The geometry of the fire compartment;
- The fire load or fuel present in the compartment;
- The openings and ventilation of the compartment;
- The material properties of the surrounding elements of the compartment.

The parametric curves assume uniform temperature in the compartment, which limits their applications to post-flashover (fully developed fire). Annexure A of EN1991-1-2 represents a method to calculate the parametric curves under the following conditions:

- The floor area of the compartments will be up to 500 m^2
- The maximum height of the compartment will be 4 m
- The upper boundary of the compartment is without openings
- Parameter b (thermal inertia) will be $100 < b < 2200 \frac{J}{m^2 s^{0.5} K}$
- The parametric curve is for cellulosic fire loads

The parametric curves assume that the fire load of the compartment is completely burnt out. The temperature curve in the heating phase can be calculated as follows:

$$T_{gas} = 20 + 1325(1 - 0.324e^{-0,2t*} - 0.204e^{-1,7t*} - 0.472e^{-19t*}) \qquad (2.4)$$

T_{gas} is the uniform gas temperature in the fire compartment

$$t^* = t.\frac{\left(\frac{O}{b}\right)^2}{\left(\frac{0.04}{1160}\right)^2}$$

$b = \sqrt{\rho c \lambda}$ $\quad 400 < b\ (J\ /\ m^2 S^{0.5} K)\ < 2200$

λ Thermal conductivity at ambient temperature

c Specific heat at ambient temperature

ρ Density of the material at ambient temperature

t Time

$O = \frac{A_v \sqrt{h_{eq}}}{A_t}$ Opening factor

A_v	Total area of the openings on walls
h_{eq}	Weighted average of the windows height
A_t	Total area of the compartment, including walls, ceiling, and floor

If the surfaces of the compartment consist of a layered material:

$$b = \frac{\sqrt{\sum s_i c_i \lambda_i}}{\sqrt{\sum \frac{s_i c_i \lambda_i}{b_i^2}}}, b_i = \sqrt{\rho_i c_i \lambda_i} \tag{2.5}$$

s_i	Thickness of the layer i
ρ_i	Density
c_i	Specific heat for layer i of the boundary
λ_i	Thermal conductivity

If different b factors of walls, ceiling, and floor are considered, the following equation can be applied:

$$b = \frac{\sum b_i A_i}{A_t - A_v} \tag{2.6}$$

A_i	Area of enclosure i

The design value of the fire load density is assumed to be $50 \leq q_{t,d} \leq 1000$. The maximum temperature in fire compartment can be calculated using the design fire load density:

$$t^*_{max} = 0{,}13 \times 10^{-3} q_{t,d} \frac{\left(\frac{O}{b}\right)^2}{\left(\frac{0.04}{1160}\right)^2} / O \tag{2.7}$$

A_i	Area of enclosure i

The temperature–time curve in the cooling phase is:

$$T_g = T_{max} - 625(t^* - t^*_{max}), \quad t^*_{max} \leq 0.5 \tag{2.8}$$

$$T_g = T_{max} - 250(3 - t^*_{max})(t^* - t^*_{max}), 0.5 < t^*_{max} \leq 0.5 \tag{2.9}$$

$$T_g = T_{max} - 250(t^* - t^*_{max}), \qquad t^*_{max} > 2 \tag{2.10}$$

In Annexure C, the determination of the parametric fire curve of an assumed fire compartment is described in detail. In this research, the parametric fire curve will be applied to obtain the temperature in the fire compartment. It will be assumed that the boundaries of the compartment consist of one layer of material. Figure 2-6 compares the ISO 834 fire curve with the parametric fire curve of a compartment by assuming the following values:

$b = \sqrt{\rho c \lambda} = 1750$ $\quad 400 < b\ (J\ /\ m^2 S^{0.5} K)\ < 2200$

$O = \dfrac{A_v \sqrt{h_{eq}}}{A_t} = 0.06$ Opening factor

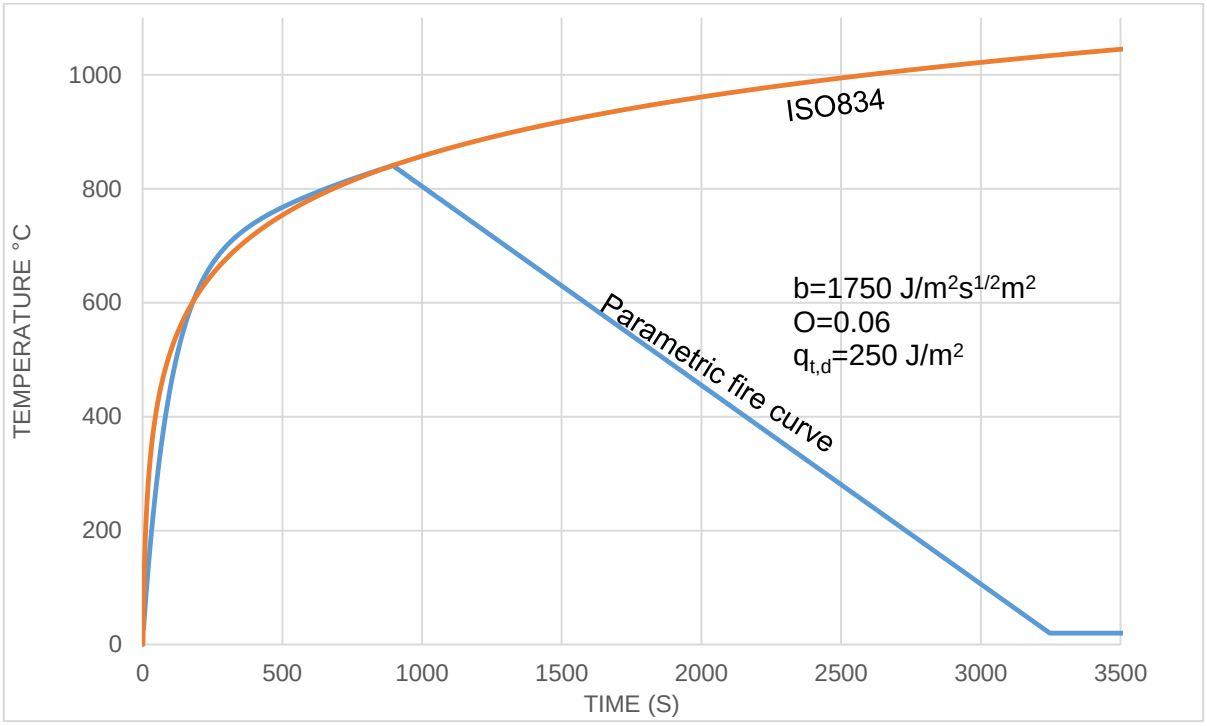

Figure 2-6: Parametric fire curve in accordance with Annexure A of EN 1991-1-2 [18] and ISO834 curve

2.7 Zone models

According to EN 1991-1-2—Annexure D [18], the development process of the fire in a compartment can be modelled by applying the zone models. Zone models divide the fire compartment into various consistent zones. They are based on the assumption of uniform temperature, gas density, and internal energy in each zone. Two fire zone models have been developed by scientists:

- One-zone model
- Two-zone model

These models are based on the conservation of mass and energy in the fire compartment. The zone models consider the rate of heat release, the fire plume, the smoke movement, the mass flow, and the gas temperature. The zone models can give a more accurate temperature curve than a parametric fire curve.

Two zone models are suitable to model the pre-flashover phase of a fire (localized fire) and the application of the one-zone model is for modelling a fully engulfed fire. The one-zone model assumes a uniform temperature distribution in the fire compartment and is suitable to model a post-flashover situation.

A two-zone situation will be developed when there is an upper zone filled with high temperature smoke and a lower layer (zone) with low temperature in the fire compartment. If the lower zone remains sufficiently high, but, above all, if the upper zone does not have a temperature above 500°C, no flashover takes place, and the natural fire may remain localized in the compartment [20]. The following parameters will be provided so as to enable one to apply a zone model:

- Geometrical data of the fire compartment, including the dimensions of the compartment, the openings, and the partitions;
- Material properties of the boundaries of the compartment;
- Fire data like combustion heat of fuel and pyrolysis rate.

In a two-zone model, the mass balance and the energy balance for each zone of the compartment will be provided, and exchanges between the two layers are considered. The result of the simulation can be the gas temperature for each layer, information on wall temperatures, and mass or heat loss through the openings. More details about zone models can be found in EN 1991-1-2 Annexure D and in Handbook 5—Design of Buildings for the fire situation [20].

2.8 Fire load density

The total heat energy released from all combustible materials in a fire compartment is defined as the fire load. The amount of energy generated by burning will heat the fire compartment. It will be released through openings. The characteristic fire load can be calculated by the method suggested in EN1991 Part 2.2, using the following equation:

$$Q_{fi,k} = \sum Q_{fi,k,i} = \sum M_{k,i} \times H_{u,i} \times m_i \times \Psi_i \qquad (2.11)$$

$0 \leq m_i \leq 1$ is the combustion factor, which depends on the combustion material and position of material in fire compartment.

$M_{k,i}$ is the amount of combustible material.

$H_{u,i}$ is the net calorific value, which depends on the humidity (u) of material and the net dry calorific of material, and can be obtained from the following equation:

$$H_u = H_{u,0} \times (1 - 0.01u) - 0.025u$$

$H_{u,0}$ The net dry calorific of the material, which can be obtained from ISO 1716.

Ψ_i Factor for assessing protected loads

The fire load divided with the reference area defines the fire load density:

$$q_{f,k} = \frac{Q_{fi,k}}{A_{area\ of\ the\ floor}} \tag{2.12}$$

The design value of the load density is defined as:

$$q_{f,d} = q_{f,k} \times m \times \gamma_{q1} \times \gamma_{q2} \times \gamma_n \tag{2.13}$$

γ_{q1} Factor to consider the fire activation risk caused by the compartment size.

γ_{q2} Atrial factor, taking into account the fire activation risk caused by the type of occupancy.

γ_n The differentiation factor, to consider the different active firefighting measures.

Partial factors γ_{q1} and γ_{q2} can be obtained from Table E.1 of EN1991-1-2.

3 Structural material at elevated temperatures

3.1 Introduction

The objective of this study is to present a simplified method to analyse structures under fire loading. This leads us to consider the thermal and mechanical properties of structural materials that depend on temperature. There are different research sources and regulations to obtain the material properties. First, the mechanical properties of structural steel—based on EN 1993-1-2 [23]—are presented, and then the properties of concrete are described, according to some sources. The valid sources that can be used for concrete to perform structural analyses may be ACI [24] and EN 1992-1-2 [2]. The values based on the second code will be used to develop the computer code. Thermal properties of steel reinforcement, concrete, and structural steel—as a function of temperature based on Eurocodes—are presented in Annexure B.

3.2 Stress–Strain curve at elevated temperatures

Imagine a test specimen in a laboratory that has to be investigated and the stress–strain curve has to be drawn at elevated temperatures for it. The stress–strain curve at elevated temperatures depends on the thermal load and can be drawn in two cases:

1- Transient thermal load: The specimen is under non-thermal loads. The thermal loads are applied afterwards. In this case, we can draw the

temperature–strain curves; the heating rate determines the shape of the curve. Figure 3-1 shows the temperature–strain curve [25].
It is important to note that the modulus of elasticity cannot be obtained from temperature curves and, in this case, is variable.

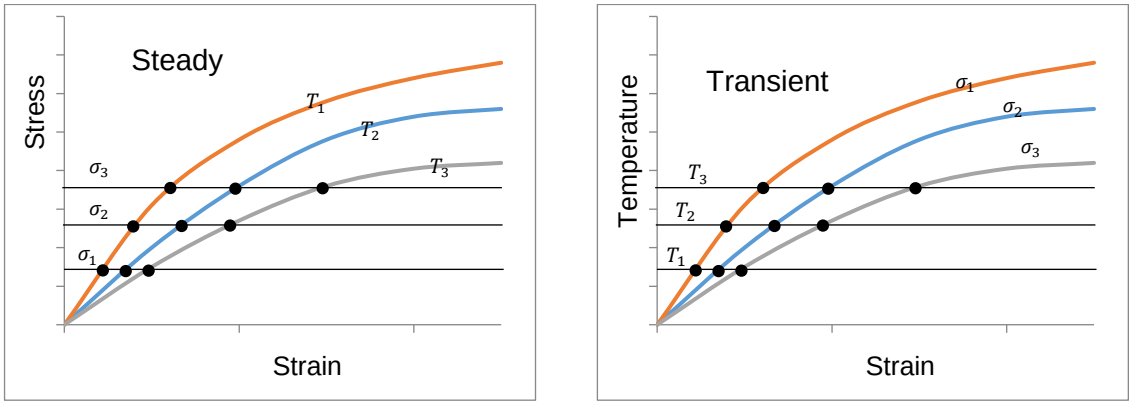

Figure 3-1: Stress–strain curve and temperature–strain curve in steady and transient analysis [25]

2- Steady state thermal load: The specimen is heated to temperature *T*, and then non-thermal loads are applied. The stress–strain curve of the specimen for each load case may be different. In this case, we can draw the stress–strain curves and the loading rate determines the form of the curve. The modulus of elasticity when a steady state thermal load is applied is constant.

The fire loading process in structural design is a transient process. The modulus of elasticity varies as the temperature increases.

3.3 Structural Steel

At present, the understanding of the behaviour of steel at elevated temperatures is more advanced than it is in relation to concrete. Quite a lot of research has been conducted on the mechanical properties of steel and concrete at elevated temperatures. The mechanical properties of structural materials in Eurocodes will be the reference values that will be used here. According to EN 1993-1-2 [23] Sections 2–3, the design values of the mechanical properties for steel are:

$$X_{d,fi} = \frac{k_T X_k}{\gamma_{M,fi}} \text{ , } \gamma_{M,fi} = 1.0 \tag{3.1}$$

$X_{d,fi}$ is the design value of the material property, X_k is the characteristic value of the material property at the normal temperature, and k_θ is the reduction factor at the elevated temperature. According to Figure 3-2, the stress–strain curve of steel at elevated temperatures can be obtained as follows:

$$\varepsilon_{p,T} = \frac{f_{p,T}}{E_{a,T}} \; (E_{a,T} = E_T \; in \; table \; 2.1) \tag{3.2}$$

$$if\ \varepsilon \le \varepsilon_{p,T} \rightarrow \sigma = \varepsilon\, E_{a,T} \tag{3.3}$$

$$if\ \varepsilon_{p,T} \le \varepsilon \le \varepsilon_{y,T} \rightarrow \sigma = f_{p,T} - c + \frac{b}{a} * \left[a^2 - \left(\varepsilon_{y,T} - \varepsilon\right)\right]^{0.5} \tag{3.4}$$

$$if\ \varepsilon_{y,T} \le \varepsilon \le \varepsilon_{t,T} \rightarrow \sigma = f_{y,T} \tag{3.5}$$

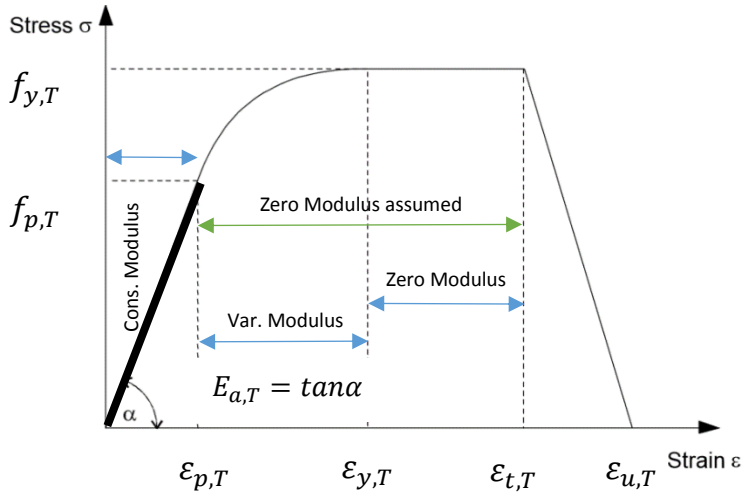

Figure 3-2: Stress–strain curve for steel at elevated temperatures, based on EN 1993-1-2, $\varepsilon_{y,T} = 0.02$

As shown in Figure 3-2, the modulus of elasticity is the tangent of the linear part of the stress–strain curve. Table 3.1 gives the values of the modulus of elasticity and yield strength of the structural carbon steel in accordance with Eurocodes. It should be noted that the variation in the modulus of elasticity for all types of steel is the same. This means that the stiffness of steel does not depend on its strength class. Here, we will assume zero stiffness for steel when the strain is bigger than $\varepsilon_{p,T}$. In this research, strain dependency of the modulus of elasticity will not be modelled. In other words,

$$if\ \varepsilon \le \varepsilon_{p,T} \rightarrow E_{a,T} = k_{E,T}\, E \tag{3.6}$$

$$if\ \varepsilon_{p,T} \le \varepsilon \le \varepsilon_{y,T} \rightarrow E = 0 \tag{3.7}$$

The upper limit of strain in the steel members—to be in the linear range of the stress–strain curve—can be seen in Table 3.1. The upper limit of linear strain for steel at elevated temperatures is smaller than the same value for lower temperatures. At elevated temperatures, the modulus of elasticity of steel depends on temperature, strain, and stress.

For steel structures facing elevated temperatures, the method of the present study that has been developed would not give valid results, since the strain dependency of the modulus of elasticity is important. Figure 3-3 shows the modulus of elasticity of steel as a function of temperature. These values do not depend on the steel strength class and are valid only when the strain is limited

to values of $\varepsilon_{p,T}$ in Table 3.1. Figure 3-4 illustrates the yield strength of different structural steels as a function of temperature.

Table 3.1: Mechanical properties of structural carbon steel [2], [17]

Temperature (°C)	$k_{E,T}$	$k_{y,T}$	$E_T\ (\frac{kg}{cm^2})$	$f_{y,T}\left(\frac{kg}{cm^2}\right)$ S235	$f_{y,T}\left(\frac{kg}{cm^2}\right)$ S275	$f_{y,T}\left(\frac{kg}{cm^2}\right)$ S355	$f_{y,T}\left(\frac{kg}{cm^2}\right)$ S450	$\varepsilon_{p,\theta}$
20	1	1	2141404	2396	2804	3620	4487	0.0011
100	1	1	2141404	2396	2804	3620	4487	0.0011
200	0.9	1	1927264	2396	2804	3620	4487	0.0010
300	0.8	1	1713123	2396	2804	3620	4487	0.0009
400	0.7	1	1498983	2396	2804	3620	4487	0.0007
500	0.6	0.78	1284842	1868.88	2187.12	2823.6	3499.86	0.0007
600	0.31	0.47	663835.2	1126.12	1317.88	1701.4	2108.89	0.0007
700	0.13	0.23	278382.5	551.08	644.92	832.6	1032.01	0.0007
800	0.09	0.11	192726.4	263.56	308.44	398.2	493.57	0.0006
900	0.0675	0.06	144544.8	143.76	168.24	217.2	269.22	0.0006
1000	0.045	0.04	96363.18	95.84	112.16	144.8	179.48	0.0006
1100	0.0225	0.02	48181.59	47.92	56.08	72.4	89.74	0.0006
1200	0	0	0	0	0	0	0	0

3.4 Reinforcement

It has been assumed that the reinforcement—designed for use in cross-sections—is hot-rolled. The cold-formed steel does not experience elevated temperatures in its production process. The mechanical properties of cold-formed cross-sections are more sensible to high temperatures and are not of interest here. The variation in the modulus of elasticity for hot-rolled reinforcements can be obtained from Table 3.1 and Figure 3-2. If the cold-formed reinforcement is considered, the reduction factors are not the same, as shown in Table 3.1.

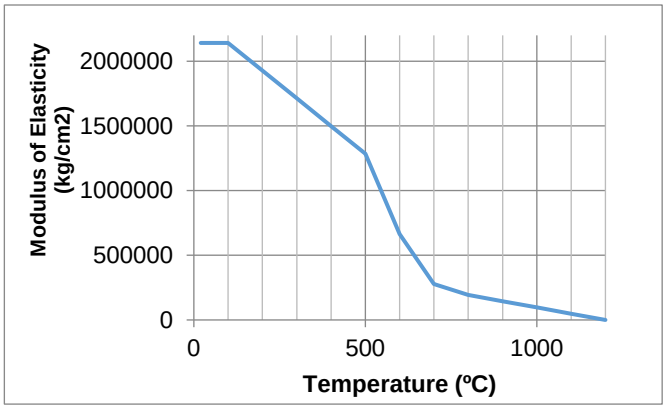

Figure 3-3: Variation in the modulus of elasticity of steel with respect to temperature

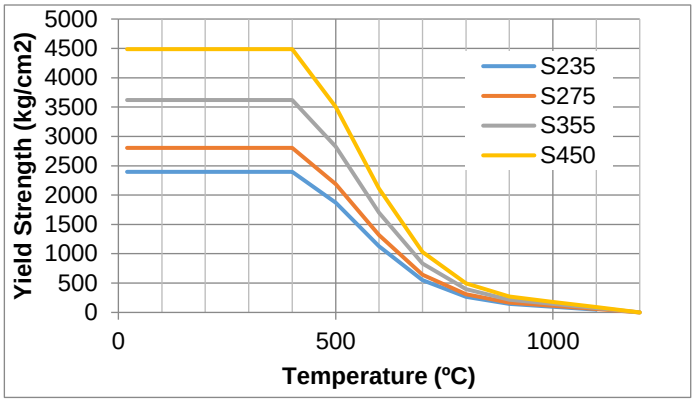

Figure 3-4: Variation in the yield strength of carbon steel with respect to temperature

3.5 Concrete

When the resistance of framed structures against fire is of interest to designers, concrete will be considered a suitable material. Concrete has nonlinear material properties at room temperature and its mechanical properties depend on time and load. Concrete is a composite material and its mechanical properties are affected by reinforcement, cement, sand, and gravel. The mechanical properties of concrete can vary over time (creep). Generally, mathematical models of concrete cannot consider all aspects, such as creep, cohesion between gravel and cement, reinforcement, and cohesion between cement and reinforcement. The most highly developed FEM software packages like ANSYS are not able to consider the nonlinear behaviour of composite structural materials like concrete at elevated temperatures. The mathematization of all aspects of nonlinear concrete material is still an interesting subject for many researchers. Till the mid-1970s, the knowledge of concrete at elevated temperatures was limited to results based on elastic theory [26]. The fundamental phenomenon that could explain the mechanical properties of concrete exposed to fire was discovered in the 1970s in Sweden [27], [28] and Germany [29]. Based on these researches, an unknown strain component—named transient strain—was identified. Transient strain was defined as a non-recoverable, time-independent, and dominating compressive strain, which develops during the first heating under simultaneous load.

Total strain of concrete at elevated temperatures:

According to EN 1992-1-2 Part 4.3.3, the total strain of concrete can be calculated as follows:

$$\varepsilon = \varepsilon_{th} + \varepsilon_{\sigma} + \varepsilon_{creep} + \varepsilon_{tr} \quad (3.8)$$

ε_{th} is the thermal strain, ε_{σ} is the instantaneous stress-dependent strain, ε_{creep} is the creep strain, and ε_{tr} is the transient state strain.

Thermal strain is caused by thermal elongations, stress-dependent strain depends on the loads, creep strain depends on the time and mechanical properties of concrete, and transient strain results from thermal deformations and variations in modulus of elasticity. Creep and transient strain are not recoverable. In this research, we do not consider creep strain, since it depends on the loads and time, and can be calculated by experimental methods. Because the stress–strain curve of concrete is nonlinear, the modulus of elasticity is determined either by the initial tangent modulus, secant modulus, or tangent modulus. Temperature can significantly affect the modulus values, causing a reduction as a result of the breakage of bonds. Drying—which increases with temperature—reduces the apparent modulus value to produce the bond rupture; it has been observed that fast drying results in a faster decrease in the modulus of elasticity than slow drying. Comparing the modulus of elasticity of temperature-loaded and temperature-unloaded specimens to those obtained from specimens tested when temperature-loaded, the retained modulus at temperature-loaded tends to be higher than that obtained from specimens permitted to cool to room temperature prior to testing. In other words, modulus of elasticity at temperatures is higher than residual modulus [30]. The decrease in elastic modulus with exposure to elevated temperature is primarily caused by the breakage of bonds in the cement paste microstructure. The following factors can affect the modulus of elasticity of hot concrete [30]: 1- Water–cement ratio; 2- Method for determination of modulus; 3- Testing hot or cold; 4- Presence of pre-load; 5- Rate of heating and cooling; 5- Rate of loading; 6- Different aggregate materials. If concrete experiences elevated temperatures, it does not recover its initial mechanical properties when temperature-unloaded. Therefore, the cooling process of concrete must be considered when the effective stiffness of the cross-section is of interest. The recommended value for the modulus of elasticity of concrete, according to [30], is:

- *Secant modulus:*

$$E_C^T = (1 - 0.0015T)E_C\,, \qquad 20 < T \leq 300 \quad (3.9)$$

$$E_C^T = (0.87 - 0.00084T)E_C\,, \qquad 300 < T \leq 700 \quad (3.10)$$

$$E_C^T = 0.28E_C\,, \qquad 700 < T \quad (3.11)$$

- *Initial tangent modulus:*

$$E_C^T = E_C\,, \qquad 20 < T \leq 60 \quad (3.12)$$

$$E_C^T = \frac{(800 - T)E_0}{740}, \qquad 60 < T \leq 800 \tag{3.13}$$

Bicanic [31] has used the following relationship to calculate the normalized modulus of elasticity in unstressed conditions:

$$\frac{E_T}{E_0} = \left(1 - 0.1\left(\frac{T - 20}{100}\right)\right)^2, \quad 0 \leq \left(\frac{T - 20}{100}\right) \leq 10 \tag{3.14}$$

He also suggested the following formula in the case of stressed conditions:

$$\frac{E_T}{E_0} = 1 - 0.1\left(\frac{T - 20}{100}\right), \quad 0 \leq \left(\frac{T - 20}{100}\right) \leq 10 \tag{3.15}$$

Cheng, Kodur, and Wang [32] performed some tests on the mechanical properties of high-strength concrete at elevated temperatures. The variation in the modulus of elasticity, based on their tests, is illustrated in Figure 3-5.

Figure 3-6 shows the variation in the modulus of elasticity based on ACI216 [24]. The maximum temperature is 1200°F (650ºC) with a reduction factor of about 0.3. ACI 216R also has some rules for Poisson's ratio and shear modulus. The variation in Poisson's ratio is not of interest here; the shear modulus can be considered a function of the modulus of elasticity.

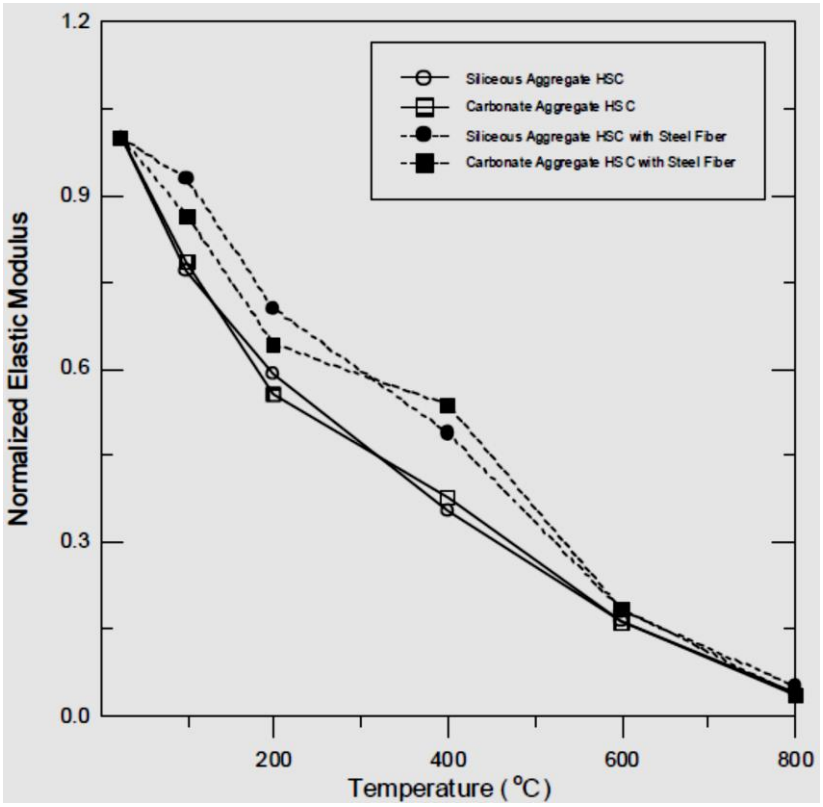

Figure 3-5: Variation in modulus of elasticity for high-strength concrete [32]

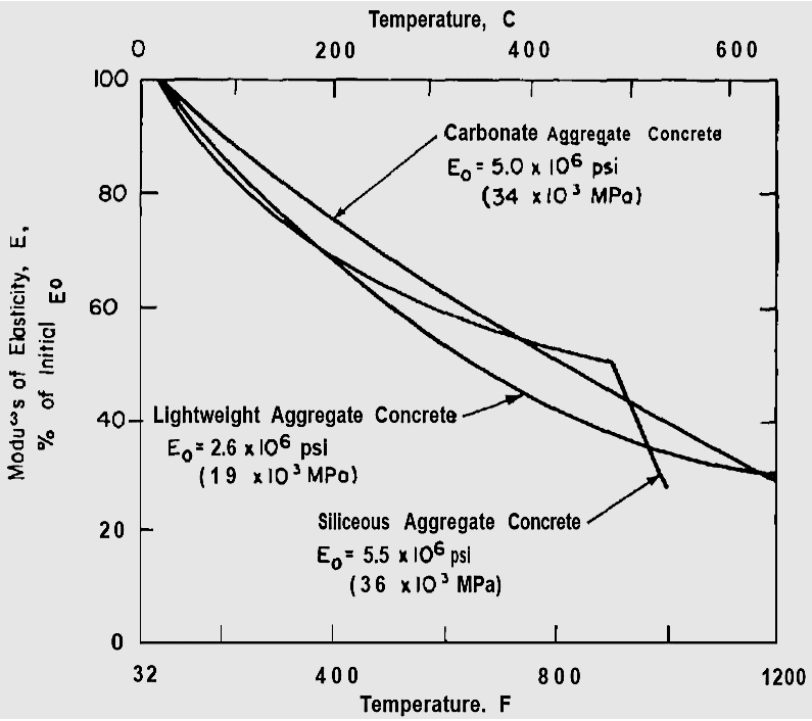

Figure 3-6: Variation in modulus of elasticity based on ACI216 [24]

Hertz [33] stated that the reduction in the short-time modulus of elasticity is the square of the reduction of the compressive strength, as follows:

$$E_{c,T} = E_{C,20} \times k_{C,T}^2 \tag{3.16}$$

Bergmann [17] used the secant modulus defined in EN 1992-1-2 to calculate the effective stiffness of concrete in composite columns. The secant modulus of elasticity, based on Eurocode, is illustrated in Figure 3-7, and can be calculated as follows:

$$E_{c,sek,20} = \frac{f_c}{\varepsilon_{cu,20°}} = \frac{f_c}{0.0025} = 400 f_c \tag{3.17}$$

$$E_{c,sek,T} = \frac{f_{c,T}}{\varepsilon_{cu,T}} = \frac{k_{c,T} f_c}{\frac{\varepsilon_{cu,T}}{\varepsilon_{cu,20°}} \varepsilon_{cu,20°}} = \frac{k_{c,T}}{\frac{\varepsilon_{cu,T}}{\varepsilon_{cu,20°}}} \times \frac{f_c}{\varepsilon_{cu,20°}} \tag{3.18}$$

$$= k_{c,E,T} \times E_{c,sek,0}$$

$E_{c,sek,T}$ is the modulus of elasticity at temperature T, $E_{c,sek,20}$ is the reference value of modulus of elasticity at 20℃, $f_{c,T}$ is the compressive strength of concrete at temperature T, and $\varepsilon_{cu,T}$ is the plastic strain of concrete at temperature T. According to EN 1992-1-2, the mechanical properties of concrete should be extracted from the stress–strain curves defined in EN 1992-1-2. These curves are as follows:

$$f = \frac{3\varepsilon f_{c,T}}{\varepsilon_{c1,T}\left(2 + \left(\frac{\varepsilon}{\varepsilon_{c1,T}}\right)^3\right)} \quad , \quad \varepsilon < \varepsilon_{c1,T} \tag{3.19}$$

$$E_{c,T} = 1.5\frac{f_{c,T}}{\varepsilon_{c1,T}} \rightarrow \frac{E_{c,T}}{E_{c,20℃}} = \frac{\frac{f_c k_{c,T}}{\varepsilon_{c1,T}}}{\frac{f_c}{\varepsilon_{c1,20}}} \tag{3.20}$$

Figure 3-7 illustrates the reference stress–strain curves based on EN 1992-1-2 in the case of warm design at 20℃. The secant modulus and tangent modulus at 20℃ can be obtained from these curves. Values of $\varepsilon_{c1,T}$ are given in EN 1992-1-2; see Table 3.2.

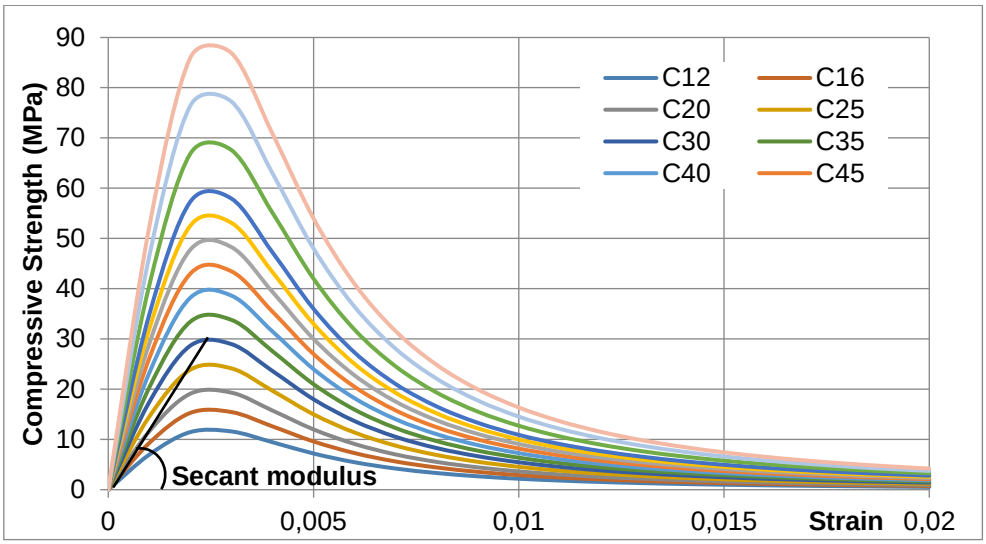

Figure 3-7: Reference stress–strain curves of concrete at room temperature, to be used in warm design; see Eq. 3.19 [2]

It should be noted that there is a significant difference between the reference value of the modulus of elasticity of concrete in warm and cold conditions. The modulus of elasticity of concrete in warm situations depends on the cooling process and cracks. In fact, the residual modulus of elasticity is not the same as the initial modulus if an elevated temperature is experienced. Table 3.3 shows the reference values of the secant modulus and tangent modulus of concrete in warm design and cold design.

The goal is to develop a simplified method to analyse the framed structures under fire loads. This simplified method is based on the strain independency of stiffness. Therefore, the stiffness of the structure or modulus of elasticity depends just on temperature. This assumption will not work for steel structures. In the current research, the variable stiffness of members has been modelled. For a strength class at each temperature, just one value for modulus is obtained, and applied to the developed code. Therefore, the non-linear part of the stress–

strain curve is not of interest. If the total strain in concrete, including thermal and residual strain, is more than the values of Table 3.2, the constant modulus of elasticity for concrete cannot be used. In other words, as long as the total strain at each temperature is between zero and the upper limit at each time step, the linear modulus of concrete—shown in Table 3.4—can be used. The reduction factors of the modulus of elasticity of concrete and the modulus of different concrete types can be seen in Tables 3.3 and 3.4 respectively. It should be mentioned that the reduction factors for concrete with siliceous aggregates are less than those with calcareous aggregates. The properties of concrete with siliceous aggregates will be used in this research. Figure 3-8 shows the normalized stress–strain curve of concrete at different temperatures. The normalized curve can be used to draw the stress–strain curve of different concrete strength classes.

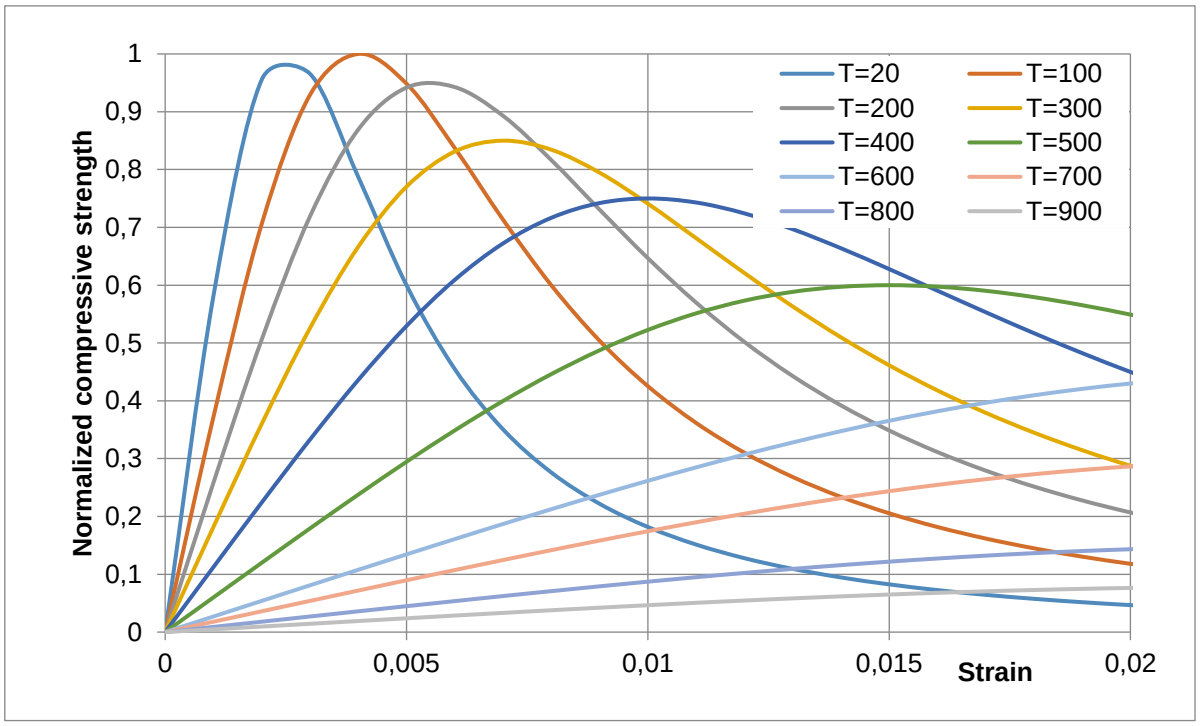

Figure 3-8: Normalized stress–strain curve for all types of concrete with calcareous aggregates, based on EN 1992-1-2

Table 3.2: Reduction factors for mechanical properties of concrete, according to EN 1992-1-2

Temperature °C	$\varepsilon_{c1,T}$	Calcareous aggregates		Siliceous aggregates	
		$k_{c,T}$	k_E	$k_{c,T}$	k_E
20	0.0025	1.000	1.000	1.000	1.000
100	0.004	1.000	0.625	1.000	0.625
200	0.0055	0.970	0.441	0.950	0.432
300	0.007	0.910	0.325	0.850	0.304
400	0.01	0.850	0.213	0.750	0.188
500	0.015	0.740	0.123	0.600	0.100
600	0.025	0.600	0.060	0.450	0.045
700	0.025	0.430	0.043	0.300	0.030
800	0.025	0.270	0.027	0.150	0.015
900	0.025	0.150	0.015	0.080	0.008
1000	0.025	0.060	0.006	0.040	0.004
1100	0.025	0.020	0.002	0.010	0.001
1200	0.025	0.000	0.000	0.000	0.000

Table 3.3: Reference values of concrete modulus of elasticity in warm and cold situations

Concrete Type	$f_{C\ MPa}$	$E_{cm,20℃\ GPa}$	$E_{tangent,fire,20\ GPa}$	$E_{secant,fire,20\ GPa}$
C12	12	27	7	4.8
C16	16	29	10	6.4
C20	20	30	12	8
C25	25	31	15	10
C30	30	33	18	12
C35	35	34	21	14
C40	40	35	24	16
C45	45	36	27	18
C50	50	37	30	20
C55	55	38	33	22
C60	60	38	36	24
C70	70	41	41	28
C80	80	42	42	32
C90	90	44	44	36

Table 3.4: Modulus of elasticity of concrete according to EN 1992-1-2 for siliceous aggregates, GPa

Temperature °C	Reduction factor	C12	C16	C20	C25	C30	C35	C40	C45	C50	C55	C60	C70	C80	C90
20	1.000	7.0	10.0	12.0	15.0	18.0	21.0	24.0	27.0	30.0	33.0	36.0	41.0	42.0	44.0
100	0.625	4.4	6.3	7.5	9.4	11.3	13.1	15.0	16.9	18.8	20.6	22.5	25.6	26.3	27.5
200	0.432	3.0	4.3	5.2	6.5	7.8	9.1	10.4	11.7	13.0	14.3	15.5	17.7	18.1	19.0
300	0.304	2.1	3.0	3.6	4.6	5.5	6.4	7.3	8.2	9.1	10.0	10.9	12.4	12.8	13.4
400	0.188	1.3	1.9	2.3	2.8	3.4	3.9	4.5	5.1	5.6	6.2	6.8	7.7	7.9	8.3
500	0.100	0.7	1.0	1.2	1.5	1.8	2.1	2.4	2.7	3.0	3.3	3.6	4.1	4.2	4.4
600	0.045	0.3	0.5	0.5	0.7	0.8	0.9	1.1	1.2	1.4	1.5	1.6	1.8	1.9	2.0
700	0.030	0.2	0.3	0.4	0.5	0.5	0.6	0.7	0.8	0.9	1.0	1.1	1.2	1.3	1.3
800	0.015	0.1	0.2	0.2	0.2	0.3	0.3	0.4	0.4	0.5	0.5	0.5	0.6	0.6	0.7
900	0.008	0.1	0.1	0.1	0.1	0.1	0.2	0.2	0.2	0.2	0.3	0.3	0.3	0.3	0.4
1000	0.004	0.0	0.0	0.0	0.1	0.1	0.1	0.1	0.1	0.1	0.1	0.1	0.2	0.2	0.2
1100	0.001	0.0	0.0	0.0	0.0	0.0	0.0	0.0	0.0	0.0	0.0	0.0	0.0	0.0	0.0
1200	0.000	0.0	0.0	0.0	0.0	0.0	0.0	0.0	0.0	0.0	0.0	0.0	0.0	0.0	0.0

Figure 3-9 compares the reduction factors of the modulus of elasticity of concrete, calculated using the method explained. The values based on Eurocodes, as shown in Table 3.4, will be applied to the FEM code sought.

On taking a look at the values of Table 3.4, it can be seen that the stiffness of concrete facing temperatures more than 450°C is negligible (under 10% of the reference value). *To develop the FEM code, parts of the cross-section that are*

made of concrete and have already experienced temperatures more than a defined temperature would be assumed to have zero stiffness. This assumption is on the safe side and is made because of unknown parameters. The upper limit of the temperature can be determined by the user in the developed code.

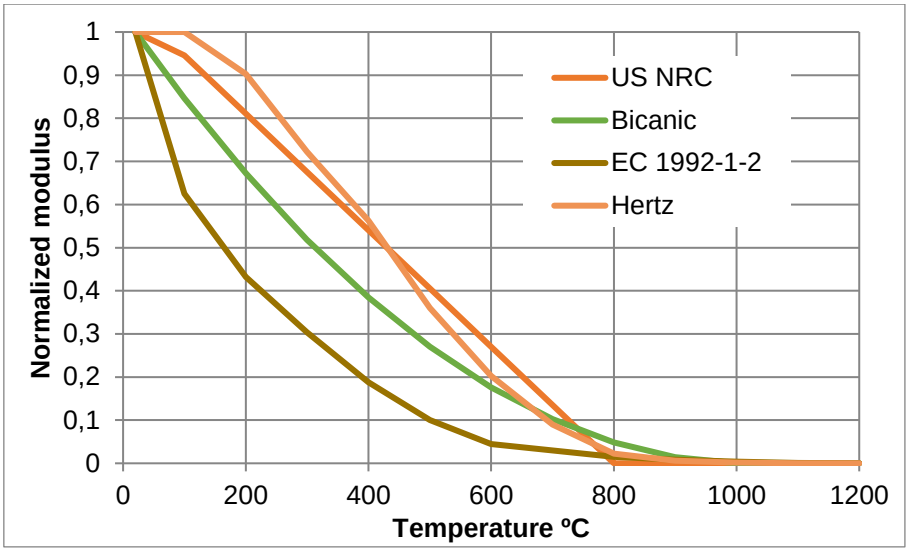

Figure 3-9: Comparison between normalized moduli of elasticity of concrete based on different studies (reduction factors)

Here, we have obtained some values for the modulus of concrete at elevated temperatures in the absence of other actions. In fact, such a situation does not exist. At first, dead load and live loads are applied to the structure, and there is some existing strain and stress in members. For example, imagine a concrete beam under dead and live load; the design plastic strain of concrete is around 0.0025. It means that members that will face elevated temperatures may have a strain of about 0.0025. Concrete members are designed to bear applied loads, so it can be assumed that the strain and tensions are limited to the plastic strain, which is defined in EN 1992-1-2. Generally, the modulus of elasticity of concrete in a warm situation depends on the temperature and temperature growth. It means that for different fire scenarios, the modulus of concrete varies in different ways, depending on the imposed loads, and temperature. Based on EN 1992-1-2, the stress–strain curves of concrete at different temperatures are presented in Annexure A. These curves are based on Eq. 3.19 for different strength classes of concrete.

3.6 Yield strain

Material properties of concrete and structural steel, including stress–strain curves and modulus of elasticity at elevated temperatures, are presented. The modulus of elasticity—illustrated in Tables 3.1 and 3.4—are applied in the FEM code. As mentioned, the strain shall be limited to the yield strain for steel and $\varepsilon_{c1,T}$ for concrete. The upper limits of strain are shown again in Table 3.5.

Table 3.5: Maximum strain for concrete and steel at elevated temperatures; the strain will be limited to these values to have a constant modulus of elasticity at temperature T.

Temperature °C	Maximum ultimate strain for concrete $\varepsilon_{c1,T}$	Yield strain of steel, $\varepsilon_{p,T}$
20	0.0025	0.0011
100	0.004	0.0011
200	0.0055	0.0010
300	0.007	0.0009
400	0.01	0.0007
500	0.015	0.0007
600	0.025	0.0007
700	0.025	0.0007
800	0.025	0.0006
900	0.025	0.0006
1000	0.025	0.0006
1100	0.025	0.0006
1200	0.025	0

3.7 Specific heat

The variation in the specific heat for steel with respect to the temperature does not show a simple trend. Owing to the latent heat effect which occurs at the transition temperature of α-into γ-crystals, there are four different ranges [34]. For simplified models, the specific heat of steel can be assumed to be constant [23].

$$C_a = 425 + 7.73 \times 10^{-1}T - 1.69 \times 10^{-3}T^2 + 2.22 \times 10^{-6}T^3 \qquad 20 \le T \le 600 \qquad (3.21)$$

$$C_a = 666 - \frac{13002}{T - 738} \qquad 600 < T \le 735 \qquad (3.22)$$

$$C_a = 545 + \frac{17820}{T - 731} \qquad 735 < T \le 900 \qquad (3.23)$$

$$C_a = 650 \qquad 900 < T \le 1200 \qquad (3.24)$$

According to EN 1992-1-2, the specific heat of normal weight dry concrete may be calculated as follows:

$$C_p = 900 \qquad 20 \leq T \leq 100 \tag{3.25}$$

$$C_p = 900 + (T - 100) \qquad 100 < T \leq 200 \tag{3.26}$$

$$C_p = 1000 + \frac{T - 200}{2} \qquad 200 < T \leq 400 \tag{3.27}$$

$$C_p = 1100 \qquad 400 < T \leq 1200 \tag{3.28}$$

In simple calculation models, the specific heat may be independent of the concrete temperature [20], [2]. The specific heat of the concrete depends on the moisture content. If the moisture content of the concrete is not available: The moisture content will not exceed 4% of the concrete weight [20].

Owing to the phase transformation of free and bound water in heated concrete, the specific heat exhibits a peak between 100°C and 200°C, with a top value at 120°C. The amount of heat which transforms the free water to vapour does not increase the temperature of the material. This peak varies with the concrete properties, water content, and other parameters [34]. In this research, to calculate the temperature field, temperature-independent specific heat—based on EN 1992-1-2 and 1993-1-2—will be assumed.

4 Thermal Analysis

4.1 Introduction

In this chapter, we consider heat transfer problems. The determination of the temperature distribution is the goal of heat transfer analysis. We can then determine the amount of heat moving into or out of a body and the thermal stresses. First of all, the heat transfer equation is presented in two-dimensional form. The two-dimensional heat transfer equation will be used to analyse the temperature distribution of a given cross-section. It is important to note that the heat transfer between cross-sections along a beam is assumed to be zero. The finite element formulation of the heat transfer equation will then be presented and the stiffness matrix and force vector will be obtained in two-dimensional form. The effects of temperature distribution on bending and the axial stiffness of cross-sections and the mathematical method to obtain bending and axial stiffness will be explained in this chapter. At the end of the chapter, the thermal FEM code will be presented.

4.2 Conservation of energy

The amount of energy that enters a system and the amount of energy that leaves a system will be in balance. The law of conservation of energy states that [35]:

> *The total energy of an isolated system remains constant; it is said to be conserved over time. Energy can be neither created nor destroyed, but is*

transformed from one form to another; for instance, chemical energy can be converted to kinetic energy in the explosion of a stick of dynamite.

The following energy balance has to be satisfied for each system:

$$E_{input} + E_{generated} = \Delta U + E_{output} \rightarrow q_x A dt + Q A dt dx = \Delta U + q_{x+dx} A dt \quad (4.1)$$

E_{in} is the amount of energy entering control volume, $E_{generated}$ is the amount of energy generated in control volume, E_{output} is the amount of energy leaving the control volume, ΔU is the change of stored energy in control volume, q_x is the heat flux at surface edge *x* (see Fig. 4.1), q_{x+dx} is the heat flux at surface *x*+*dx*, t is time, Q is the internal heat generated by internal heat source, and A is the cross-sectional area perpendicular to heat flow.

- *Rate equations*

To calculate the amount of energy that enters or leaves a control volume, the rate of energy change will have to be known. The rate equations, which describe the rates of energy flow by different energy transportation methods, are given by the following equations.

Conduction: The rate of heat flow in x direction by conduction (q) is given by

$$q_x = -K_{xx} \frac{dT}{dx} \quad (4.2)$$

K_{xx} is the thermal conductivity in x direction and $\frac{dT}{dx}$ is the temperature gradient.

Equation 4.2 shows that the heat flux is proportional to the gradient of the temperature. The minus sign implies the fact that the heat flow is positive in the direction opposite to the direction of increase in temperature. This equation is similar to the one-dimensional stress-strain law, which is $\sigma_x = E(\frac{du}{dx})$. For *x*=*x*+*dx,* we have:

$$q_{x+dx} = -K_{xx} \frac{dT}{dx}\Big| x + dx \quad (4.3)$$

Convection: When a solid is flowing in a fluid, heat transfer between the solid and the fluid will occur when a temperature difference occurs. The rate of heat flow by convective heat transfer between solid faces and fluid can be obtained by [36]:

$$q_h = hA(T - T_\infty) \quad (4.4)$$

where h is the heat transfer or convection coefficient, A is the area of the surface facing heat, T is the temperature of the solid surface at the solid/fluid interface, and T_∞ is the temperature of fluid.

Free convection occurs when, for instance, a hot plate is exposed to ambient room air without an external source of motion. This movement of the air, experienced as a result of the density gradients near the plate, is called free convection. Forced convection is experienced, for instance, in the case of a fan blowing air over a plate. Approximate values of heat convection coefficient are given in Table 4.1.

Table 4.1: Heat convection coefficients [37]

Mode	$h\ (\frac{W}{(m^2\,°C}$)
Free convection, air	5–25
Forced convection, air	10–500
Forced convection, water	100–15000
Boiling water	2500–25000
Condensation of water vapour	5000–100000

Radiation: Radiation heat transfer is the process by which the thermal energy is exchanged between two surfaces, obeying the laws of electromagnetics. Radiation plays a significant role in structural fire design. The radiation energy can be of three kinds: reflected, transmitted, or absorbed. The absorbed radiation energy is converted into heat energy and increases the material temperature. The radiation in fire compartments accelerates the temperature rise inside the compartment because the fire compartments are enclosed areas. The rate of heat flow by radiation can be obtained by [36]:

$$q = \varepsilon\sigma A(T^4 - T_\infty^4) \tag{4.5}$$

where σ is the Stefan-Boltzmann constant, ε is the emissivity of the surface, A is the surface area of the body through which heat flows, T is the absolute surface temperature of the body, and T_∞ is the absolute surrounding temperature.

4.3 Governing equation of heat transfer

4.3.1 One-dimensional form

The objective is to present a physical insight into the heat transfer phenomena, which needs to be understood so that the finite element formulation of the problem is fully understood. Imagine the one-dimensional heat transfer

problems without convection, as shown in Figure 4-1. The temperature gradient will be evaluated at *x*=*x*+*dx*. Using the two-term Taylor's series, we have:

$$q_{x+dx} = -\left(K_{xx}\frac{dT}{dx} + \frac{d}{dx}\left(K_{xx}\frac{dT}{dx}\right)dx\right) \tag{4.6}$$

The variation of stored energy in control volume is:

$$\Delta U = Specific\ heat\ \times mass\ \times temperature\ changes = c(\rho A dx)dT \tag{4.7}$$

c is the specific heat and ρ is the density. By substituting Eq. 4.7 in Eq. 4.6 and dividing Eq. 4.6 by $Adxdt$, we have:

$$\frac{\partial}{\partial x}\left(K_{xx}\frac{\partial T}{\partial x}\right) + Q = \rho c\frac{\partial T}{\partial t} \tag{4.8}$$

For steady state heat conduction, we have $\frac{dT}{dt} = 0$.

$$K_{xx}\frac{d^2T}{dx^2} + Q = 0 \tag{4.9}$$

If the boundary conditions are available, the temperature field can be calculated. For example, the boundary conditions can be heat flux or temperature at the boundaries. If the heat is flowing out of the body, the heat flux is negative; and if the heat is flowing into the body, the heat flux is positive. Eq. 4.8 is the one-dimensional heat transfer equation that will be used to obtain the temperature field in one-dimensional domains, such as bars or beams, when modelled by neutral axis.

$$heat\ flux = -K_{xx}\frac{dT}{dx} \tag{4.10}$$

4.3.2 Two-dimensional heat conduction

Imagine the two-dimensional heat transfer, as shown in Figure 4-2. The two-dimensional heat conduction equation can be obtained in a similar manner to the one-dimensional case. For the steady state case, we have:

$$K_{xx}\frac{\partial^2 T}{\partial x^2} + K_{yy}\frac{\partial^2 T}{\partial y^2} + Q = 0 \tag{4.11}$$

For the transient state:

$$K_{xx}\frac{\partial^2 T}{\partial x^2} + K_{yy}\frac{\partial^2 T}{\partial y^2} + Q = \rho c\frac{\partial T}{\partial t} \tag{4.12}$$

If the heat sources are absent and $K = K_{xx} = K_{yy}$, we can obtain:

$$\frac{\partial^2 T}{\partial x^2} + \frac{\partial^2 T}{\partial y^2} = \frac{1}{\alpha}\frac{\partial T}{\partial t} \tag{4.13}$$

where $\alpha = \frac{K}{\rho c}$

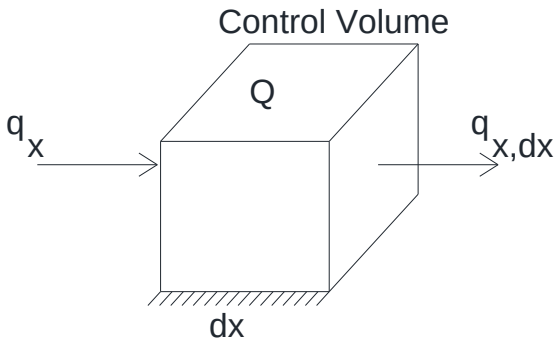

Figure 4-1: Control volume for one-dimensional heat conduction

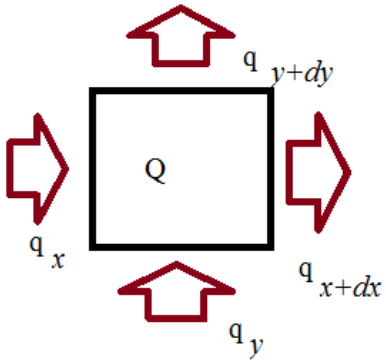

Figure 4-2: Control volume for two-dimensional heat conduction

4.4 Boundary and initial conditions

The differential equation of heat transfer is a second-order one; therefore, two boundary conditions are required to solve the equations. Possible boundary and initial conditions are:

$$T(x,y,z,t) = T_0\,, t > 0 \tag{4.14}$$

$$k_x \frac{\partial T}{\partial x} l_x + k_y \frac{\partial T}{\partial y} l_y + k_z \frac{\partial T}{\partial z} l_z + q = 0\,, t > 0 \tag{4.15}$$

$$k_x \frac{\partial T}{\partial x} l_x + k_y \frac{\partial T}{\partial y} l_y + k_z \frac{\partial T}{\partial z} l_z + h(T - T_\infty) = 0\,, t > 0 \tag{4.16}$$

where q_0 is the boundary heat flux, h is the convection heat transfer coefficient, T_∞ is the surrounding temperature, and l_x, l_y, l_z are the direction cosines of the outward drawn normal to the boundary.

Equation 4.14 indicates that the temperature is specified as T_0 on the surface of the element. This boundary condition is applicable when the temperature change is forced to a boundary—for example, faces which are in contact with a melting metal or a boiling fluid. Equation 4.15 represents the existence of a fixed or constant heat flux q_0 at the boundary. Equation 4.16 denotes the existence of convection heat transfer (heating or cooling of the body) at the boundary. This boundary condition is realized when cold (or hot) air flows around the hot (or cold) surface. The air may be blown by a fan to increase the convection heat transfer coefficient. Equation 4.14 is known as the Dirichlet condition and Equations 4.15 and 416 are called Neumann conditions. Equations 4.15 and 4.16 give the variations of a variable (here, the temperature) on the boundary. The initial condition of each system—when dealing with the heat transfer problem—is the temperature field at time *t=0*. At each time step, the temperature field that is calculated in the previous time step is the initial condition.

$$T(x,y,z,t=0) = T(x,y,z) \tag{4.17}$$

$T_{t=0}$ is the specified temperature distribution at time zero.

4.5 Variational form of heat transfer equation

The two-dimensional heat conduction problem can be stated in an equivalent variational form, as follows [36]:

Finding the temperature distribution *T(x, y, z, t)* inside the solid body that minimizes the integral

$$I = \frac{1}{2}\iiint_V \left[k\frac{\partial^2 T}{\partial x^2} + k\frac{\partial^2 T}{\partial y^2} + 2(\rho c\ \frac{\partial T}{\partial t})T\right] dV \tag{4.18}$$

and satisfies the required boundary and initial conditions. In case of heat transfer with convection and existence of heat source inside the domain, we have:

$$I = \frac{1}{2}\iiint_V \left[k\frac{\partial^2 T}{\partial x^2} + k\frac{\partial^2 T}{\partial y^2} + 2(\rho c\ \frac{\partial T}{\partial t})T\right] dV + \iint_S q_0 T dS + \frac{1}{2}\iint_S h(T - T_\infty)^2 dS \tag{4.19}$$

S indicates the surfaces of the finite volume and *V* indicates the volume of the finite volume. The finite element method might be applied to obtain the temperature field that satisfies Eq. 4.19.

4.6 Two-dimensional finite element formulation

4.6.1 Formulation

The finite element equations for the heat conduction problem can be derived by using a variational approach or a Galerkin approach. In the present study, the temperature field of cross-sections at elevated temperatures is of interest. When the heat flux along the structural members—such as beam and columns—is zero, the temperature field of each cross-section can be modelled using a two-dimensional formulation. To solve the problem using a two-dimensional formulation, the following steps will be performed.

Step 1: Element type and meshing

To mathematize a phenomenon using finite element formulation, the first step is the formation of elements and choice of the element type, which is named meshing. The 2d linear triangular element with three nodes has been considered, so as to calculate the temperature field. The element is illustrated in Figure 4-3. This element is suitable and simple for modelling the temperature fields inside solids.

- *Two-dimensional linear triangular element with three nodes*

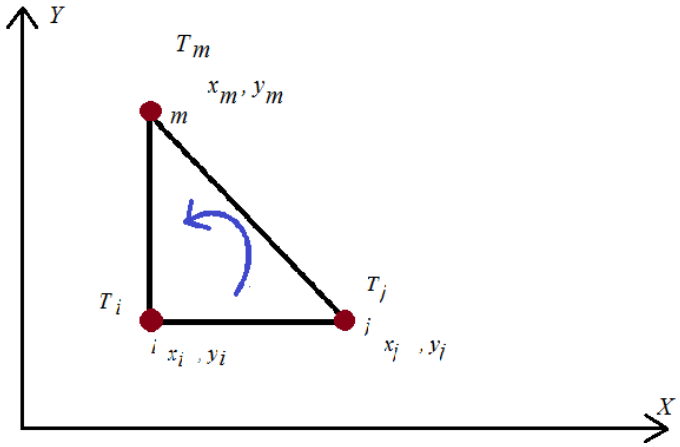

Figure 4-3: Two-dimensional triangular element

Triangular elements have three nodes named *i*, *j*, and *m* with coordinates (x_i , y_i), (x_j , y_j), and (x_m , y_m). In Figure 4-3, T_i, T_j, and T_m are the nodal temperatures. Shape functions for the linear triangular elements are [38]:

$$N_k = \frac{1}{2A}(a_k + b_k x + c_k y), \qquad k = i, j, m \tag{4.20}$$

A is the area of the element, a, b, and c are constants, and *x*, *y* are the nodal coordinates in the Cartesian system. N_i is the shape function which estimates the purposed variables over the element. To know more about shape functions and their characteristics, the reader is referred to [38]. Each element possesses three shape functions. The constants of shape functions, a, b, and c, can be obtained as follows:

$$a_i = x_j y_m - x_m y_j \tag{4.21}$$

$$b_i = y_j - y_m \tag{4.22}$$

$$c_i = x_m - x_j \tag{4.23}$$

The other coefficients are obtained by a cycle permutation of subscripts in the order *i*, *j*, *k* and the area of the element:

$$2A = det \begin{vmatrix} 1 & x_i & y_i \\ 1 & x_j & y_j \\ 1 & x_m & y_m \end{vmatrix} \tag{4.24}$$

Step 2: Temperature function

We define the temperature vector, ***T***, for each element and the ***N*** vector as follows:

$$[\boldsymbol{T}] = \begin{bmatrix} T_i \\ T_j \\ T_m \end{bmatrix} \text{ and } [\boldsymbol{N}] = [N_i \quad N_j \quad N_m] \tag{4.25}$$

Therefore, we have:

$$T_{element} = [\boldsymbol{N}].[\boldsymbol{T}] = [N_i \quad N_j \quad N_m]\begin{bmatrix} T_i \\ T_j \\ T_m \end{bmatrix} \tag{4.26}$$

$$\rightarrow \frac{\partial T}{\partial x} = \left[\frac{\partial N_i}{\partial x} \quad \frac{\partial N_j}{\partial x} \quad \frac{\partial N_m}{\partial x}\right]\begin{bmatrix} T_i \\ T_j \\ T_m \end{bmatrix}$$

Step 3: Derivation of the element conduction matrix and equations

Using the variational form of the finite element formulation, we express the functional ***I*** as a sum of ***ELE*** elemental quantities ***I****(e)* as:

$$I = \sum_{e=1}^{ELE} I^{(e)}, \qquad ELE = number\ of\ elements \tag{4.27}$$

$$I^{(e)} = \frac{1}{2}\iiint_V \left[k\frac{\partial^2 T}{\partial x^2} + k\frac{\partial^2 T}{\partial y^2} + 2(\rho c\ \frac{\partial T}{\partial t})T\right]dV + \iint_S q_0 T dS + \frac{1}{2}\iint_S h(T - T_\infty)^2 dS \tag{4.28}$$

The variational function is a function of the temperature field *T*. To minimize the function ***I***, the following equation will have to be satisfied:

$$\frac{\partial I}{\partial T_i} = \sum_{e=1}^{ELE} \frac{\partial I^{(e)}}{\partial T_i}\ , ELE = number\ of\ elements\ , i = total\ number\ of\ nodes \tag{4.29}$$

Assuming zero convection and in the absence of heat sources, we can write:

$$\frac{\partial I^{(e)}}{\partial T_i} = \iiint_V \left[k\frac{\partial T}{\partial x}\frac{\partial}{\partial T_i}\left(\frac{\partial T}{\partial x}\right) + k\frac{\partial T}{\partial y}\frac{\partial}{\partial T_i}\left(\frac{\partial T}{\partial y}\right) - 2(\rho c\ \frac{\partial T}{\partial t})\frac{\partial T}{\partial T_i}\right]dV \tag{4.30}$$

The terms of Equation 4.30 can be obtained as:

$$\begin{cases} \begin{bmatrix} \frac{\partial T}{\partial x} \\ \frac{\partial T}{\partial y} \end{bmatrix} = \begin{bmatrix} \frac{\partial N_i}{\partial x} & \frac{\partial N_j}{\partial x} & \frac{\partial N_m}{\partial x} \\ \frac{\partial N_i}{\partial y} & \frac{\partial N_j}{\partial y} & \frac{\partial N_m}{\partial y} \end{bmatrix}\begin{bmatrix} T_i \\ T_j \\ T_m \end{bmatrix} = [B][T] & (4.31) \\ \frac{\partial}{\partial T_i}\left(\frac{\partial T}{\partial x}\right) = \frac{\partial N_i}{\partial x}\ (See\ Eq. 4.26) & (4.32) \\ \frac{\partial T}{\partial T_i} = N_i\ (See\ Eq. 4.26) & (4.33) \\ \frac{\partial T}{\partial t} = N\begin{bmatrix} \frac{\partial T_i}{\partial t} \\ \frac{\partial T_j}{\partial t} \\ \frac{\partial T_m}{\partial t} \end{bmatrix} & (4.34) \end{cases}$$

Therefore, Equation 4.30 can be expressed as:

$$\frac{\partial I^{(e)}}{\partial T_i} = [K]_1[T] + [K]_3\frac{\partial T}{\partial t} \tag{4.35}$$

$$[K]_{1_{i,j}} = \iiint_V \left[k\frac{\partial T}{\partial x}\frac{\partial}{\partial T_i}\left(\frac{\partial T}{\partial x}\right) + k\frac{\partial T}{\partial y}\frac{\partial}{\partial T_i}\left(\frac{\partial T}{\partial y}\right)\right]dV \tag{4.36}$$

$$= \iiint_V \left[k\frac{\partial N_i}{\partial x}\frac{\partial N_j}{\partial x} + k\frac{\partial N_i}{\partial y}\frac{\partial N_j}{\partial y}\right]dV$$

$$[K]_{3_{i,j}} = \iiint_V \rho c N_i N_j dV \tag{4.37}$$

$[B]$ matrix can be obtained by substituting Eq. 4.20 into Eq. 4.31. By differentiation, we have:

$$[B] = \begin{bmatrix} \frac{\partial N_i}{\partial x} & \frac{\partial N_j}{\partial x} & \frac{\partial N_m}{\partial x} \\ \frac{\partial N_i}{\partial y} & \frac{\partial N_j}{\partial y} & \frac{\partial N_m}{\partial y} \end{bmatrix} = \frac{1}{2A}\begin{bmatrix} b_i & b_j & b_m \\ c_i & c_j & c_m \end{bmatrix} \tag{4.38}$$

The material properties matrix of the element is:

$$[D] = \begin{bmatrix} K_{xx} & 0 \\ 0 & K_{yy} \end{bmatrix} \tag{4.39}$$

$$[K]_1 = \iiint_V [B]^T[D][B]dV \tag{4.40}$$

$$[K]_1 = \iiint_V \frac{1}{4A^2}\begin{bmatrix} b_i & c_i \\ b_j & c_j \\ b_m & c_m \end{bmatrix}\begin{bmatrix} K_{xx} & 0 \\ 0 & K_{yy} \end{bmatrix}\begin{bmatrix} b_i & b_j & b_m \\ c_i & c_j & c_m \end{bmatrix}dV \tag{4.41}$$

If the elements' thickness, *t*, is constant, we are able to simplify the integration as follows:

$$[K]_1 = \frac{t}{4A}\begin{bmatrix} b_i & c_i \\ b_j & c_j \\ b_m & c_m \end{bmatrix}\begin{bmatrix} K_{xx} & 0 \\ 0 & K_{yy} \end{bmatrix}\begin{bmatrix} b_i & b_j & b_m \\ c_i & c_j & c_m \end{bmatrix} \rightarrow \tag{4.42}$$

$$if\ K_{xx} = K_{yy} = K\ and\ thickness\ of\ element = 1 \rightarrow [K]_1$$

$$= \frac{K}{4A}\begin{bmatrix} b_i^2 + c_i^2 & b_ib_j + c_ic_j & b_ib_m + c_ic_m \\ b_ib_j + c_ic_j & b_j^2 + c_j^2 & b_jb_m + c_jc_m \\ b_ib_m + c_ic_m & b_jb_m + c_jc_m & b_m^2 + c_m^2 \end{bmatrix}$$

$[K]_1$ is the stiffness matrix of the element related to conduction part of the heat transformation. If we consider convection on boundaries, there will be another stiffness, which will be added to $[K]_1$.The stiffness matrix related to convection effects is:

$$[K]_2 = \iint_S h[N]^T [N] dS = h \iint_S \begin{bmatrix} N_i N_i & N_i N_j & N_i N_m \\ N_j N_i & N_j N_j & N_j N_m \\ N_m N_i & N_m N_j & N_m N_m \end{bmatrix} dS \quad (4.43)$$

Equation 4.43 will be integrated over the boundaries. Nodes that are located on boundaries with convection heat transfer will have non-zero convective stiffness in the element and global stiffness matrix. The unsteady portion of the stiffness matrix, which is represented by $[K]_3 \frac{\partial T}{\partial t}$, can be obtained as follows:

$$[K]_3 = \frac{\rho c A}{12} \begin{bmatrix} 2 & 1 & 1 \\ 1 & 2 & 1 \\ 1 & 1 & 2 \end{bmatrix} \quad (4.44)$$

Equation 4.44 is the consistent matrix for triangular elements. Here, the lumped matrix can also be applied, which is:

$$[K]_3 = \frac{\rho c A}{3} \begin{bmatrix} 1 & 0 & 0 \\ 0 & 1 & 0 \\ 0 & 0 & 1 \end{bmatrix} \quad (4.45)$$

The lumped-mass matrix has diagonal terms only. This facilitates the computation of the global equations. Hence, the lumped-mass matrix will be used in the current research. The solution accuracy is usually not as good as when a consistent-mass matrix is used [37].

Step 4: Evaluation of force matrix

$$[f] = \iiint_V Q[N]^T dV = Q \iiint_V [N]^T dV \quad (4.46)$$

As mentioned earlier, in the present study, the heat source is not inside the body. Therefore, Equation 4.46 is equal to zero. The boundary condition of the problem is variable temperature as a function of time.

Step 5: Assembly of the global stiffness and force matrix

The global stiffness matrix of the system can now be calculated. The stiffness of each node as a member of the total stiffness matrix is the summation of the stiffness of that node related to each element. Figure 4-4 shows a system consisting of two triangular elements and the stiffness matrix of the system. The procedure of Figure 4-4 will be applied to all elements.

$$[K]_{Total} = \sum_{e=1}^{ELE} [K]^{element}, ELE = number\ of\ elements \quad (4.47)$$

$$[F]_{Total} = \sum_{e=1}^{ELE} [F]^{element} \quad (4.48)$$

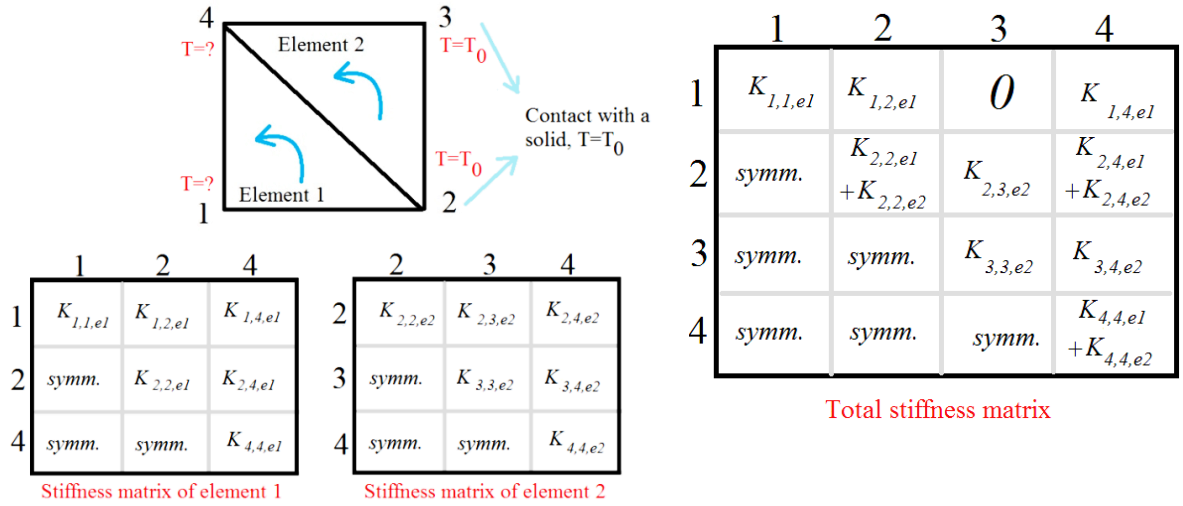

Figure 4-4: Assembly of the stiffness matrix for the whole system

The force matrix, which considers the boundary conditions in FEM formulation, can be obtained in accordance with the procedure shown in Figure 4-5.

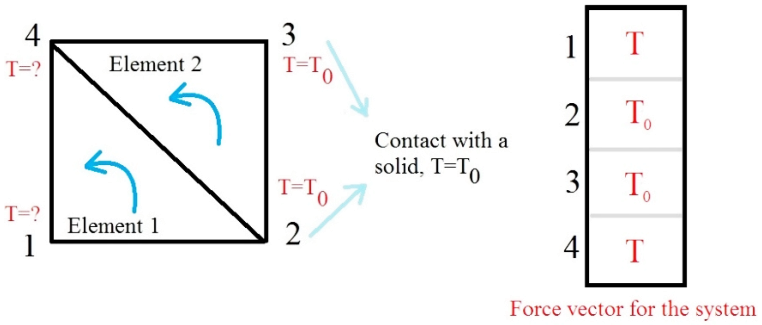

Figure 4-5: Force vector when boundary condition is the given temperatures

Step 6: Solution

If the total force vector and stiffness matrix are known, including convection, conduction, and radiation effects, the system of equations can be solved as follows:

$$[K_1].[T] + [K_3].[\dot{T}] = [F] \tag{4.49}$$

We will apply the finite difference scheme in the time domain for solving Eq. 4.49. This scheme is based on approximating the first-time derivative of *T* as:

$$[\dot{T}] \approx \frac{\Delta T}{\Delta t} = \frac{[T_1] - [T_0]}{\Delta t} \tag{4.50}$$

$$[K_1].[T] + [K_3].\frac{[T_1] - [T_0]}{\Delta t} = [F] \tag{4.51}$$

$[T_1]$ and $[T_0]$ are the temperature fields at time steps *t+1* and *t* respectively. $[\dot{T}]$ is evaluated at the middle point of time interval Δt; therefore, other quantities like $[T]$ or force vector will also be calculated at this point of time domain as follows:

$$[T] = \frac{[T_1] + [T_0]}{2} \tag{4.52}$$

$$[F] = \frac{[F_1] + [F_0]}{2} \tag{4.53}$$

By substituting Eq. 4.53 and 4.52 into Eq. 4.51, we have:

$$[K_1]\frac{[T_1] + [T_0]}{2} + [K_3]\frac{[T_1] - [T_0]}{\Delta t} = \frac{[F_1] + [F_0]}{2} \tag{4.54}$$

$$\left([K_1] + \frac{2}{\Delta t}[K_3]\right)[T_1] = \left(-[K_1] + \frac{2}{\Delta t}[K_3]\right)[T_0] + [F_1] + [F_0] \tag{4.55}$$

Eq. 4.55 shows that the temperature field at time *t+1,* $[T_1]$, can be calculated once the temperature field at time step *t*, $[T_0]$, is known. The boundary nodes can be adjacent to heat sources or in contact with a fluid. When the domain is divided into some nodes and triangular elements, the boundary nodes can be determined by convex hull algorithm. To know more about convex hull algorithms, the reader is referred to Computational Geometry, Chapter: Convex Hulls [39]. We have to mention that if the boundary condition is the group of given temperatures for some nodes, the stiffness matrix must be modified to be inverse-able. Figure 4-6 illustrates the modified stiffness matrix for the system shown in Figure 4-5.

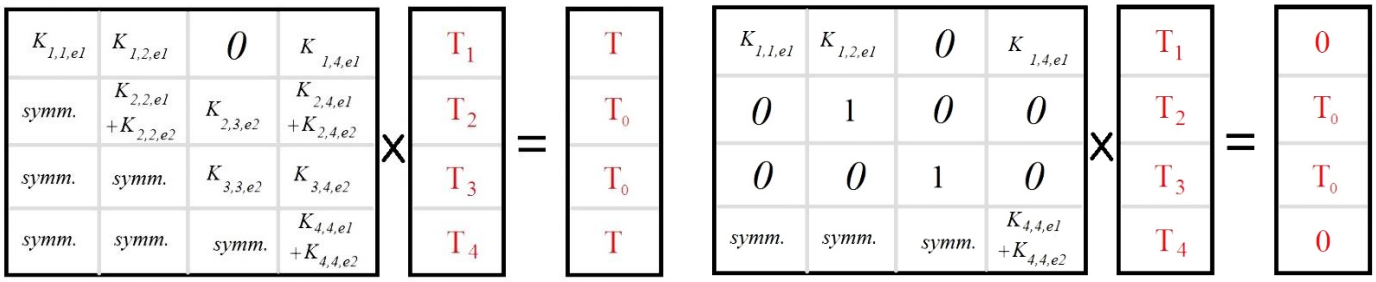

Figure 4-6: Modified stiffness matrix for the system shown in Fig. 4-4

4.6.2 Thermal FEM code

Figure 4-7 shows the code developed for heat transfer analysis. It needs to be mentioned that the developed code cannot generate the FEM mesh for a given domain. The FEM mesh, including material properties of each element, nodal coordinates, and nodes of elements, will be imported as an Excel worksheet. Applying the FEM formulation in Section 4.6.1, a FEM code in Microsoft Visual Studio C# (C sharp) has been developed. Microsoft Visual Studio is an integrated development environment (IDE) from Microsoft. It is used to develop computer programs for Microsoft Windows, as well as websites, web applications, and web services [40]. The developed code is a Windows Form Application written in Visual C#. Fire load, FEM mesh, and material properties will be imported to computer code. It computes the temperature distribution for

concrete and steel members at each time step and saves the temperature field to be used in calculation of the stiffness curves.

<THERMAL ANALYSIS>

Mesh the domain using triangular elements and import the coordinates and the element formation matrix into the code. Element formation matrix contains the nodal indexes for each element. Here matrix **E**;
X,Y = Vector of nodal coordinates;
Node = Number of nodes;
TOTALSTEPS = Number of time steps based on the fire curve;
T0 = Vector of initial condition, here initial temperature of all nodes, when time is 0, the initial temperature is equal to room temperature 20°C;
TEMPERATURE (Node X TOTALSTEPS) = A matrix which saves the calculated temperatures at the end of time step;
HULLINDEXES = A vector to save the index of boundary nodes. The convex hull algorithm will be applied;
KTOTAL (Node X Node), K1ELEMENT(3X3) = Define the element and total stiffness;
K3TOTAL (Node X Node), K3ELEMENT(3X3) = Define the element and total lumped matrix for transient analysis;
P = Define the force vector;
CONDUCTIVITY, DENSITY, SPECIFIC HEAT = Define the variables of heat transfer formulation, including conductivity, specific heat, and density for concrete and steel.
MATERIAL = A matrix to determine the element material; 1 means concrete and 0 means steel. This vector will be imported to the code as a property for each element.
Begin a loop through all elements, element number variable **e**;
    Calculate the thermal properties of each element, based on the calculated temperature in the last time step and save them;
    AELE = Area of the element, see Eq. 4.24;
    K1ELEMENT, K3ELEMENT = Calculate the element stiffness and consistent matrix, see Eq. 4.42 and Eq. 4.45;
End of the loop;
KTOTAL, K3TOTAL = Assembly of the total stiffness matrix and total consistent matrix for all elements;

<Solution>

The stiffness matrix will be changed to consider boundary effects (see Fig. 4.6). The stiffness matrix is symmetric. Therefore, it is not inverse-able and the system of equations does not have a special solution (see Eq. 4.55).

STMATRIX1 = $[K_1] + \frac{2}{\Delta t}[K_3]$, Inverse-able stiffness matrix;
Begin of a loop through all time steps, time variable **step**;
    STMATRIX1 = Change the stiffness matrix of the system based on the indexes obtained from convex hull algorithm and known temperatures;
    Solve the system of equations based on the analysis type, see Eq. 4.55;
    Save the temperature field obtained for the current time step in matrix **TEMPERATURE (Node, step)**;
End of the loop;
Return the variable **TEMPERATURE**;

Figure 4-7: FEM procedure for heat transfer analysis

5 Linear and Nonlinear Mechanical Analysis

5.1 Introduction

Finite element formulation and principles have already been developed for the mechanics of solids, especially frame elements. A frame element is a line in space with two nodes at both ends and has six degrees of freedom at each node, translation in *x*, *y,* and *z* directions, and rotation about *x*, *y,* and *z* axes (see Fig. 5.1). Frame element is suitable for modelling Euler and Timoshenko beams [41]. Curved frames can also be modelled by these two theories; they just need to be divided into some straight lines. Timoshenko beam theory accounts for shear deformations that are applicable in thick beams, but Euler beam theory does not consider deep and short beams. In Chapter 4, we calculated the temperature field for a cross-section under a given fire curve and the stiffness curves for warm members are drawn. Stiffness curves give the variation of bending and axial stiffness of members (here, space frames) as a function of time when facing fire. In Chapter 5, the mechanical analysis of a structure—as the stiffness of warm members varies in accordance with the stiffness curves—is proposed. A large deformation analysis will be applied to make the mathematical model of the structure more realistic.

Nonlinear behaviour of structures may be divided into two forms: 1- Material nonlinearity and 2- Geometric nonlinearity. When stress is not linearly proportional to strain or unloading and loading path are different, we have

material nonlinearity. Elasto-plastic behaviour is categorized under material nonlinearity behaviour. If the loading part of the stress–strain graph includes a linear relationship between stress and strain, the deformation includes elasto-plastic behaviour [42]. When the deformations of a solid reach a state for which the undeformed and deformed shapes are substantially different, a state of finite deformation occurs, and it is no longer possible to write linear equations for the undeformed geometry [38]. It is said the system includes geometric nonlinearity. The effects of these finite deformations on the behaviour of a system will be considered. In Section 4.3, we present the basic equation of linear systems and finite element formulation for linear space frame element. Afterwards, the geometric nonlinear formulation, which permits large deformations but small strains, and the nonlinear space frame element will be presented. Structures under fire loads show nonlinear behaviour and large strains but, in this research, these are modelled by assuming the variable stiffness of warm members. We note that strains will be limited to the values given in Table 3.5. Large strain analyses do not have applications in buildings and civil structures. In civil engineering, large displacements mean structural collapse, in both warm and normal design cases. Building regulations include some serviceability limits to control the deformations of structures, but large displacement analysis can be applied to obtain accurate results.

5.2 Basic equations of solid mechanics

The aim of problems in structural analysis or solid mechanics is to find the displacement and stresses under given loads and boundary conditions. Imagine the free body shown in Figure 5-2. We assume that this body is in equilibrium under the given static loads. If a body is in equilibrium under specified static loads, actions must be in balance with support reactions. In such a situation, the force and moment equilibrium for the whole body will be satisfied. Assume that B_x, B_y, B_z are body forces like self-weight, P_x, P_y, P_z are external point forces, and W_x, W_y, W_z are distributed loads. *S* is the boundary surface of the body and *V* is its volume; therefore, we have:

$$\sum F_x = 0 \rightarrow \int_S W_x ds + \int_V B_x dV + \sum P_x = 0 \tag{5.1}$$

$$\sum F_y = 0 \rightarrow \int_S W_y ds + \int_V B_y dV + \sum P_y = 0 \tag{5.2}$$

$$\sum F_z = 0 \rightarrow \int_S W_z ds + \int_V B_z dV + \sum P_z = 0 \tag{5.3}$$

Equations 5.1, 5.2, and 5.3 may be written for moment equilibrium in an analogous way. When a system is in equilibrium, there will be internal and

external equilibriums. Equations 5.1, 5.2, and 5.3 represent the external equilibrium of a system.

5.2.1 Differential equations

Stresses will develop inside the body because the body is under external actions. If we consider an element of material inside the body, it must be in equilibrium as a result of the internal stresses that have developed. This leads to equations known as internal equilibrium equations. To write the internal equilibrium, first the Cauchy stress tensor will be defined. If we denote the Cartesian coordinates as *x*, *y,* and *z*—or in index form x_1, x_2, and x_3—the unknown quantities are:

1. Displacements and rotations:
   $[u \quad v \quad w \quad \theta_x \quad \theta_y \quad \theta_z]=[u_1 \quad u_2 \quad u_3 \quad \theta_1 \quad \theta_2 \quad \theta_3]$;
2. Stresses $[\sigma_{xx} \quad \sigma_{yy} \quad \sigma_{zz} \quad \sigma_{xy} \quad \sigma_{yz} \quad \sigma_{zx}] = [\sigma_{11} \quad \sigma_{22} \quad \sigma_{33} \quad \sigma_{12} \quad \sigma_{23} \quad \sigma_{31}]$;
3. Strains $[\varepsilon_{xx} \quad \varepsilon_{yy} \quad \varepsilon_{zz} \quad \varepsilon_{xy} \quad \varepsilon_{yz} \quad \varepsilon_{zx}] = [\varepsilon_{11} \quad \varepsilon_{22} \quad \varepsilon_{33} \quad \varepsilon_{12} \quad \varepsilon_{23} \quad \varepsilon_{31}]$;

σ_{ij} is the Cauchy stress tensor or true stress tensor that completely defines the state of stress at a point inside a material in the deformed placement or configuration.

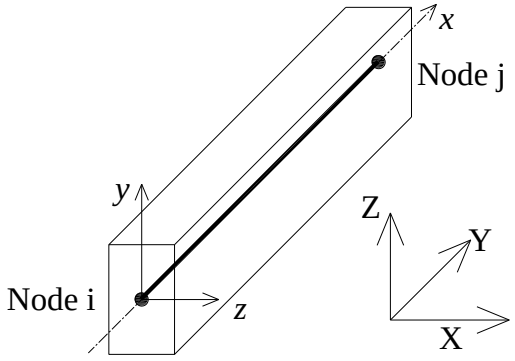

Figure 5-1: Three-dimensional beam with six degrees of freedom at each node and local and global coordinate systems

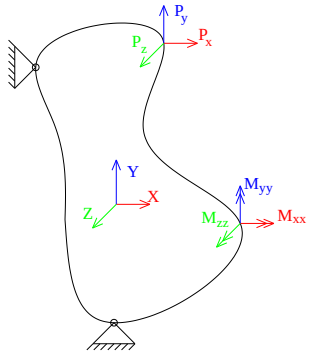

Figure 5-2: Free body in equilibrium

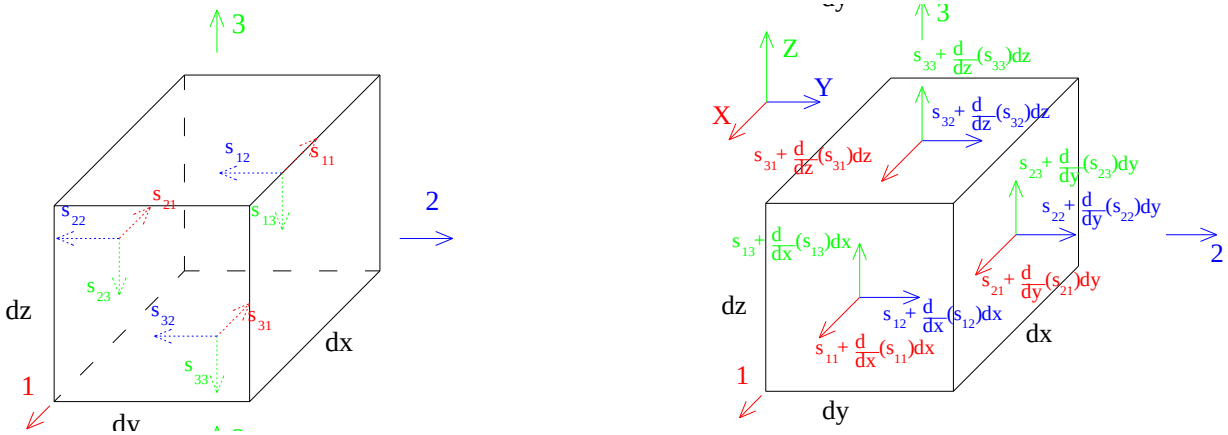

Figure 5-3: An element inside a body under loads, true stresses of an element in tensor form

$$Stress = [\boldsymbol{\sigma}] = \begin{bmatrix} \sigma_{xx} & \sigma_{xy} & \sigma_{xz} \\ \sigma_{yx} & \sigma_{yy} & \sigma_{yz} \\ \sigma_{zx} & \sigma_{zy} & \sigma_{zz} \end{bmatrix} \tag{5.4}$$

$$Strain = [\boldsymbol{\varepsilon}] = \begin{bmatrix} \varepsilon_{xx} & \varepsilon_{xy} & \varepsilon_{xz} \\ \varepsilon_{yx} & \varepsilon_{yy} & \varepsilon_{yz} \\ \varepsilon_{zx} & \varepsilon_{zy} & \varepsilon_{zz} \end{bmatrix} \tag{5.5}$$

The stress and strain inside a body under external loads is defined by nine components of Equations 5.4 and 5.5. σ_{ii} are normal stress components and σ_{ij} are the shear stresses. Moment equilibrium of an element (Fig. 5.3) gives:

$$\sigma_{ij} = \sigma_{ji} \tag{5.6}$$

Therefore, we can write the strain and stress matrix in vector form as follows:

$$[\boldsymbol{\sigma}] = \begin{bmatrix} \sigma_{xx} \\ \sigma_{yy} \\ \sigma_{zz} \\ \sigma_{xy} \\ \sigma_{yz} \\ \sigma_{zx} \end{bmatrix} \; and \; [\boldsymbol{\varepsilon}] = \begin{bmatrix} \varepsilon_{xx} \\ \varepsilon_{yy} \\ \varepsilon_{zz} \\ \varepsilon_{xy} \\ \varepsilon_{yz} \\ \varepsilon_{zx} \end{bmatrix} \tag{5.7}$$

If b_i is the body force per unit volume in *x*, *y*, and *z* directions, we can write the second law of Newton or the equilibrium of internal forces in the *x*, *y*, and *z* directions for the element of Figure 5-3 as follows:

$$F = ma \rightarrow \begin{cases} \dfrac{\partial \sigma_{xx}}{\partial x} + \dfrac{\partial \sigma_{xy}}{\partial y} + \dfrac{\partial \sigma_{xz}}{\partial z} + b_x = \rho \ddot{u}_x \\ \dfrac{\partial \sigma_{xy}}{\partial x} + \dfrac{\partial \sigma_{yy}}{\partial y} + \dfrac{\partial \sigma_{yz}}{\partial z} + b_y = \rho \ddot{u}_y \\ \dfrac{\partial \sigma_{zx}}{\partial x} + \dfrac{\partial \sigma_{yz}}{\partial y} + \dfrac{\partial \sigma_{zz}}{\partial z} + b_z = \rho \ddot{u}_z \end{cases} \tag{5.8}$$

where $\ddot{u}_i$ gives the partial differentiation of deformations with respect to time or acceleration of the body and ρ is mass density. Solution of Equation 5.8 gives the stresses and deformations for a body. For a complicated system, Equation 5.8 cannot be solved, and finding an exact solution is impossible; numerical methods will be applied. In some cases, the problem can be simplified by making some assumptions. For example, we can simplify equations by eliminating the *z* and *y* components of stress. Equations 5.9 and 5.10 represent the two-dimensional and one-dimensional forms of the equation of motion. The one-dimensional form is valid for truss members. Truss members are tension- or compression-only members, without transverse loads.

$$Two-dimensional\ form: \begin{cases} \frac{\partial \sigma_{xx}}{\partial x} + \frac{\partial \sigma_{xy}}{\partial y} + b_x = \rho \ddot{u}_x \\ \frac{\partial \sigma_{xy}}{\partial x} + \frac{\partial \sigma_{yy}}{\partial y} + b_y = \rho \ddot{u}_y \end{cases} \quad (5.9)$$

$$One-dimensional\ form: \frac{\partial \sigma_{xx}}{\partial x} + b_x = \rho \ddot{u}_x \quad (5.10)$$

5.2.2 Stress–strain relationship

For the one-dimensional form and linear material, Hooke's law is valid. Hooke's law states that the force *F* needed to extend or compress a spring by some distance *X* is proportional to that distance. For a finite element, we have stresses instead of force:

$$\sigma = E\varepsilon \ or \ \sigma_{xx} = E\varepsilon_{xx} \quad (5.11)$$

In case of a linear (based on Hooke's law) and isotropic material (when material properties are not a function of orientation, it is said that *the material is isotropic*), we can develop Equation 5.11 in three-dimensional form, as follows:

$$[\boldsymbol{\sigma}] = \begin{bmatrix} \sigma_{xx} \\ \sigma_{yy} \\ \sigma_{zz} \\ \sigma_{xy} \\ \sigma_{yz} \\ \sigma_{zx} \end{bmatrix} = [\boldsymbol{D}] \begin{bmatrix} \varepsilon_{xx} \\ \varepsilon_{yy} \\ \varepsilon_{zz} \\ \varepsilon_{xy} \\ \varepsilon_{yz} \\ \varepsilon_{zx} \end{bmatrix} \rightarrow \quad (5.12)$$

$$= \frac{E}{(1+\vartheta)(1-2\vartheta)} \times \begin{bmatrix} 1-\vartheta & \vartheta & \vartheta & 0 & 0 & 0 \\ \vartheta & 1-\vartheta & \vartheta & 0 & 0 & 0 \\ \vartheta & \vartheta & 1-\vartheta & 0 & 0 & 0 \\ 0 & 0 & 0 & 0.5(1-2\vartheta) & 0 & 0 \\ 0 & 0 & 0 & 0 & 0.5(1-2\vartheta) & 0 \\ 0 & 0 & 0 & 0 & 0 & 0.5(1-2\vartheta) \end{bmatrix} \begin{bmatrix} \varepsilon_{xx} \\ \varepsilon_{yy} \\ \varepsilon_{zz} \\ \varepsilon_{xy} \\ \varepsilon_{yz} \\ \varepsilon_{zx} \end{bmatrix}$$

E is the Young's modulus and ϑ is the Poisson's ratio. When there is some initial strain in members like thermal strains, we can write:

$$[\boldsymbol{\varepsilon_0}] = \begin{bmatrix} \varepsilon_{xx0} \\ \varepsilon_{yy0} \\ \varepsilon_{zz0} \\ \varepsilon_{xy0} \\ \varepsilon_{yz0} \\ \varepsilon_{zx0} \end{bmatrix} = \begin{bmatrix} \alpha\Delta T \\ \alpha\Delta T \\ \alpha\Delta T \\ 0 \\ 0 \\ 0 \end{bmatrix} \rightarrow [\boldsymbol{\sigma}] = [\boldsymbol{D}]([\boldsymbol{\varepsilon}] - [\boldsymbol{\varepsilon_0}]) \quad (5.13)$$

It should be noted that concrete is not an isotropic material. Material properties of concrete are different in *x*, *y,* and *z* directions, but in calculations based on Eurocodes and other building regulations, isotropic properties are assumed for concrete. Formwork, aggregates, reinforcement, and other parameters can change the mechanical properties of concrete (as a composite material) in each direction.

5.2.3 Strain–displacement relationship

The deformation of a point of a body can be described by three components *u*, *v, w* or u_1, u_2, u_3 in *x*, *y,* and *z* directions and three rotations, if there exist some moments. Each of these six deformation components is a function of coordinates and loads. Strains in a body can be introduced as a function of displacements. Equation 5.14 presents the relationship between normal strain and displacements related to normal stresses [36]. In the case of small strains and displacements, Equation 5.15 may be written for shear strains in three directions, related to shear stresses.

$$\varepsilon_{xx} = \frac{\partial u}{\partial x}, \varepsilon_{yy} = \frac{\partial v}{\partial y}, \varepsilon_{zz} = \frac{\partial w}{\partial z} \tag{5.14}$$

$$\varepsilon_{xy} = \varepsilon_{yx} = \frac{\partial u}{\partial y} + \frac{\partial v}{\partial x}, \varepsilon_{zy} = \varepsilon_{yz} = \frac{\partial w}{\partial y} + \frac{\partial v}{\partial z}, \varepsilon_{xz} = \varepsilon_{zx} = \frac{\partial u}{\partial z} + \frac{\partial w}{\partial x} \tag{5.15}$$

5.2.4 Variational form

Most of the problems can be formulated in accordance with one of these methods: 1- Differential equations, for example, Galerkin approach [38] ; and 2- Variational method. Finite element formulation can be extracted by applying one of these two methods [38]. We use the minimum potential energy by applying the variational principles to extract the formulation.

Galerkin method

If the unknown function $\boldsymbol{u}$ is approximated by the following equation:

$$\boldsymbol{u} \approx \hat{\boldsymbol{u}} = \sum_{1}^{n} \boldsymbol{N}_i \boldsymbol{a}_i = \boldsymbol{N}\boldsymbol{a} \tag{5.16}$$

And the following statement in domain $\boldsymbol{\Omega}$ with boundary Γ shall be satisfied:

$$\int_{\Omega} \boldsymbol{V}^T \boldsymbol{A}(\boldsymbol{u})\, d\Omega + \int_{\Gamma} \overline{\boldsymbol{V}}^T \boldsymbol{B}(\boldsymbol{u})\, d\Gamma = 0 \tag{5.17}$$

A finite set of approximation can be put in place of $\boldsymbol{V}$:

$$\boldsymbol{V} = \sum_{j=1}^{n} \boldsymbol{w}_j \delta \boldsymbol{a}_j\,,\ \overline{\boldsymbol{V}} = \sum_{j=1}^{n} \overline{\boldsymbol{w}}_j \delta \boldsymbol{a}_j, \tag{5.18}$$

$$\delta \boldsymbol{a}_j = arbitary\ parameters\ and\ n = number\ of\ unknowns$$

$$\int_{\Omega} \boldsymbol{w}_j{}^T \boldsymbol{A}(\boldsymbol{N}\boldsymbol{a})\, d\Omega + \int_{\Gamma} \overline{\boldsymbol{w}_j}^T \boldsymbol{B}(\boldsymbol{N}\boldsymbol{a})\, d\Gamma = 0, j = 1\ to\ n \tag{5.19}$$

$\boldsymbol{A}(\boldsymbol{N}\boldsymbol{a})$ represents the residual or error obtained by the substation of the approximation into the differential equation and $\boldsymbol{B}(\boldsymbol{N}\boldsymbol{a})$ the residual of the boundary conditions. Equation 5.19 is the weighted integral of errors or

residuals. Almost any set of functions $\boldsymbol{w}_j$ may be used. The Galerkin method assumes $\boldsymbol{w}_j = \boldsymbol{N}_j$. The original shape functions are used as weighting [38].

Variational principle

A variational principle gives a scalar quantity (for example, potential energy), which is defined by the following integral:

$$\Pi = \int_v F\left(\boldsymbol{u}, \frac{\partial \boldsymbol{u}}{\partial x}, \dots\right) dv + \int_s E\left(\boldsymbol{u}, \frac{\partial \boldsymbol{u}}{\partial x}, \dots\right) ds \tag{5.20}$$

$\boldsymbol{u}$ is the unknown function and *F* and *E* are differential operations. The solution of the problem is a function $\boldsymbol{u}$ which minimizes the variational Π. If a variational form can be written for a problem, it means the approximate solution of the problem can be found by applying the variational principle [38]. The function $\boldsymbol{u}$ shall be approximated as follows:

$$\boldsymbol{u} \approx \hat{\boldsymbol{u}} = \sum_1^n \boldsymbol{N}_i \boldsymbol{a}_i \rightarrow \boldsymbol{u} = \hat{\boldsymbol{u}}(\boldsymbol{a}_1 + \boldsymbol{a}_2 + \cdots) \tag{5.21}$$

$\boldsymbol{N}_i$ are the shape functions. To minimize the variational function:

$$\frac{\delta \Pi}{\delta \boldsymbol{a}} = \begin{bmatrix} \frac{\delta \Pi}{\delta \boldsymbol{a}_1} \\ \vdots \\ \frac{\delta \Pi}{\delta \boldsymbol{a}_n} \end{bmatrix} = 0 \tag{5.22}$$

Parameters $\boldsymbol{a}_i$ will be found as the solution of the variational function.

The potential energy of an elastic body π_p is defined as:

$$\pi_p = Internal\ work\ done\ by\ stress\ or\ strain\ energy - External\ work\ done\ by\ forces = \pi - W_{ext} \tag{5.23}$$

The principle of minimum energy states: If there are some possible displacement states for a body (*u*, *v, w*) under some loads, displacements that satisfy the kinematic or displacement boundary conditions and the equilibrium, make the potential energy function π_p minimum. For example, a piece of spherical stone placed in a bowl moves to the bottom and rests there, till new loads are applied to it. Therefore, each body in equilibrium has the lowest possible potential energy. This principle is also valid for fluids. If the potential energy of the body is a function of displacements, and forces and stresses are assumed to be constant, we can write:

$$\pi_p(u, v, w) = \pi(u, v, w) - W_{ext}(u, v, w) \tag{5.24}$$

If *V* denotes the volume of the body and *T* the transpose operation in matrix algebra, the strain energy or the amount of work done by stress is (this work is equal to the area under the stress–strain curve):

$$\pi(u,v,w) = \frac{1}{2}\iiint_V [\boldsymbol{\varepsilon}]^T[\boldsymbol{\sigma}]dv \rightarrow \tag{5.25}$$

$$\pi(u,v,w) = \frac{1}{2}\iiint_V \begin{bmatrix}\varepsilon_{xx} & \varepsilon_{yy} & \varepsilon_{zz} & \varepsilon_{xy} & \varepsilon_{yz} & \varepsilon_{zx}\end{bmatrix}\begin{bmatrix}\sigma_{xx}\\ \sigma_{yy}\\ \sigma_{zz}\\ \sigma_{xy}\\ \sigma_{yz}\\ \sigma_{zx}\end{bmatrix}dv$$

If there is some initial strain $[\varepsilon_0]$ in the body, and using the stress–strain relationship in accordance with Equation 5.13, we can write:

$$\begin{aligned}\pi(u,v,w) &= \frac{1}{2}\iiint_V [\boldsymbol{\varepsilon}]^T[\boldsymbol{D}]([\boldsymbol{\varepsilon}] - 2[\boldsymbol{\varepsilon_0}])dv \\ &= \frac{1}{2}\iiint_V [\boldsymbol{\varepsilon}]^T[\boldsymbol{D}][\boldsymbol{\varepsilon}]dv - \iiint_V [\boldsymbol{\varepsilon}]^T[\boldsymbol{D}][\boldsymbol{\varepsilon_0}]dv\end{aligned} \tag{5.26}$$

The first term of Equation 5.26 represents the amount of work done by stress due to new strains, and the second term the amount of work done by stress due to initial strains. Initial strain can be, for example, thermal strain. The work done by external forces can be expressed as:

$$W_{ext} = \iiint_V [\boldsymbol{B}]^T[\boldsymbol{U}]dv + \iint_S [\boldsymbol{P}]^T[\boldsymbol{U}]ds \tag{5.27}$$

$$\text{Where } [\boldsymbol{U}] = \begin{bmatrix}u\\ v\\ w\\ \theta_x\\ \theta_y\\ \theta_z\end{bmatrix}, [\boldsymbol{b}] = \begin{bmatrix}b_x\\ b_y\\ b_z\end{bmatrix}, [\boldsymbol{P}] = \begin{bmatrix}P_x\\ P_y\\ P_z\\ M_x\\ M_y\\ M_z\end{bmatrix}$$

$[\boldsymbol{P}]$ is the surface force and moment vector and $[\boldsymbol{b}]$ is the body force vector. It can be noticed that the energy terms related to rotations are just included in external terms. By substituting Equations 5.26 and 5.27 into Equation 5.24, we can write the potential energy function of a deformed body as follows:

$$\begin{aligned}\pi_p = I &= \frac{1}{2}\iiint_V [\boldsymbol{\varepsilon}]^T[\boldsymbol{D}][\boldsymbol{\varepsilon}]dv - \iiint_V [\boldsymbol{\varepsilon}]^T[\boldsymbol{D}][\boldsymbol{\varepsilon_0}]dv \\ &\quad - \iiint_V [\boldsymbol{b}]^T[\boldsymbol{U}]dv - \iint_S [\boldsymbol{P}]^T[\boldsymbol{U}]ds\end{aligned} \tag{5.28}$$

The minimization of Equation 5.28 leads to the deformed form of the body that satisfies the boundary conditions and equilibrium. To minimize Equation 5.28, the deformation vector $[u \quad v \quad w]$, which satisfies Equation 5.29, will be found. To achieve this, the derivatives of Equation 5.28 with respect to deformations u_i will be taken.

$$\frac{\partial I}{\partial u_i} = 0 \tag{5.29}$$

5.3 Finite element formulation of frame elements

5.3.1 Formulation

The variational principle and minimum potential energy have been applied to derive the three-dimensional equation of equilibrium for an element. As explained in Section 5.2.4, the function of potential energy is assumed to be a function of nodal displacements (see Equation 5.26). The partial derivatives of variational function will be taken and set equal to zero. In Section 4.6, the derivation of FEM formulation for heat transfer problems was divided into six steps. Here, we will again state the process of extracting FEM formulation in solid mechanics problems in some steps, as follows:

Step 1: Defining the finite element mesh

The current study deals with the framed structures, which are modelled by line elements. The structure will be divided into some lines that are normally the centreline or the neutral axis of elements. It is not possible to model all structures as framed members. Some structures like houses, offices, hospitals, and industrial buildings can normally be modelled as framed ones.

Step 2: The displacement function or shape functions

In case of line elements, there are two nodes at both ends, which are boundaries of the element. If we approximate the displacement at any point within the element as a function of nodal displacement:

$$[\boldsymbol{u}] \approx [\widehat{\boldsymbol{u}}] = \sum_{nodes} N_{nodes} a_{nodes} = [N_i \quad N_j \quad ...] \begin{bmatrix} a_i \\ a_j \\ \vdots \end{bmatrix} = [\boldsymbol{N}][\boldsymbol{a}] \tag{5.30}$$

N_i are the shape functions, they relate nodal displacements, while a_i are nodal displacements for element *e*.

Step 3: Variational form of equations

The variational function and its derivatives related to deformations will be written. See Eq. 5.28.

Step 4: Element and global stiffness matrix

Strain and internal and external forces will be inserted into Equation 5.28. Therefore:

$$[\boldsymbol{\varepsilon}] = \begin{bmatrix} \varepsilon_{xx} \\ \varepsilon_{yy} \\ \varepsilon_{zz} \\ \varepsilon_{xy} \\ \varepsilon_{yz} \\ \varepsilon_{zx} \end{bmatrix} = \begin{bmatrix} \frac{\partial u}{\partial x} \\ \frac{\partial v}{\partial y} \\ \frac{\partial w}{\partial z} \\ \frac{\partial u}{\partial y} + \frac{\partial v}{\partial x} \\ \frac{\partial v}{\partial z} + \frac{\partial w}{\partial y} \\ \frac{\partial u}{\partial z} + \frac{\partial w}{\partial x} \end{bmatrix} = \begin{bmatrix} \frac{\partial}{\partial x} & 0 & 0 \\ 0 & \frac{\partial}{\partial y} & 0 \\ 0 & 0 & \frac{\partial}{\partial z} \\ \frac{\partial}{\partial y} & \frac{\partial}{\partial x} & 0 \\ 0 & \frac{\partial}{\partial z} & \frac{\partial}{\partial y} \\ \frac{\partial}{\partial z} & 0 & \frac{\partial}{\partial x} \end{bmatrix} \begin{bmatrix} u \\ v \\ w \end{bmatrix} = [\boldsymbol{B}][\boldsymbol{U}] \tag{5.31}$$

$$[\boldsymbol{\varepsilon}]^T[\boldsymbol{D}][\boldsymbol{\varepsilon}] = [\boldsymbol{U}]^T[\boldsymbol{B}]^T[\boldsymbol{D}][\boldsymbol{B}][\boldsymbol{U}] \tag{5.32}$$

$$[\boldsymbol{\varepsilon}]^T[\boldsymbol{D}][\boldsymbol{\varepsilon_0}] = [\boldsymbol{U}]^T[\boldsymbol{B}]^T[\boldsymbol{D}][\boldsymbol{\varepsilon_0}] \tag{5.33}$$

By substituting Equations 5.32 and 5.33 into Equation 5.28:

$$\begin{aligned} {\pi_p}^e = I^e = \frac{1}{2}\iiint_V [\boldsymbol{U}]^T[\boldsymbol{B}]^T[\boldsymbol{D}][\boldsymbol{B}][\boldsymbol{U}]dv - \iiint_V [\boldsymbol{U}]^T[\boldsymbol{B}]^T[\boldsymbol{D}][\boldsymbol{\varepsilon_0}]dv \\ - \iiint_V [\boldsymbol{U}]^T[\boldsymbol{N}]^T[\boldsymbol{b}]dv - \iint_S [\boldsymbol{U}]^T[\boldsymbol{N}]^T[\boldsymbol{P}]ds \end{aligned} \tag{5.34}$$

Equation 5.34 is the total potential energy of an element. To obtain the total potential energy of the whole system:

$$\begin{aligned} \pi_p = \sum_{e=1}^{E} {\pi_p}^e = \sum_{e=1}^{E} \Bigg(\frac{1}{2}\iiint_V [\boldsymbol{U}]^T[\boldsymbol{B}]^T[\boldsymbol{D}][\boldsymbol{B}][\boldsymbol{U}]dv \\ - \iiint_V [\boldsymbol{U}]^T[\boldsymbol{B}]^T[\boldsymbol{D}][\boldsymbol{\varepsilon_0}]dv - \iiint_V [\boldsymbol{U}]^T[\boldsymbol{N}]^T[\boldsymbol{b}]dv \\ - \iint_S [\boldsymbol{U}]^T[\boldsymbol{N}]^T[\boldsymbol{P}]ds \Bigg) \rightarrow \\ \pi_p = \frac{1}{2}[\boldsymbol{U}]^T \sum \left(\iiint_V [\boldsymbol{B}]^T[\boldsymbol{D}][\boldsymbol{B}]dv \right)[\boldsymbol{U}] - [\boldsymbol{U}]^T \sum \left(\iiint_V [\boldsymbol{B}]^T[\boldsymbol{D}][\boldsymbol{\varepsilon_0}]dv \right) \\ - [\boldsymbol{U}]^T \sum \left(\iiint_V [\boldsymbol{N}]^T[\boldsymbol{b}]dv \right) - [\boldsymbol{U}]^T \sum \left(\iint_S [\boldsymbol{N}]^T[\boldsymbol{P}]ds \right) \end{aligned} \tag{5.35}$$

Equation 5.35 is the total potential energy of a system as a function of displacement vector $[\boldsymbol{U}]$. To minimize Equation 5.35, its derivatives with respect to displacements (*u*, *v, w*) will be equal to zero.

$$\frac{\partial \pi_p}{\partial u_i} = \frac{\partial I}{\partial u_i} = 0 \rightarrow \frac{\partial \pi_p}{\partial u} = \frac{\partial \pi_p}{\partial v} = \frac{\partial \pi_p}{\partial w} = 0 \tag{5.36}$$

For example, in case of one-dimensional problems, we can write:

$$\begin{aligned} \pi_p = \frac{1}{2} u \sum \left(\iiint_V [\boldsymbol{B}]^T [\boldsymbol{D}][\boldsymbol{B}] dv \right) u \\ - u \sum \left(\iiint_V [\boldsymbol{B}]^T [\boldsymbol{D}][\boldsymbol{\varepsilon_0}] dv \right) \\ - u \sum \left(\iiint_V [\boldsymbol{N}]^T [\boldsymbol{b}] dv \right) - u \sum \left(\iint_S [\boldsymbol{N}]^T [\boldsymbol{P}] ds \right) \\ \rightarrow \end{aligned} \tag{5.37}$$

$$\begin{aligned} \frac{\partial \pi_p}{\partial u} = \sum \left(\iiint_V [\boldsymbol{B}]^T [\boldsymbol{D}][\boldsymbol{B}] dv \right) u - \sum \left(\iiint_V [\boldsymbol{B}]^T [\boldsymbol{D}][\boldsymbol{\varepsilon_0}] dv \right) \\ - \sum \left(\iiint_V [\boldsymbol{N}]^T [\boldsymbol{b}] dv \right) - \sum \left(\iint_S [\boldsymbol{N}]^T [\boldsymbol{P}] ds \right) \end{aligned} \tag{5.38}$$

One-dimensional formulation is valid for truss structures or axially loaded members (tension or compression). Two-dimensional and three-dimensional forms of Equation 5.37 can be written in a similar manner. Defining:

$$[K]_e = element\ stiffness\ matrix = \iiint_V [\boldsymbol{B}]^T [\boldsymbol{D}][\boldsymbol{B}] dv \tag{5.39}$$

$$\begin{aligned} [P]_{e,initial} &= element\ force\ vector\ due\ to\ initial\ strain \\ &= \sum \left(\iiint_V [\boldsymbol{B}]^T [\boldsymbol{D}][\boldsymbol{\varepsilon_0}] dv \right) \end{aligned} \tag{5.40}$$

$$\begin{aligned} [F]_{e,body} &= element\ force\ vector\ due\ to\ body\ forces\ like\ self \\ &- weight = \iiint_V [\boldsymbol{N}]^T [\boldsymbol{b}] dv \end{aligned} \tag{5.41}$$

$$\begin{aligned} [F]_{e,surface} &= element\ force\ vector\ due\ to\ surface\ forces \\ &= \iint_S [\boldsymbol{N}]^T [\boldsymbol{P}] ds \end{aligned} \tag{5.42}$$

Therefore, Equation 5.38 can be written in the following form:

$$\left(\sum_{e=1}^{E} [K]_e \right) [\boldsymbol{U}] - \sum_{e=1}^{E} \left([P]_{e,ini.} + [F]_{e,b.} + [F]_{e,sur.} \right) - \sum_{i=1}^{Node} \left([P]_{i,con.} \right) = 0 \tag{5.43}$$

$[P]_{i,con.}$ is the nodal concentrated force vector in the global coordinate system. In some cases, some terms of Equation 5.43 can be zero. For example, in the absence of initial conditions, $[P]_{e,initial}$ may be zero. Boundary elements or elements without actions have zero surface loads. The surface force vector of an element can consist of force and moments in three directions, generally six

components. Equation 5.43 gives the equilibrium of the desired structure and can be written as follows:

$$[\boldsymbol{K}][\boldsymbol{U}] = [\boldsymbol{P}] \tag{5.44}$$

$[\boldsymbol{K}]$ is the stiffness matrix of the system, $[\boldsymbol{P}]$ the total force vector, and $[\boldsymbol{U}]$ nodal displacements. Equation 5.44 is a system of equations consisting of *n* unknown parameters or degrees of freedom. The number of the degrees of freedom depends on element type and unknown displacements. For example, for three-dimensional frame elements, there are three displacements and three rotations at each node. A three-dimensional frame element includes at least two nodes. Hence, the element stiffness matrix consists of 12 rows and 12 columns.

Step 5: Solution

The solution of Equation 5.44 for steady state and linear problems can be simply obtained as follows:

$$[\boldsymbol{U}] = [\boldsymbol{K}]^{-1}[\boldsymbol{P}] \tag{5.45}$$

- The formation of the FEM formulation requires evaluation of integrals of Equations 5.39, 5.40, 5.41, and 5.42. For some elements, integration is simple, but in most cases, integration will be carried out by numerical methods.
- The order of the element stiffness matrix and load vector depends on the degrees of freedom and element.
- The element stiffness matrix and total stiffness matrix are always symmetric.
- To calculate the integrals of stiffness matrix and load vectors, it is more convenient and simpler to use the local coordinate system of elements. To obtain the matrices in the global coordinate system, a transformation matrix can be used. Transformation of loads, displacements, and stiffness matrices can be complicated, especially in nonlinear systems, where it requires more attention because it can cause inaccuracy or errors.
- When the stiffness matrix is singular, it is not inversible, and there is more than one possible solution for Equation 5.44. A singular stiffness matrix represents a rigid body motion of a structure. Every displacement vector that describes rigid body motion of the structure in space might be the solution of Equation 5.44. To prevent this, the effects of boundary conditions and supports will be considered in the formation of the stiffness matrix. Columns and rows related to supported nodes will be removed from the stiffness matrix and load vector.

5.3.2 Coordinate transformation

Normally, it is more convenient to obtain the characteristics of an element in a coordinate system that is attached to an element. External forces and displacements are measured in a global coordinate system. Therefore, there will be always two or more coordinate systems—local and global. The solution of the system of equations and results are always in the global coordinate system while integrations are done in the local coordinate system. Before the element equations can be assembled, it is necessary to transform the element matrices and vectors derived in local coordinate systems, so that all the elemental equations are referred to a common global coordinate system. The transformation of coordinates can be simply performed by transformation matrix. In linear algebra, linear transformations can be represented by matrices. If *T* is a linear transformation mapping a space to another space and $[\boldsymbol{X}]$ is a column vector with *n* entries, then:

$$T([\boldsymbol{X}]) = [\boldsymbol{A}][\boldsymbol{X}] \tag{5.46}$$

The $m \times n$ matrix $\boldsymbol{A}$ is called the transformation matrix of T. [43]. Therefore, the displacement components of an element can be simply transformed as follows:

$$[\boldsymbol{a}]_{loc.} = [\boldsymbol{A}][\boldsymbol{a}]_{glob.} \tag{5.47}$$

The amount of work or virtual work done by external and internal forces in both local and global systems will be the same:

$$[\boldsymbol{F}]^T_{loc.}[\boldsymbol{a}]_{loc.} = [\boldsymbol{F}]^T_{glob.}[\boldsymbol{a}]_{glob.} \rightarrow [\boldsymbol{F}]^T_{loc.}[\boldsymbol{A}][\boldsymbol{a}]_{glob.} = [\boldsymbol{F}]^T_{glob.}[\boldsymbol{a}]_{glob.} \tag{5.48}$$
$$\rightarrow [\boldsymbol{F}]^T_{loc.}[\boldsymbol{A}] = [\boldsymbol{F}]^T_{glob.} \rightarrow [\boldsymbol{F}]_{glob.} = [\boldsymbol{A}]^T[\boldsymbol{F}]_{loc.}$$

To obtain the transformated stiffness matrix, an analogous procedure will be applied:

$$[\boldsymbol{F}]_{loc.} = [\boldsymbol{K}]_{loc.}[\boldsymbol{a}]_{loc.} and\ [\boldsymbol{F}]_{glob.} = [\boldsymbol{K}]_{glob.}[\boldsymbol{a}]_{glob.} \tag{5.49}$$
$$\rightarrow [\boldsymbol{A}]^T[\boldsymbol{F}]_{loc.} = [\boldsymbol{K}]_{glob.}[\boldsymbol{A}]^T[\boldsymbol{a}]_{loc.} \rightarrow [\boldsymbol{F}]_{loc.} = [\boldsymbol{A}][\boldsymbol{K}]_{glob.}[\boldsymbol{A}]^T[\boldsymbol{a}]_{loc.}$$
$$\rightarrow [\boldsymbol{K}]_{loc.} = [\boldsymbol{A}][\boldsymbol{K}]_{glob.}[\boldsymbol{A}]^T\ and\ [\boldsymbol{K}]_{glob.} = [\boldsymbol{A}]^T[\boldsymbol{K}]_{loc.}[\boldsymbol{A}]$$

The coordinate transformation is necessary when the field variable is a vector quantity, such as displacement or velocity. The solution of a problem does not depend on coordinate systems. Depending on the element and degrees of freedom, the size of the transformation matrix can vary. The transformation matrix of frame elements in three-dimensional space will be presented in Section 5.6.

5.4 Linear beam element

One-dimensional structural elements or lines are considered to model the behaviour of framed structures. These elements can be used to mathematize the skeletal-type structures, such as trusses, beams, girders, and space frames.

A truss element is able to resist only axial forces, including tension and compression forces. Truss members can deform in just the axial direction. If there exist some transverse forces, bending moments will not be zero. A frame or a beam element is a bar able to resist axial and transverse forces and bending moments. For a space frame (see Figure 5-4), each end of the frame element will have three translational displacement components (three translational degrees of freedom) and three rotational components. In the present study, frames are assumed to be uniform (a cross-section of a frame does not change along it).

5.4.1 Axial deformation

As explained in Section 5.4, five steps have to be fulfilled to obtain the FEM formulation of problems of solid mechanics. Step One has been already done and the frame element has been selected to build the mathematized model. The next step entails determination of the shape functions, as follows:

$$u \approx \hat{u} = \sum_{1}^{n} N_i a_i = N_i u_i + N_j u_j \tag{5.50}$$

$$[\boldsymbol{N}] = [N_i \quad N_j] = \left[1 - \frac{x}{l} \quad \frac{x}{l}\right], [\boldsymbol{U}]^T = [u_i \quad u_j] \tag{5.51}$$

u_i and u_j are shown in Figure 5-4 and N_i and N_j are shape functions that give the relationship between deformation of any point within the element and deformation of nodes i and j. l is the length of element and x is the distance from end i, measured in the local coordinate system. The origin of the local coordinate system is assumed to be attached to node i and its *x*-axis is parallel to the frame.

$$\varepsilon_{xx} = \frac{\partial u}{\partial x} = \frac{u_j - u_i}{l} = [\boldsymbol{B}][\boldsymbol{U}] \tag{5.52}$$

$$[\boldsymbol{B}][\boldsymbol{U}] = \left[-\frac{1}{l} \quad \frac{1}{l}\right] \begin{bmatrix} u_i \\ u_j \end{bmatrix} \tag{5.53}$$

The stress-strain relationship in one-dimensional form can be written as follows; see Eq. 5.13:

$$\sigma_{xx} = [E](\varepsilon_{xx} - \varepsilon_{xx0}) \tag{5.54}$$

For the stiffness matrix which explains the axial behaviour of a space element:

$$[K]_e = \iiint_V [\boldsymbol{B}]^T [\boldsymbol{D}][\boldsymbol{B}] dv = A \int_{x=0}^{l} \begin{bmatrix} -\frac{1}{l} \\ \frac{1}{l} \end{bmatrix} E \left[-\frac{1}{l} \quad \frac{1}{l}\right] dx \tag{5.55}$$

Equation 5.55 gives the stiffness matrix (related to the axial behaviour of a beam) in the local coordinate system. Body force load vector, initial strains like thermal strain, and surface forces can be calculated as follows:

$$[P]_{e,i} = \sum \left(\iiint_V [\boldsymbol{B}]^T [\boldsymbol{D}][\boldsymbol{\varepsilon_0}] dv \right) = AE\alpha\Delta T \int_{x=0}^{l} \begin{bmatrix} -\frac{1}{l} \\ \frac{1}{l} \end{bmatrix} dx \tag{5.56}$$

$$[F]_{e,b} = \iiint_V [\boldsymbol{N}]^T [\boldsymbol{b}] dv = A \int_{x=0}^{l} \begin{bmatrix} 1 - \frac{x}{l} \\ \frac{x}{l} \end{bmatrix} b dx = \begin{bmatrix} \frac{bAl}{2} \\ \frac{bAl}{2} \end{bmatrix} \tag{5.57}$$

If there are some axial distributed loads parallel to Axis 1 in the local coordinate system, we have (see Figure 5-5):

$$[F]_{e,s} = \iint_S [\boldsymbol{N}]^T [\boldsymbol{P}] ds = \int_{x=0}^{l} \begin{bmatrix} 1 - \frac{x}{l} \\ \frac{x}{l} \end{bmatrix} q_{xx} dx = \begin{bmatrix} \frac{q_{xx} l}{2} \\ \frac{q_{xx} l}{2} \end{bmatrix} \tag{5.58}$$

5.4.2 Bending deformations

Beams are subjected to transverse loads. Deformation of a beam is described by the transverse displacement and the rotation or slope of the beam. Therefore, there are two translational and two rotational degrees of freedom at each end of the beam element, related to the bending behaviour of the beam (see Figure 5-5). Positive rotations are counter-clockwise or the rotation vector is in the positive direction of the coordinate system. The vector of the degrees of freedom related to the bending behaviour of a beam is (in the local coordinate system):

$$[\boldsymbol{U}]^T{}_{bending} = [v_i \quad w_i \quad \theta_{2i} \quad \theta_{3i} \quad v_j \quad w_j \quad \theta_{2j} \quad \theta_{3j}] \tag{5.59}$$

Shape function vectors to estimate the deformation of a beam are:

$$[\boldsymbol{N}] = [N_1 \quad N_2 \quad N_3 \quad N_4 \quad N_5 \quad N_6 \quad N_7 \quad N_8] \rightarrow \tag{5.60}$$

$$[\boldsymbol{N}]^T = \begin{bmatrix} \frac{2x^3 - 3lx^2 + l^3}{l^3} \\ \frac{2x^3 - 3lx^2 + l^3}{l^3} \\ \frac{x^3 - 2lx^2 + l^2x}{l^2} \\ \frac{x^3 - 2lx^2 + l^2x}{l^2} \\ -\frac{2x^3 - 3lx^2}{l^3} \\ -\frac{2x^3 - 3lx^2}{l^3} \\ \frac{x^3 - lx^2}{l^2} \\ \frac{x^3 - lx^2}{l^2} \end{bmatrix}$$

It can be noticed that rotation of beam $\theta_{3i,j}$ and $\theta_{2i,j}$ are derivatives of deformations:

$$\theta_{3i} = \frac{dv_i}{dx}, \theta_{2i} = \frac{dw_i}{dx} \; at \; x = 0 \tag{5.61}$$

$$\theta_{3j} = \frac{dv_j}{dx}, \theta_{2j} = \frac{dw_j}{dx} \; at \; x = l$$

x is defined in the local coordinate system, as shown in Figures 5-4 and 5-5. j and i indicate the end points of the element.

To calculate the deformation of a beam, the simple beam theory or Euler beam theory can be applied. The Euler-Bernoulli beam theory (also known as engineer's beam theory or classical beam theory) [44] considers the linear theory of elasticity, which provides a mean to calculate the load-carrying and deflection characteristics of beams. Euler beam theory covers small bending deflections. It is a simplified Timoshenko beam and does not consider deformations related to shear strain and cannot be applied to deep beams and columns. The theory describes the bending deflection of beams as follows:

$$\frac{d^2}{dx^2}\left(EI_{yy}\frac{d^2w}{dx^2}\right) = q_{zz} \; For \; bending \; about \; local \; axis \; y \; (2) \tag{5.62}$$

$$\frac{d^2}{dx^2}\left(EI_{zz}\frac{d^2v}{dx^2}\right) = q_{yy} \; For \; bending \; about \; local \; axis \; z \; (3) \tag{5.63}$$

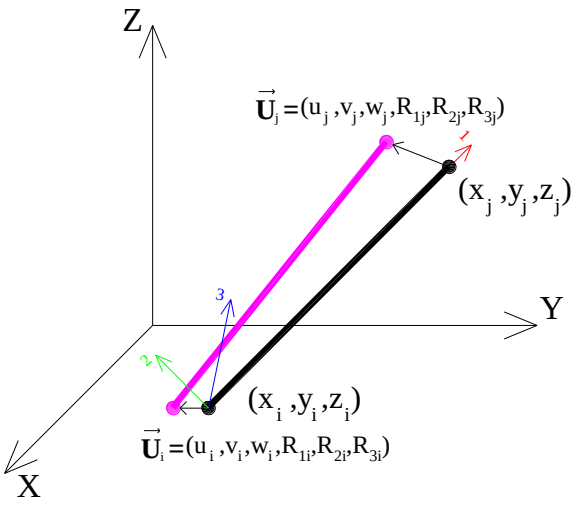

Figure 5-4: Three-dimensional frame element and global and local coordinate systems

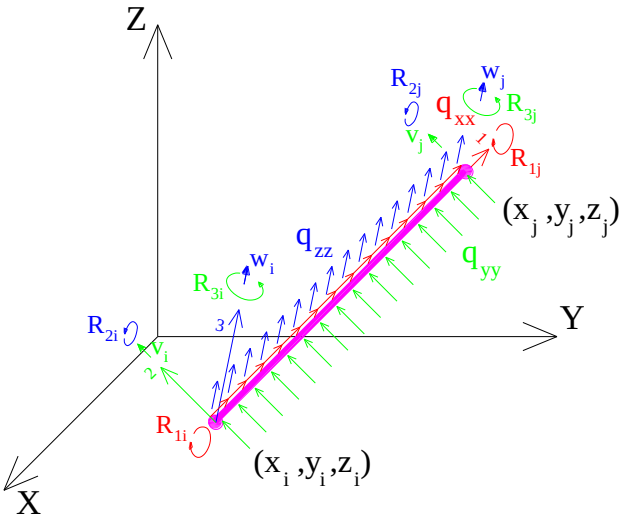

Figure 5-5: Deformations and distributed loads applied to a frame element

$w(x)$ and $v(x)$ describe the bending deflection of a beam and $\frac{dv(x)}{dx}$ and $\frac{dw(x)}{dx}$ give the rotation of beam about local *z* and *y* axes. q_{yy} and q_{zz} are distributed loads as a function of *x*. I_{zz} and I_{yy} are the second moment of inertia and *E* is the modulus of elasticity. EI is named the bending stiffness or flexural rigidity and is the main parameter in the current research. EI is assumed to be variable as a function of the temperature curve. To obtain EI_{zz} and EI_{yy}, numerical integration over the cross-section has been used. In the case of constant modulus and second moment of inertia (uniform beam):

$$EI_{yy}\frac{d^4w}{dx^4}=q_{zz} \tag{5.64}$$

$$EI_{zz}\frac{d^4v}{dx^4}=q_{yy} \tag{5.65}$$

If we assume that the plane sections of the beam remain plane after deformation (Timoshenko beam), the axial displacement can be related to transverse deformation:

$$u=-y\frac{\partial v}{\partial x}\ For\ bending\ about\ local\ z\ axis \tag{5.66}$$

$$u=-z\frac{\partial w}{\partial x}\ For\ bending\ about\ local\ y\ axis \tag{5.67}$$

z and y are the distances from the neutral axis of the cross-section. The axial strain is:

$$\varepsilon_{xx} = \frac{\partial u}{\partial x} = -y\frac{\partial^2 v}{\partial x^2} - z\frac{\partial^2 w}{\partial x^2} = [\boldsymbol{B}][\boldsymbol{U}] \tag{5.68}$$

The element stiffness matrix and load vectors can be calculated with Equations 5.39–42. $[\boldsymbol{B}]$ matrix defines the differential equations between displacement and strains and can be found with the help of Equation 5.69.

$$[\boldsymbol{B}]^T = \begin{bmatrix} \frac{-y(12x-6l)}{l^3} \\ \frac{-z(12x-6l)}{l^3} \\ \frac{-z(6x-4l)}{l^2} \\ \frac{-y(6x-4l)}{l^2} \\ \frac{y(12-6l)}{l^3} \\ \frac{z(12-6l)}{l^3} \\ \frac{-z(6x-2l)}{l^2} \\ \frac{-y(6x-2l)}{l^2} \end{bmatrix} \tag{5.69}$$

5.4.3 Torsion

The torsional rotation of a bar can be estimated by linear variation along the beam as a function of beam length.

$$\varepsilon_{rotation,x} = r\frac{d\theta_x}{dx} \tag{5.70}$$

r is distance of the fibre from the centre of rotation or, here, centroidal axis of the cross section. θ_x is the rotation of beam (in radians) about *x* local axis or axis 1. Designers can prevent torsional deformation because they include unknown effects that cannot be modelled by simple theories of beams and columns. The developed code cannot consider variable torsional stiffness of cross-sections, but a constant torsional stiffness. The torsional stiffness is assumed to be constant while fire curves are being applied to the structure. Shape functions for torsion are similar to shape functions considered for axial displacement of the beam.

$$\theta_x \approx \widehat{\theta_x} = \sum_{1}^{n} N_i a_i = N_i\theta_{x,i} + N_j\theta_{x,j} \tag{5.71}$$

$$[\boldsymbol{N}] = [N_i \quad N_j] = \left[1 - \frac{x}{l} \quad \frac{x}{l}\right], [\boldsymbol{U}]^T = [\theta_{x,i} \quad \theta_{x,j}] \tag{5.72}$$

$$\varepsilon_{rotation,x} = [\boldsymbol{B}][\boldsymbol{U}] \tag{5.73}$$

$$[\boldsymbol{B}][\boldsymbol{U}] = \begin{bmatrix} -\frac{r}{l} & \frac{r}{l} \end{bmatrix} \begin{bmatrix} \theta_{x,i} \\ \\ \theta_{x,j} \end{bmatrix} \tag{5.74}$$

The stress-strain relationship for torsion can be written as follows:

$$\sigma_{rotation} = [G]\left(\varepsilon_{rotation,x}\right) \tag{5.75}$$

G is the shear modulus of the material. The stiffness matrix that explains the torsional behaviour of a uniform space beam in a local coordinate system is:

$$[K]_e = \iiint_V [\boldsymbol{B}]^T[\boldsymbol{D}][\boldsymbol{B}]dv = G\int_0^l dx \iint_A r^2 dA \begin{bmatrix} -\frac{1}{l} \\ \\ \frac{1}{l} \end{bmatrix} \begin{bmatrix} -\frac{1}{l} & \frac{1}{l} \end{bmatrix} \tag{5.76}$$

5.4.4 Stiffness matrix of space frames

If the axial, torsional, and bending components of the stiffness matrix are available, the stiffness matrix of a beam element in a local coordinate system can be written as follows:

	u^i	v^i	w^i	θ_x^i	θ_y^i	θ_z^i	u^j	v^j	w^j	θ_x^j	θ_y^j	θ_z^j
u^i	$\frac{EA}{l}$	0	0	0	0	0	$-\frac{EA}{l}$	0	0	0	0	0
v^i	0	$\frac{12EI_{zz}}{l^3}$	0	0	0	$\frac{6EI_{zz}}{l^2}$	0	$-\frac{12EI_{zz}}{l^3}$	0	0	0	$\frac{6EI_{zz}}{l^2}$
w^i	0	0	$\frac{12EI_{yy}}{l^3}$	0	$\frac{6EI_{yy}}{l^2}$	0	0	0	$-\frac{12EI_{yy}}{l^3}$	0	$\frac{6EI_{yy}}{l^2}$	0
θ_x^i	0	0	0	$\frac{GJ}{l}$	0	0	0	0	0	$-\frac{GJ}{l}$	0	0
θ_y^i	0	0	$\frac{6EI_{yy}}{l^2}$	0	$\frac{4EI_{yy}}{l}$	0	0	0	$-\frac{6EI_{yy}}{l^2}$	0	$\frac{2EI_{yy}}{l}$	0
θ_z^i	0	$\frac{6EI_{zz}}{l^2}$	0	0	0	$\frac{4EI_{zz}}{l}$	0	$-\frac{6EI_{zz}}{l^2}$	0	0	0	$\frac{2EI_{zz}}{l}$
u^j	$-\frac{EA}{l}$	0	0	0	0	0	$\frac{EA}{l}$	0	0	0	0	0
v^j	0	$-\frac{12EI_{zz}}{l^3}$	0	0	0	$-\frac{6EI_{zz}}{l^2}$	0	$\frac{12EI_{zz}}{l^3}$	0	0	0	$-\frac{6EI_{zz}}{l^2}$
w^j	0	0	$-\frac{12EI_{yy}}{l^3}$	0	$-\frac{6EI_{yy}}{l^2}$	0	0	0	$\frac{12EI_{yy}}{l^3}$	0	$-\frac{6EI_{yy}}{l^2}$	0
θ_x^j	0	0	0	$-\frac{GJ}{l}$	0	0	0	0	0	$\frac{GJ}{l}$	0	0
θ_y^j	0	0	$\frac{6EI_{yy}}{l^2}$	0	$\frac{2EI_{yy}}{l}$	0	0	0	$-\frac{6EI_{yy}}{l^2}$	0	$\frac{4EI_{yy}}{l}$	0
θ_z^j	0	$\frac{6EI_{zz}}{l^2}$	0	0	0	$\frac{2EI_{zz}}{l}$	0	$-\frac{6EI_{zz}}{l^2}$	0	0	0	$\frac{4EI_{zz}}{l}$

Figure 5-6: Linear portion of the stiffness matrix of a space frame

As mentioned earlier, the stiffness matrix is calculated in the local coordinate system and will be transformed to the global coordinate system. Equations 5.39–43 give the global stiffness matrix, displacement vector, and force vector for a space frame as follows:

$$\begin{bmatrix} U^i \\ V^i \\ W^i \\ \theta_X^i \\ \theta_Y^i \\ \theta_Z^i \\ U^j \\ V^j \\ W^j \\ \theta_X^j \\ \theta_Y^j \\ \theta_Z^j \end{bmatrix} = \begin{bmatrix} l_1 & m_1 & n_1 & 0 & 0 & 0 & 0 & 0 & 0 & 0 & 0 & 0 \\ l_2 & m_2 & n_2 & 0 & 0 & 0 & 0 & 0 & 0 & 0 & 0 & 0 \\ l_3 & m_3 & n_3 & 0 & 0 & 0 & 0 & 0 & 0 & 0 & 0 & 0 \\ 0 & 0 & 0 & l_1 & m_1 & n_1 & 0 & 0 & 0 & 0 & 0 & 0 \\ 0 & 0 & 0 & l_2 & m_2 & n_2 & 0 & 0 & 0 & 0 & 0 & 0 \\ 0 & 0 & 0 & l_3 & m_3 & n_3 & 0 & 0 & 0 & 0 & 0 & 0 \\ 0 & 0 & 0 & 0 & 0 & 0 & l_1 & m_1 & n_1 & 0 & 0 & 0 \\ 0 & 0 & 0 & 0 & 0 & 0 & l_2 & m_2 & n_2 & 0 & 0 & 0 \\ 0 & 0 & 0 & 0 & 0 & 0 & l_3 & m_3 & n_3 & 0 & 0 & 0 \\ 0 & 0 & 0 & 0 & 0 & 0 & 0 & 0 & 0 & l_1 & m_1 & n_1 \\ 0 & 0 & 0 & 0 & 0 & 0 & 0 & 0 & 0 & l_2 & m_2 & n_2 \\ 0 & 0 & 0 & 0 & 0 & 0 & 0 & 0 & 0 & l_3 & m_3 & n_3 \end{bmatrix} \times \begin{bmatrix} u^i \\ v^i \\ w^i \\ \theta_x^i \\ \theta_y^i \\ \theta_z^i \\ u^j \\ v^j \\ w^j \\ \theta_x^j \\ \theta_y^j \\ \theta_z^j \end{bmatrix} \tag{5.77}$$

We define:

$$[\boldsymbol{A}] = \begin{bmatrix} l_1 & m_1 & n_1 \\ l_2 & m_2 & n_2 \\ l_3 & m_3 & n_3 \end{bmatrix} \tag{5.78}$$

l_1, m_1, and n_1 are the direction cosines of a line exactly on frame element in space or local *x* axis. Nodes *i* and *j* are located at both ends of line. l_2, m_2, and n_2 are the direction cosines of *y* axis and l_3, m_3, and n_3 indicate the directions cosines of *z* axis of local coordinate system with respect to the global coordinate system. Local and global coordinate systems are shown in Figures 5-4 and 5-5. The direction cosines (or directional cosines) of a vector are the cosines of the angles between the vector and the three coordinate axes [45]. Imagine line *i-j* or *x* axis of local coordinate system as a vector named $[\boldsymbol{V}]$. Direction cosines of vector $[\boldsymbol{V}]$ shown in Figure 5-7 are:

$$l_1 = \cos(a) = \frac{\boldsymbol{V}.\boldsymbol{e}_X}{|\boldsymbol{V}|} = \frac{X_j - X_i}{l} \tag{5.79}$$

$$m_1 = \cos(b) = \frac{\boldsymbol{V}.\boldsymbol{e}_Y}{|\boldsymbol{V}|} = \frac{Y_j - Y_i}{l} \tag{5.80}$$

$$n_1 = \cos(c) = \frac{\boldsymbol{V}.\boldsymbol{e}_Z}{|\boldsymbol{V}|} = \frac{Z_j - Z_i}{l} \tag{5.81}$$

X, *Y,* and *Z* indicate the coordinate of end points of line *i-j* in the global coordinate system. To determine the other components, the following equations will be applied:

$$l_3 = \frac{-n_1}{\sqrt{l_1^2 + n_1^2}}, \qquad m_3 = 0, \qquad n_3 = \frac{l_1}{\sqrt{l_1^2 + n_1^2}} \tag{5.82}$$

$$l_2 = \frac{-l_1 m_1}{\sqrt{l_1^2 + n_1^2}}, \qquad m_2 = \frac{l_1^2 + n_1^2}{\sqrt{l_1^2 + n_1^2}}, \qquad n_2 = \frac{-n_1 m_1}{\sqrt{l_1^2 + n_1^2}} \tag{5.83}$$

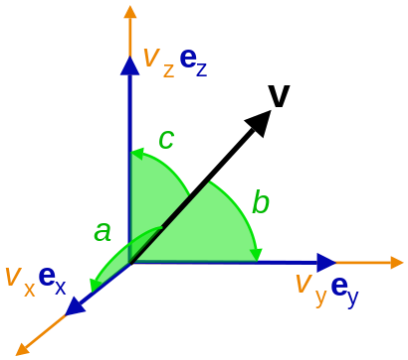

Figure 5-7: Direction cosines of vector $[\boldsymbol{V}]$, $\boldsymbol{e}_X$, $\boldsymbol{e}_Y$, and $\boldsymbol{e}_Z$ form the standard basis of the global Cartesian coordinate system

Finally, the transformation matrix from the global coordinate system to the local system can be determined by Equation 5.78:

$$[\boldsymbol{A}] = \begin{bmatrix} l_1 & m_1 & n_1 \\ l_2 & m_2 & n_2 \\ l_3 & m_3 & n_3 \end{bmatrix} = \begin{bmatrix} l_1 = \dfrac{X_j - X_i}{l} & m_1 = \dfrac{Y_j - Y_i}{l} & n_1 = \dfrac{Z_j - Z_i}{l} \\ \dfrac{-l_1 m_1}{\sqrt{l_1^2 + n_1^2}} & \dfrac{l_1^2 + n_1^2}{\sqrt{l_1^2 + n_1^2}} & \dfrac{-n_1 m_1}{\sqrt{l_1^2 + n_1^2}} \\ \dfrac{-n_1}{\sqrt{l_1^2 + n_1^2}} & 0 & \dfrac{l_1}{\sqrt{l_1^2 + n_1^2}} \end{bmatrix} \tag{5.84}$$

In some cases, the cross-section is rotated about the *x* axis of the local coordinate system. If α indicates the rotation angle in radians, the transformation matrix can be obtained as follows:

$$[\boldsymbol{A}] = \begin{bmatrix} 1 & 0 & 0 \\ 0 & \cos\alpha & \sin\alpha \\ 0 & -\sin\alpha & \cos\alpha \end{bmatrix} \begin{bmatrix} l_1 & m_1 & n_1 \\ l_2 & m_2 & n_2 \\ l_3 & m_3 & n_3 \end{bmatrix} \tag{5.85}$$

5.4.5 Force vector of space frames

Beams can be subjected to transverse distributed/point loads, axial loads, and moments. Load vectors for each case (distributed moments and forces or point forces and moments) will be calculated. The computer code developed is able to consider distributed transverse loads/moments and point loads/moments, which are applied just at the end points of elements. Therefore, there will be a point where a point load will exist. Nodal point loads are defined in a global coordinate system for joints, not elements. If the constant distributed loads are indicated by q_{xx}, q_{yy}, q_{zz}, then, in the case of a uniform beam, the force vector can be obtained in accordance with Equation 5.42 as follows:

	Distributed loads in local coordinate system for joint *I*	Point loads at joint *I* in global coordinate system		Distributed loads in local coordinate system for joint *J*
u^i	$\frac{q_{xx}l}{2}$	$P_{x,I}$	u^j	$\frac{q_{xx}l}{2}$
v^i	$\frac{q_{yy}l}{2}$	$P_{y,I}$	v^j	$\frac{q_{yy}l}{2}$
w^i	$\frac{q_{zz}l}{2}$	$P_{z,I}$	w^j	$\frac{q_{zz}l}{2}$
θ_x^i	$\frac{M_{torsion}l}{2}$	$M_{x,I}$	θ_x^j	$\frac{M_{torsion}l}{2}$
θ_y^i	$\frac{q_{zz}l^2}{12}$	$M_{y,I}$	θ_y^j	$-\frac{q_{zz}l^2}{12}$
θ_z^i	$\frac{q_{yy}l^2}{12}$	$M_{z,I}$	θ_z^j	$-\frac{q_{yy}l^2}{12}$

Figure 5-8: Force vector for distributed loads and point forces

5.4.6 Assembly of total force and stiffness matrix

Some points of the FEM mesh might be shared between two or more elements. This means that the stiffness of shared points in the global stiffness matrix is the summation of stiffness related to all elements containing that shared point. The same procedure as that shown in Figure 5-4 will be used to obtain the assembled stiffness matrix of the whole system. In thermal analysis, there is just one degree of freedom to be found for each point, but here, there are six degrees of freedom to be calculated for each point. Therefore, there are 36 stiffness components, to be determined for each point. For example, for the system shown in Figure 5-9, the assembled stiffness matrix can be calculated as follows:

$$[\boldsymbol{K}]_{assembled_{[18\times18]}} = \tag{5.86}$$

$$= \overbrace{\begin{bmatrix} K_{11_{[6\times6]}} & K_{12_{[6\times6]}} & 0_{[6\times6]} \\ K_{21_{[6\times6]}} & K_{22,e1_{[6\times6]}} & 0_{[6\times6]} \\ 0_{[6\times6]} & 0_{[6\times6]} & 0_{[6\times6]} \end{bmatrix}}^{Stiffness\ of\ element\ 1} + \overbrace{\begin{bmatrix} 0_{[6\times6]} & 0_{[6\times6]} & 0_{[6\times6]} \\ 0_{[6\times6]} & K_{22,e2_{[6\times6]}} & K_{23_{[6\times6]}} \\ 0_{[6\times6]} & K_{32_{[6\times6]}} & K_{33_{[6\times6]}} \end{bmatrix}}^{Stiffness\ of\ element\ 2}$$

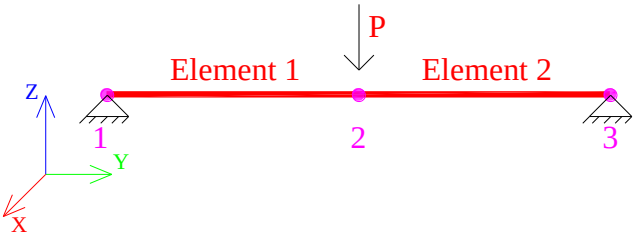

Figure 5-9: A simply supported beam under point load *P* at the mid-point

$K_{ij_{[6\times6]}}$ is the stiffness of joint i related to joint j. $K_{ij_{[6\times6]}}$ is zero if joint i and j are not connected with a frame element. It should be noted that at first, the stiffness

matrix of element e is transformed to the global coordinate system; next, it is assembled with the stiffness matrix of other elements. The force vector can also be determined by applying the same procedure. For example, in the absence of distributed loads, the force vector of the system shown in Figure 5-9 in the global coordinate system is:

$$[\boldsymbol{F}]^{T}_{assembled} = \left[\overbrace{0 \quad 0 \quad 0}^{Joint\ 1} \quad \overbrace{0 \quad 0 \quad 0}^{} \quad \overbrace{0 \quad 0 \quad -P}^{Joint\ 2} \quad \overbrace{0 \quad 0 \quad 0}^{} \quad \overbrace{0 \quad 0 \quad 0}^{Joint\ 3} \quad \overbrace{0 \quad 0 \quad 0}^{}\right] \tag{5.87}$$

5.4.7 Solution

The element and assembled stiffness matrices are singular. It means that the determinant of matrix $[\boldsymbol{K}]$ is zero. To obtain the deformation vector of a system, the following system of equations will be solved:

$$[\boldsymbol{U}] = displacement\ vector = [\boldsymbol{K}]^{-1}[\boldsymbol{P}] \tag{5.88}$$

A solution of Equation 5.88 is possible when $[\boldsymbol{K}]$ matrix in inversible. A stiffness matrix with a determinant equal to zero represents a rigid body motion. To solve the system of equations, the stiffness of restrained joints will be removed from the stiffness matrix and load vector. For example, for the system shown in Figure 5-9, the translational stiffness in three directions of Joints 1 and 3 will be removed from matrix $[\boldsymbol{K}]$. Displacement of these two joints represents the boundary condition of the problem and is equal to zero. Equation 5.88 is valid for linear systems in steady state conditions. In case of nonlinear structures and unsteady problems, the system of equations cannot be solved simply. In Section 4.6, nonlinear systems, geometric nonlinearity, and solution of nonlinear problems will be explained.

5.5 Nonlinear analysis

The nonlinear behaviour of structures entails numerous problems in solid mechanics. Nonlinearity can include three types of problems: 1- Geometric nonlinearity; 2- Physical or material nonlinearity; and 3- Nonlinearity caused by boundary condition. In some books, the third type is classified under Geometric nonlinearity. These three types of nonlinearity are explained in this section with some examples. To satisfy the safety of structures, including stress limit and serviceability limit states, it is usually sufficient to consider the small strain behaviour for materials. Structural nonlinearity, especially in civil engineering, will include problems with small strain assumptions.

Geometric nonlinearity: Geometric nonlinearities involve nonlinearities in kinematic quantities, such as the strain-displacement relationships in solids. Such nonlinearities can occur because of large displacements, large strains, large rotations, and so on. Contact between two plastic bodies can also be

classified as a geometric nonlinearity because the area of contact is a function of the deformation [46]. An example of geometric nonlinearity is a rigid beam, as shown in Figure 5-10. The beam is supported with a rotational spring with stiffness K at the end point A. The equilibrium equation for the deformed beam is (the equilibrium of the deformed beam considers the effects of deformations in stress calculations, or the geometric parameters are included in the equilibrium equation):

$$\sum_A M = 0 \rightarrow Pl\cos(a) = Ka \tag{5.89}$$

Equation 5.89 represents the nonlinear relationship between actions (here P) and rotation a. Therefore, this type of behaviour is known as geometrical nonlinearity. If the rotation angle of spring remains small $cos(a) = 1$, we will have $P = \frac{Ka}{l}$. If angle a is big enough, the calculated nonlinear force P (see Eq. 5.79) will not be equal to linear force $\frac{Ka}{l}$.

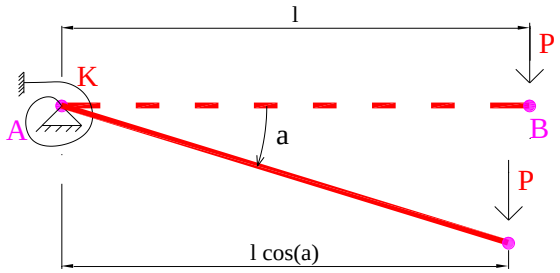

Figure 5-10: Rigid beam under point load and supported by a rotational spring

The second order theory is normally applied to consider the effects of deformations in mechanical models. The idea is to describe the nonlinear terms using a Taylor series, which is terminated after the second term. For the rigid beam of Figure 5-10, we can write (Taylor series for cosine $\cos(a) = 1 - \frac{a^2}{2}$):

$$P = \frac{Ka}{l\left(1 - \frac{a^2}{2}\right)} \tag{5.90}$$

Physical nonlinearity: In the last section, to calculate the force as a function of deformation, Hooke's law was considered to be valid. Hooke's law considers the linear relationship between deformation and force (here, the stiffness of spring K). This assumption is valid for many materials, but only under some circumstances. Deformations will be limited to the upper boundary of linear deformation. The nonlinear relationship between stress and strain is called plastic flow and the limiting stress or the upper boundary stress is known as yield stress. Nonlinear materials produce responses that are not proportional to the influences. An example of material nonlinearity is the behaviour of steel and

concrete. In Chapter 3, stress-strain curves of steel and concrete have been discussed. Concrete represents a plastic material. The deformation of a plastic material is irreversible. Steel is an elasto-plastic material. The stress-strain curve of steel has both an elastic part and a plastic part. Elastic deformation of steel is reversible, but its plastic deformation is irreversible.

Nonlinearity caused by boundary conditions: A source of nonlinearity is related to variable boundaries as a function of time or as a function of the deformation path—for example, when the boundaries are in contact with another body that deforms during the process of analysis. This can happen in contact problems. In some problems, the force will vary as a function of time, which will cause the nonlinear behaviour of the structure. The source of nonlinear behaviour is quite different. In Section 5.7, the geometric nonlinearity of three-dimensional beam elements will be explained. The FEM formulation, which considers the nonlinear effects, is applied. It should be noted that nonlinear material behaviour, like plastic or elasto-plastic behaviour, are not considered in the current study.

5.6 Nonlinear beam element

The objective of this section is to present large deformation formulations of beam elements. In Sections 5.4 and 5.5, we explained the linear FEM formulation of three-dimensional frame elements. The stiffness matrix, force vector, and solution procedure of linear problems have been discussed. To mathematize the structural behaviour of frames under fire loads, nonlinear deformations will be considered. Large strains can only occur if the displacement gradients are also large, but the reverse does not necessarily hold true: large displacement gradients can be observed in structural behaviour while the strains are still limited, smaller than, say, 2% [47]. For large displacement gradients, but small strains, the usual constitutive relationships—for example, Hooke's law of linear elasticity—remain valid. To develop a geometrically nonlinear beam element, an Updated Lagrangian (UL) or Total Lagrangian (TL) formulation can be employed [48]. Both formulations result in the same solution. The choice of a total Lagrangian or an updated Lagrangian formulation should be decided only by the relative numerical effectiveness of each formulation. The beam elements are assumed to be straight, and the conventional beam displacement functions are employed to express the displacements of the elements in converted coordinates. The updated Lagrangian-based element is computationally more effective [48]. Warmed structural materials behave in a nonlinear manner and may be damaged. Elastic material with variable modulus of elasticity has been assumed to mathematize the structural behaviour. We need to mention that exact solution of structures under fire loading is not possible and we are trying to obtain an acceptable solution to the problem. Therefore, geometric nonlinearity with small limited strains and large

deformations have been chosen to perform the analysis. A three-dimensional beam can be a suitable element to be applied in the case of structural fire analysis. Figure 5-11 shows a moving beam element in a fixed Cartesian coordinate system, with two nodes at both ends. The objective is to obtain the deformation of the element at all-time steps. Solution time step t will be used to solve the problem at time $t + dt$.

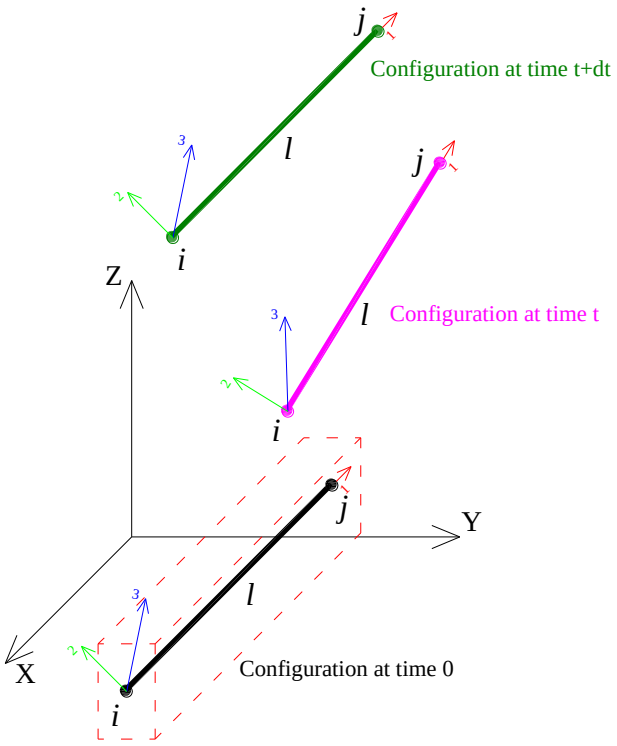

Figure 5-11: Large deformations of a three-dimensional frame element and its attached local coordinate system

In TL formulation, all parameters refer to the initial configuration at time 0. For the deformed element at time $t + dt$, we can write the principle of virtual displacements for the current time or load step as follows:

$$\int_V \sigma_{ij}^{t+dt} \delta^{t+dt} \varepsilon_{ij}^t dv = \int_A t_k^{t+dt} \delta u_k^t ds + \int_V \rho\, b_k \delta u_k^t dv \tag{5.91}$$

The right side of Equation 5.91 represents the internal virtual work and the left side the external virtual work done by body forces b_k and surface forces t_k^{t+dt} when virtual displacement δu_k is considered. Here, we will assume that body and surface forces remain constant as the element deforms. $\delta^{t+dt} \varepsilon_{ij}^t$ are virtual variations in Cartesian components of Green-Lagrange strain tensor at time $t + dt$ in the local coordinate system at time t and σ_{ij}^{t+dt} are the Cartesian components of the 2nd Piola-Kirchhoff stress tensor at time $t + dt$, which will be measured in local coordinate system at time t [48]. The theory of beams states that the normal stresses perpendicular to the centreline must vanish [47]. It

should be noted that the strain and stresses are measured in the local coordinate system attached to the deformed beam. Therefore, the strain tensor will be:

$$Piola\text{–}Kirchhof\ Stress = [\boldsymbol{\sigma}] = \begin{bmatrix} \sigma_{xx} & \sigma_{xy} & \sigma_{xz} \\ \sigma_{yx} & \sigma_{yy} = 0 & \sigma_{yz} = 0 \\ \sigma_{zx} & \sigma_{zy} = 0 & \sigma_{zz} = 0 \end{bmatrix} \tag{5.92}$$

The Green strain tensor, referred to in the local coordinate system at time t, includes linear and nonlinear strain; its components can be written as follows:

$$\varepsilon_{xx} = \overbrace{\frac{\partial u}{\partial x}}^{Linear\ strain} + \overbrace{\frac{1}{2}\left(\left(\frac{\partial u}{\partial x}\right)^2 + \left(\frac{\partial v}{\partial x}\right)^2 + \left(\frac{\partial w}{\partial x}\right)^2\right)}^{Nonlinear\ strain} = \varepsilon_{xx,L} + \eta_{xx,NL} \tag{5.93}$$

$$\varepsilon_{xy} = \overbrace{\frac{\partial u}{\partial y} + \frac{\partial v}{\partial x}}^{Linear\ strain} + \overbrace{\frac{\partial u}{\partial x}\frac{\partial u}{\partial y} + \frac{\partial v}{\partial x}\frac{\partial v}{\partial y} + \frac{\partial w}{\partial x}\frac{\partial w}{\partial y}}^{Nonlinear\ strain} = \varepsilon_{xy,L} + \eta_{xy,NL} \tag{5.94}$$

$$\varepsilon_{xz} = \overbrace{\frac{\partial u}{\partial z} + \frac{\partial w}{\partial x}}^{Linear\ strain} + \overbrace{\frac{\partial u}{\partial x}\frac{\partial u}{\partial z} + \frac{\partial v}{\partial x}\frac{\partial v}{\partial z} + \frac{\partial w}{\partial x}\frac{\partial w}{\partial z}}^{Nonlinear\ strain} = \varepsilon_{xz,L} + \eta_{xz,NL} \tag{5.95}$$

The constitutive relations with tensor components can be used to relate the virtual incremental strains to Piola-Kirchhoff's stresses. The stress at time $t + dt$ can be divided into two components σ_{ij}^t and $\Delta\sigma_{ij}^t$. σ_{ij}^t is known and calculated at the last time step. In the updated Lagrangian system, we can write Equation 5.91 as follows:

$$\begin{aligned} \int_V \sigma_{ij}^{t+dt}\delta\varepsilon_{ij}dv &= \int_V \sigma_{ij}^t\delta\varepsilon_{ij}dv + \int_V \Delta\sigma_{ij}^t\delta\varepsilon_{ij}dv \\ &= \int_A t_k^{t+dt}\delta u_k^t ds + \int_V \rho\, b_k \delta u_k^t dv \end{aligned} \tag{5.96}$$

For small strains, a linear relationship between stress increment $\Delta\sigma_{ij}^t$ and strain increment can be assumed:

$$\Delta\boldsymbol{\sigma} = \boldsymbol{D}\Delta\boldsymbol{\varepsilon} \rightarrow in\ tensor\ form\ \Delta\sigma_{ij}^t = D_{ij}\Delta\varepsilon_{ij} \tag{5.97}$$

The matrix $\boldsymbol{D}$ contains the instantaneous stiffness moduli of the material. In case of elastic material, it is Hooke's law. Substitution of Equation 5.97 into Equation 5.96 gives (in matrix form):

$$\int_V \delta\boldsymbol{\varepsilon}^T\boldsymbol{\sigma}dv + \int_V \delta\boldsymbol{\varepsilon}^T\boldsymbol{D}\Delta\boldsymbol{\varepsilon}dv = \int_A \delta\boldsymbol{u}^T\boldsymbol{t_0}ds + \int_V \delta\boldsymbol{u}^T\boldsymbol{B}dv \tag{5.98}$$

$\boldsymbol{B}$ is the body force vector, $\boldsymbol{t_0}$ the surface force vector, and $\boldsymbol{u}^T$ is the displacement-components vector. The strain increment contains linear and nonlinear contributions.

$$\Delta\boldsymbol{\varepsilon} = \Delta\boldsymbol{\varepsilon_L} + \Delta\boldsymbol{\eta}_{NL} \tag{5.99}$$

$$\begin{aligned}\int_V \delta\Delta{\boldsymbol{\varepsilon}_L}^T \boldsymbol{D}\Delta\boldsymbol{\varepsilon}_L dv + \int_V \delta\Delta{\boldsymbol{\varepsilon}_L}^T \boldsymbol{D}\Delta\boldsymbol{\eta}_{NL} dv + \int_V \delta\Delta{\boldsymbol{\eta}_{NL}}^T \boldsymbol{D}\Delta\boldsymbol{\varepsilon}_L dv \\ + \int_V \delta\Delta{\boldsymbol{\eta}_{NL}}^T \boldsymbol{D}\Delta\boldsymbol{\eta}_{NL} dv + \int_V \delta{\boldsymbol{\varepsilon}_L}^T \boldsymbol{\sigma}^t dv + \int_V \delta{\boldsymbol{\eta}_{NL}}^T \boldsymbol{\sigma}^t dv \\ = \int_A \delta\boldsymbol{u}^T \boldsymbol{t_0} ds + \int_V \delta\boldsymbol{u}^T \boldsymbol{B} dv\end{aligned} \tag{5.100}$$

Because of the linear stress-strain relationship, in order to derive the stiffness matrix related to linear deformations and geometric nonlinearity, we can only use those contributions that are linear in the displacement increment [47]. The second, third, and fourth terms of Equation 5.100 include nonlinear displacements, and so will be removed. Therefore:

$$\overbrace{\int_V \delta\Delta{\boldsymbol{\varepsilon}_L}^T \boldsymbol{D}\Delta\boldsymbol{\varepsilon}_L dv}^{Term\ 1} + \overbrace{\int_V \delta{\boldsymbol{\eta}_{NL}}^T \boldsymbol{\sigma}^t dv}^{Term\ 2} = \overbrace{\int_A \delta\boldsymbol{u}^T \boldsymbol{t_0} ds}^{Term\ 3} + \overbrace{\int_V \delta\boldsymbol{u}^T \boldsymbol{B} dv}^{Term\ 4} - \overbrace{\int_V \delta{\boldsymbol{\varepsilon}_L}^T \boldsymbol{\sigma}^t dv}^{Term\ 5} \tag{5.101}$$

The nonlinear space frame is formulated on the basis of the theory summarized above. As can be seen in Figure 5-11, the element has two nodes with six degrees of freedom at each node. Beam elements can transmit axial force, shear force, and bending and torsional moments. Bending moments and forces at each node of the element are shown in Figure 5-5. The element is assumed to be straight and uniform (constant cross-section). Euler assumptions for beams and columns are valid for this element (plane sections of the beam element remain plane during deformation). The proposed element can model large deflections and rotations but not large strains. It is very important to consider the constant length and volume for the element. The element has two nodes i and j. Node i is the origin of the attached local coordinate system and the x-axis of local coordinate system is parallel to the element.

Shape functions: To obtain the finite element formulation (like linear analysis), the first step involves defining the FEM mesh. Afterwards, shape functions to estimate deformations along the element will be chosen [38] [49]. Shape functions are the same as those that have been defined for the linear element in the last section.

$$[\boldsymbol{N}]^T = \begin{bmatrix} 1-\frac{x}{l} \\ \frac{2x^3-3lx^2+l^3}{l^3} \\ \frac{2x^3-3lx^2+l^3}{l^3} \\ 1-\frac{x}{l} \\ \frac{x^3-2lx^2+l^2x}{l^2} \\ \frac{x^3-2lx^2+l^2x}{l^2} \\ \frac{x}{l} \\ -\frac{2x^3-3lx^2}{l^3} \\ -\frac{2x^3-3lx^2}{l^3} \\ \frac{x}{l} \\ \frac{x^3-lx^2}{l^2} \\ \frac{x^3-lx^2}{l^2} \end{bmatrix} \quad , \frac{d[\boldsymbol{N}]^T}{dx} = \begin{bmatrix} -\frac{1}{l} \\ \frac{6x^2-6lx}{l^3} \\ \frac{6x^2-6lx}{l^3} \\ -\frac{1}{l} \\ \frac{3x^2-4xl+l^2}{l^2} \\ \frac{3x^2-4xl+l^2}{l^2} \\ \frac{1}{l} \\ -\frac{6x^2-6xl}{l^3} \\ -\frac{6x^2-6xl}{l^3} \\ \frac{1}{l} \\ \frac{3x^2-2xl}{l^2} \\ \frac{3x^2-2xl}{l^2} \end{bmatrix} \tag{5.102}$$

Strain-displacement relationship: The next step is to define the strain-displacement relations for linear and nonlinear analysis. According to Equations 5.93–95, total strain contains two components—linear and nonlinear ones. The same process used for linear analysis will be applied to obtain the linear and nonlinear stiffness matrices. It should be mentioned that $[\Delta \boldsymbol{U}]$ in Equations 5.103 and 5.104 represents the incremental displacement of each step.

$$Nonlinear\ strain = [\boldsymbol{\eta}]_{NL} = [\boldsymbol{B}]_{NL}[\Delta \boldsymbol{U}] \tag{5.103}$$

$$Linear\ strain = [\boldsymbol{\varepsilon}]_{L} = [\boldsymbol{B}]_{L}[\Delta \boldsymbol{U}] \tag{5.104}$$

Stiffness matrix: By substitution of Equation 5.103 into Equation 5.101, the finite element formulation of the problem can be obtained. All terms of Equation 5.101 can be written in a matrix form. The second term of Equation 5.101 considers large deformation effects on internal forces at the previous load step. For more details on nonlinear finite element formulation, see references [38], [48], [50], and [47].

$$1 - \int_V \delta \Delta {\boldsymbol{\varepsilon}_L}^T \boldsymbol{D} \Delta \boldsymbol{\varepsilon}_L dv = [\Delta \boldsymbol{U}]^T \left(\int_V [\boldsymbol{B}]_L^T \boldsymbol{D} [\boldsymbol{B}]_L dv \right) [\Delta \boldsymbol{U}] = [\Delta \boldsymbol{U}]^T [\boldsymbol{K}]_L [\Delta \boldsymbol{U}] \tag{5.105}$$

$$\begin{aligned} 2 - \int_V \delta {\boldsymbol{\eta}_{NL}}^T \boldsymbol{\sigma}^t dv &= [\Delta \boldsymbol{U}]^T \left(\int_V [\boldsymbol{B}]_{NL}^T \boldsymbol{\sigma}^t [\boldsymbol{B}]_{NL} dv \right) [\Delta \boldsymbol{U}] \\ &= [\Delta \boldsymbol{U}]^T [\boldsymbol{K}]_{NL} [\Delta \boldsymbol{U}] \end{aligned} \tag{5.106}$$

$$3 - \int_A \delta \boldsymbol{u}^T \boldsymbol{t_0} ds = [\Delta \boldsymbol{U}]^T \int_A [\boldsymbol{B}]_L^T \boldsymbol{t_0} ds = [\Delta \boldsymbol{U}]^T [\boldsymbol{F}]_{external,surface}^{t+dt} \tag{5.107}$$

$$4-\int_V \delta \boldsymbol{u}^T \boldsymbol{B}_{bodyforce} dv = [\Delta \boldsymbol{U}]^T \int_A [\boldsymbol{B}]_L^T \boldsymbol{B}_{bodyforce} dv = [\Delta \boldsymbol{U}]^T [\boldsymbol{F}]_{external,body}^{t+dt} \quad (5.108)$$

$$5-\int_V \delta {\boldsymbol{\varepsilon}_L}^T \boldsymbol{\sigma}^t dv = [\Delta \boldsymbol{U}]^T \left(\int_V [\boldsymbol{B}]_L^T \boldsymbol{\sigma}^t dv \right) = [\Delta \boldsymbol{U}]^T [\boldsymbol{F}]_{internal,initial}^t \quad (5.109)$$

$$\rightarrow [\Delta \boldsymbol{U}]^T [\boldsymbol{K}]_L [\Delta \boldsymbol{U}] + [\Delta \boldsymbol{U}]^T [\boldsymbol{K}]_{NL} [\Delta \boldsymbol{U}] = [\Delta \boldsymbol{U}]^T [\boldsymbol{F}]_{external,surface}^{t+dt} + [\Delta \boldsymbol{U}]^T [\boldsymbol{F}]_{external,body}^{t+dt} - [\Delta \boldsymbol{U}]^T [\boldsymbol{F}]_{internal,initial}^t \quad (5.110)$$

$$\rightarrow \boxed{([\boldsymbol{K}]_L + [\boldsymbol{K}]_{NL})[\Delta \boldsymbol{U}] = [\boldsymbol{F}]_{ext.}^{t+dt} - [\boldsymbol{F}]_{int.,ini.}^t}$$

The linear stiffness matrix is extracted in Section 5.5. If the element length and volume remain constant, the force matrix can be obtained in accordance with Section 5.5. As mentioned, constant length and volume are the basic assumptions of the solution. The nonlinear stiffness matrix of three-dimensional beams can be obtained by Equation 5.111 [38]. The nonlinear geometric stiffness matrix, shown in Figure 5-12, does not contain shear deformation effects. Large deformations but small rotations of three-dimensional beams can be modelled by the formulation obtained. The assumption of small rotations and large deformations is appropriate for many skeletal structures.

$$[\boldsymbol{K}]_{NL} = [\boldsymbol{K}]_G = \frac{EA}{l_0}(u_j - u_j) \int_V \frac{\partial N_i}{\partial x} \frac{\partial N_j}{\partial x} = \frac{EA}{l_0}(u_j - u_j) \begin{bmatrix} [[\boldsymbol{K}]_{G,1,1}]_{6\times6} & [[\boldsymbol{K}]_{G,1,2}]_{6\times6} \\ [[\boldsymbol{K}]_{G,2,1}]_{6\times6} & [[\boldsymbol{K}]_{G,2,2}]_{6\times6} \end{bmatrix} \quad (5.111)$$

$$T_t = \frac{EA}{l_0}(u_j - u_j) = Axial\ internal\ force$$

Force vector: The force vector for body forces and external forces can be obtained, as explained, for the linear elements.

$$For\ small\ rotations: sin(\alpha) \approx \alpha\ and \cos(\alpha) \approx 1 \quad (5.112)$$

	u^i	v^i	w^i	θ_x^i	θ_y^i	θ_z^i	u^j	v^j	w^j	θ_x^j	θ_y^j	θ_z^j
u^i	$\frac{T_t}{l_0}$	0	0	0	0	0	$-\frac{T_t}{l_0}$	0	0	0	0	0
v^i	0	$1.2\frac{T_t}{l_0}$	0	0	0	$0.1T_t$	0	$-1.2\frac{T_t}{l_0}$	0	0	0	$-0.1T_t$
w^i	0	0	$1.2\frac{T_t}{l_0}$	0	$0.1T_t$	0	0	0	$-1.2\frac{T_t}{l_0}$	0	$-0.1T_t$	0
θ_x^i	0	0	0	0	0	0	0	0	0	0	0	0
θ_y^i	0	0	$0.1T_t$	0	$0.1333T_t l_0$	0	0	0	$0.1T_t$	0	$0.0333T_t l_0$	0
θ_z^i	0	$0.1T_t$	0	0	0	$0.1333T_t l_0$	0	$0.1T_t$	0	0	0	$0.0333T_t l_0$
u^j	$-\frac{T_t}{l_0}$	0	0	0	0	0	$\frac{T_t}{l_0}$	0	0	0	0	0
v^j	0	$-1.2\frac{T_t}{l_0}$	0	0	0	$0.1T_t$	0	$1.2\frac{T_t}{l_0}$	0	0	0	$-0.1T_t$
w^j	0	0	$-1.2\frac{T_t}{l_0}$	0	$0.1T_t$	0	0	0	$1.2\frac{T_t}{l_0}$	0	$-0.1T_t$	0
θ_x^j	0	0	0	0	0	0	0	0	0	0	0	0
θ_y^j	0	0	$-0.1T_t$	0	$0.0333T_t l_0$	0	0	0	$-0.1T_t$	0	$0.1333T_t l_0$	0
θ_z^j	0	$-0.1T_t$	0	0	0	$0.0333T_t l_0$	0	$-0.1T_t$	0	0	0	$0.1333T_t l_0$

Figure 5-12: Nonlinear geometric stiffness matrix of a space frame

$[K]_{G,1,1} =$	$\int \frac{\partial N_1}{\partial x}\frac{\partial N_1}{\partial x}dx$	0	0	0	0	0
	0	$\int \frac{\partial N_2}{\partial x}\frac{\partial N_2}{\partial x}dx$	0	0	0	$\int \frac{\partial N_6}{\partial x}\frac{\partial N_2}{\partial x}dx$
	0	0	$\int \frac{\partial N_3}{\partial x}\frac{\partial N_3}{\partial x}dx$	0	$\int \frac{\partial N_5}{\partial x}\frac{\partial N_3}{\partial x}dx$	0
	0	0	0	0	0	0
	0	0	$\int \frac{\partial N_5}{\partial x}\frac{\partial N_3}{\partial x}dx$	0	$\int \frac{\partial N_5}{\partial x}\frac{\partial N_5}{\partial x}dx$	0
	0	$\int \frac{\partial N_6}{\partial x}\frac{\partial N_2}{\partial x}dx$	0	0	0	$\int \frac{\partial N_6}{\partial x}\frac{\partial N_6}{\partial x}dx$
$[K]_{G,2,2} =$	$\int \frac{\partial N_7}{\partial x}\frac{\partial N_7}{\partial x}dx$	0	0	0	0	0
	0	$\int \frac{\partial N_8}{\partial x}\frac{\partial N_8}{\partial x}dx$	0	0	0	$\int \frac{\partial N_8}{\partial x}\frac{\partial N_{12}}{\partial x}dx$
	0	0	$\int \frac{\partial N_9}{\partial x}\frac{\partial N_9}{\partial x}dx$	0	$\int \frac{\partial N_9}{\partial x}\frac{\partial N_{11}}{\partial x}dx$	0
	0	0	0	0	0	0
	0	0	$\int \frac{\partial N_9}{\partial x}\frac{\partial N_{11}}{\partial x}dx$	0	$\int \frac{\partial N_{11}}{\partial x}\frac{\partial N_{11}}{\partial x}dx$	0
	0	$\int \frac{\partial N_8}{\partial x}\frac{\partial N_{12}}{\partial x}dx$	0	0	0	$\int \frac{\partial N_{12}}{\partial x}\frac{\partial N_{12}}{\partial x}dx$
$[K]_{G,1,2} =$	$\int \frac{\partial N_1}{\partial x}\frac{\partial N_7}{\partial x}dx$	0	0	0	0	0
	0	$\int \frac{\partial N_2}{\partial x}\frac{\partial N_8}{\partial x}dx$	0	0	0	$\int \frac{\partial N_2}{\partial x}\frac{\partial N_{12}}{\partial x}dx$
	0	0	$\int \frac{\partial N_3}{\partial x}\frac{\partial N_9}{\partial x}dx$	0	$\int \frac{\partial N_3}{\partial x}\frac{\partial N_{11}}{\partial x}dx$	0
	0	0	0	0	0	0
	0	0	$\int \frac{\partial N_5}{\partial x}\frac{\partial N_{11}}{\partial x}dx$	0	$\int \frac{\partial N_5}{\partial x}\frac{\partial N_{11}}{\partial x}dx$	0
	0	$\int \frac{\partial N_8}{\partial x}\frac{\partial N_6}{\partial x}dx$	0	0	0	$\int \frac{\partial N_6}{\partial x}\frac{\partial N_{12}}{\partial x}dx$
$[K]_{G,2,1} =$	$\int \frac{\partial N_7}{\partial x}\frac{\partial N_1}{\partial x}dx$	0	0	0	0	0
	0	$\int \frac{\partial N_2}{\partial x}\frac{\partial N_8}{\partial x}dx$	0	0	0	$\int \frac{\partial N_8}{\partial x}\frac{\partial N_6}{\partial x}dx$
	0	0	$\int \frac{\partial N_3}{\partial x}\frac{\partial N_9}{\partial x}dx$	0	$\int \frac{\partial N_5}{\partial x}\frac{\partial N_{11}}{\partial x}dx$	0
	0	0	0	0	0	0
	0	0	$\int \frac{\partial N_3}{\partial x}\frac{\partial N_{11}}{\partial x}dx$	0	$\int \frac{\partial N_5}{\partial x}\frac{\partial N_{11}}{\partial x}dx$	0
	0	$\int \frac{\partial N_2}{\partial x}\frac{\partial N_{12}}{\partial x}dx$	0	0	0	$\int \frac{\partial N_6}{\partial x}\frac{\partial N_{12}}{\partial x}dx$

Figure 5-13: Components of nonlinear geometric matrix

5.6.1 Transformation

In an updated Lagrangian formulation, the transformation between coordinate systems requires special attention. The transformation matrix between local coordinate system at time t, local coordinate system at time $t + dt$, and global coordinate system will be obtained. It is important to consider that vectors and matrices can be added just when they are transformed into a reference coordinate system. For example, to obtain the nonlinear geometric stiffness matrix, the axial force from the previous load or time step is required. To use the vector of internal forces at time $t + dt$, it will first be transformed from the local coordinate system at time t to the local coordinate system at time $t + dt$. The same process will be repeated for force vectors and displacement vectors. The solution process of Equation 5.110 will be performed in the global coordinate system. Therefore, at every load step, the stiffness matrix and load vectors will be transformed to the global coordinate system. The mathematical process of obtaining the transformation matrices can be found in reference books of finite element and mathematics [48]. Equations 5.113–114 give the transformations between coordinates. Transformation matrices are the function of incremental deformations at every load step. For large incremental displacements, the results would not be accurate because the transformation matrices may contain errors.

1. *Transform from local coordinate at time 0 (local0) to local at time t (localt):*

$$du = u_{j,local0} - u_{i,local0}\,, dv = v_{j,local0} - v_{i,local0} \quad (5.113)$$

$$dw = w_{j,local0} - w_{i,local0}\,, \gamma = \theta^{j}_{x,local0} - \theta^{i}_{x,local0}$$

$$l = (l_0 + du)^2 + dw^2\,, \qquad ll = \sqrt{(l + dv^2)}$$

$$\cos(A) = \frac{(du + l_0)}{\sqrt{l}}, \qquad \sin(B) = \frac{dv}{ll}$$

$$\sin(A) = \sqrt{1 - \cos(A)^2}\ \cos(B) = \sqrt{1 - \sin(B)^2}$$

$$R_1 = \begin{bmatrix} \cos(A)\cos(B) & \sin(B) & \sin(A)\cos(B) \\ -\cos(A)\sin(B) & \cos(B) & -\sin(A)\sin(B) \\ -\sin(A) & 0 & \cos(A) \end{bmatrix} \begin{bmatrix} 1 & 0 & 0 \\ 0 & \cos(\gamma) & \sin(\gamma) \\ 0 & -\sin(\gamma) & \cos(\gamma) \end{bmatrix}$$

2. *Transform from local coordinate at time t (localt1) to local at time $t + dt$ (localt2):*

$$du = u_{j,localt} - u_{i,localt}\,, dv = v_{j,localt} - v_{i,localt} \quad (5.114)$$

$$dw = w_{j,localt} - w_{i,localt}\,, \gamma = \theta^{j}_{x,localt} - \theta^{i}_{x,localt}$$

$$l = (l_0 + du)^2 + dw^2\,, \qquad ll = \sqrt{(l + dv^2)}$$

$$\cos(A) = \frac{(du + l_0)}{\sqrt{l}}, \qquad \sin(B) = \frac{dv}{ll}$$

$$\sin(A) = \sqrt{1 - \cos(A)^2}\ \cos(B) = \sqrt{1 - \sin(B)^2}$$

$$R_2 = \begin{bmatrix} \cos(A)\cos(B) & \sin(B) & \sin(A)\cos(B) \\ -\cos(A)\sin(B) & \cos(B) & -\sin(A)\sin(B) \\ -\sin(A) & 0 & \cos(A) \end{bmatrix} \begin{bmatrix} 1 & 0 & 0 \\ 0 & \cos(\gamma) & \sin(\gamma) \\ 0 & -\sin(\gamma) & \cos(\gamma) \end{bmatrix}$$

3. *Transform from local coordinate at time 0 (localt1) to global:* Transformation matrix from the local coordinate system at time t=0 to the global coordinate system is obtained in Section 5.4 (see Equation 5.78).

5.6.2 Thermal strains

Temperature change can affect the molecular structure of a material. Many materials expand when temperature rises. We have to consider the thermal strains within a body that emerge when material deforms as a result of temperature changes. Temperature changes in a structure can result in large strains. In case of fire, there will emerge 3D thermal strains in a warm member. Thermal strains may be variable over a cross-section area, which cannot be modelled by the developed method. By assuming a cumulative thermal strain over a cross-section, the thermal strain and stresses are modelled. Under this assumption, the developed method is not suitable to model the local thermal effects. Consider a bar as shown in Figure 5-14, one that is unconstrained (there are no supports), and undergoing uniform temperature change.

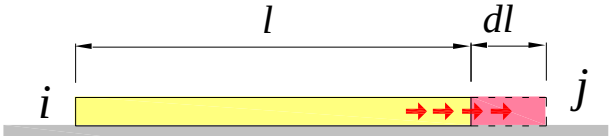

Figure 5-14: An element lying on a surface subjected to temperature

$$dl = \Delta l = \alpha \times \Delta T_N \times l \tag{5.115}$$

$$\varepsilon_{Th} = thermal\ strain = \frac{\Delta l}{l} = \alpha \Delta T_N \tag{5.116}$$

Since the bar is free to expand and there is no support to prevent longitudinal deformations, thermal stresses in the bar cannot develop. In general, for statically determinate structures, a uniform temperature change in one or more members does not result in stress in any of the members [37]. For statically indeterminate structures, a uniform temperature change in one or more members of the structure usually results in stress. It is possible to have thermal strain without having thermal stress, or have thermal stresses without thermal deformations. For one-dimensional problems, we will have:

$$\varepsilon_x = \frac{\sigma_x}{E} + \varepsilon_{Th} \tag{5.117}$$

Let $E = D$ and let us solve Equation 5.117 for σ_x as follows:

$$\sigma = D(\varepsilon - \varepsilon_{Th}) \tag{5.118}$$

The strain energy per unit volume is the area under the $\sigma - \varepsilon$ curve as follows:

$$dE = \frac{1}{2}\sigma(\varepsilon - \varepsilon_{Th}) \rightarrow In\ matrix\ form: \frac{1}{2}(\boldsymbol{\varepsilon} - \boldsymbol{\varepsilon}_{Th})^T \boldsymbol{D}(\boldsymbol{\varepsilon} - \boldsymbol{\varepsilon}_{Th}) \quad (5.119)$$

The total energy is the integration of strain energy over the body:

$$E = \int_V \frac{1}{2}(\boldsymbol{\varepsilon} - \boldsymbol{\varepsilon}_{Th})^T \boldsymbol{D}(\boldsymbol{\varepsilon} - \boldsymbol{\varepsilon}_{Th}) dv \quad (5.120)$$

We have $\boldsymbol{\varepsilon} = [\boldsymbol{B}][\boldsymbol{U}]$. Therefore, Equation 5.119 can be written as follows:

$$E = \int_V \frac{1}{2}([\boldsymbol{B}][\boldsymbol{U}] - \boldsymbol{\varepsilon}_{Th})^T \boldsymbol{D}([\boldsymbol{B}][\boldsymbol{U}] - \boldsymbol{\varepsilon}_{Th}) dv \quad (5.121)$$

Simplifying Equation 5.121 gives the following equation:

$$E = \frac{1}{2}\int_V \left(\overbrace{\boldsymbol{B^T U^T D B U}}^{Term\ 1} - \overbrace{\boldsymbol{B^T U^T D \varepsilon}_T}^{Term\ 2} - \overbrace{\boldsymbol{\varepsilon}_{Th}{}^T \boldsymbol{D B U}}^{Term\ 3} + \overbrace{\boldsymbol{\varepsilon}_{Th}{}^T \boldsymbol{D \varepsilon}_{Th}}^{Term\ 4} \right) dv \quad (5.122)$$

The first term of Equation 5.122 is the strain caused by non-thermal loads or mechanical actions. Terms 2 and 3 are identical and can be added together. The last term is constant and, by applying the principle of minimum energy, it gives zero derivatives. Finally, the contribution of thermal energy to total energy can be presented by Equation 5.123.

$$E_{Th} = \frac{1}{2}\int_V (\boldsymbol{\varepsilon}_{Th}{}^T \boldsymbol{D B U} + \boldsymbol{B^T U^T D \varepsilon}_{Th}) dv = \int_V (\boldsymbol{\varepsilon}_{Th}{}^T \boldsymbol{D B U}) dv \quad (5.123)$$

By applying the principle of minimum energy, we have:

$$\frac{\partial E_{Th}}{\partial U} = \int_V (\boldsymbol{B D \varepsilon}_{Th}{}^T) dv = \boldsymbol{F}_{Th} = Thermal\ force\ vector \quad (5.124)$$

$\boldsymbol{F}_{Th}$ is the force vector caused by temperature change in the element. Considering one-dimensional thermal effects, which are appropriate to be applied in frame element problems and Equation 5.118 for one-dimensional thermal strain, we can write Equation 5.125 for frame elements.

$$\boldsymbol{F}_{Th} = A\int_0^l \boldsymbol{B^T D}\alpha\Delta T_N = A\int_0^l \begin{bmatrix} -\frac{1}{l} \\ \frac{1}{l} \end{bmatrix} \boldsymbol{D}\alpha\Delta T_N = \begin{bmatrix} -EA\alpha\Delta T_N \\ EA\alpha\Delta T_N \end{bmatrix} \quad (5.125)$$

There are no shear strains in isotropic material. Thermal strains are just expansions or contractions. Therefore, the thermal force vector of a beam element is:

$$[\boldsymbol{F}]_{Th}^T = \left[\overbrace{-EA\alpha\Delta T_N \quad 0 \quad 0 \quad 0 \quad 0 \quad 0}^{Joint\ i\ of\ the\ element} \quad \overbrace{EA\alpha\Delta T_N \quad 0 \quad 0 \quad 0 \quad 0 \quad 0}^{Joint\ j\ of\ the\ element} \right] \quad (5.126)$$

5.6.3 Solution

For the solution of linear problems, we need to always solve the system of equations. If the $[\boldsymbol{K}]$ matrix is non-singular, the solution is unique. In the solution of non-linear problems, we always have a set of nonlinear equations in the following form:

$$R(\boldsymbol{a}) = \boldsymbol{f} - \boldsymbol{P}(\boldsymbol{a}) = 0 \tag{5.127}$$

where $\boldsymbol{a}$ is the set of parameters to be obtained, $\boldsymbol{f}$ a vector which is independent from parameters, and $\boldsymbol{P}$ a vector dependent on the parameters. Here, $\boldsymbol{a}$ is displacements, or $\boldsymbol{U}$, of nodes, and $\boldsymbol{f}$ is the vector of actions including surface and body forces. The solution of Equation 5.127 may not necessarily be unique. Having an appropriate physical insight into the problem and small load step in length are essential to obtain a realistic solution. If the physical behaviour of a system is path-dependent, an incremental solution is always required. The solution at every load step depends on the answers of the solved last load step [38]. If $\boldsymbol{U}_{n+1}$ is the answer vector of load step $n+1$, the problem will be formulated as follows:

$$R(\boldsymbol{U}_{n+1}) = \boldsymbol{f}_{n+1} - \boldsymbol{P}(\boldsymbol{U}_{n+1}) = 0 \tag{5.128}$$

To obtain the solution of load step $n+1$, the answers—including load vector and properties of load step n—are required. As explained, the solution will be incremental so as to be able to follow the solution path. The force vector of every load step[1] and answer, which are displacements here, can be written as:

$$\boldsymbol{f}_{n+1} = \boldsymbol{f}_n + \Delta\boldsymbol{f}_n \tag{5.129}$$

$$\boldsymbol{U}_{n+1} = \boldsymbol{U}_n + \Delta\boldsymbol{U}_n \tag{5.130}$$

The load increments will be kept small enough to be able to consider the path dependence behaviour. $\Delta\boldsymbol{f}_n$ may be positive or negative. Converged answers cannot be reached directly and some iterations at each load step are always required. Therefore, at each load step, we have to solve the incremental equation in the following form:

$$(\boldsymbol{K}_n d\boldsymbol{U}_n)_i = (\Delta\boldsymbol{f}_n)_i \tag{5.131}$$

i indicates the iteration number and n load step number. The solution increment $d\boldsymbol{U}_n$ will be computed in some iterations till it is converged. The solution procedure of nonlinear problems for each load step is described in the following steps:

1. Set $d\boldsymbol{U}_{i=0} = 0$ for the current load step;

[1] A load step is indicated by the variable n and is defined as the solution within each load increment. A time step is the solution of a problem within each time increment. A time step may be discretized into several load steps.

2. Compute the external force vector of the current load step $(\boldsymbol{f}_{n+1})_{external}$;
3. Calculate the stiffness matrix of current load step $\boldsymbol{K}_n$;
4. Solve the linear system of equations

$$d\boldsymbol{U}_n = \overbrace{\boldsymbol{K}_n^{-1}(\boldsymbol{f}_{n+1})_{external}}^{\substack{Represents\ the\ virtual\ work\ done\ by\ external\ forces}} - \overbrace{\boldsymbol{K}_n^{-1}(\boldsymbol{f}_n)_{internal}}^{\substack{Represents\ the\ stored\ energy\ in\ system\\ in\ previous\ load\ steps}} \tag{5.132}$$

5. Update the deformation vector of the system
   $\boldsymbol{U}_{n+1} = \boldsymbol{U}_n + \Delta\boldsymbol{U}_n$ $(\Delta\boldsymbol{U}_n = \sum d\boldsymbol{U}_n)$;
6. Compute the stress increment $\Delta\boldsymbol{\sigma}_{n+1}$ of the current load step;
7. Update the stress vector of the system $\boldsymbol{\sigma}_{n+1} = \boldsymbol{\sigma}_n + \Delta\boldsymbol{\sigma}_{n+1}$;
8. Compute the internal force vector $(\boldsymbol{f}_{n+1})_{internal} = \boldsymbol{K}_n\boldsymbol{U}_{n+1}$;
9. Check the convergence criteria.

To solve Equation 5.131, the Newton-Raphson method has been applied. Each load step is divided into some sub-steps or iterations. The number of iterations depends on the convergence criteria. Figure 5-15 represents the n-load step of the solution domain. According to this figure, we have [38]:

$$R((\boldsymbol{U}_{n+1})_{i+1}) \approx R((\boldsymbol{U}_{n+1})_i) - \left(\frac{\partial R}{\partial \boldsymbol{U}}\right)_{n+1}(d\boldsymbol{U}_n)_i = 0 \tag{5.133}$$

To start the solution, $(\boldsymbol{U}_{n+1})_1$ is required, which is assumed to be equal to the converged answer of the last load step $\boldsymbol{U}_n$. The structural stiffness matrix is given by:

$$K_T = -\left(\frac{\partial R}{\partial \boldsymbol{U}}\right) \tag{5.134}$$

$$\left(K_T^i\right)d\boldsymbol{U}_n^i = R_{n+1}^i \rightarrow d\boldsymbol{U}_n^i = \left(K_T^i\right)^{-1}R_{n+1}^i \tag{5.135}$$

A new K_T matrix will be computed at every iteration of the load step. The transformations between coordinates, in particular, may require lots of time. Based on Eurocodes, in fire loading analysis, external actions—including live load and dead load—are assumed to be constant. The stiffness matrix of the structure will vary as the temperature distribution changes. To consider the path dependency, it is important to choose small load increments and small time steps.

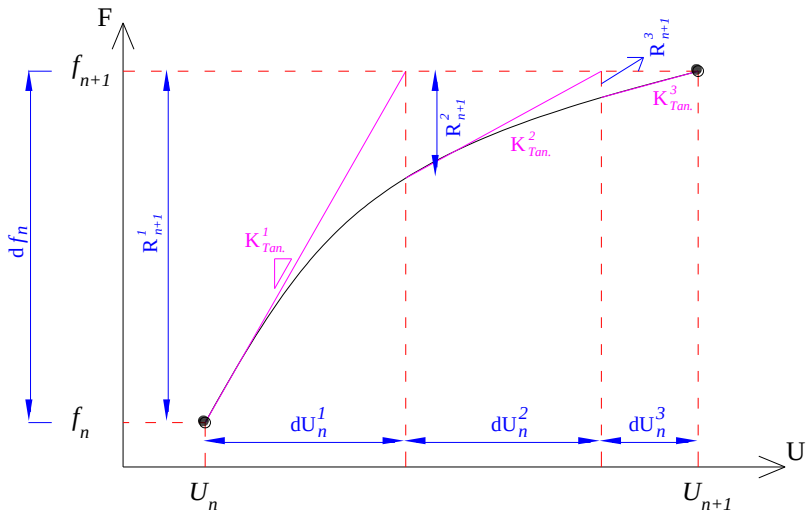

Figure 5-15: Newton-Raphson method

5.7 FEM Code

In Chapter 3, the FEM code of heat transfer is presented. Stiffness curves are required to calculate deformations of every load step. Three vectors—which save the axial and bending stiffness about weak and strong axes of warm members—will be imported to the mechanical analysis code. These vectors take into account the solution path. The solution path is a function of fire curves or the fire scenario.

<MECHANICAL ANALYSIS>
Import mesh;
X,Y,Z= Vector of nodal coordinates in global coordinate system;
Node = Number of nodes;
TOTALSTEPS = Number of time steps based on the fire curve;
EI22, EI33, EA → Import the stiffness curves for warm elements;
FORCEVECTOR = Define the external force vector;
<Solution of the first time step>
Begin a loop through all load steps for the first time increment of stiffness curves, load step variable n;

Begin a loop to converge the answers of the current load step;
Begin a loop through all beam elements, element number variable **e**;
K(e) = Calculate the linear element stiffness matrix for element e, see Fig. 5.6;
KG (e) = Calculate the geometric nonlinear stiffness matrix for element e, see Fig. 5.12.
Transform the stiffness matrices to global coordinate system;
End of the loop;
dF = FORCEVECTOR / n - FINTERNAL, incremental load vector;
DELTADIS = DELTADIS + (KTOTAL^{-1}).dF; incremental deformation
Begin a loop through all beam elements, element number variable **e**;
K(e), KG(e) = Calculate the stiffness matrix of element e in local coordinate system;
Calculate the force vector of element e in local coordinate system;

DELTADISLOCALT = Transfer the displacement of node i and j of element e to local coordinate system, $\Delta U_{local,t}$;
FINTERNALLOCAL = Calculate the internal forces of element including internal axial force T, $\left(KG(e) + K(e)\right)\Delta U_{local,t}$;
End of the loop;
Check the convergence criteria; if this is satisfied, terminate the loop;
End of the loop;

Update the displacement $U_{n+1} = U_n + \Delta U_n$;
Move the local coordinate system to the new position;
Update the internal force vector which represents the stored energy in system;
End of the loop;
<Solution of next time steps>
Begin a loop through all time steps, variable t;
Begin a loop through load steps of every time step, n;

Begin a loop to converge the answers of the current load step;
Begin of a loop through all beam elements, element number variable **e**;
K(e) = Calculate the linear element stiffness matrix for element e, see Fig. 5.6;
KG(e) = Calculate the geometric nonlinear stiffness matrix for element e, see figure 5.12. The stiffness matrices are calculated in local coordinate systems attached to the element;
KTOTAL = Place the element stiffness matrix into the stiffness matrix of the whole system;
End of the loop;
FINTERNAL = Calculate the internal force vector in global coordinate system, $(KTOTAL)\Delta U$;
dF = FORCEVECTOR – FINTERNAL;
DELTADIS = DELTADIS + ($KTOTAL^{-1}$).dF Calculate the displacement increment;
Begin a loop through all beam elements, element number variable **e**;
K(e), KG(e) = Calculate the stiffness matrix of element e in local coordinate system;
Calculate the force vector in local coordinate system;
DELTADISLOCALT = Transfer the displacement of node i and j of element e to local coordinate system, $\Delta U_{local,t}$;
FINTERNALLOCAL = Calculate the internal forces of element including internal axial force T, $\left(KG(e) + K(e)\right)\Delta U_{local,t}$;
End of the loop;
Check the convergence criteria; if these are satisfied, terminate the loop;
End of the loop;

Update the displacement $U_{n+1} = U_n + \Delta U_n$;
End of the loop;
End of the loop;

Figure 5-16: FEM procedure

6 The simplified method

6.1 Introduction

In the earlier chapters, only the thermal and mechanical finite element theories and material properties of concrete and steel in warm situations—which were required—were discussed. Details of the finite element theories can be found in different references. In this chapter, the basics of fire loading in Eurocodes and the simplified method will be presented. The finite element theories and material properties represented are implemented in a computer code. Using the developed code, deformation curves for the point of the structural model—which is presumed to have maximum deformation—are drawn. The method, which has been developed by applying some simplified assumptions, reduces the time required for the analysis, and makes it more convenient.

6.2 General regulations of Eurocodes—Fire design

In the current study, a new method—which is not categorized under simplified methods of Eurocodes—is researched. There are three levels of fire safety analysis in EN 1991-1-2: 1- Analysis of a member; 2- Analysis of a part of the structure; and 3- Analysis of the entire structure. To know about the structural analysis in Eurocodes and to place the simplified method between the existing methods of the Eurocode, the basic definitions of the simplified methods of Eurocodes are explained [18].

Global structural analysis: Structural analysis of the entire structure, when the whole structure—or some part of it—is exposed to fire. Indirect actions, such as

thermal expansion, are also included. According to EN 1990 [51], the global analysis of a structure is the determination of a consistent set of either internal forces and moments, or stresses that are in equilibrium with a particular defined set of actions on the structure.
Global structural analysis will consider the concepts of the Global Fire Safety, which are: [20]

- Building characteristics relevant to fire growth and development of fire in compartments to determine compartment type, fire scenario, and fire load;
- The risk function to start a fire. The risk of starting a fire can be a function of compartment, fire load, size of fire compartment, and firefighting measures and devices. Statistical data about the building type and occupancy can help the designer calculate the fire risk;
- Determination of fire load based on the fire risk analysis and design fire curve;
- Performance of the global structural and thermal analysis to check the global safety of structure under fire load (a part of the current study);
- Calculation of the design resistance time of the structure and comparison with the required time. The design resistance time of the building can be unlimited when the structure is able to bear the fire load.

To satisfy the fire safety, based on code regulations, some fire scenarios will first be defined. For each fire scenario, structural and thermal analyses will be performed, and the mechanical behaviour of the structure will be calculated. According to EN 1991-1-2, two approaches are available to consider the fire loads: the prescriptive approach or nominal curves, and the performance-based approach or natural curves. The prescriptive approach uses nominal fires to generate thermal actions. The performance-based approach, using fire safety engineering, refers to thermal actions based on the physical and chemical parameters of the fire compartment. These two approaches can be applied in the following cases: 1- Normal buildings with a fire load related to a building and its occupancy; and 2- They do not cover the assessment of the damage of a structure after a fire.

When the thermal actions or the fire curve are determined, hot members will be analysed and verified for the equivalent time of fire exposure. The required resistance of the structure exposed to fire will be verified by test results or methods given in building code. Based on the Eurocode, there are three valid methods of analysis: advanced calculation methods, simplified methods, and tabulated data.

According to EN 1991-1-2 [18], a structural fire design analysis should take into account the following steps:

1. **Selection of the relevant design fire scenarios**

The selection of the design fire scenario depends on boundary conditions, material to be burnt, openings for example windows, and fire protection equipment. The choice of the relevant design fire scenario is made by appropriate qualified and experienced personnel, or is given by the relevant national regulation. The total amount of thermal energies that will be released by the combustion of all combustible material in a space and the rate of heat release are important factors to calculate the fire curve of the compartments, which will be determined by the designer. In this research, the gas temperature and the energy transformation form—such as radiation, convection, conduction, or advection—are obtained, based on the regulations of EN1991-1-2 [18]. The standard fire scenario and fire curve for a fire compartment are assumed to calculate the temperature distribution in hot members.

2. **Design fire**

Design fires can be obtained when possible fire scenarios are determined. For each design fire scenario, a design fire in a fire compartment will be calculated. Depending on the design fire, the following procedures should be used:

- With a given nominal temperature–time curve, the temperature analysis of the structural members is made for a specified period of time, without any cooling phase. Nominal curves are explained in Annexure C.
- With a given natural fire model, the temperature analysis of the structural members is made for the full duration of the fire, including the cooling phase. In Annexure C, the process of obtaining the design fire for a fire compartment is explained.

3. **Temperature distribution**

Temperature distribution can be obtained by thermal analysis, simplified models, and tabulated data given in Eurocodes. In order to know the temperature distribution, we need to know the amount of heat transmitted to structural members. The amount of heat transmitted is known as heat flux. Heat transfers from hot material to cold material. Heat can be transmitted by radiation, convection, and conduction. Inside a fire compartment, heat transfers by convection and radiation between structural members and hot gas surrounding these members. Conduction occurs inside and between beams, columns, walls, and floors. The simplified method performs the thermal analysis for a member and the mechanical analysis for the whole structure.

In the current research, the simulation procedure of Level 2 based on Eurocode will be applied to obtain the reduced cumulative (integrated over the cross-section area) time-dependent stiffness of warm members as a function of time. The variable stiffness of warm members will be exercised to mathematize the global structural behaviour and calculate the distribution of internal forces after taking geometrical nonlinearity into consideration (Figure 6-1).

4. Mechanical analysis

The global structural analysis will take into account the relevant failure mode under thermal actions, the temperature-dependent material properties and member stiffness, and the effects of thermal expansions, thermal gradients, and thermal deformations. According to Eurocodes the verification can be based on Temperature, time and design resistance. The design resistance of members will be obtained in accordance with EN 1992-1-2 to 1996-1-2. Based on these codes, three methods are available to determine the design resistance: 1- Tabulated data, which can be used for special structures; 2- Simple calculation models for members, which satisfy the code limitations. (This method can be used to analyse one member or a part of the structure); 3- Advanced calculation models, which can be used for all types of members and structures. In case of the analysis of a part of the structure, appropriate subassemblies should be selected on the basis of the potential thermal expansions and deformations, such that their interaction with other parts of the structure may be approximated by time-independent support and boundary conditions during fire exposure. The internal forces, support reactions, and loads are assumed to be constant and equal to the values at time zero of the fire time domain. When analysing one member, it is also assumed that the external actions, internal forces, and support reactions do not depend on time and temperature. The analysis of a member and a part of the structure do not give the redistribution of internal forces for the global structure.

To verify the design resistance, resistance time and temperature of members facing fire, the following equation will have to be satisfied:

$$E_{fire,d,t} \leq R_{fire,d,t} \quad (6.1)$$

$E_{fire,d,t}$ is the internal force for the fire situation at time t and $R_{fire,d,t}$ is the design resistance of a member facing fire at time t. The current study considers just the left side of Equation 6.1. The right side of this equation will be obtained by using the given regulations in codes. In Annexure D, an example is solved by using the simplified method of Eurocode. The simplified and tabulated methods of the Eurocode are based on laboratory tests and give conservative results.

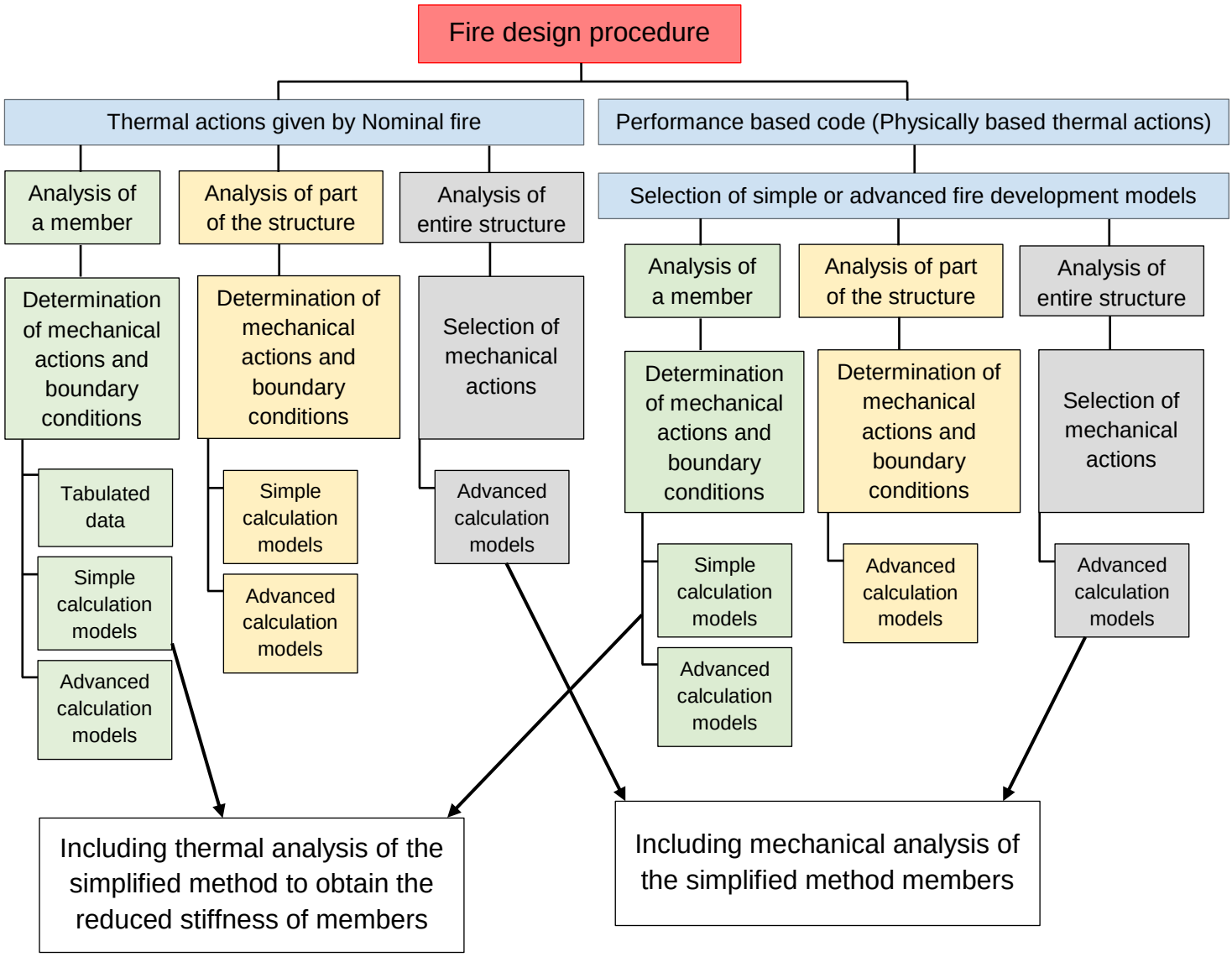

Figure 6-1: Design procedures for fire situation based on EN 1991-1-2 [18]

6.3 Modulus of elasticity of concrete

Figure 6-2 gives the modulus of elasticity of concrete type C30 at temperatures based on Eurocodes. In Chapter 3, we obtained the modulus of elasticity of concrete for all types of concrete defined in Eurocodes. The modulus curve will be modified for use in computer code or ANSYS. In the computer code, it may be assumed that the modulus of members that have already experienced temperatures more than a given critical temperature is zero and remains zero for the next few time steps. For example, if a fibre of the frame section reaches the given critical temperature at time step t, the modulus of that part will be zero at time steps $t + 1,2,3,\ldots$. The developed method assumes the mean value of stiffness of all parts of the frame section as the stiffness of a warmed member. The modulus of elasticity for three-dimensional brick elements of ANSYS Workbench will not be less than a predetermined value. If the stiffness or modulus of elasticity of 3D brick elements of ANSYS Workbench turns to zero

at time step t, the analysis would be unstable, and not 'convergable'. The modulus of elasticity will be chosen bigger than a critical value to have the stability. In ANSYS Workbench, the lower limit of modulus of elasticity is assumed to be 1 GPa (=100 kN/cm^2) for concrete type C30.

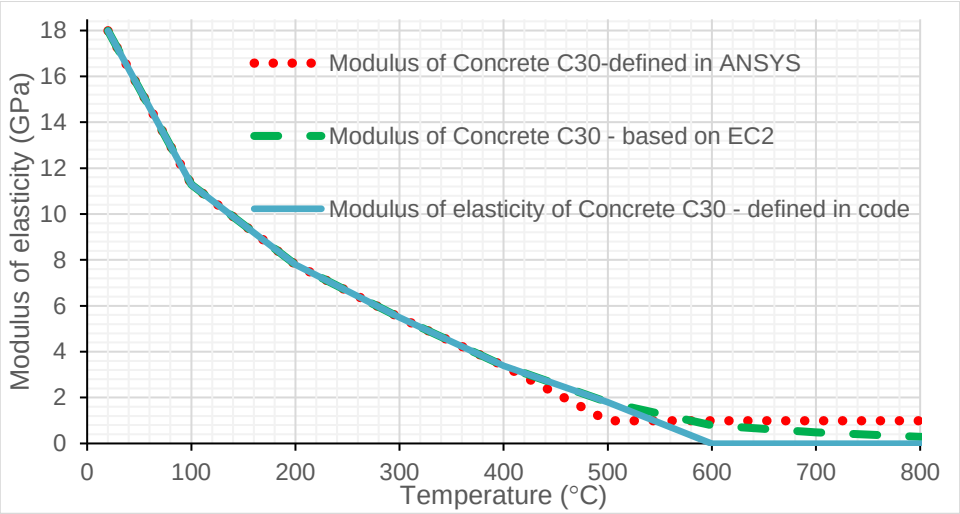

Figure 6-2: Modulus of elasticity of concrete type C30, as defined in ANSYS Workbench and the computer code

6.4 Effective stiffness

The effective bending and axial stiffness can be calculated by numerical integration of bending and axial stiffness of each element over a cross-section. The cross-section will just be divided into some elements that consist of different materials with different moduli of elasticity—here, triangular elements. *Depending on the temperature calculated at time t for each element, material properties of each element vary.* The following simple method has been used to calculate the cross-section properties:

According to EN 1994-1-2 Section 4.3.5.1, the effective bending stiffness is [3]:

$$(EI)_{eff,T} = \sum_j (\varphi_{s,T} E_{s,T} I_{s,T}) + \sum_i (\varphi_{c,T} E_{c,sec,T} I_{c,T}) \quad (6.2)$$

where $\varphi_{s,T}, \varphi_{c,T}$ are the reduction coefficients, depending on the effects of thermal stresses for concrete and steel; here, these are assumed to be unity. Having temperature distribution at time *t* and modulus of elasticity for steel and concrete as a function of temperature, the bending (*EI*) and axial (*EA*) stiffness of the cross-section at temperature T_e can be calculated. A numerical integration over the cross-section will be performed to obtain the total stiffness of all elements about the neutral axis of the cross-section. If the elements are small enough, their bending stiffness about element neutral axis may be neglected. The last equation can be written in the following form:

$$EI_{total,T} = \int E_T y^2 dA \approx \sum_{element\ 1}^{element\ N} E_{e,T} y_e^2 A_e \quad (6.3)$$

where $EI_{total,t}$ is the bending stiffness at time *t*, $E_{e,T}$ is the modulus of elasticity for element *e* at temperature T_e , y_e is the distance between centroid of the element and elastic bending axis, A_e is the area of element *e*. For example, imagine we have the cross-section of Figure 6-3 under the fire load. Since the temperature field is known, we are able to calculate the bending and axial stiffness of the cross-section, as shown in this figure.

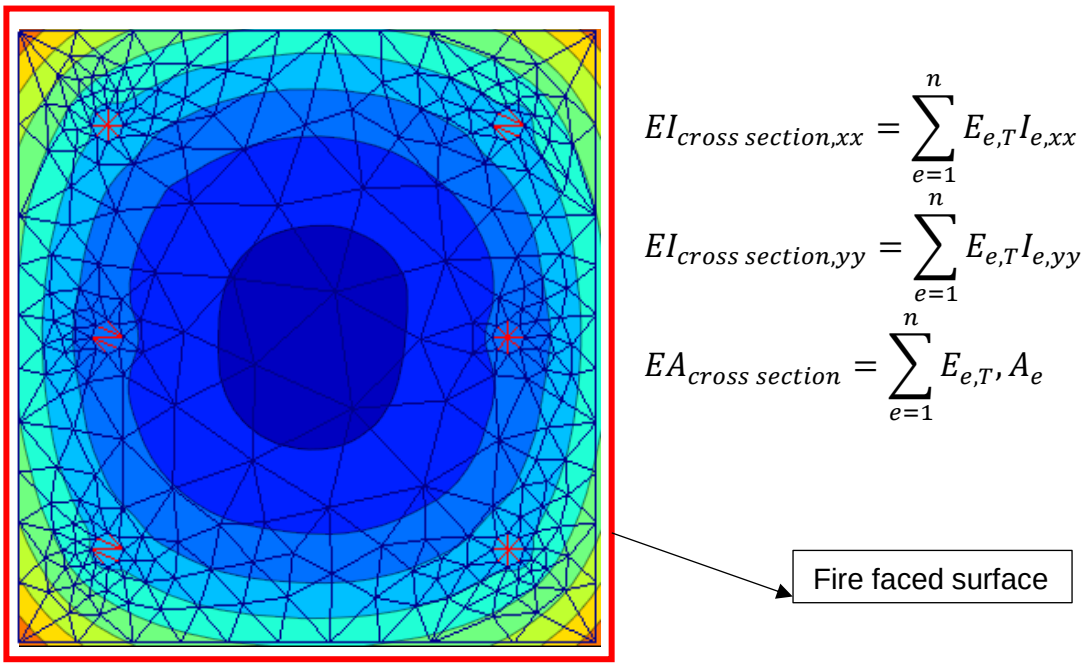

Figure 6-3: Stiffness of composite cross-sections

During the cooling phase, structural members do not recover their initial stiffness (EI or EA) because concrete elements which experience temperatures more than a predefined temperature (here, 500–800 °C) are assumed to have zero modulus of elasticity from that time step to the end of the time domain. Apart from this issue, concrete cannot recover 100% of its initial modulus of elasticity, which is not modelled in the current research. To calculate the bending and axial stiffness of members faced to thermal loads in cooling phase, the modulus of elasticity is obtained from the Eurocode regulations.

By assigning the temperature curve, which consists of the warming and cooling phases of a fire scenario, the temperature field of cross-sections has been calculated. Afterwards, the variation of cross-section stiffness, which depends on material properties of hot members, is obtained. To obtain these curves, the following points will be considered:

1. The structural members under fire-loading are assumed to be similar to composite cross-sections with different materials and stiffness. Therefore, if the temperature field is available, the bending stiffness and axial stiffness of cross-sections under fire-loading can be obtained by replacing the warmed cross-section with a composite one.
2. It is important to note that the neutral axis of the cross-section may vary when temperature changes. If the thermal load and the geometry of the cross-section are symmetric, the neutral axes will not vary. If the thermal load or the geometry is asymmetric, the neutral axis will move as the temperature varies. The movement of the neutral axis exerts a considerable influence on bending stiffness and second order effects, which may increase the internal forces. For columns with a significant axial load, the eccentricity of the axial load is quite important. The eccentricity of the axial load will vary as the temperature field of the cross-section changes. Structural members facing asymmetrical thermal loads, such as end columns or beams that face fire at the bottom face, are members with eccentricity of neutral axis under fire loads.

<STIFFNESS CURVES>

TEMPERATURE = Import the results of thermal analysis for all time steps;

X,Y = Vector of nodal coordinates;

Node = Number of nodes;

TOTALSTEPS = Number of time steps based on the fire curve;

EITOTALY, EITOTALX, EATOTAL = Define three matrixes to save the stiffness in all time steps;

ELEDIE = define a vector to determine the existence of each element at each time step. If **ELEDIE** is 0 element stiffness will be zero, and if ELEDIE is one, element stiffness will be taken into account.

Begin of a loop through all time steps, time variable **step**;

    Set the cross-section properties zero for the current time step;

    Begin of a loop through all elements, element counter **e**;

        T = Call the temperature of element **e** at time step ***step***;

        If element **e** is a concrete element

            If (**T** > 450) (See Sec. 2.5)

                Element will die, and the modulus of elasticity for this element is zero;

                Set the **ELEDIE** variable equal to zero for this element;

```
            If (T < 450) (See Sec. 2.5)

                 Calculate the modulus of elasticity for concrete at
                 temperature T, see Table 2.4;

                 Set the ELEDIE equal to one for this element;

        If element e is a steel element

            If (T > 250)

                 Set the modulus of elasticity for steel equal to zero;

            If (T < 250)

                 Calculate the modulus of elasticity for steel at temperature
                 T, see Table 2.1;

        AELE = Calculate the area of the element;

        XELE, YELE = Calculate the coordinates of the centre of the element;

        EIXX, EIYY = Calculate the moment of inertia about X and Y axis for that
        element, I=E.A.d2;

        EA = Calculate the axial stiffness for the element;

          EITOTALY = EIYY + EITOTALY;

          EITOTALX = EITOTALX + EIXX;

          EATOTAL = EATOTAL + EA;

        Calculate the coordinate of neutral axis for each time step;

    End of the loop;

    Save the calculated stiffness for the current time step and set all variables
    equal to zero for the next time step;

End of the loop;
```

Figure 6-4: Process of calculating the effective stiffness

6.5 Applying the developed method

In this section, we solve a simple multi-storeyed structure by applying the computer code. The computer code includes eight tabs. In each tab, one step of analysis will be performed.

To consider all parameters—such as path dependency, redistribution of internal forces and moments, nonlinear effects, and thermal strains—advanced methods of analysis will be applied. These methods cannot be suitable for complicated systems, such as multi-storeyed buildings. The developed method can reduce the cost of analysis and time, and is simple in its application. Figure 6-5 illustrates the flowchart of the simplified method.

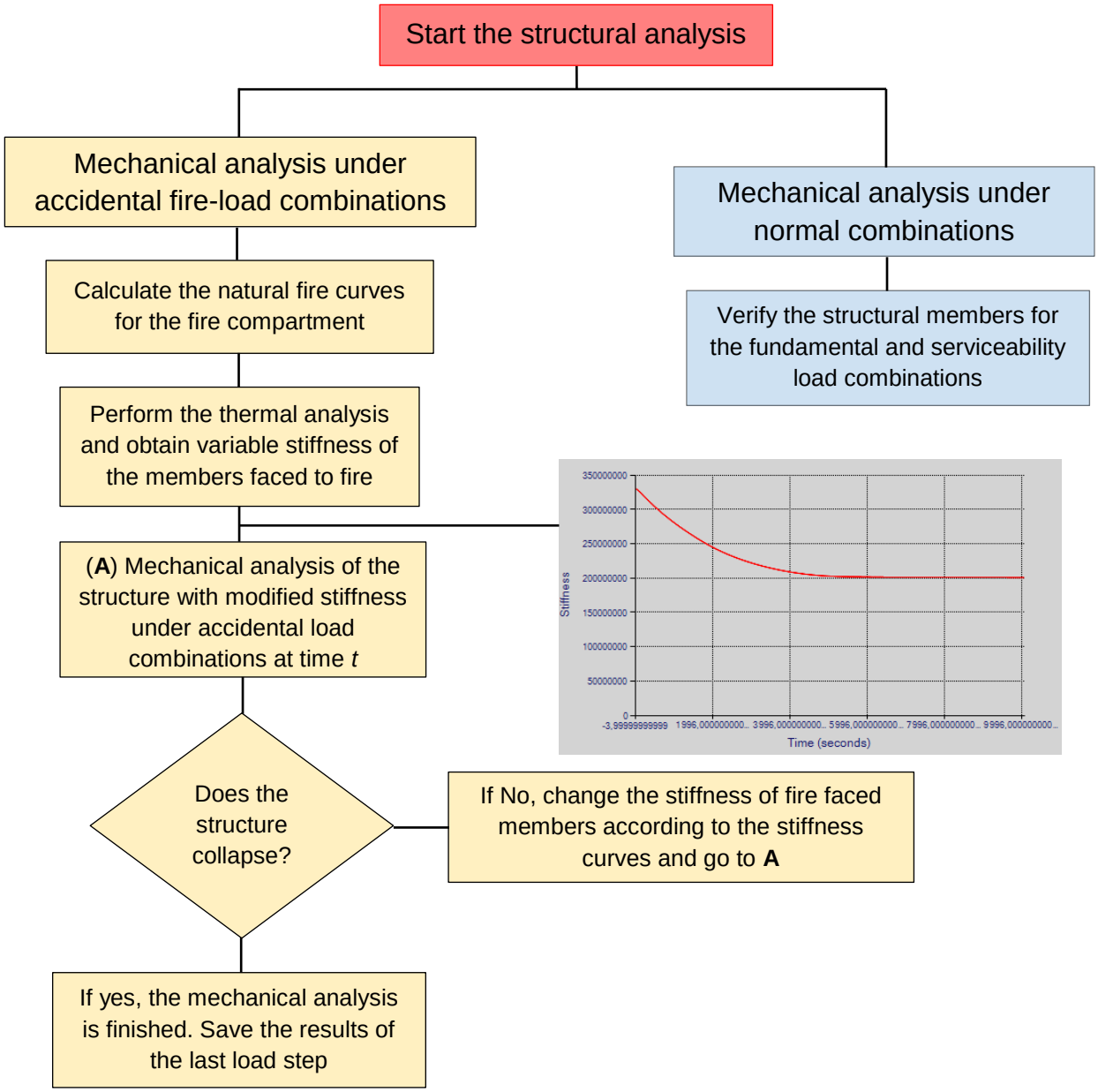

Figure 6-5 Flowchart of proposed process of analysis of fire loading

The designer will first analyse the structure for cold loads and design the members to withstand the cold situation. The results of cold design will be

considered the initial condition of warm design at time t=0. Afterwards, the possible fire scenarios will be chosen, and the variable stiffness of members facing fire can be calculated. On having the variable stiffness of warm members, an analysis can be performed to obtain the internal forces and check the safety of the structure. The failure criteria might be large deformations that are not accepted in buildings, stress, or large strains. Small deformations caused by fire loads mean small-scale redistribution of internal forces and changes in material properties.

To apply the fire loads using the developed method, five steps will be performed. First, the type of analysis—linear or nonlinear—will be determined. The computer code is able to consider geometric nonlinearities and variable stiffness of material, which is a type of nonlinearity. Here, we will explain the necessary steps in the course of a worked example. Imagine a multi-storeyed hospital with reinforced concrete columns and beams; see Figure 6-6. The modelling of the system shown in Figure 6-6 is proposed. It will be assumed that the highlighted elements are facing fire. The gravity loads including imposed loads and dead loads are assumed; see Equation 6.4. Table 6.1 represents the cross-section dimensions and material of the columns and beams of the example.

$$Dead\ Load = 600\frac{kg}{m^2}\ \&\ Live\ load = 500\ \frac{kg}{m^2}\ for\ hospitals \tag{6.4}$$

The developed software is a Microsoft Windows Form consisting of eight tabs. The first tab explains the local and global coordinate systems and loads. Here, the type of analysis—linear or nonlinear—will be determined. If the geometric nonlinearities are considered, the number of load steps and iterations per load step will be given by the user.

In the case of thermal analysis, fire curves will be defined and imported to code. All inputs of the code will be in .xlsx format (Microsoft Excel worksheets). Sample input files can be generated by the software. Figure 6-8 shows the first tab. The figure shows the local and global axes of the element, which should be considered as the user defines the structural model in Microsoft Excel.

Table 6.1: Cross-section dimensions and material of the example

Storey	Typical column cross-section	Typical beam cross-section	Deep columns assumed as shear walls	Storey height
1	Concrete C50 - 60x60	Concrete C50 – 60x60	Concrete C50 - 120x60cm	450cm
2	Concrete C50 - 60x60	Concrete C50 – 50x40	Concrete C50 - 120x40cm	450cm
3	Concrete C50 - 50x50	Concrete C50 – 50x40	Concrete C50 - 120x40cm	450cm
4	Concrete C50 - 50x50	Concrete C50 – 50x40	Concrete C50 - 120x40cm	450cm
5	Concrete C50 - 50x50	Concrete C50 – 40x40	Concrete C50 - 120x40cm	450cm
6	Concrete C50 - 50x50	Concrete C50 – 40x40	Concrete C50 - 120x40cm	450cm
7	Concrete C50 - 50x50	Concrete C50 – 40x40	-	450cm

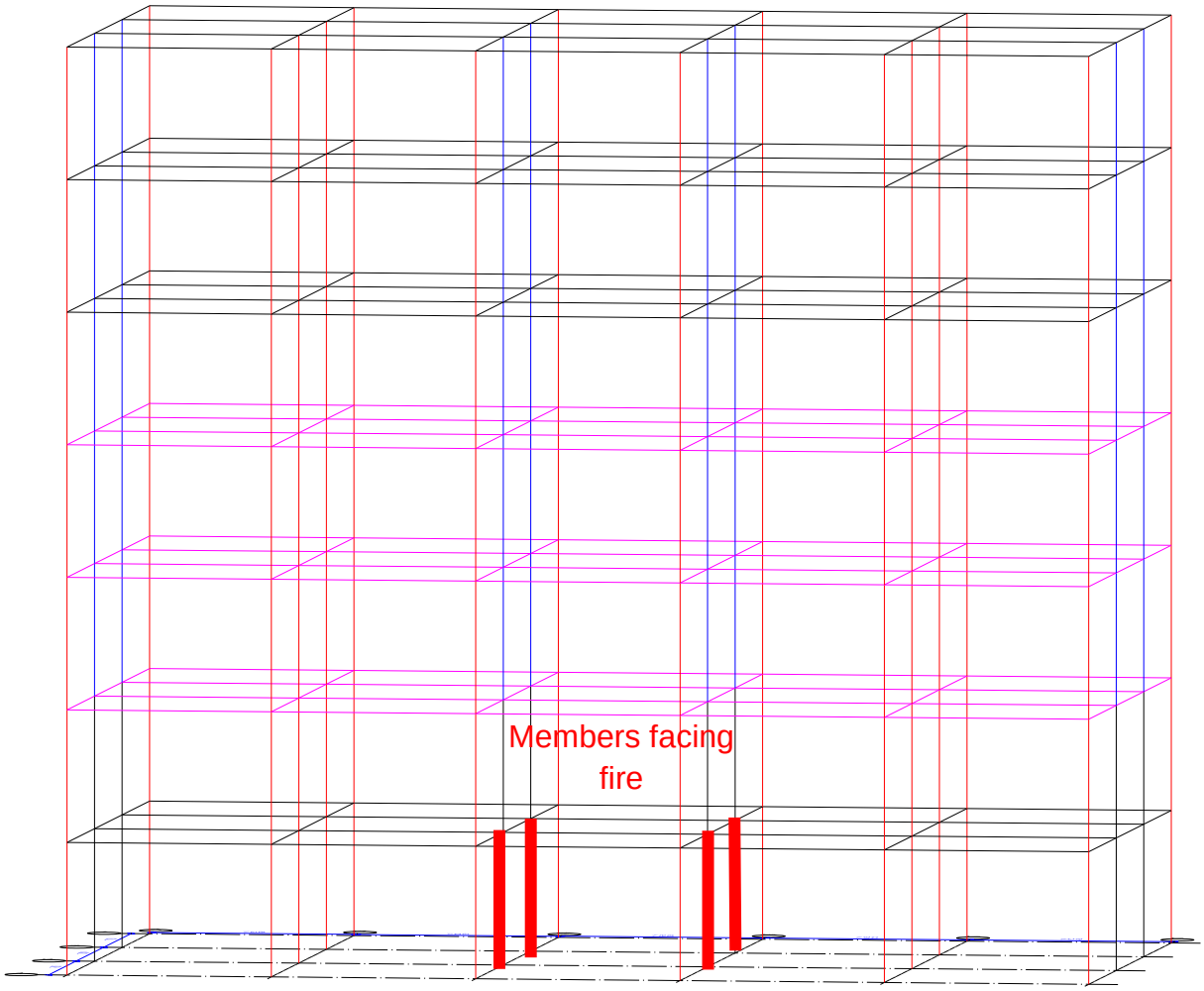

Figure 6-6: 3D view of the static model—the marked columns are on four sides exposed to fire. Cross-section dimensions and material properties are given in Table 6.1

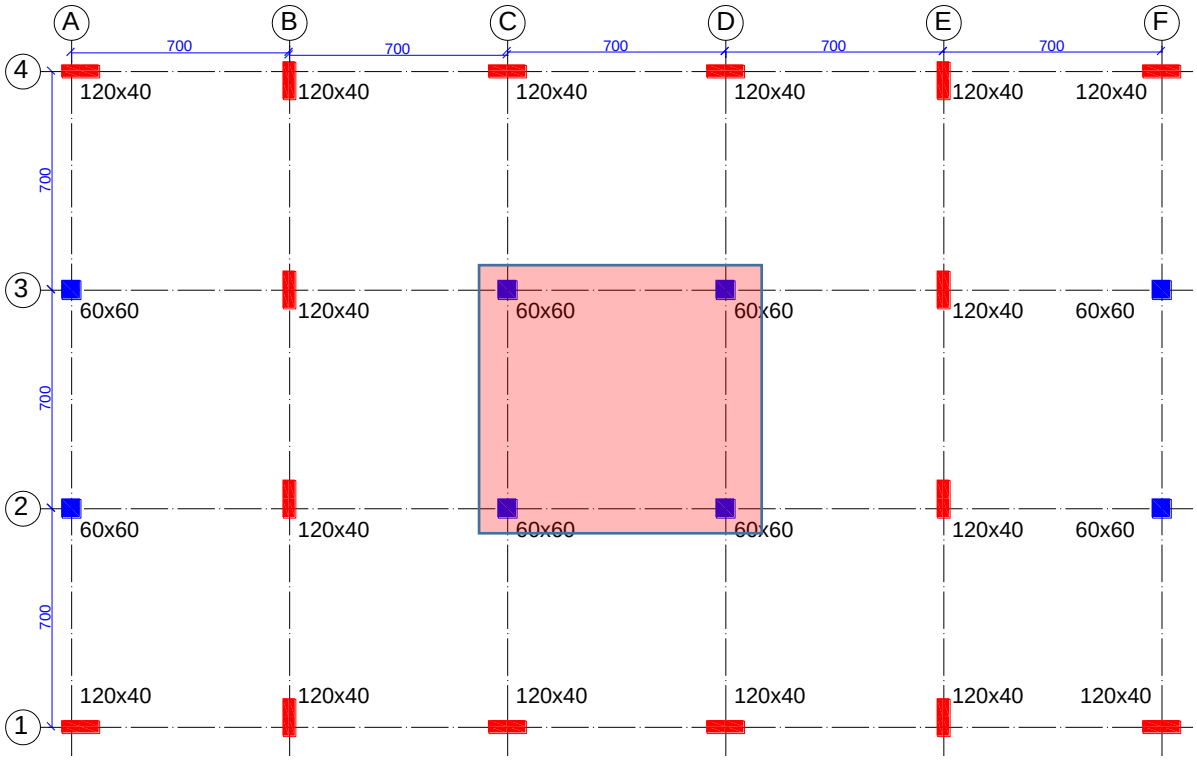

Figure 6-7: Base plan of the hospital

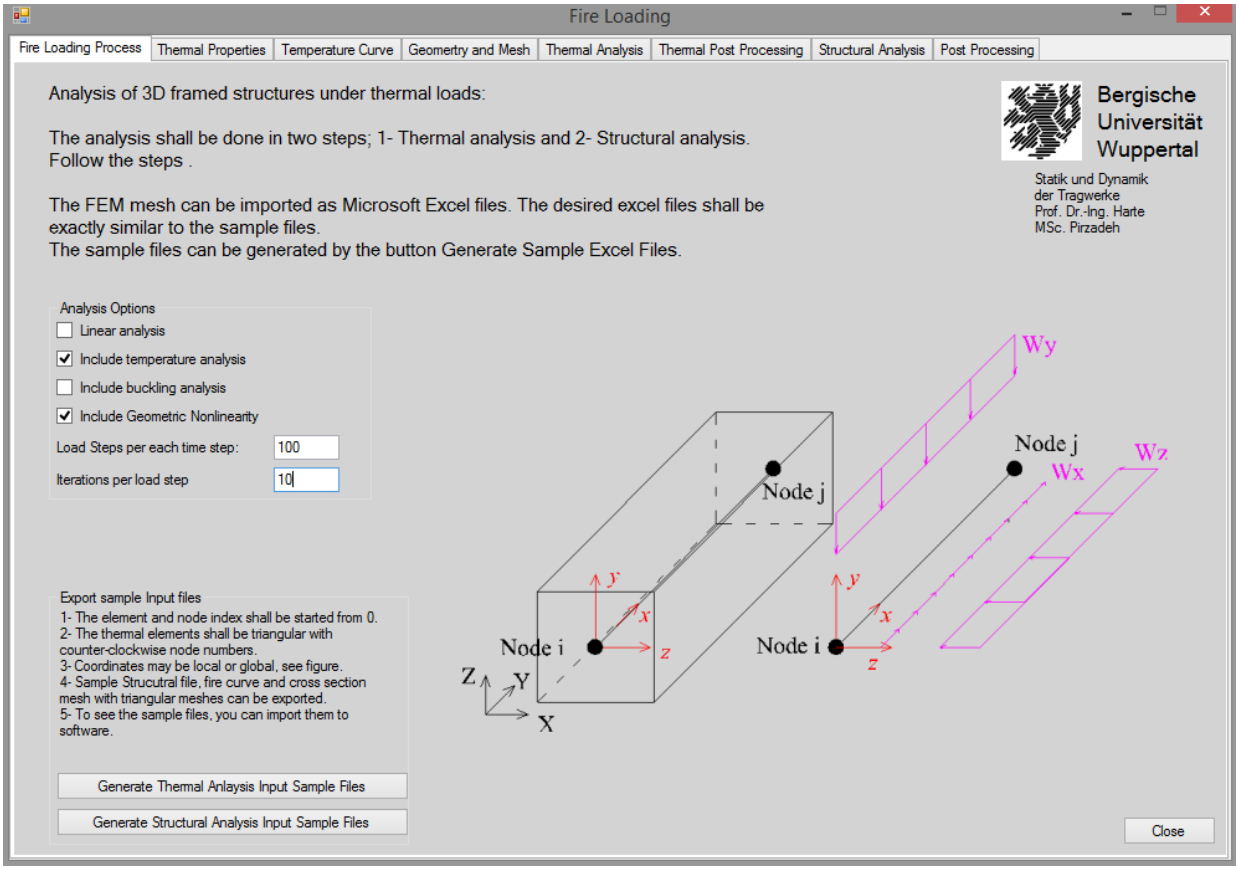

Figure 6-8: First tab of the code—options of analysis

6.5.1 Step 1: Material properties

The properties of concrete and steel based on Eurocodes (see Chapter 3)—including specific heat, modulus of elasticity, heat conductivity, and coefficient of thermal expansion—are defined in Windows Form and can be determined in the second tab. For steel structures, the simplified method is valid at low temperatures. For composite structures consisting of steel and concrete, the method would be valid at high temperatures only if the strain limits are respected. It should be considered that in the case of estimating the behaviour of concrete structures, the simplified method can be an estimating tool for fires with maximum element[2] temperatures less than 600°C.

The problems of fire engineering can be divided into two categories: a) investigating the residual resistance and obtaining the redistributed internal forces of a building that has already experienced fire loads, and b) designing a structure for a given fire scenario. In both cases, the developed method can be applied under some conditions. The choice of maximum element temperature, material properties, and protection method depend on the engineering judgement. The simplified method can mathematize and estimate the structural behaviour in the following conditions:

1- Steel structures: The simplified method may be applied if the maximum element temperature during a fire process is less than 200°C. At temperatures lower than 200°C, the maximum strain for steel does not depend on temperature (see Table 3.5). Generally, analysing an unprotected steel construction is not of interest. It will be assumed that unprotected steel members are not fire-resisting members.

2- Concrete and composite structures: Concrete is a composite material consisting of steel, aggregates, and cement. Concrete has low thermal conductivity and conducts heat very slowly. It is suitable for use as a fire-resisting structural member or to protect such members. The method may give better estimation for application to concrete constructions.

The material properties of different types of concrete, according to Eurocodes—including modulus of elasticity, thermal conductivity, thermal expansion, and specific heat—are defined in computer code as a function of temperature. The user will just change the concrete type. Figure 6-9 shows the second tab of the computer code to define the temperature-dependent material properties for steel and concrete.

[2] Element temperature is defined as the temperature of structural members and gas temperature is the temperature of surrounding gas. The gas temperature is the fire curves, based on Eurocodes.

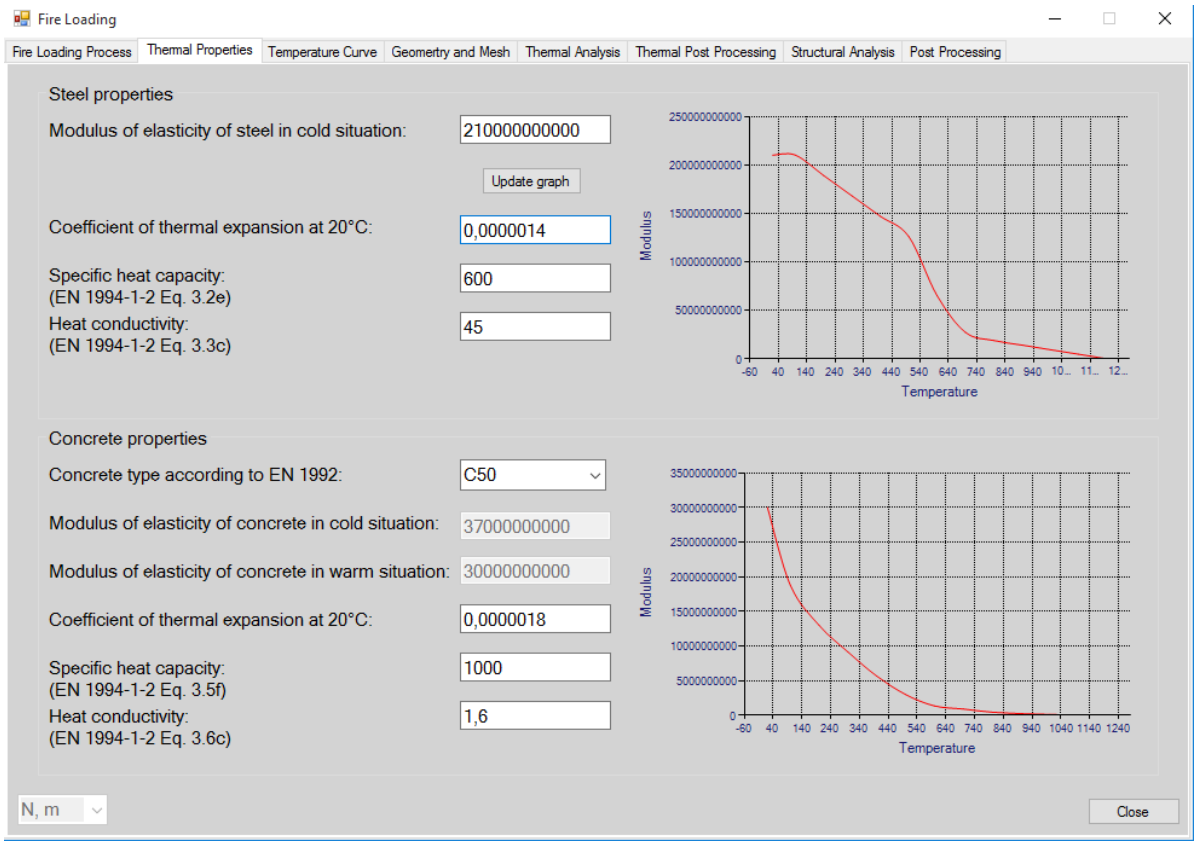

Figure 6-9: Defining concrete and steel material properties

6.5.2 Step 2: Fire curves

Thermal analysis of structures under fire loads can be divided into two categories: a) thermal analysis using nominal curves and b) analysis by applying natural ones. Nominal curves are calculated for a fire compartment based on load density and compartment boundaries, such as walls and windows. Nominal curves can be calculated by the suggested process in Eurocodes. Annexure C gives the calculation method of nominal curves in accordance with Eurocodes. The fire curve calculated in Annexure C will be imported using Microsoft Excel worksheets. Figure 6-10 shows the imported fire curve to software. The upper limit of element temperature can be defined in the third tab. When calculating stiffness curves, the software removes bending and axial stiffness of elements with temperatures higher than the upper limit.

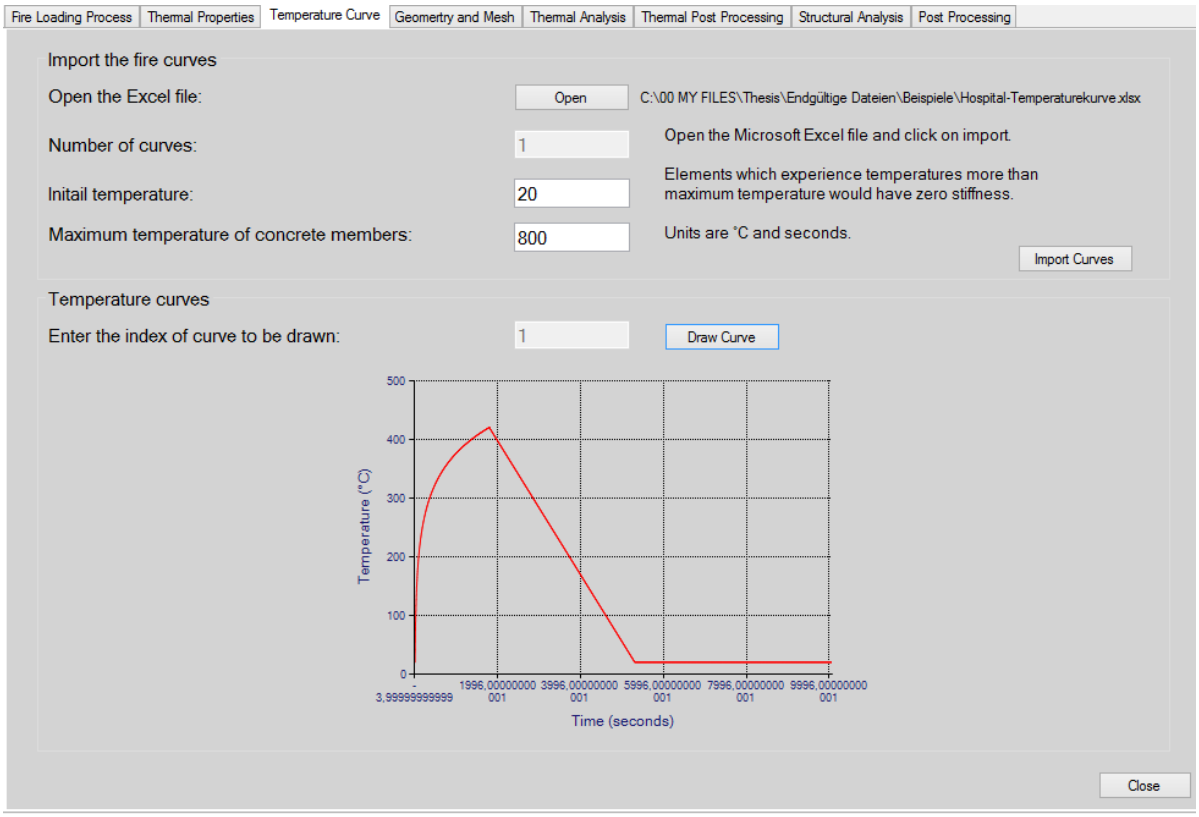

Figure 6-10: Parametric fire curve, including cooling phase, imported to the program

6.5.3 Step 3: Geometry and mesh

Skeletal structures will be meshed and imported to the software. Microsoft Excel should be used to define the mesh. A finer mesh can yield more accurate results. When nonlinear structural analysis is applied, time step size and element size should be small enough to obtain the converged solution. If the stiffness of warm members varies during time, time steps should be small enough to be able to model large deformations. For time steps more than 3 seconds, in some cases, the analysis may not converge.

Loads—including thermal loads and distributed and point loads—can be modelled by software. The input file contains loads, coordinates, and mesh of the structure. Figure 6-11 illustrates the isometric view of the imported mesh to the software.

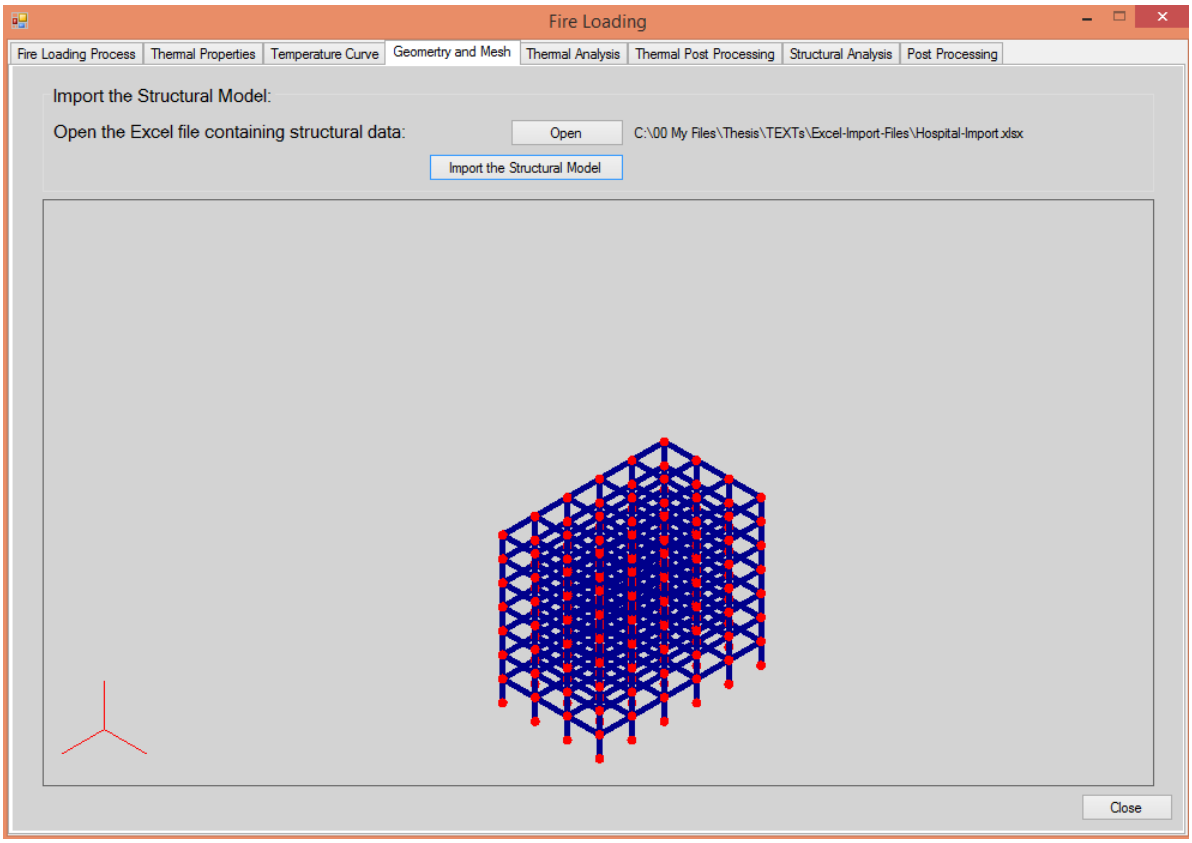

Figure 6-11: Structural mesh imported to computer code

6.5.4 Step 4: Thermal analysis

The members that face elevated temperatures will be defined and the cross-section mesh for warm members will be imported to software. Afterwards, the temperature distribution and stiffness curves can be calculated. Figure 6-12 shows the calculated stiffness curves. At the next step, the stiffness of warm members will vary in accordance with the curves calculated here. Bending and axial stiffness of warm members are $EI_{yy}, EI_{yy}, and\ EA$.

It has been assumed that the marked columns at the first storey are facing the fire. The cross-section of warmed members: 60cm x 60cm. The FEM code is able to draw a contour plot of temperature distribution at each time step and calculate the variable stiffness of members facing the thermal load; see Figure 6-12. Figures 6-13a–e show the temperature distribution for beams of structure in Figure 6-11.

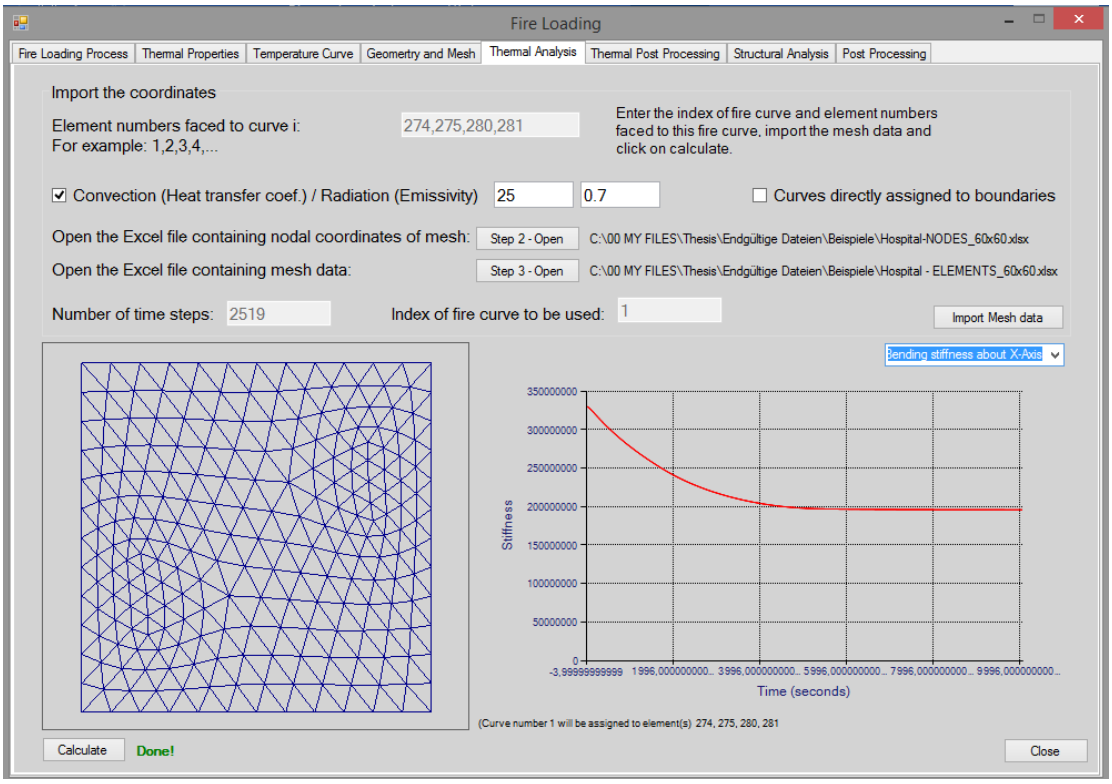

Figure 6-12: (a) Bending stiffness curves of hot members, for cross-section 60x60cm

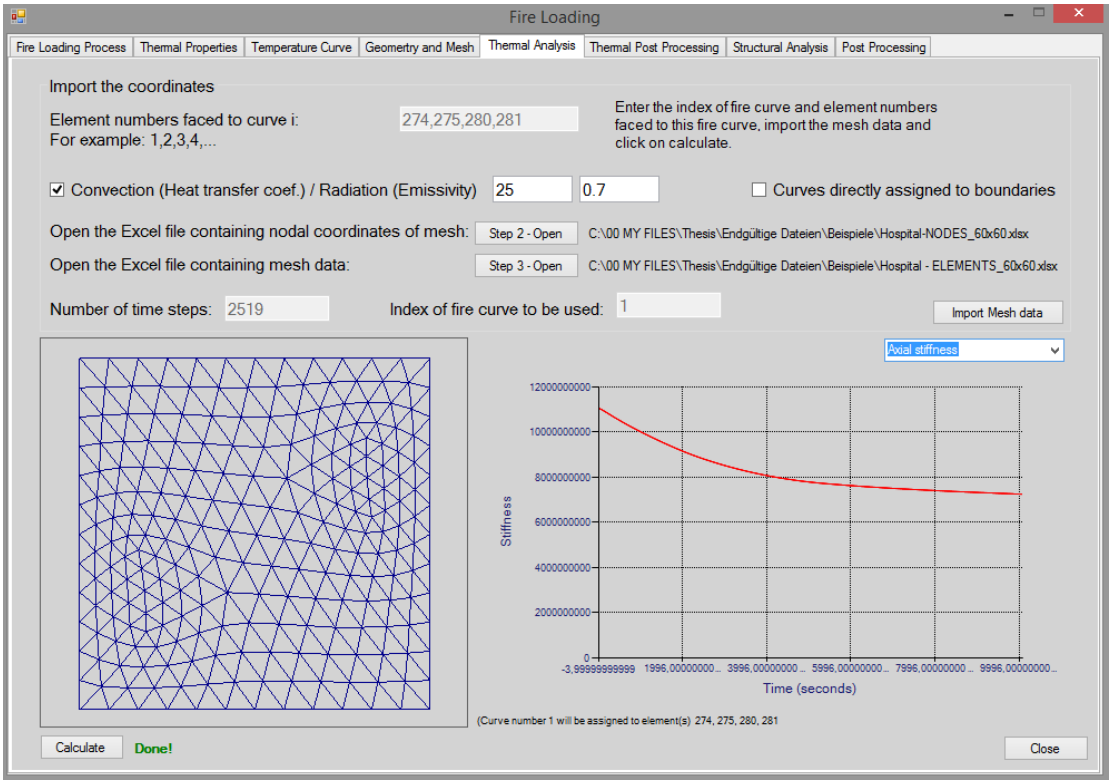

Figure 6-12: (b) Axial stiffness curve of hot members, for cross-section 60x60cm

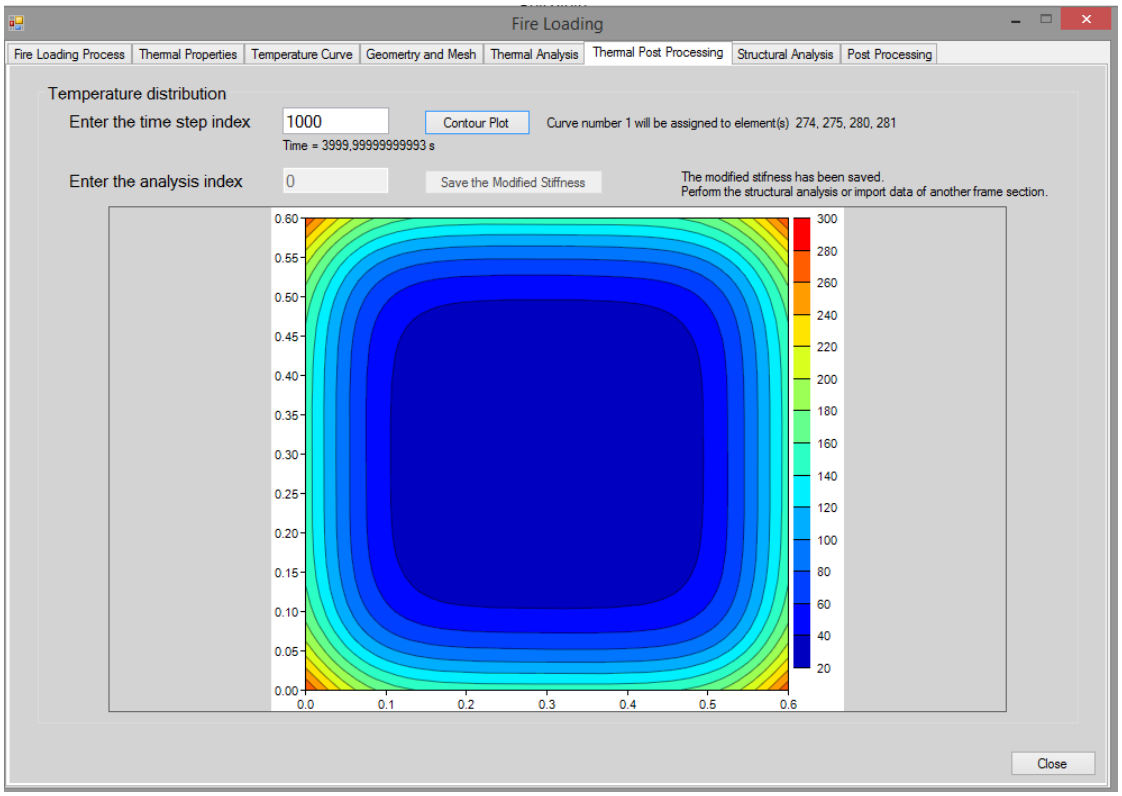

(a)Temperature distribution, for cross-section 60cmx60cm, time=4000s

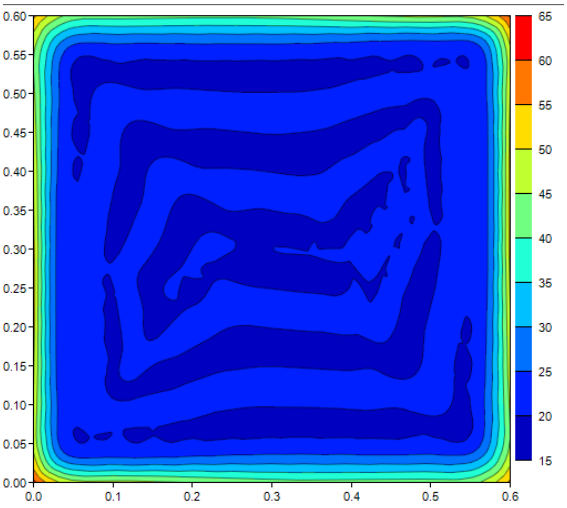

(b): Time=400s

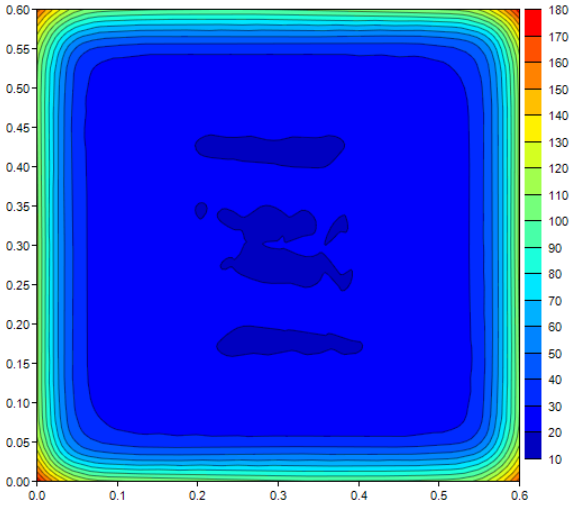

(c) Time=1400s

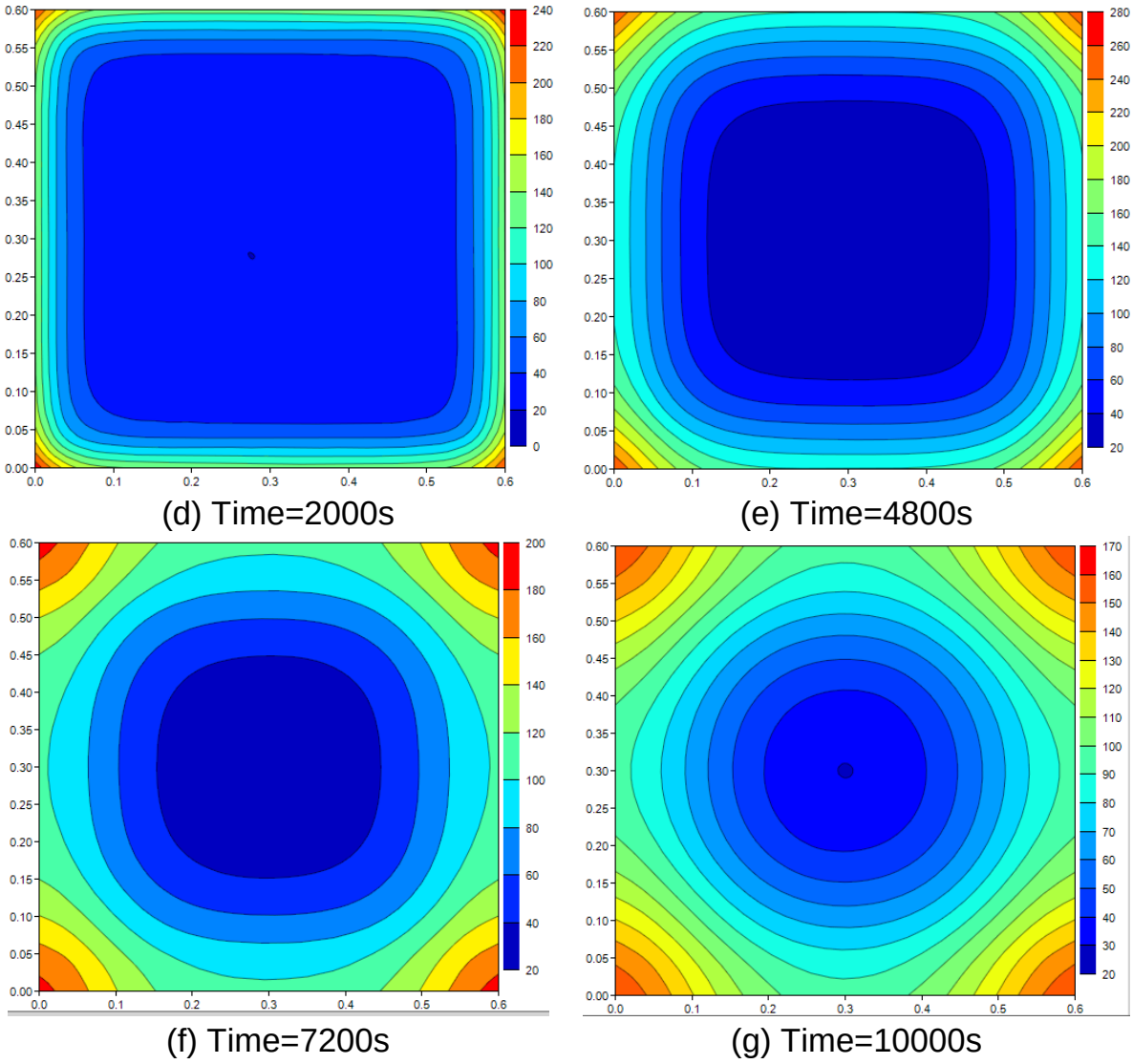

Figure 6-13: Temperature distribution, for cross-section 60cmx60cm

6.5.5 Step 5: Mechanical analysis

The path of analysis depends on the stiffness curves. It is important to check the maximum deformation of members to obtain converged results. The computer code is able to draw the deformation path of joints and internal forces of members.

The results of the computer code for the structure shown in Figure 6-6 can be seen in Figures 6-14–17. The analysis time is about 10 hours for 4s time step size and ca. 10000s time domain size.

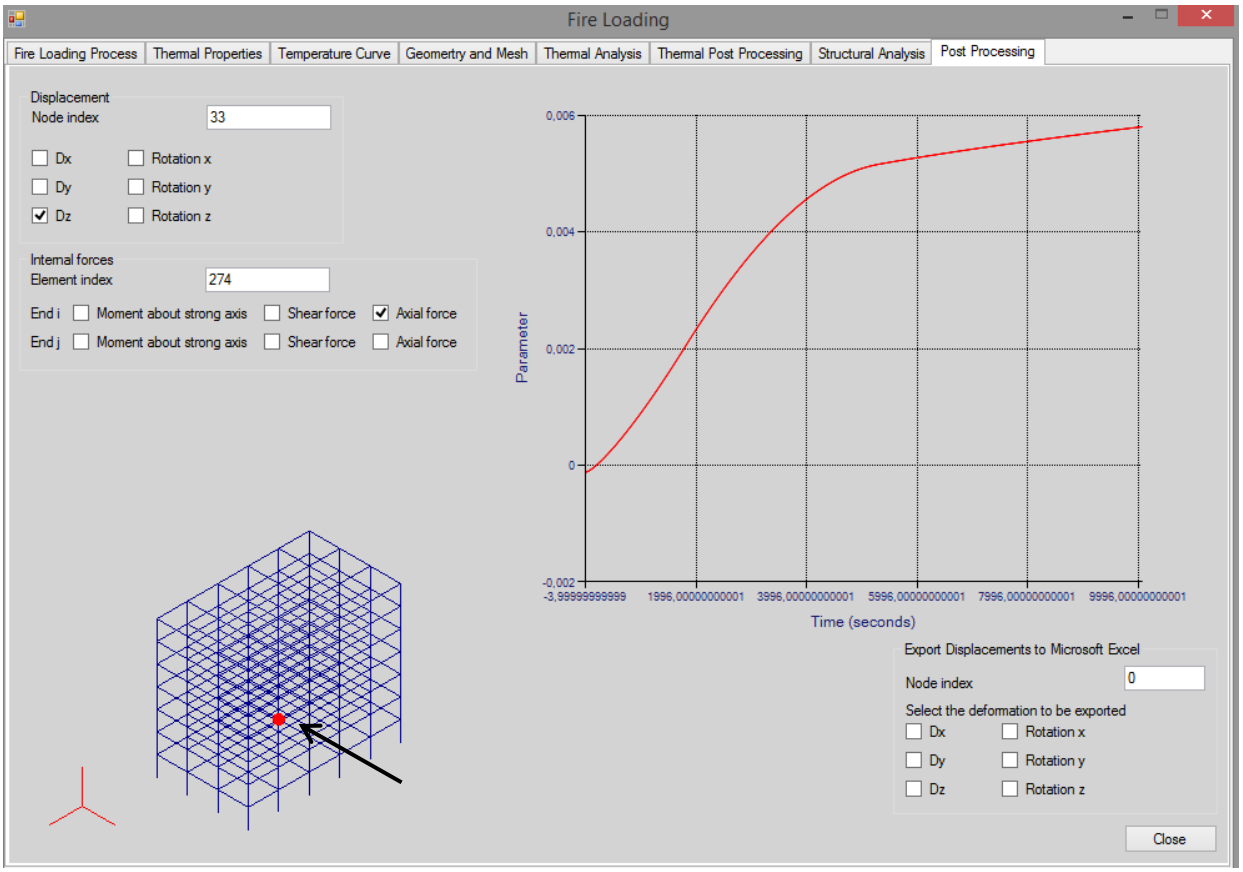

Figure 6-14: Deformation (m) of Point 33 (end of the warmed column) as a function of time in z-direction

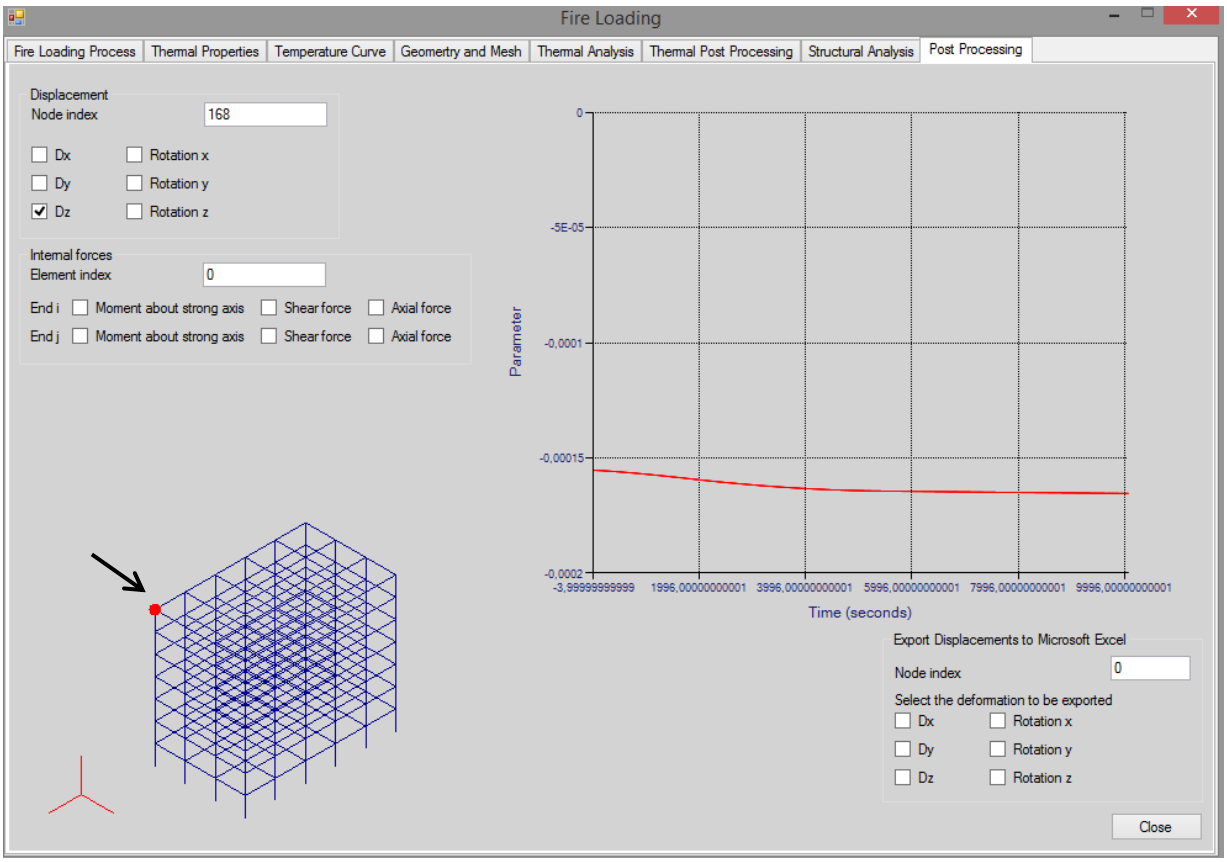

Figure 6-15: Deformation (m) of Point 168 as a function of time

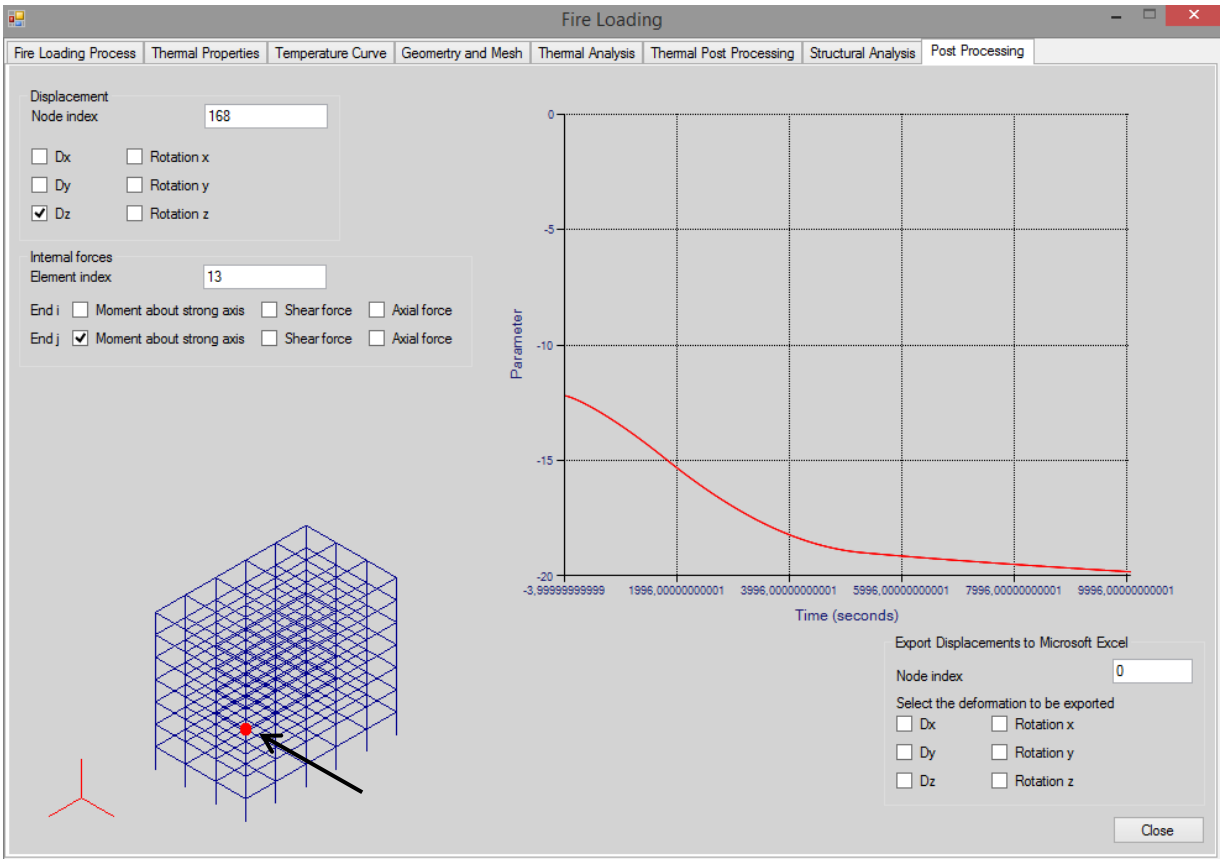

Figure 6-16: Bending moment ($kN.m$) for Element No. 13 as a function of time

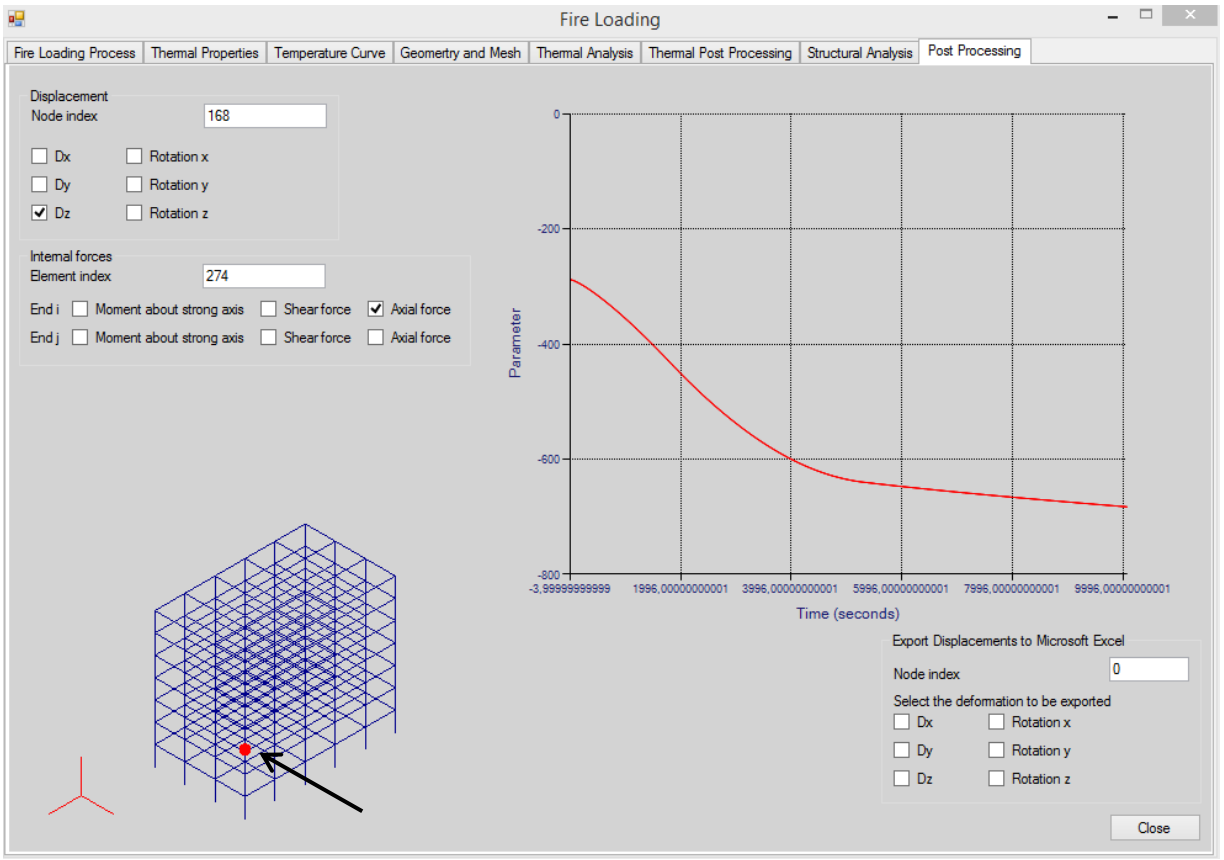

Figure 6-17: Axial force (kN) for Element No. 274 as a function of time

7 Validation and verification

7.1 Introduction

In Chapter 7, we will validate the results of the computer code by applying the multi-phase analysis of ANSYS Workbench software. To do this, seven examples are solved with the help of the developed code and ANSYS Workbench.

The warm design of structures requires the determination of temperature distribution. Three-dimensional elements in ANSYS Workbench are able to model the temperature field and take into account material and geometric nonlinearity of beams and columns. The temperature-dependent material properties of concrete or steel will be defined in ANSYS Workbench. Based on the thermal properties of materials, ANSYS Workbench obtains the temperature distribution at each time step. With the temperature distribution and the deformation of the system at time step $t - 1$, ANSYS Workbench will be able to calculate the structural response of the system at time t. The temperature distribution can be obtained before mechanical analysis—or parallel to mechanical analysis—at each time step. Since the deformations are not too big and the finite element mesh does not move, the temperature distribution will be independent of deformations. Therefore, the thermal analysis can be executed independently from the structural analysis.

To obtain the temperature distribution and variation in stiffness of beams and columns, three-dimensional solid brick elements will be used in ANSYS Workbench. The element has six translational and rotational degrees of freedom and one thermal degree at each point: see Figure 7-1.

To learn more about ANSYS Workbench software, the reader is referred to ANSYS Workbench help documentation, which can be found online or is delivered with the software [52]. There are various solved examples, which can be found in ANSYS Workbench documentation about thermal and structural analysis. In the current study, a multi-phase analysis of ANSYS Workbench has been used to model the thermal and structural behaviour of beams and columns. In the ANSYS Workbench, two thermal and structural transient analyses will be defined. The results of transient thermal analysis will be imported to the transient structural analysis as body temperatures. Performing time history analysis—when 3D brick elements are applied—can be time-consuming. For example, the analysis, including structural and thermal effects, may take about 18 hours for a simply supported beam 8m in length. The time required for analysis depends on the number of time steps, nonlinearity, and the speed of the processor. When the objective is to investigate structural fires, the time domain will be longer than 10 hours to be able to consider the cooling phase. The results of the code developed are also compared with Example No. 10 of Annexure CC of DIN EN 1991-1-2/NA:2010-12.

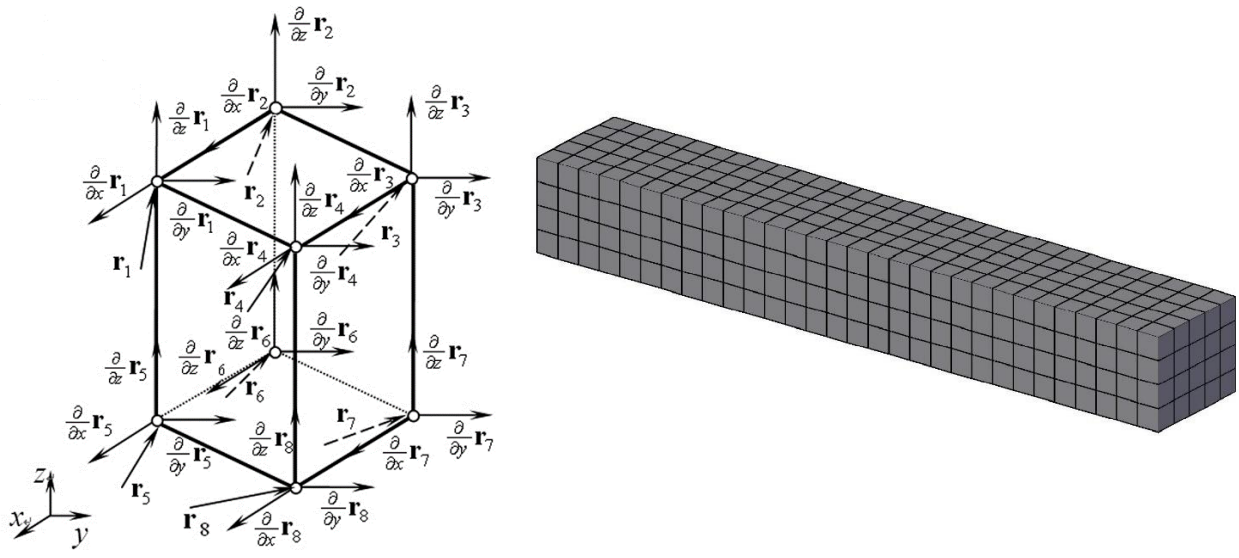

Figure 7-1: Three-dimensional brick elements

7.2 Comparison with results of ANSYS

Some examples will be solved by ANSYS Workbench software and the code developed. We will consider only unprotected concrete members, which can resist elevated temperatures. The analysis will be performed by using two fire curves: 1- The nominal fire curve, which is obtained at the end of Annexure C—

see Figure 7-2a; and 2- The fire curve of Annexure C, divided by 2 in the warming phase—see Figure 7-2b. The calculated fire curves are used for all examples. The maximum deformation of the beam obtained by ANSYS Workbench and the computer code are drawn as a function of time. The curves compare the results of ANSYS Workbench with the results of the computer code.

Maximum temperature in the software developed can be determined by the user. Elements of the cross-section that experience temperatures more than the determined maximum temperature are assumed to have zero stiffness. The variation of the stiffness of the structure as a function of assumed max-temperature may be interested to investigate the effects of the fire loads. Determination of the max-temperature might be based on the structural system and material. Examples are solved by assuming different maximum temperatures (800°C, 500°C, and 400°C). The maximum temperature in ANSYS Workbench is assumed to be 500°C. Therefore, the results at 500°C may have the best agreement.

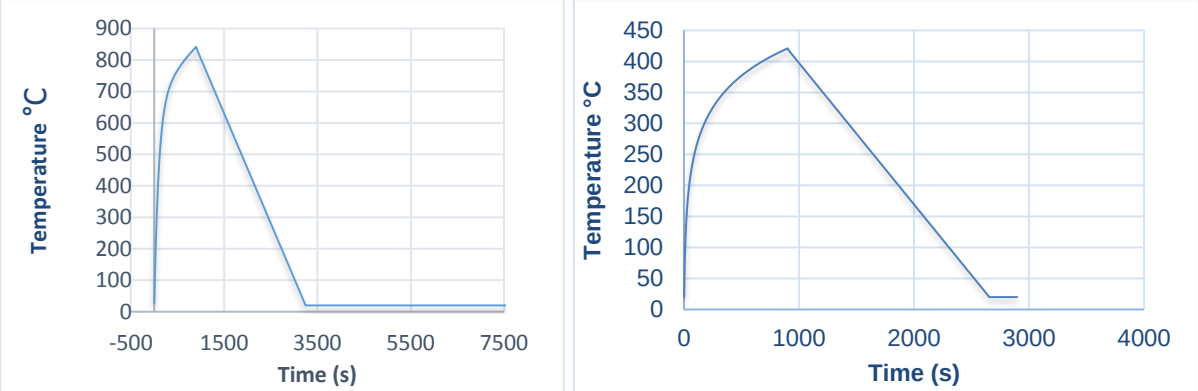

(a) (b)

Figure 7-2: (a)Parametric fire curve 1 - T_{max}=840°C and (b) Fire curve 2 - T_{max}=420°C (parametric fire curve divided by 2—just for a comparison between results at lower temperatures)

7.2.1 Example 1

The first example is a cantilevered beam under uniform load. The objective is to obtain the deformation and internal forces of the beam when the whole beam is subjected to Fire Curves 1 and 2. The results are obtained by ANSYS and the code. The beam is divided into five elements. Each element is 1m long. The cross-section of the beam is assumed to be rectangular, with dimensions $50 \times 35cm$. See Figure 7-3. It is assumed that the beam is facing the fire on all four sides of the cross-section. The end point of the beam is unrestrained and free to deform in axial and transverse directions. There would not be any thermal stresses in the beam. Loads and material properties are given in Figure 7-3a. External loads are applied in one load step and then the temperature effect—

which is the variable stiffness of the warm beam—is assigned. Figures 7-3b and c give the deformation of Point 5 of the beam. As can be seen, the results of the code developed match better with the results of ANSYS Workbench, when the maximum temperature is assumed to be 500°C.

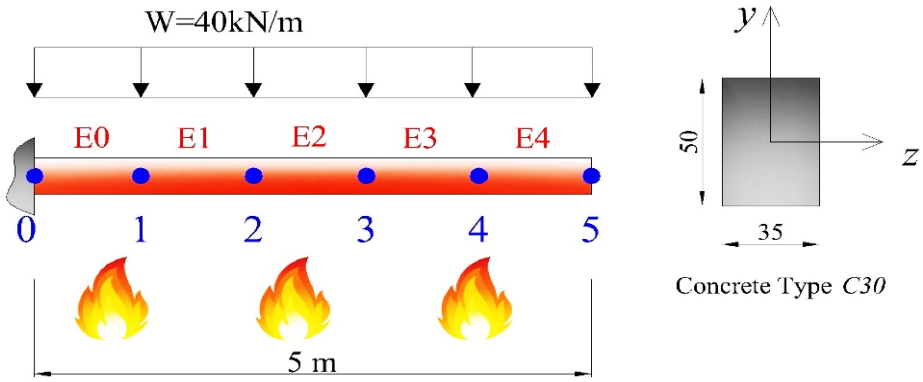

(a) Cantilevered beam under fire load from all four sides

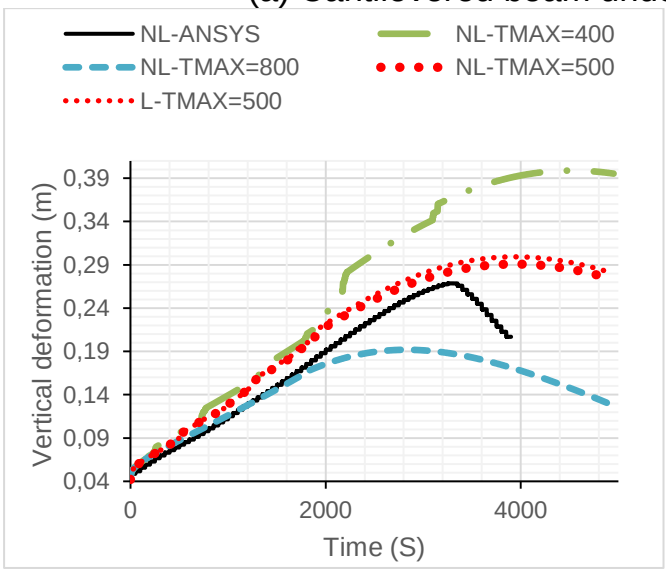

(b) Vertical deformation of Point 5 when Curve 1 is subjected to the beam; see Fig. 7-2a—NL denotes geometric nonlinearity

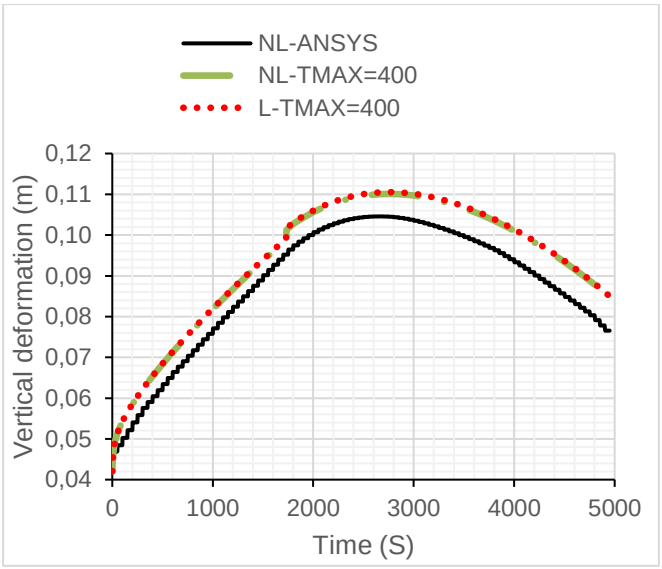

(c) Vertical deformation of Point 5 facing Curve 2; see Fig. 7-2b

Figure 7-3: Example 1-Cantilevered beam under thermal loads

Figure 7-3b gives the deformation path of Point 5, calculated by ANSYS Workbench and the developed code, when the geometric nonlinear behaviour of the beam is considered. In case of maximum temperatures equal to 500°C, the beam is also analysed without considering geometric nonlinearity, apart from nonlinear analysis. It should be mentioned that the variable stiffness of warm members is a nonlinear behaviour.

The deformations of the first load step form the initial condition for the next time steps. Time step size is assumed to be 2 seconds. Longer time steps may cause instability in analysis. The use of 3D solid brick elements of ANSYS Workbench

takes about 20 hours to analyse the beam, but the code developed requires just about 15 minutes to perform the analysis.

7.2.2 Example 2

Here, we will investigate the structural response of a 3m-long cantilevered concrete beam. Example 2 is similar to example 1 but the non-linear deformations are smaller. Example 2 is considered to investigate the influence of nonlinear effects and to compare the nonlinear deformations with those of example 1. The beam consists of three elements with 1m length and 4 nodes. All elements are subjected to a uniform distributed load. The uniform load may be self-weight, dead load plus live load, which might be applied in one load step. Afterwards, the thermal effects will be applied in the next time steps. The results of the first load step are initial conditions of the first time-step. Figure 7-4 gives the schematic view of the beam. Figures 7-4b and 7-4c give the deformation of Point 3 of beam for both fire scenarios. As is obvious, the geometric nonlinear deformations are negligible. In this case, the results of ANSYS Workbench and the developed method have a better agreement. There is a significant difference between the two methods in the cooling phase. It will be because of the recovered modulus of elasticity in ANSYS.

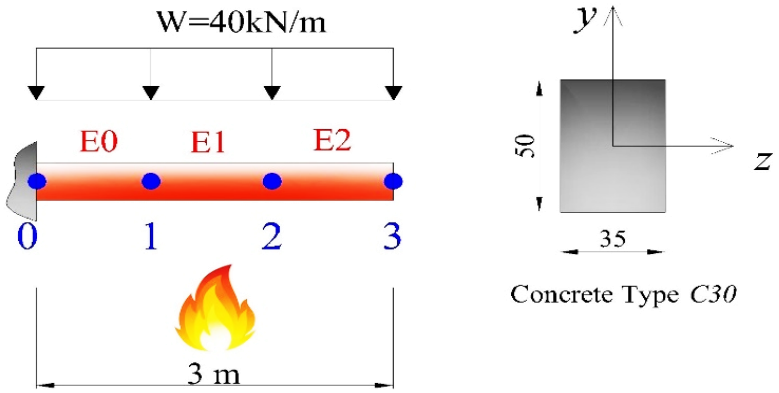

(a) Example 2—Cantilevered beam under fire load from all four sides

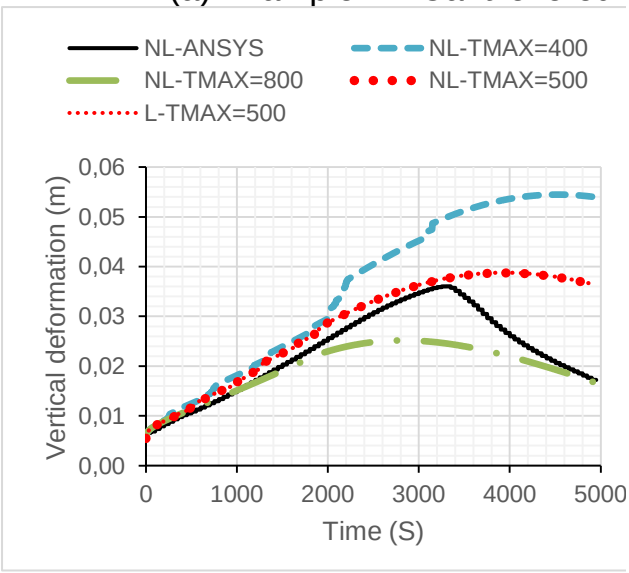

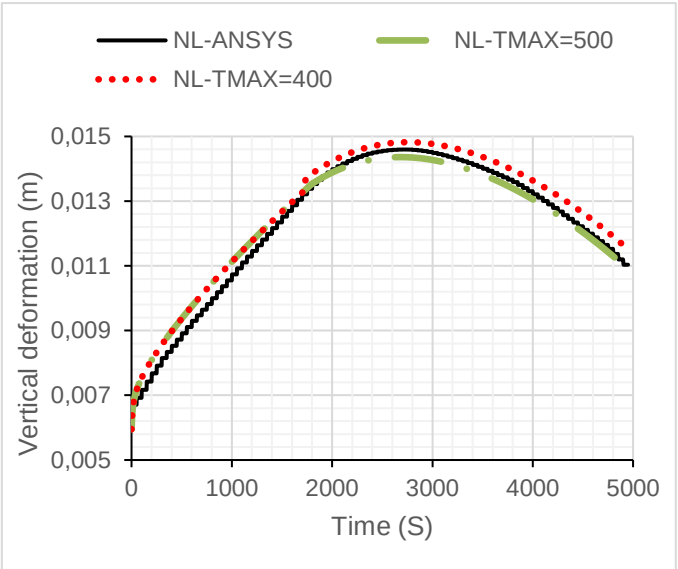

(b) Vertical deformation of end point of beam facing Curve 1

(c) Vertical deformation of end point of beam facing Curve 2

Figure 7-4: Example 2—Cantilevered beam under thermal loads

7.2.3 Example 3

This example compares the results of the developed method and ANSYS Workbench for a 6m-long concrete beam. The beam is fully restrained at both ends and the beam is subjected to a uniform distributed load with an intensity of $40\ kN/m$. The beam is divided into six elements and seven nodes. Figure 7-5a illustrates the beam and Figures 7-5b and c compare the results of ANSYS Workbench and code. Other assumptions are similar to the examples last discussed. The deformation paths obtained by both methods show an acceptable agreement for this example. The difference between two methods is obvious in the cooling phase.

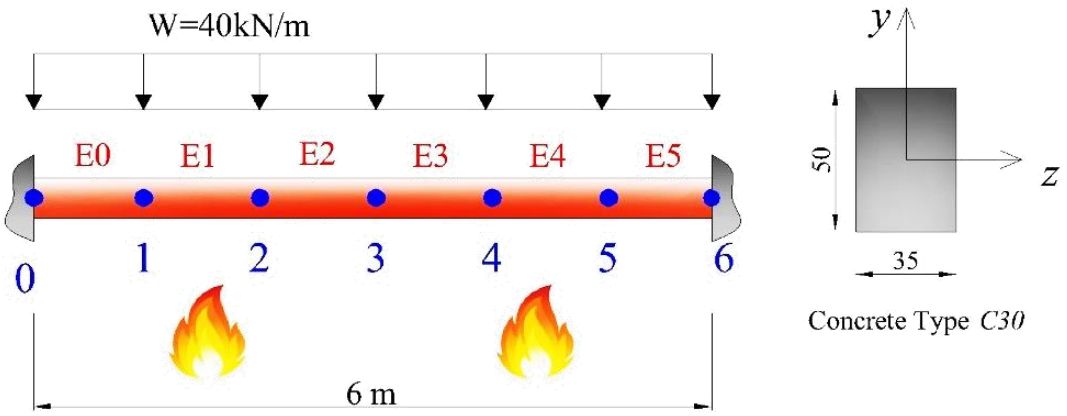

(a) Example 3—Fixed beam at both ends under fire load from all four sides

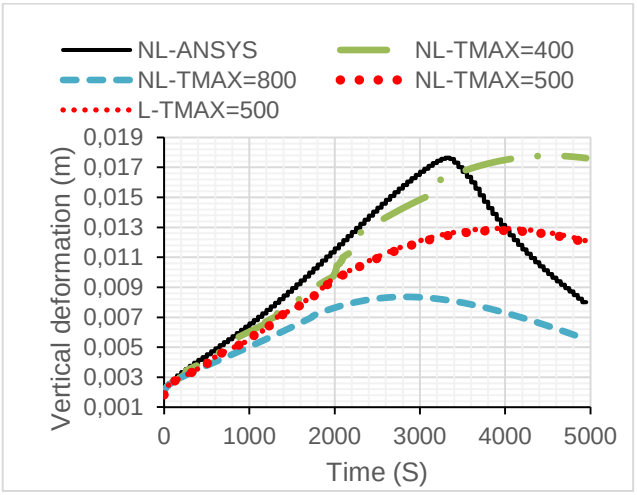

(b) Vertical deformation of beam mid-point facing Curve 1

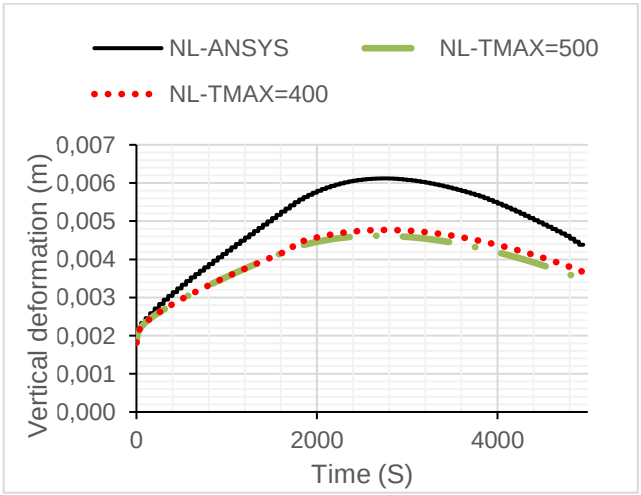

(c) Vertical deformation of beam mid-point facing Curve 2

Figure 7-5: Example 3—Fixed beam at both ends

7.2.4 Example 4

The analysis of complicated systems in ANSYS Workbench with 3D brick elements is time-consuming and not simple. Example 4 validates the results of the simplified method by comparing the results of ANSYS Workbench and the method for a simple 2D frame structure. As shown in Figure 7-6a, the FEM model consists of 16 elements and 17 nodes. Figure 7-6b compares the deformation of Point 4, as indicated in Figure 7-6a. The results of ANSYS and the code show a better agreement when the maximum temperature is assumed to be 500°C. Again, the difference here is in the cooling phase, in which the material properties in ANSYS Workbench are completely different.

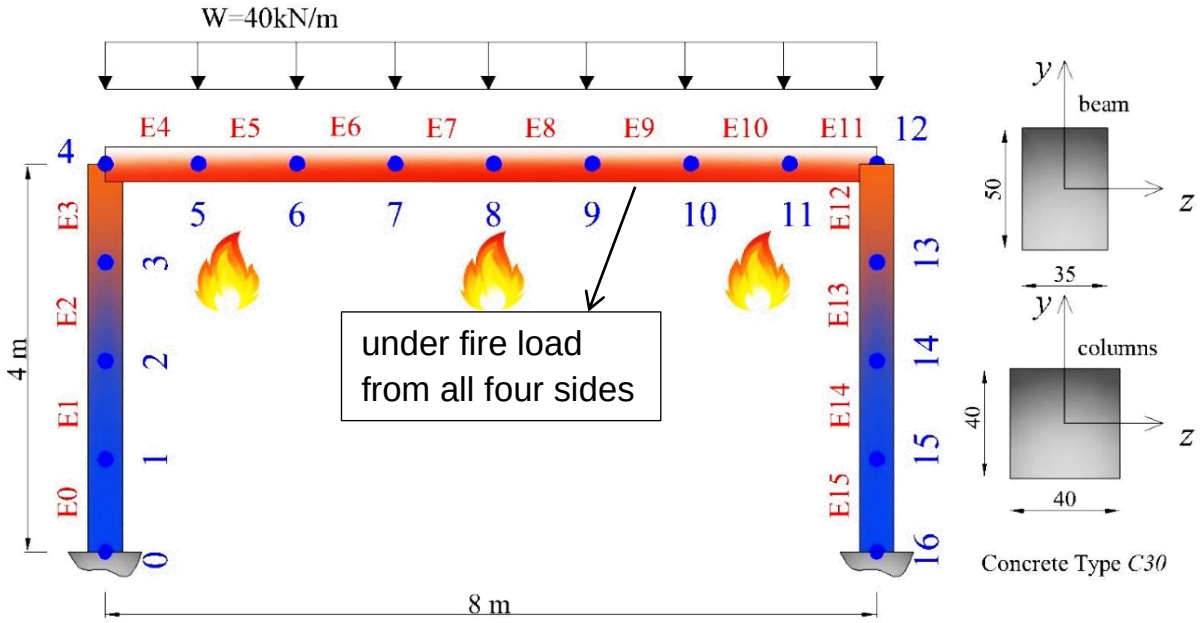

(a) Example 4—Rigid concrete frame

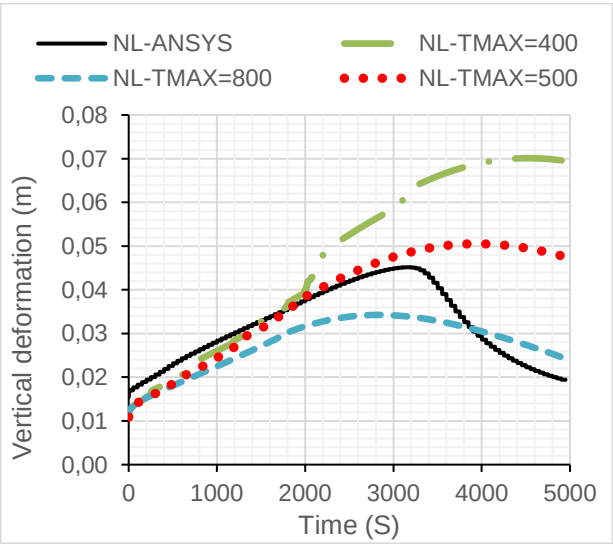

(b) Vertical deformation of beam mid-point facing Curve 1

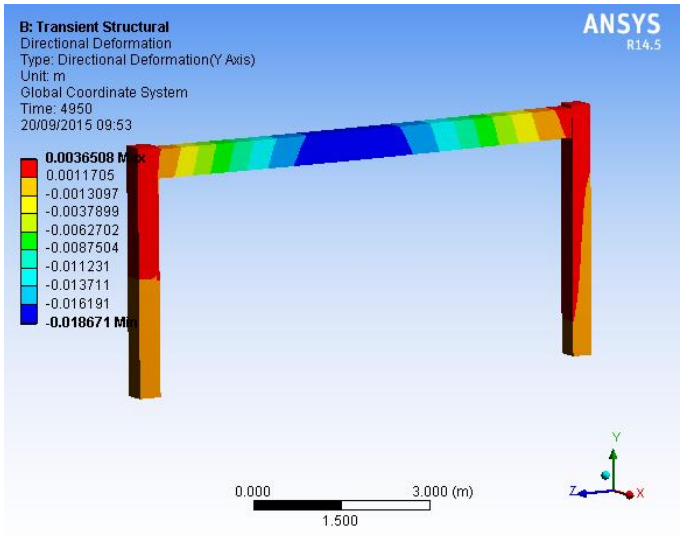

(c) The desired frame modelled in ANSYS

Figure 7-6: Example 4—Rigid concrete frame

7.3 Comparison with Example 10 of DIN EN 1991-1-2/NA:2010-1-2

Imagine a composite column fixed at one end and subjected to wind, concentrated moment, and fire load, as shown in Figure 7-7. The column is 7m long with $36 \times 36cm$ cross-section dimensions and is assumed to consist of concrete type C20/25 and 6Ø20 steel bars. The nominal fire curve (ETK) is subjected to the column.

According to Example 10 of the abovementioned code—after 90min fire time—the maximum calculated horizontal deformation of column shall be about 381mm with 15 per cent acceptable error. Assuming the maximum temperature to be equal to 500°C, the calculated deformation will be obtained in the desired range. Elements with temperatures more than maximum temperature are assumed to have zero stiffness. The deformation obtained by the simplified method is 415 mm, which is within the requested limits. The temperature of reinforcements at time = 90 min is less than the reference values, but the horizontal deformation of point 7 is bigger than the reference values. Therefore, a smaller failure time ($t_{\Delta=381mm} = 86$ min) is obtained.

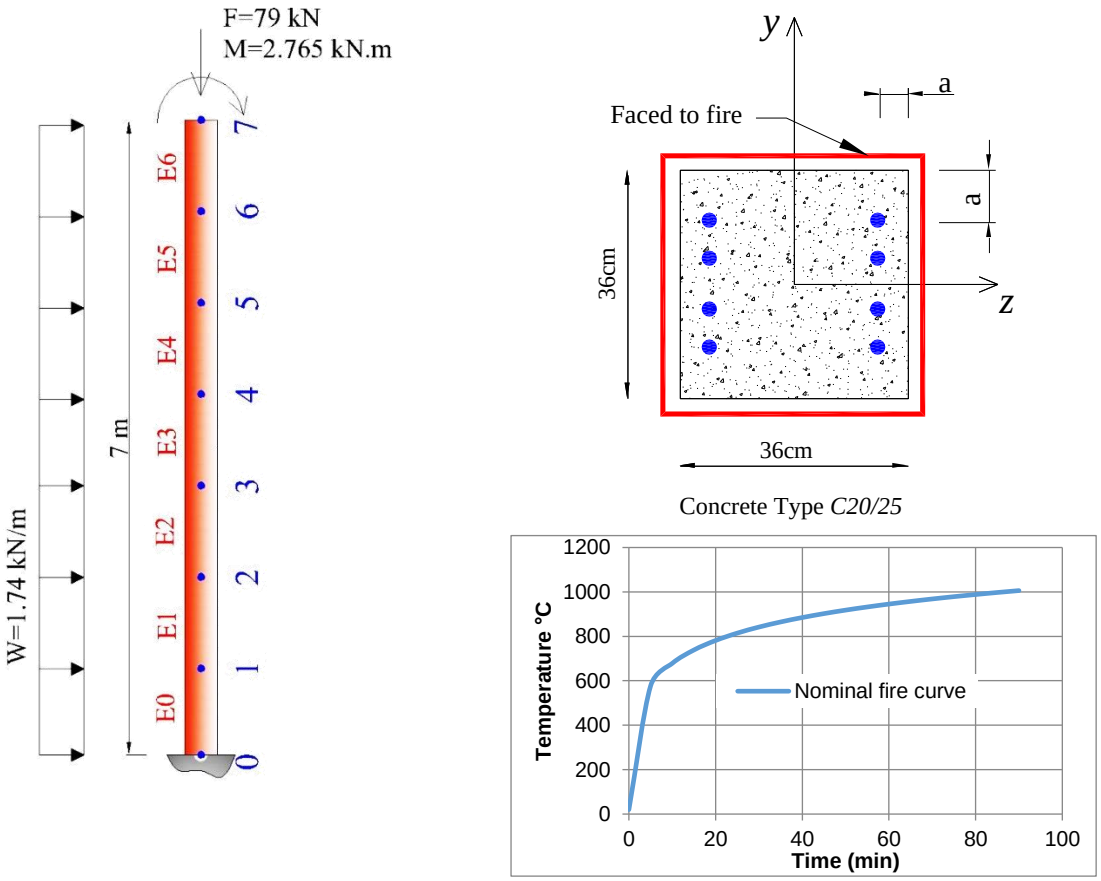

Figure 7-7: Example of DIN EN 1991-1-2/NA:2010-12 and nominal fire curve (Einheitstemperaturkurve), subjected to column

Table 7.1: Reference and calculated values (the latter by the simplified method) of the example

	Reference Value	Calculated Value – developed FEM code	Error (%) developed FEM code	Tolerance (%)
Failure Time (min)	93	86	7.5%	±3%
Horizontal deformation of point 7, t=90 min (mm)	381	415 T_{max}=500 °C	8.9%	±15%
Bending Moment at footplate, kNm	75.5	81	7.3%	±5%
Temperature in corner Reinforcement, °C	502	463	-7.7%	-
Temperature in middle Reinforcement, °C	319	291	-8.7%	-

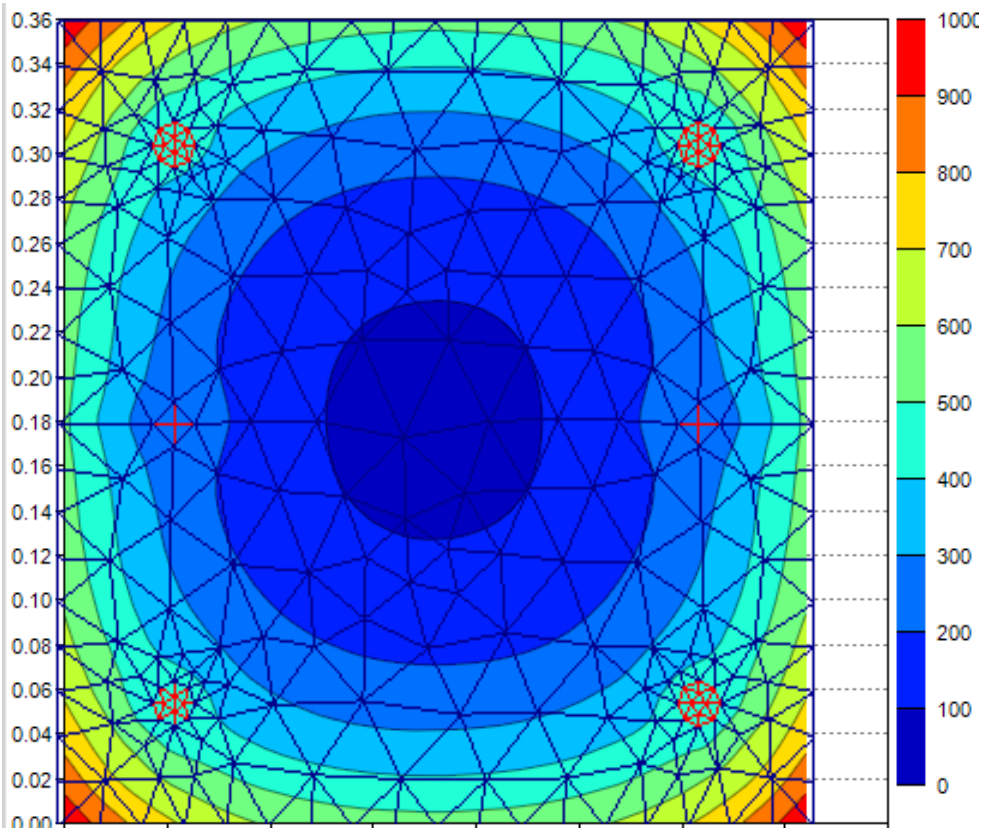

Figure 7-8: Temperature distribution at t=90 min

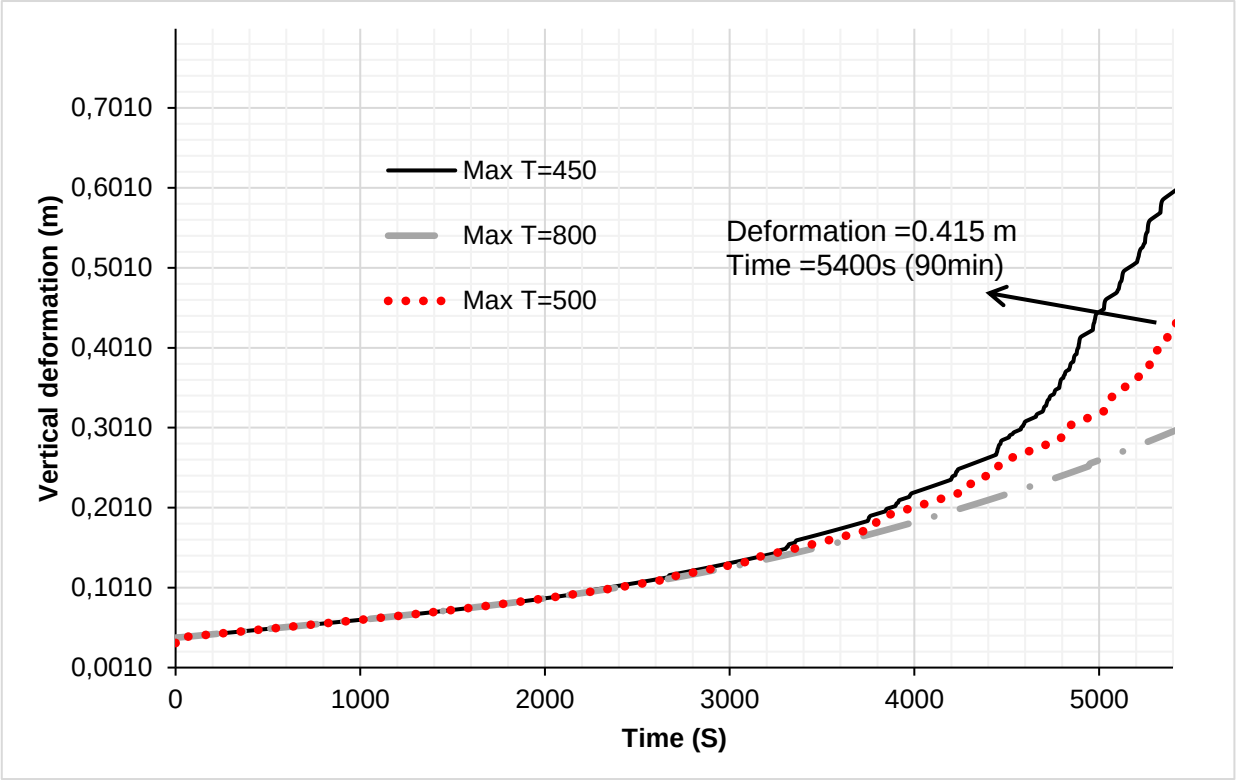

Figure 7-9: Horizontal deformation of Point 7; see Figure 7.7
Assuming maximum temperature equal to 500°C, deformation is 0.415 m

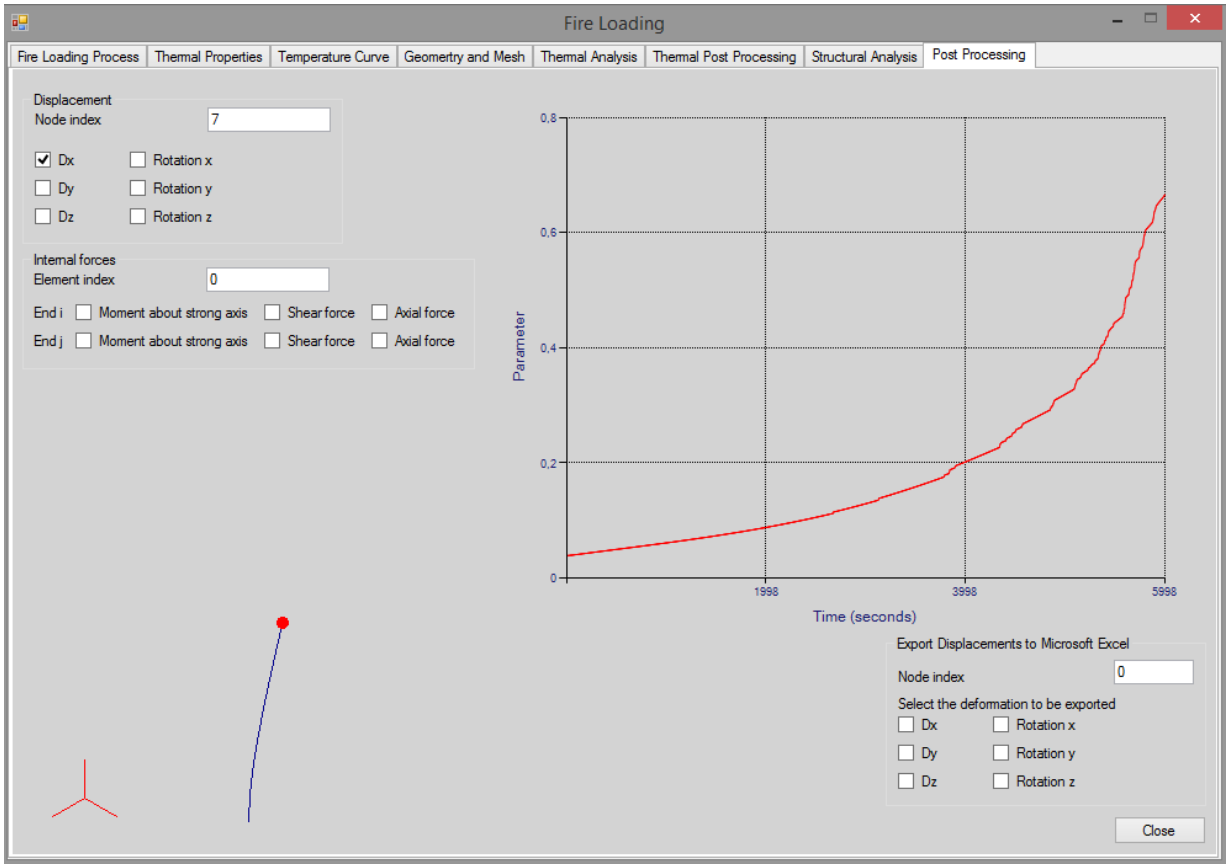

Figure 7-10: Deformed shape of column

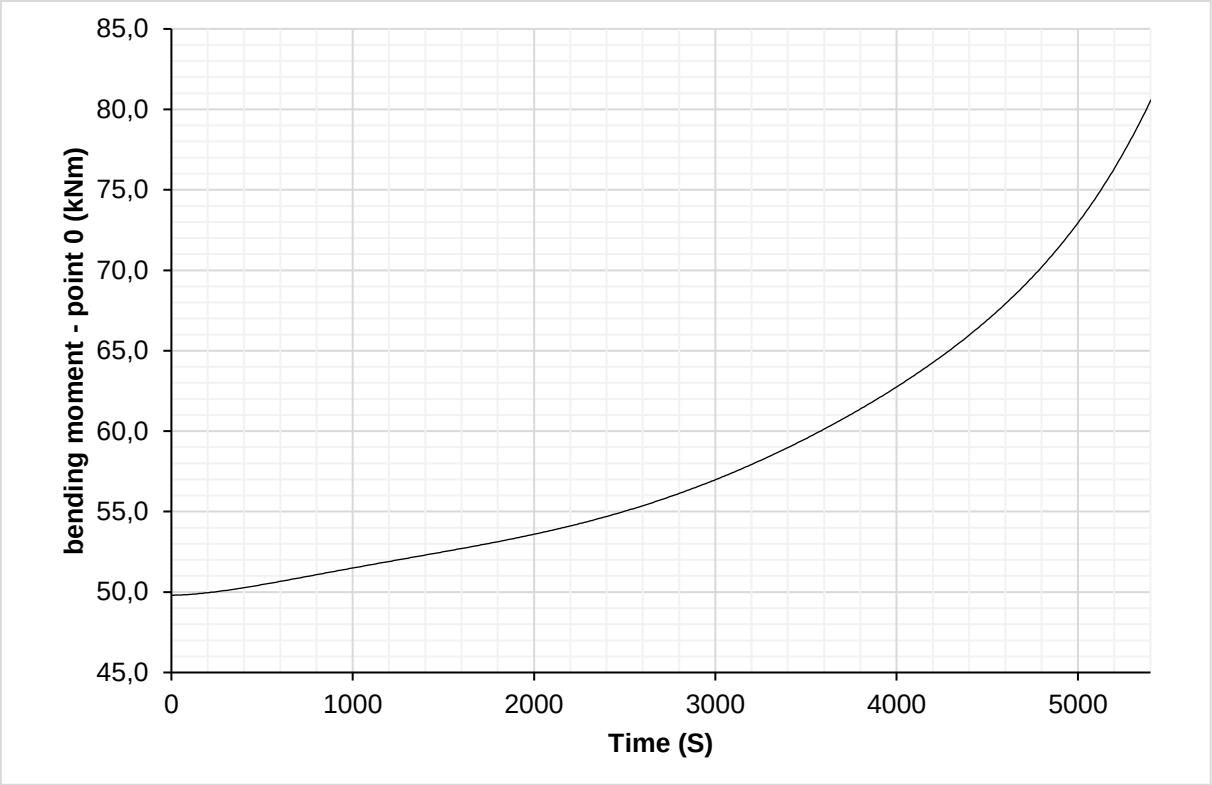

Figure 7-11: Bending moment at point 0

7.4 Limitations of the simplified method

In this chapter, some simple structures are modelled by applying the simplified method; the results have been compared with transient thermal structural analysis of ANSYS Workbench. To make the model in ANSYS Workbench, it has been assumed that the maximum resistible temperature is 500°C. For temperatures more than this value, the modulus of elasticity is assumed to be negligible.

Considering the results of the current chapter:

1. In increasing phase, the results of the FEM code depend on the max-temperature. Max-temperature might be determined based on the structural material-properties or fire load density.
2. The deformation path, obtained by ANSYS, and the written FEM code in the cooling phase do not perfectly match. This is because of the difference between material properties defined in ANSYS and the computer code. In the cooling phase, the beam model in ANSYS exactly recovers its initial material properties. The developed element does not recover its initial stiffness. Therefore, the results of the cooling phase cannot be verified by ANSYS Workbench.
3. In the case of extreme loss of stiffness (which may depend on the geometry of the structure, material properties and fire loads) there might

be extra-large deformations in the domain of analysis. Having extra-large deformations, the simplified method might not yield acceptable results.

4. To investigate the fire resistance of steel structures, the developed method would not give convincing results. It will be assumed that unprotected steel members are not fire-resistant.
5. Although the structural response path calculated by the ANSYS and the simplified method do not agree perfectly, there is, however, a better agreement between the results at the beginning and the end of the analysis.
6. The developed method is a first step and attempts to decrease the analysis time and give a rough estimation of structural response. The application of the method in structural designing might be investigated in further researches. The method might be applied to obtain an estimation of the behaviour of structure during a fire scenario. The results depend directly on stiffness curves and the assumptions.
7. The developed simplified method is not suitable to determine the exact and accurate structural behaviour. Material non-linearity, crashes in concrete members, 3D thermal stresses and strains in cross-sections, buckling, and shear deformations are some of the important parameters that are not considered by the developed method. The developed method considers a cold analysis under an assumption of variable stiffness for the warm members and so is just suitable to determine an estimation.

Although the simplified method is faster (more than 10 times) than the enhanced solutions, the robustness and precision of the method could not be achieved, as expected, in all cases.

8 Summary and Outlook

With the increase in the possibilities of numerical calculation methods in recent decades, it is possible to mathematize the structural behaviour under fire loads (by applying the advanced calculation methods). Fire loads are accidental and difficult to be mathematized when using the advanced calculation method. In the current research, the regulations of Eurocodes are implemented in many advanced structural analysis software which can perform thermal and non-linear structural analysis.

By combining the simulation procedure of Levels 2 and 3, based on Eurocodes, a FEM model of analysis (a frame element with six degrees of freedom which is written in Microsoft Visual C#) for mathematizing the fire-loading process is developed. The developed method considers a cold geometric non-linear analysis, under an assumption of variable stiffness for the warm members/frames, which is dependent just on the temperature field. The structural members under fire loading are assumed to be similar to composite cross-sections with different materials and stiffness. On having the variable stiffness of warm members, an analysis can be performed. The thermal axial stress along the frame members' length is considered as a cumulative stress. Conductivity, convection, and radiation are taken into account. The material properties of concrete and steel, based on Eurocodes, are applied to develop the FEM element.

The developed element consists of the following steps: 1- determination of the material properties; 2- defining the fire scenarios and curves; 3- definition of the geometry and mesh; 4- performing the thermal analysis and calculating the variable stiffness, and 5- exerting the mechanical analysis and calculating the structural response.

The results are compared with those of the ANSYS Workbench software (using three-dimensional solid brick elements) and with those of example 10 of DIN EN 1991-1-2/NA: 2010-1-2.

- In comparison with the example 10 of DIN EN1991-1-2/NA, the calculated deformation is within the requested limits. However, the failure time and the bending moment are not in the acceptable range.
- In increasing phase, the results of the developed element depend on the max-temperature and in the cooling-phase do not perfectly match with those obtained by ANSYS.

Material non-linearity, crashes in concrete, 3D thermal stresses and strains in cross-sections, buckling and shear deformations are some of the important parameters that are not considered by the developed method. The developed simplified method is not suitable to determine the exact and accurate structural behaviour. In the case of extreme loss of stiffness, the simplified method might not yield acceptable results.

The results depend on the stiffness curves and the stiffness curves are a function of the assumed max-temperature and fire curve. Determination of the stiffness curves and the max-temperature needs further research. Determination of the stiffness curves may be based on experimental data. Max-temperature might be determined based on the structural material-properties or fire load density.

Literature

[1] S. Olive, M. Feeney and P. Bevan Jones, Dependable Performance of Steel Structures in Fire with Case Studies, New Zealand - California: Holmes Culley San Francisco, California - Holmes Fire & Safety Auckland, New Zealand, 2008.

[2] EN 1992-1-2: Design of concrete structures - Part 1-2, Brussels: European committee for standardization, 2005.

[3] EN 1994-1-2: Design of composite steel and concrete structures - Part 1-2: General rules - Structural fire design, Brussel: European committee for standardization, 2004.

[4] H. Bizri, “Structural capacity of reinforced concrete columns subjected to fire induced thermal gradients,” Department of Civil Engineering, University of California Berkeley, California, 1973.

[5] J. Becker and B. Bresler, “Reinforced concrete frames in fire environments,” *Journal of the Structural Division, vol 103,* pp. 211-224, 01 1977.

[6] V. Chandrasekaran and N. Mulcahy, “Analysis Of Time Of Collapse Of Steel Columns Exposed To Fire,” *Fire safety science 5,* pp. 1141-1152, 1997.

[7] B. Ellingwood and J. Shaver, “Reliability of RC Beams Subjected to Fire,” *Journal of the Structural Division, vol. 103,* May No. ST5 1977.

[8] V. Kodur, D. Nwosu, M. Sultan and J. Franssen, “Application of the SAFIR computer program for evaluating fire resistance,” *Third International Conference on Fire Research and Engineering,* 1999.

[9] J. Myllymaki and D. Barboudi, “Simple Method to Predict Fire Resistance of Composite Columns,” *Fire Safety Science,* pp. 879-890.

[10] H. A. Saab, Non-linear finite element analysis of steel frames in fire condition, University of Sheffield, 1990.

[11] K. Lien, Y. Chiou, R. Wang and P. Hsiao, “Nonlinear behavior of steel structures considering the cooling phase of a fire,” *Journal of Constructional Steel Research,* p. 1776–1786, 2009.

[12] M. Gelien, Ein Beitrag zur Bemessung von Stahlbetonstützen im Brandfall, Bergische Universität Wuppertal, 2011.

[13] E. Spacone and S. El-Tawil, “Nonlinear Analysis of Steel-Concrete Composite Structures:,” *ASCE,* pp. 159-168, 2004.

[14] V. Mihajlov, Numerical Model for Spatial Steel and Composite Frame-Structures Exposed to Fire and Elevated Temperatures, Bergische Universität Wuppertal, 2009.

[15] J. Pauli, The Behaviour of Steel Columns in fire, Institute of Structural Engineering Zurich, 2012.

[16] Y. Zhuang, Storey-based Stability Analysis of Unbraced Steel Frames at Ambient and Elevated Temperatures, Canada: Waterloo, Ontario, 2013 .

[17] M. Bergmann, Zur Bemessung von Hohlprofilverbundstützen, Institut für Konstruktiven Ingenieurbau Bergische Universität Wuppertal, 2013.

[18] EN 1991-1-2: Actions on structures - Part 1-2: General actions -Actions on structures exposed to fire, Brussel: European committee for standardization, 2002.

[19] P. Stollard and J. Abrahams, Fire from First Principles, New York: Routledge, 1999.

[20] Book by Leonardo da Vinci Pilot Project CZ/02/B/F/PP-134007, Implementation of Eurocodes (Handbook 5): Design of Buildings for the Fire Situation, Luxembourg: https://eurocodes.jrc.ec.europa.eu/, 2005.

[21] K. O.-K. 006, EN13501-2 - Klassifizierung von Bauprodukten und Bauarten zu, Austrian Standards Institute, 2010.

[22] J. M. Franssen, J. F. Cadorin, D. Guibert, G. Aurtenetxe, D. Joyeuxm, J. Kruppa , S. Pustorino, J. B. Schleich, L. G. Cajot and M. Pierre, “Competitive Steel Buildings Through Natural Fire Safety Concept, Report Part 2, Working Group 1: Natural Fire Models, CEO Agreement 7220-SA/125,126,213,214,323,423,623,839,937,” 1999.

[23] EN 1993-1-2 : Design of steel structures - Part 1-2: General rules - Structural fire design, Brussel: European committee for standardization, 2005.

[24] ACI216-Cmmittee, "Guide for Determining the Fire Endurance of Concrete Elements," in *ACI 216R*, 1994.

[25] J. Outinen and P. Mäkeläinen, “Mechanical properties of structural steel at elevated temperatures and after cooling down,” John Wiley & Sons, Ltd, 2004.

[26] Y. Anderberg, “The impact of various material models on structural fire behaviour prediction, in Proceedings of the fifth international workshop Structures in Fire.,” pp. 253-265, 2008 - Singapore.

[27] S. Thelanderson, “Mechanical Behaviour of Heated Concrete Under Torsional Loading at Transient High Temperature Conditions, Bulletin No. 46,,” Lund Institute of Technology, Sweden, 1974.

[28] Y. Anderberg and S. Thelanderson, “Stress and Deformation Characteristics of Concrete at High Temperatures: Experimental Investigation and Material Behaviour Model,” Lund Institute of Technology, Sweden, 1976.

[29] U. Schneider, Loss of strength due to kinetic reactions of normal concretes up to 1000ºC: Ph.D. thesis, Braunschweig, Germany: Technical University, 1973.

[30] U.S.NRC, "A Compilation of Elevated Temperature Concrete Material Property Data and Information for Use in Assessments of Nuclear Power Plant Reinforced Concrete Structures," United States Nuclear Regulary Commission, 2010.

[31] C. Nielsen, C. Pearce and N. Bicanic, "Improved phenomenological modeling of transient thermal strains for concrete at high temperature," *Computers and Concrete,* vol. 2, pp. 189-201, 2004.

[32] F.-P. Cheng, V. Kodur and T.-C. Wang, "Stress-Strain Curves for High Strength Concrete at Elevated Temperatures," *Journal of Materials in Civil Engineering,* Feb 2004.

[33] K. Hertz, "Simplified calculation method for fire exposed concrete structures (Supporting document for CEN-PR-ENV 1992-1-2)," Technical University of Denmark, 1993.

[34] W. Kaspar, X. Yunping, L. Keun and K. Byunhun, Thermal response of reinforced concrete structures in nuclear power plants, University of Colorado at Boulder: Department of Civil, Environmental, and Architectural Engineering, 2009.

[35] M. Planck, Treatise on Thermodynamics, third English edition translated by A. Ogg from the seventh German edition, London: Longmans, Green & Co., 1927.

[36] Rao and S. S., The Finite Element Method in Engineering - Fifth Edition, USA: Butterworth–Heinemann, 2011.

[37] D. L. Logan, A first course in the finite element method, Fifth Edition, University of Wisconsin–Platteville, 2012.

[38] O. Zienkiewicz and R. Taylor, The Finite Element Method, Volume 1, 2 and 3 - Fifth Edition, Bristol, England: Butterworth-Heinemann, 2000.

[39] F. P. Preparata and M. Ian Shamos, Computational Geometry, Chapter: Convex Hulls: Basic Algorithms, New York: Springer, 1985.

[40] Microsoft, “DreamSpark - Software Catalog,” 31 05 2013. [Online]. Available: https://www.dreamspark.com/Student/Software-Catalog.aspx.

[41] S. Timoshenko, Strength of Material part I, Elementary theory and problems, Newyork: D. Van Nostrand Company, Inc., 1948.

[42] S. Timoshenko, Strength of Material part II, Advanced theory and problems, Newyork: D. Van Nostrand Company, Inc., 1947.

[43] J. E. Gentle, Matrix Algebra: Theory, Computations, and Applications in Statistics, USA: Springer, 2007.

[44] S. Timoshenko, History of strength of materials, New York: McGraw-Hill, 1953.

[45] D. C. Kay, Tensor Calculus. Schaum’s Outlines, USA: McGraw Hill, 1988.

[46] P. Wriggers, Nonlinear Finite Element Methods, Germany : Springer, 2008.

[47] R. de Borst, M. A. Crisfield, J. J. Remmers and C. V. Verhoosel, Non-linear finite element analysis of solids and structures, India: John Wiley & Sons, 2012.

[48] K.-J. Bathe and S. Bolourchi, “Large displacement analysis of three-Dimensional beam structures,” *International jounrnal for numerical methods in engineering,* Vols. VOL. 14,961-986, 1979.

[49] M. L. Bucalem and K.-J. Bathe, The Mechanics of Solids and Structures – Hierarchical Modeling and the Finite Element Solution, London, New York: Springer, 2011.

[50] V. Ivančo, Nonlinear finite element analysis, Slovakia: Technical University of Košice, 2011.

[51] EN 1990 - Basis of structural design, Brussel: European committee for standardization, 2002.

[52] ANSYS, “ANSYS Help - Version 14.5”.

[53] Code of Practice for Fire Safety in Buildings 2011, Hong Kong: Building Surveyor/Legislation Hong Kong , 2012 .

[54] V. Illingworth, The Penguin Dictionary of Physics, London: Books, Penguin, 1991.

[55] NFPA, Fire Protection Handbook, 20th Edition, USA: 20th Edition, 2008.

[56] AISC, Fire Resistance of Structural Steel Framing, USA: AISC, 2003.

[57] M. G. Goode, Fire Protection of Structural Steel in High-Rise Buildings, USA: Department of Commerce Technology Administration , 2004.

[58] Buildings Department , Code of Practice for Fire Safety in Buildings 2011, Hong Kong : Buildings Department , 2012.

[59] M. A. Crisfield, Non-linear Finite Element Analysis of Solids and Structures, London: JOHN WILEY & SONS , 2000.

[60] A. Ferreira, MATLAB Codes for Finite Element Analysis, Portugal: Springer, 2009.

[61] E. Oñate, Structural Analysis with the Finite Element Method, Barcelona: Springer, 2009.

[62] P. Krysl, A Pragmatic Introduction to the Finite Element Method for Thermal and Stress Analysis, Pressure Cooker Press: San Diego , 2005.

[63] R. Iding, B. Bresler and Z. Nizamuddin, FIRES - RCII, California: University of california, Berkeley, 1977.

[64] P. Stollard and J. Abrahams, Fire from First Principles, London and New York: E & FN SPON, 1999.

[65] R. W. Lewis, P. Nithiarasu and K. N. Seetharamu, Fundamentals of the Finite Element Method for Heat and Fluid Flow, England: John Wiley & Sons, 2004.

[66] R. Kindmann and M. Kraus, Steel Structures: Design using FEM, Bochum - Germany: Ernst & Sohn, 2011.

[67] C. Üstündağ, Beitrag zur Bemessung von Verbundträgern unter ermüdungswirksamen Beanspruchungen, Bergische Universität Wuppertal, 2007.

[68] M. Schäfer, Zum Tragverhalten von Flachdecken mit integrierten hohlkastenförmigen Stahlprofilen, Institut für Konstruktiven Ingenieurbau Bergische Universität Wuppertal, 2007.

[69] F. Wald, “Fire Engineering of steel structures,” Czech Technical University in Prague, Prague.

[70] J. Bonet and R. D. Wood, Nonlinear continuum mechanics for dinite element analysis, United States of America: Cambridge University Press, 1997.

[71] F. Ricketts, S. Merritt and T. Jonathan, Building design and construction handbook, New York: McGRAW-HILL, 2000.

[72] R. W. Bukowski, “Fire as a building design load,” *Interflam,* vol. Volume 1, no. 17-11-2001, 2001.

[73] Background documents to EN 1992-1-2, European committee for standardization, 2004.

[74] EN1992-1-1: Design of concrete structures - Part 1-1, Brussel: European committee for standardization, 2004.

[75] J. Chessa, “Programming the Finite Element Method with Matlab,” 2002.

[76] Fire resistance design manual sound control-Gypsum systems, USA, 2009.

Annexure A: Stress–Strain curves

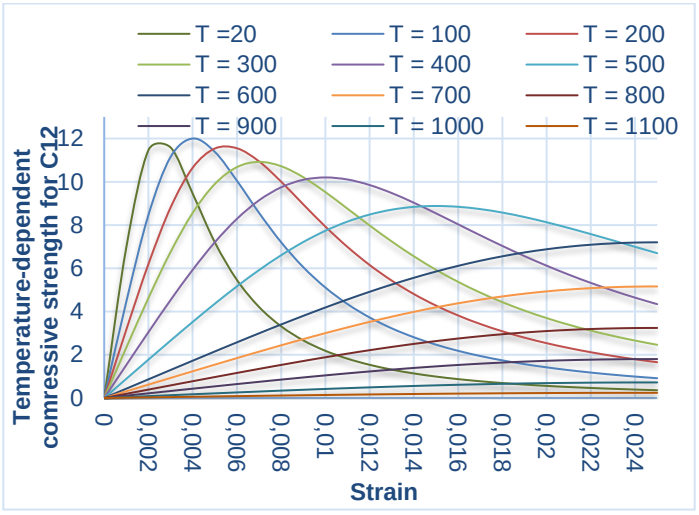

Figure A.1: Stress–Strain curves of concrete type C12 at elevated temperatures

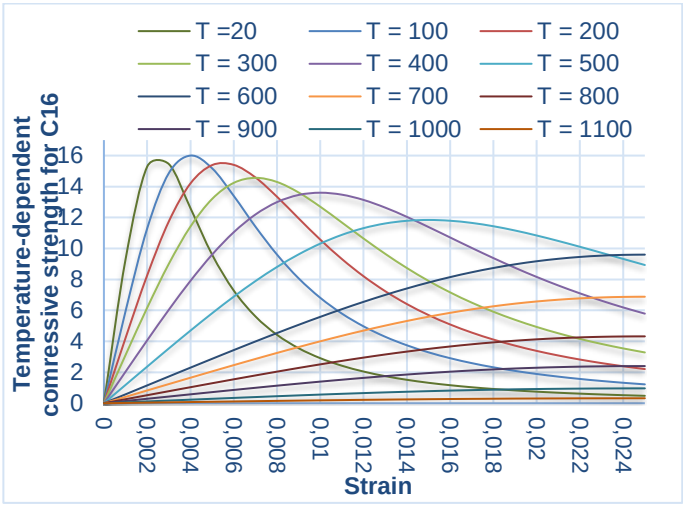

Figure A.2: Stress–Strain curves of concrete type C16 at elevated temperatures

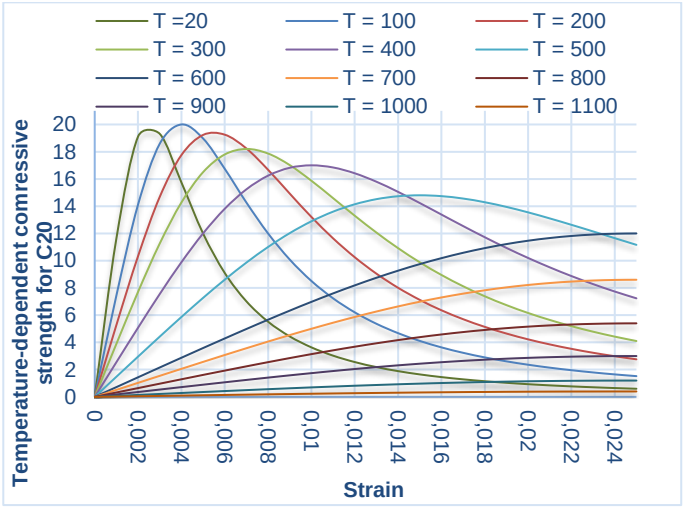

Figure A.3: Stress–Strain curves of concrete type C20 at elevated temperatures

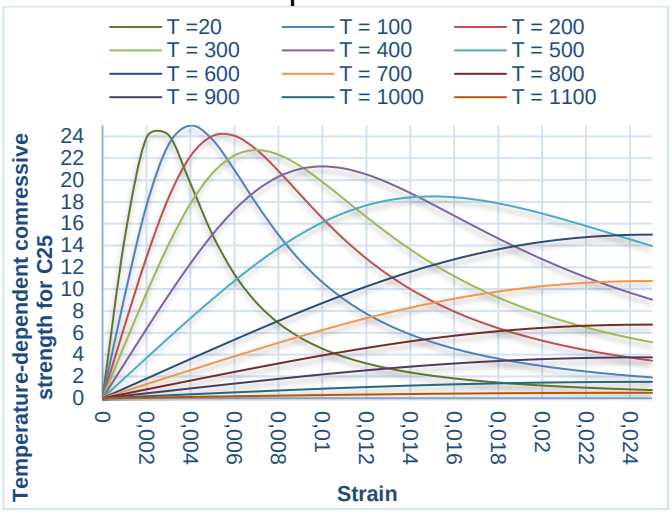

Figure A.4: Stress–Strain curves of concrete type C25 at elevated temperatures

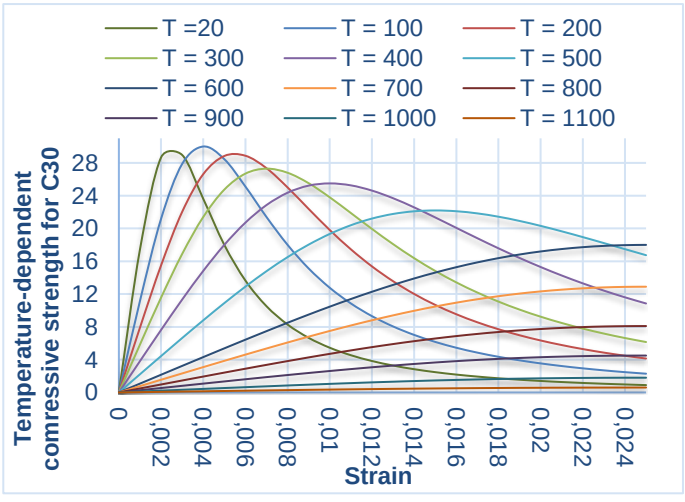

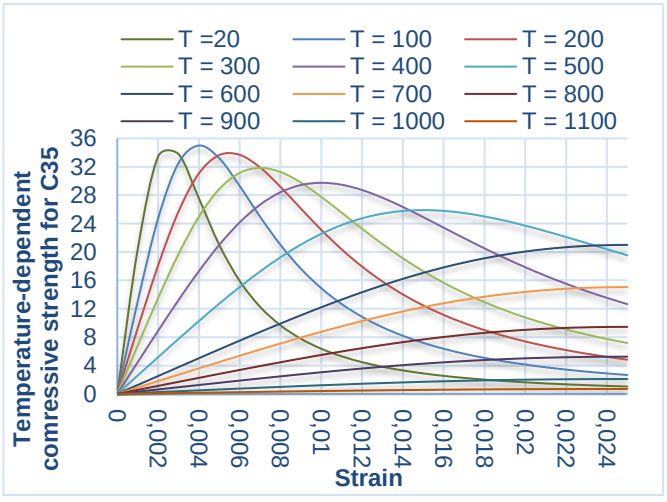

Figure A.5: Stress–Strain curves of concrete type C30 at elevated temperatures

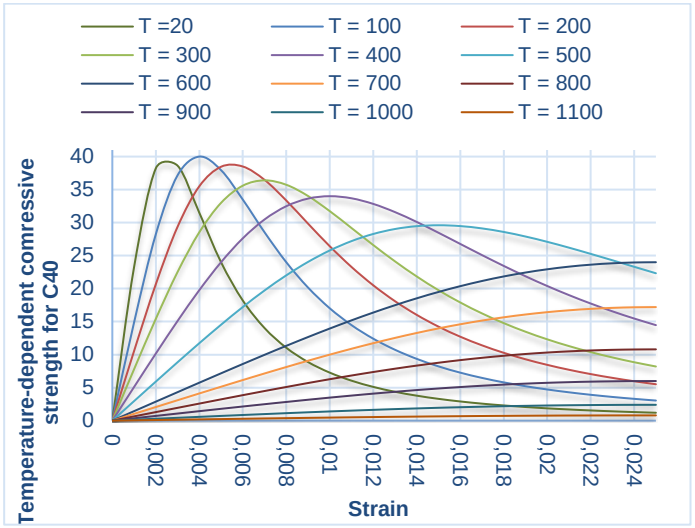

Figure A.6: Stress–Strain curves of concrete type C35 at elevated temperatures

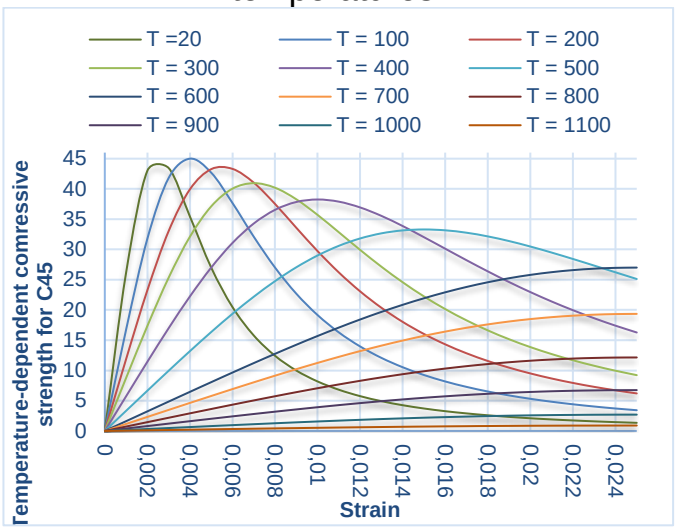

Figure A.7: Stress–Strain curves of concrete type C40 at elevated temperatures

Figure A.8: Stress–Strain curves of concrete type C45 at elevated temperatures

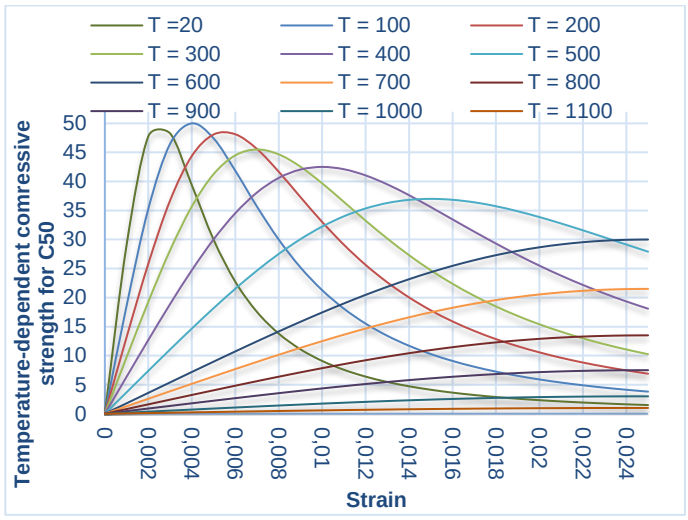

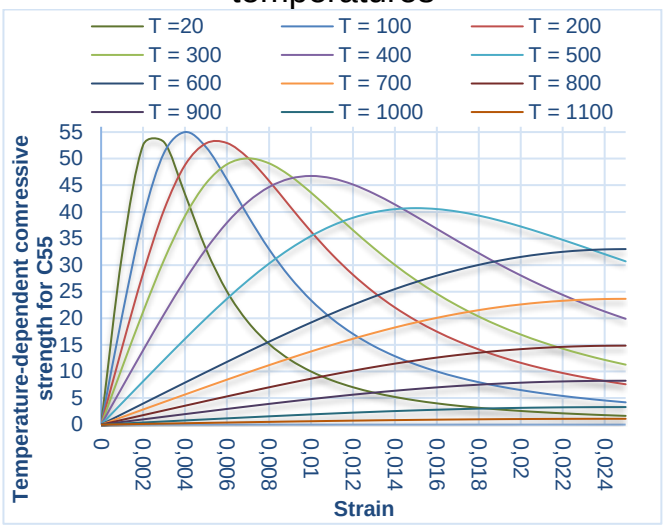

Figure A.9: Stress–Strain curves of concrete type C50 at elevated temperatures

Figure A.10: Stress–Strain curves of concrete type C55 at elevated temperatures

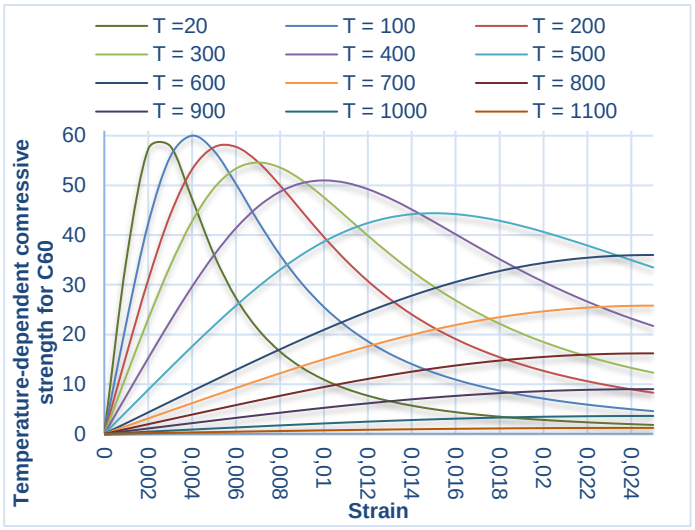

Figure A.11: Stress–Strain curves of concrete type C60 at elevated temperatures

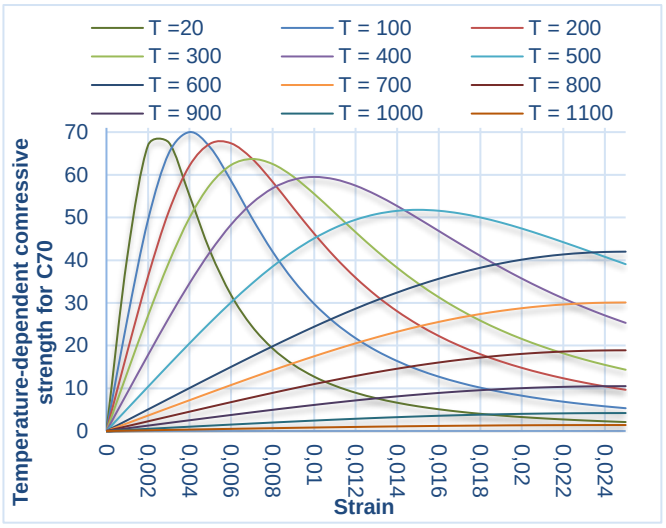

Figure A.12: Stress–Strain curves of concrete type C70 at elevated temperatures

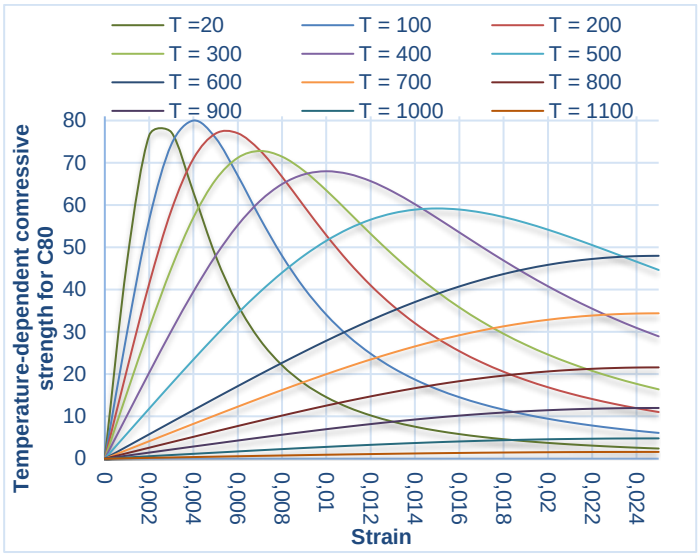

Figure A.13: Stress–Strain curves of concrete type C80 at elevated temperatures

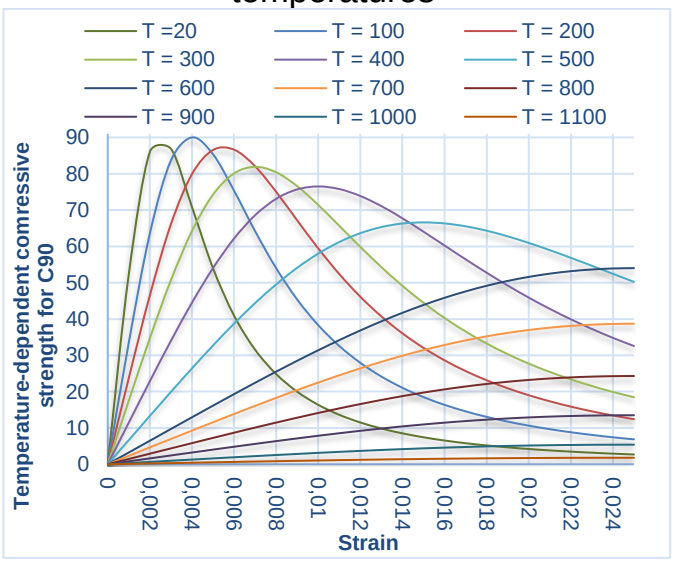

Figure A.14: Stress–Strain curves of concrete type C90 at elevated temperatures

Annexure B: Thermal properties

Concrete: Thermal properties of concrete according to EN 1992-1-2:

- *Thermal elongation:*

$$\frac{\Delta l}{l} = -1.8 \times 10^{-4} + 9 \times 10^{-6}T + 2.3 \times 10^{-11}T^3 \qquad 20 \le T \le 700 \qquad \text{(B.1)}$$

$$\frac{\Delta l}{l} = 14 \times 10^{-3} \qquad 700 < T \le 1200 \qquad \text{(B.2)}$$

- *Specific heat* ($J/kg.K$):

$$C_p = 900 \qquad 20 \le T \le 100 \qquad \text{(B.3)}$$

$$C_p = 900 + (T - 100) \qquad 100 < T \le 200 \qquad \text{(B.4)}$$

$$C_p = 1000 + \frac{T - 200}{2} \qquad 200 < T \le 400 \qquad \text{(B.5)}$$

$$C_p = 1100 \qquad 400 < T \le 1200 \qquad \text{(B.6)}$$

- *Density* (kg/m^3):

$$\rho(T) = \rho(20℃) \qquad 20 \le T \le 115 \qquad \text{(B.7)}$$

$$\rho(T) = \rho(20℃)\left(1 - \frac{0.02(T - 115)}{85}\right) \qquad 115 < T \le 200 \qquad \text{(B.8)}$$

$$\rho(T) = \rho(20℃)\left(0.98 - \frac{0.03(T - 200)}{200}\right) \qquad 200 < T \le 400 \qquad \text{(B.9)}$$

$$\rho(T) = \rho(20℃)\left(0.95 - \frac{0.07(T - 400)}{800}\right) \qquad 400 < T \le 1200 \qquad \text{(B.10)}$$

- *Thermal conductivity* ($W/m.K$):

$$Upper\ limit: \lambda_c = 2 - 0.2451\frac{T}{100} + 0.0107\left(\frac{T}{100}\right)^2 \qquad 20 \le T \le 1200 \qquad \text{(B.11)}$$

$$Lower\ limit: \lambda_c = 1.36 - 0.136\frac{T}{100} + 0.0057\left(\frac{T}{100}\right)^2 \qquad 20 \le T \le 1200 \qquad \text{(B.12)}$$

Steel: Thermal properties of steel according to EN 1994-1-2:

- *Thermal elongation:*

$$\frac{\Delta l}{l} = -2.416 \times 10^{-4} + 1.2 \times 10^{-5}T + 0.4 \times 10^{-8}T^2 \qquad 20 \le T \le 750 \qquad \text{(B.13)}$$

$$\frac{\Delta l}{l} = 11 \times 10^{-3} \qquad 750 < T \le 860 \qquad \text{(B.14)}$$

$$\frac{\Delta l}{l} = -6.2 \times 10^{-3} + 2 \times 10^{-5} T \qquad 860 < T \leq 1200 \qquad \text{(B.15)}$$

- *Specific heat* $(J/kg.K)$:

$$C_a = 425 + 7.73 \times 10^{-1} T - 1.69 \times 10^{-3} T^2 + 2.22 \times 10^{-6} T^3 \qquad 20 \leq T \leq 600 \qquad \text{(B.16)}$$

$$C_a = 666 - \frac{13002}{T - 738} \qquad 600 < T \leq 735 \qquad \text{(B.17)}$$

$$C_a = 545 + \frac{17820}{T - 731} \qquad 735 < T \leq 900 \qquad \text{(B.18)}$$

$$C_a = 650 \qquad 900 < T \leq 1200 \qquad \text{(B.19)}$$

- *Thermal conductivity* $(W/m.K)$:

$$\lambda_a = 54 - 3.33 \times 10^{-2} T \qquad 20 \leq T \leq 800 \qquad \text{(B.20)}$$

$$\lambda_c = 27.3 \qquad 800 < T \leq 1200 \qquad \text{(B.21)}$$

- The *density* of steel shall be considered to be independent of steel temperature. $\rho_{steel} = 7850 \ \frac{kg}{m^3}$

Table B.1: Thermal properties of concrete and steel at elevated temperatures

Temperature °C	Concrete				Steel		
	Thermal Elongation	Specific Heat $\frac{J}{kgK}$	Density $\frac{kg}{m^3}$	Thermal Conductivity $\frac{W}{mK}$	Thermal Elongation	Specific Heat $\frac{J}{kgK}$	Thermal conductivity $\frac{W}{mK}$
20	1.84E-07	900	2450	1.95	0.0000	439.8	53.33
100	7.43E-04	900	2450	1.77	0.0010	487.6	50.67
200	1.80E-03	1000	2401	1.55	0.0023	529.8	47.34
300	3.14E-03	1050	2364	1.36	0.0037	564.7	44.01
400	4.89E-03	1100	2328	1.19	0.0052	605.9	40.68
500	7.20E-03	1100	2306	1.04	0.0068	666.5	37.35
600	1.02E-02	1100	2285	0.91	0.0084	759.9	34.02
700	1.40E-02	1100	2263	0.81	0.0101	1008.2	30.69
800	1.40E-02	1100	2242	0.72	0.0110	803.3	27.36
900	1.40E-02	1100	2220	0.66	0.0118	650.4	27.30
1000	1.40E-02	1100	2199	0.62	0.0138	650.0	27.30
1100	1.40E-02	1100	2177	0.60	0.0158	650.0	27.30
1200	1.40E-02	1100	2156	0.60	0.0178	650.0	27.30

Annexure C: Parametric curve of a fire compartment

Consider the fire compartment of Figure C-1. We assume the compartment is a part of an office building with concrete walls and roof. Concrete members are fire-resistant and stop the fire from spreading to other rooms. Some openings are provided in the walls. Here, we want to calculate the parametric fire curve for the fire compartment, based on Annexure A of EN 1991-1-2. Structural members, including floors, walls, and columns, are made of reinforced concrete.

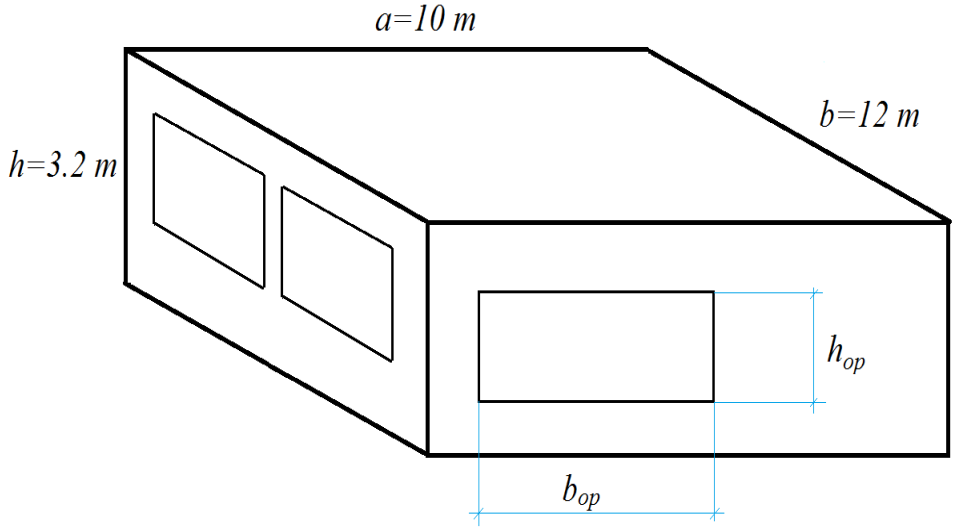

Figure C.1: Dimensions of fire compartment and openings

Density: $= 2300\ kg/m^3$, specific heat: $C = 840\ J/(kg.K)$,thermal conductivity: $\lambda = 1.57\ W/(m.K)$

The characteristic fire load density related to floor area for office buildings is given in Table E.4 of EN 1991-1-2:

$q_{f,k} = 511 \frac{MJ}{m^2}$, $A_{floor} = a.b = 10 \times 12 = 120\ m^2$

The factor of fire activation risk can be calculated by interpolation from Table E.1 of EN 1991-1-2, as follows:

$$\delta_{q1} = 1{,}1 + 0.4\frac{120 - 25}{250 - 25} = 1.27 \quad \text{(C.4)}$$

Fire activation risk caused by the compartment type for office buildings is:

$$\delta_{q2} = 1.00 \quad \text{(C.5)}$$

The design fire load density can be calculated as:

$$q_{fd} = \delta_{q1}\delta_{q2}q_{fk} = 1.27 \times 511 \times 1 = 649\frac{MJ}{m^2} \quad \text{(C.6)}$$

The total area of the enclosure and openings is:

$$A_{total} = 2A_f + 2(a+b)h = 2 \times 120 + 2 \times (22 \times 3.2) = 380.8\, m^2 \quad \text{(C.7)}$$

$$A_{op} = 3 \times 3 \times 1.6 = 14.4\, m^2 \quad \text{(C.8)}$$

The surface factor for floor and ceiling and the surface factor of the compartment can be obtained as:

$$b = \sqrt{\rho c \lambda} = \sqrt{2300 \times 840 \times 1.57} = 1741.62 \frac{J}{m^2 s^{0.5} K} \quad \text{(C.9)}$$

$$\bar{b} = \frac{\sum b_i A_i}{A_{total} - A_{opening}} = \frac{380.8 \times 1741.62}{380.8 - 14.4} = 1810 \frac{J}{m^2 s^{0.5} K} \quad \text{(C.10)}$$

The opening factor is:

$$O = \frac{A_{op}\sqrt{h_{op}}}{A_{total}} = \frac{14.4 \times \sqrt{1.6}}{380.8} = 0.05\sqrt{m} \quad \text{(C.11)}$$

According to Annexure A, the opening factor will be more than 0.02 and less than 0.2. The limitation is satisfied. The time factor can be obtained as:

$$\Gamma = \frac{\left(\frac{O}{b}\right)^2}{\left(\frac{0.04}{1160}\right)^2} = \frac{\left(\frac{0.05}{1810}\right)^2}{\left(\frac{0.04}{1160}\right)^2} = 0.64 \quad \text{(C.12)}$$

Fire load density related to the surface area can be calculated as follows:

$$q_{t,d} = \frac{q_{f,d} A_{floor}}{A_{total}} = \frac{649 \times 120}{380.8} = 204 \frac{MJ}{m^2} \quad \text{(C.13)}$$

The limiting time and the maximum temperature in fire compartment can be obtained as follows. Medium fire growth rate is expected at $t_{lim} = 30min = 0.5hour$.

$$t_{max} = max\begin{cases} \frac{0.0002 q_{t,d}}{O} \\ t_{lim} \end{cases} = max\begin{cases} 0.0002 \times \frac{204}{0.05} = 0.81 \\ 0.5hour \end{cases} \quad \text{(C.14)}$$

Just three openings are assumed for the compartment. Therefore, as can be seen above, the fire is ventilation-controlled; t_{max} is given by the first term. The time to achieve maximum temperature is:

$$t^*_{max} = t_{max}\Gamma = 0.81 \times 0.64 = 0.51\, hours = 31\, min \quad \text{(C.15)}$$

And the maximum temperature:

$$T_{max} = 20 + 1325\left(1 - 0.324e^{-0.2t^*} - 0.204e^{-1.7t^*} - 0.472 * e^{-19.2t^*}\right) = 844 \quad \text{(C.16)}$$

Finally, the temperature curve, including the cooling phase, is:

$$T = \begin{cases} 20 + 1325(1 - 0.324e^{-0.2t} - 0.204e^{-1.7t} - 0.472 * e^{-19.2t}) \\ T_{max} - 250(t - t_{max}) = 844 - 250(t - 0.51) \end{cases} \quad \text{(C.17)}$$

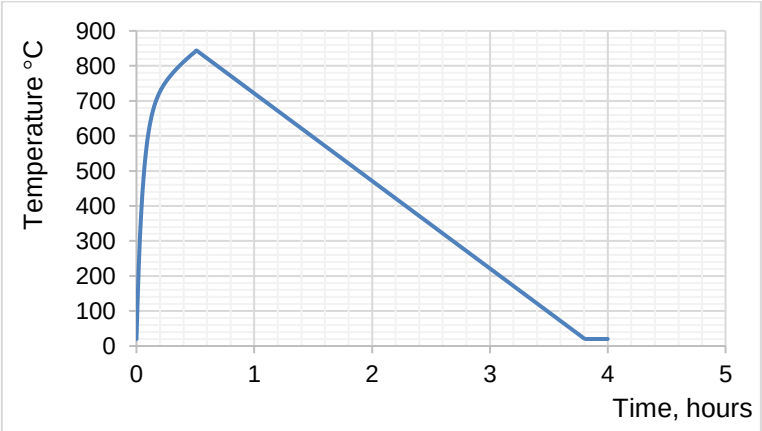

Figure C.2: Calculated parametric temperature curve for the fire compartment

Annexure D: Fire resistance of composite columns

Imagine a composite column as a part of a structure, as shown in Figure D.1. Here, the fire resistance of the column—based on EN 1994-1-2—is proposed. This example shows the design process of a member as a part of a structure. It has been assumed that the structure is a frame of an office building and the fire resistance required is R30. This means that the structure shall resist at least 30 minutes in a fire situation. The column length is 3m; therefore, the buckling length of column is $0.5 \times 3 = 1.5m$. Figure D.2 shows the composite cross-section of the column.

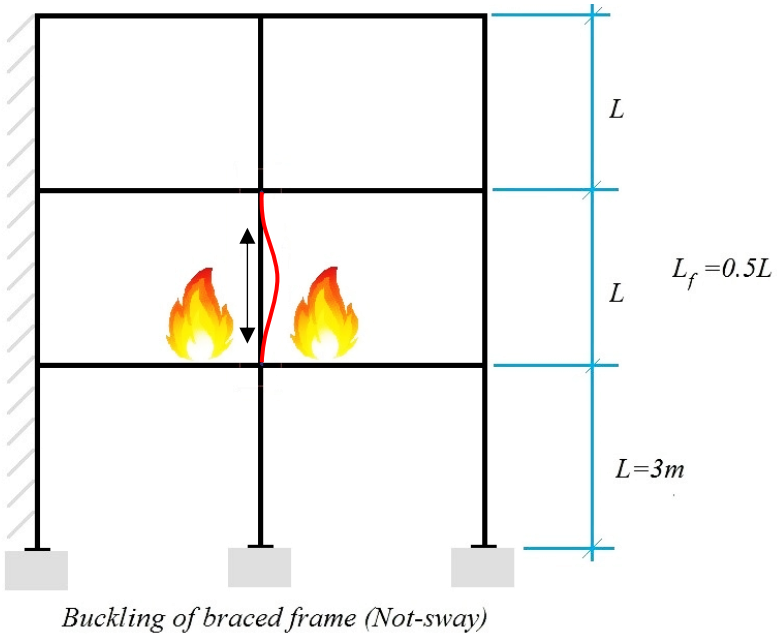

Figure D.1: The proposed frame

The accidental load combinations for fire design is written as follows:

$\psi_{2,1} = 0.3$

$$E_{Ed} = \sum G_k + \sum \psi_{2,i} Q_{k,i} + A_d = 1.0 \times 800 + 0.3 \times 650 = 995\ kN \quad \text{(D.1)}$$

The simple calculation method has been used to verify the column in a fire situation as follows:

➢ *Simple calculation method*

The fire resistance can be verified as follows:

$$\frac{N_{fi,d}}{N_{fi,Rd}} \leq 1 \quad \text{(D.2)}$$

Which $N_{fi,Rd,z} = \chi_z N_{fi,pl,Rd}$

- Steel profile HEB300, Material S235

$h = 300mm$
$b = 300mm$
$e_w = thickness\ of\ web = 11mm$
$e_f = thickness\ of\ flange = 19mm$
$A_{crossSection} = 14900mm^2$

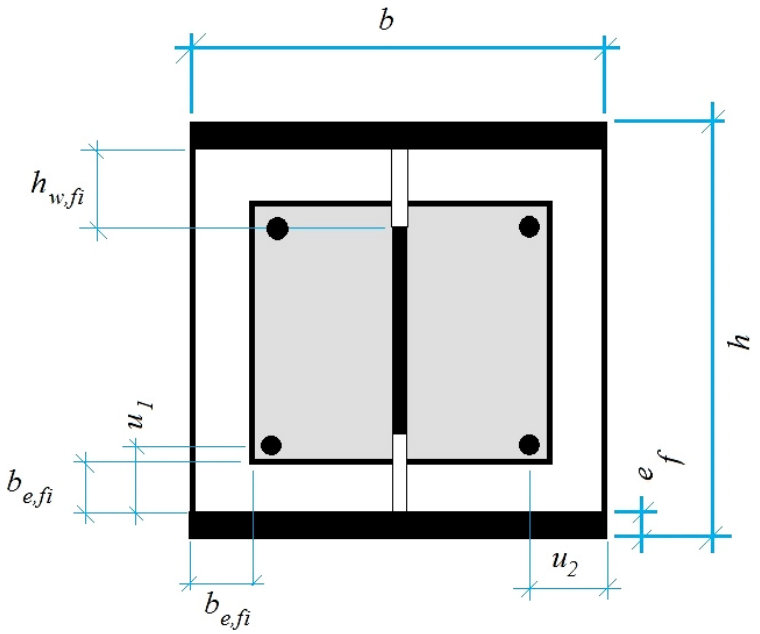

$f_y = yield\ stress = 235\frac{N}{mm^2}$, $E_s = modulus\ of\ elasticity = 210000\frac{N}{mm^2}$
$Moment\ of\ Inertia = I_z = 8.56 \times 10^7 mm^4$

- Concrete, Material C25/30

$A_C = area = 300 \times 300 - 14900 = 75100mm^2$
$f_c = compressive\ strength = 25\frac{N}{mm^2}$, $E_C = 30500\frac{N}{mm^2}$
$Moment\ of\ Inertia = I_z = 300 \times \frac{300^3}{12} - 8.56 \times 10^7 = 589400000\ mm^4$

- Internal forces

$M = 0$, $N_{permanent} = 800\ kN$, $N_{variable} = 650\ kN$

Figure D.2: cross section properties

χ_z is the reduction factor for buckling, which depends on the buckling curve c and the slenderness of the column, and $N_{fi,pl,Rd}$ is the plastic axial design resistance of the cross-section in a fire situation. The axial resistance here is the compression resistance. The simple calculation method has some limitations, which can be seen in Table D.1. At first, these limitations will be satisfied. At elevated temperatures, the material strength will be reduced. The reduction will be taken into account with reducing the cross-sectional area of the concrete. Figure D.2 shows the reduced cross-section at elevated temperatures. It has been assumed that the cross-section is heated on four sides. The reduced height of the web for the steel profile can be obtained as:

$$T_{f,t} = T_{o,t} + \frac{k_t A_m}{V} \quad (D.3)$$

The temperature $T_{o,t}$ and the reduction factor k_t are given in Table D.2. The section factor can be calculated as:

$$\frac{A_m}{V} = \frac{2h + 2b}{hb} = \frac{2 \times 0.3 + 2 \times 0.3}{0.3 \times 0.3} = 13.3 \quad \text{(D.4)}$$

Table D.1: Limitations of the simplified method

Limitation	Calculation	
$l_{Temp} \leq 13.5$	$1.5 \leq 4.05m$	*OK*
$230\ mm \leq h\ or\ b \leq 1100\ mm$	$h = b = 300mm$	*OK*
$1\% \leq \frac{A_{reinforcement}}{A_C} \leq 6\%$	$\frac{A_{reinforcement}}{A_C} = 1$ Assuming 1% reinforcement.	*OK*
Maximum fire resistance 120min	R30	*OK*
$l_T < 10b\ if \begin{cases} 230 \leq b \leq 300 \\ \frac{h}{b} > 3 \end{cases}$	$h = b = 300mm$ $\frac{h}{b} = 1$ $l_T = 1.5m < 10 \times 0.3 = 3m$	*OK*

Therefore, we have:

$T_{f,t} = 550 + 9.65 \times 13.3 = 665$ ℃

Table D.2: Parameters for calculating the average temperature for flange

Fire resistance category	$T_{o,t}$℃	k_t m℃
R30	550	9.65
R60	680	9.55
R90	805	6.15
R120	900	3.65

Having $T_{f,t}$, average flange temperature, the reduction factors for modulus of elasticity and yield strength can be obtained from Table 3.2 of EN 1994-1-2.

$$k_{y,T} = 0.314 \quad \text{(D.5)}$$

$$k_{E,T} = 0.193 \quad \text{(D.6)}$$

The axial resistance of the flanges of the steel profile is:

$$N_{fi,pl,Rd,flange} = \frac{2be_f k_{y,T} f_{ay,f}}{\gamma_{M,fi,a}} = 2 \times 300 \times 19 \times 235 \times \frac{0.314}{1} = 841.206\ kN \quad \text{(D.7)}$$

$$EI_{fi,f} = 2\frac{k_{E,T} E_{a,f} e_f b^3}{12} = 0.193 \times 210000 \times 19 \times 300 \times 300 \times \frac{300}{6} = 3.46 \times 10^9\ kNmm \quad \text{(D.8)}$$

For the web of the steel profile, we have:

$$h_{w,fi} = 0.5(h - 2 \times 19)\left(1 - \sqrt{1 - 0.16\frac{H_t}{h}}\right) \quad \text{(D.9)}$$

According to Annexure G of EN 1994-1-2 for fire resistance category R30, we have $H_t = 350mm$.

$h_{w,fi} = 0.5(300 - 38)(0.0983) = 12.88\,mm$

The reduced yield stress is:

$$f_{ay,w,t} = f_{ay,w}\sqrt{1 - 0.16\frac{H_t}{h}} = 212\frac{N}{mm^2} \quad \text{(D.10)}$$

The axial resistance of the web is:

$$N_{fi,pl,Rd,web} = \frac{e_w(h - 2e_f - 2h_{w,fi})\,f_{ay,w}}{\gamma_{M,fi,a}} = 550.35\,kN \quad \text{(D.11)}$$

In comparison with the concrete part and flanges, the bending stiffness of the web is assumed to be negligible. A layer of concrete around the perimeter with a thickness of 4mm needs to be neglected. The thickness of the layer that will be neglected is given in Annexure G of EN 1994-1-2 as a function of the fire resistance category. The area of concrete will be reduced using the reduction factor, which can be obtained using the values given in Table G.4 of EN 1994-1-2. These values depend on section factor $\frac{A_m}{V}$ and the fire resistance category. Using the linear interpolation, for R30 we have:

$T_{c,t} = 220.5℃$

The reduction factors of compressive strength and the ultimate strain for concrete are given in Table 3.3 of EN 1994-1-2. According to this table:

$$\varepsilon_{cu,T} = 5.8 \times 10^{-3} \quad \text{(D.12)}$$

$$k_{C,T} = 0.93 \quad \text{(D.13)}$$

The secant modulus of elasticity of concrete can be obtained from Figure 3-12 or the following relationship:

$$E_{c,sec,T} = \frac{k_{c,T}f_c}{\varepsilon_{cu,T}} = \frac{0.93 \times 0.025}{5.8 \times 10^{-3}} = 4.0\frac{kN}{mm^2} \quad \text{(D.14)}$$

Using the calculated values, the axial resistance of the concrete part of the cross-section can be determined:

$$N_{fi,pl,Rd,c} = 0.86A_C k_{c,T}\frac{f_c}{\gamma_{M,fi,c}} = 254 \times 292 \times 0.93 \times \frac{25}{1} = 1724.4\,kN \quad \text{(D.15)}$$

$$EI_{f,c,z} = E_{c,sec,T} \times 292^3 \times \frac{254}{12} = 21.08 \times 10^8\,kNmm^2 \quad \text{(D.16)}$$

Here, we assume that the axial resistance of reinforcing bars and their bending stiffness is zero. Finally, the design compressive resistance of the whole cross-section is:

$$N_{fi,pl,Rd} = N_{fi,pl,Rd,c} + N_{fi,pl,Rd,web} + N_{fi,pl,Rd,flange} = 1724 + 550 + 841 = 3115\,kN \quad \text{(D.17)}$$

The effective flexural bending stiffness can be determined when the reduction coefficients $\varphi_{i,T}$ are chosen. These values are given in Table G.7 of EN 1994-1-2. These values are given for each part of the cross-section, depending on the fire resistance category.

$$\varphi_{concrete,T} = 0.8, \qquad \varphi_{flange,T} = 1, \qquad \varphi_{web,T} = 1 \tag{D.18}$$

$$EI_{fi,eff,z} = \varphi_{concrete,T} EI_{f,c,z} + \varphi_{flange,T} EI_{fi,f} + 0$$
$$= 0.8 \times 2.108 \times 10^9 + 3.46 \times 10^9 = 5.14 \times 10^9$$

The axial buckling load at elevated temperatures or the Euler buckling load for the column is:

$$N_{fi,critical,z} = \frac{\pi^2 EI_{fi,eff,z}}{l_T^2} = 22523\ kN \tag{D.19}$$

l_T is the buckling length of the column in a fire situation or warm design. The non-dimensional slenderness is:

$$\lambda_T = \sqrt{\frac{N_{fi,pl,Rd}}{N_{fi,critical,z}}} = \sqrt{\frac{3115}{22523}} = 0.372 \tag{D.20}$$

The buckling curves c of Table 4.5.2 of EN 1993-1-1 and non-dimensional slenderness will be used to determine the reduction factor.

$$\chi_z = \frac{1}{\phi + \sqrt{\phi^2 - \lambda_T^2}} = \frac{1}{0.55 + \sqrt{0.55^2 - 0.372^2}} = 1.04 \tag{D.21}$$

$$\phi = 0.5(1 + \alpha(\lambda_T^2 - 0.2) + \lambda_T^2) = 0.554 \tag{D.22}$$

The buckling design resistance is:

$$N_{fi,Rd,z} = \chi_z N_{fi,pl,Rd} = 1.04 \times 3115 = 3240\ kN \tag{D.23}$$

Verification: $\frac{N_{fi,d}}{N_{fi,Rd,z}} = \frac{995}{3240} = 0.307 < 1$ OK